This is a excerpt from:
ICES. 2022. Working Group on the Integrated Assessments of the Barents Sea (WGIBAR). ICES Scientific Reports. 4:50. 235 pp.
http://doi.org/10.17895/ices.pub.20051438

Annex 5: The state and trends of the Barents Sea ecosystem in 2021

Edited by Elena Eriksen and Anatoly Filin

Contributing Authors (Alphabetic):

Institute of Marine Research (IMR), Norway:

Bagøien, E., Boitsov. S., Bogstad, B., Dalpadado. P., Eriksen, E., Fall, J., Frantzen, S., Gjøsæter, H., Grøsvik, BE., Heldal, HE., Hjelset, AM., Husson, B., Hvingel, C., Ingvaldsen, R., Johannesen, E., Jørgensen, LL., Mikkelsen. N., van der Meeren, G., Karlson, S., Rønning, J., Skaret, G., Solvang H., Øien, N.

Polar Branch of the Federal State Budget Scientific Institution, Russian Federal Research Institute of Fisheries and Oceanography ("PINRO" named after N. M. Knipovich), Russia: Benzik , A., Dolgov, A., Filin, A., Gordeeva, A., Klepikovskiy RN., Kovalev, Yu., Krivosheya, P., Kudryashova, AS., Mikhina, A., Novikov, MA., Prokhorova, T., Prokopchuk, I., Prozorkevich, D., Russkikh, A., Stesko, A., Strelkova, N., Trofimov, A., Zacharov, DV.

The Norwegian Polar Institute (NPI): Aars, J., Johnsen, H., Kovacs, K.

The Norwegian Institute for Nature Research (NINA), Norway: Per Fauchald

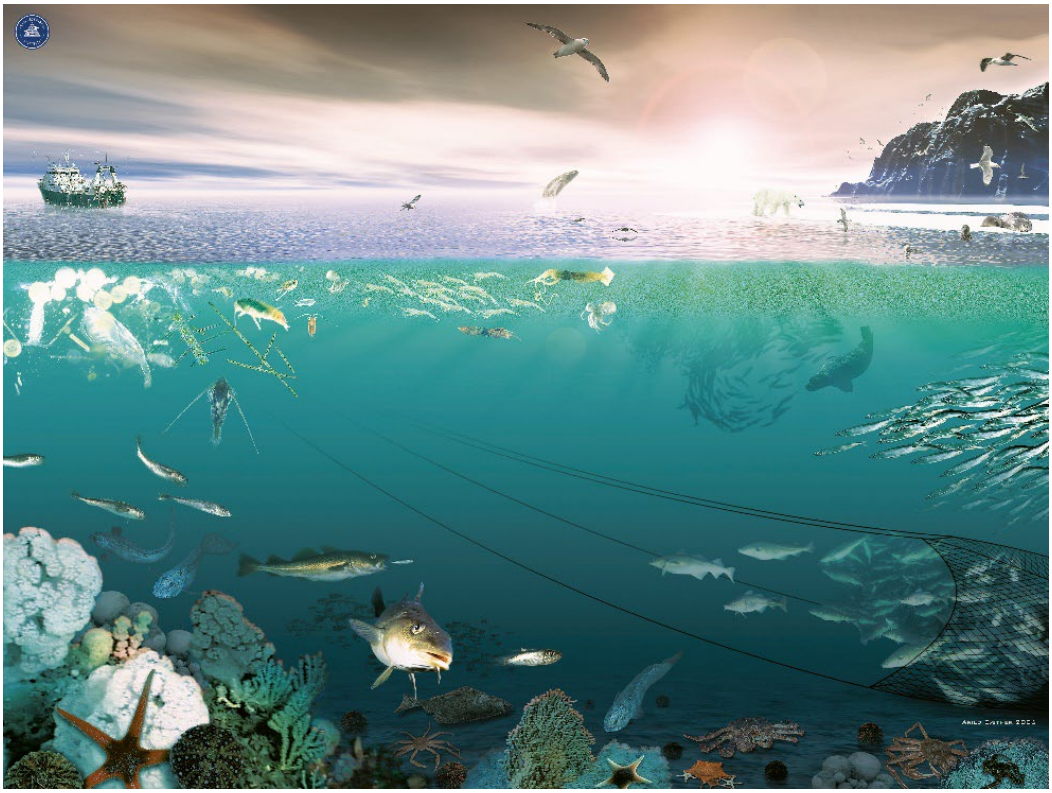

Summary

The Barents Sea has experienced a warming trend since 1970s, while becoming colder after 2015–2016. Temperatures in 2021 were still typical of warm years. The areas covered by Atlantic and Arctic Waters in autumn were similar to 2020, while the area covered by cold bottom waters

increased slightly and turned out to be the largest since 2011. Ice coverage of the Barents Sea has increased since 2016 due to lower temperatures and lower area covered by Atlantic Water, but the ice coverage in 2021 was still below average (1981–2010).

Some decrease in mesozooplankton biomass, mainly in some western and central areas, measured in autumn 2021 could be influenced by high predation pressure due to a large capelin stock, possibly a lower advection of mesozooplankton with inflowing waters into the Barents Sea (BS) and variation in local production. Krill indices of biomass have shown increasing trends over recent decades to the increased contribution from *M. norvegica* in the BS. The total biomass of amphipods was slightly higher than long term mean (2003–2021) but the lowest since 2014.

The 2021-year classes of cod and haddock were strong, while those of polar cod, redfish seem to be weak. Capelin and herring year classes was moderate. In 2021, the total biomass of 0-group in the Barents Sea was slightly below long term mean and was close to 1 million tonnes.

The total stock of capelin was estimated to about 4 million tonnes, which is the highest estimated biomass since 2008 and above the long-term level. The biomass of polar cod in the Barents Sea recovered after a long time decline and in 2021 was estimated 1.3 million tonnes.

Most of the main demersal fish stocks (cod, haddock, Greenland halibut, beaked redfish, long rough dab, saithe) in the BS are in a healthy state and at a level at or above the long term mean. Cod food consumption in 2021 was close to the level of 2020. Capelin is still the most important food item for cod. Importance of euphausiids, hyperiids, polar cod and snow crab has increased in cod diet, while importance of haddock, shrimp and herring has decreased.

The northern shrimp stock is relatively stable. The snow crab population distribution and abundance is stable. Aggregations of the red king crab have been shifted eastward and north-eastward last decade, however in 2021 compared 2020 location of main aggregations of red king crab were stable.

The distribution of megabenthos may show relative stable large-scale patterns but with slightly increasing biomass. This may indicate a long-term change toward warmer seabed conditions. Two new boreal species was recorded in the SW where also the general biomass of benthos increases the most.

The centre of gravity of the most common species shifted northward for several species the last 11 years. In the same period, the abundance of pelagic surface feeding birds has decreased.

The abundances of minke, fin and humpback whales in the BS increased after 2000 and have stayed at high levels. Their distributions, especially of minke and humpback whales, generally overlap with capelin distributions in late summer-autumn

Temporal development

Statistical spatial trend analyses to investigate association/linkage among biotic and abiotic conditions.

By Hiroko Solvang and Elena Eriksen (IMR)

Common trends refer to trends that are similar across ecosystem components. Identifying common trends can be useful as a diagnostic tool to reveal past changes and to explore the relationships among biological communities, as well as between these communities and environmental conditions. In the present investigation, trend estimation and classification analyses (TREC, Solvang and Planque 2020) are applied to WGIBAR time-series data. Based on the discussion in the

meeting, the time-series data should be analysed by dividing into two groups, before 2004 (148 biotic and abiotic) and after 2005.

Since 1990 and up to 2004, the BS has experienced colder conditions with an increase of Arctic Water area and ice coverage, of volume of water transport between Svalbard and Franz Josef Land (January–August) and increased days with storm, water salinity at Kola section and stratification (SE and SW). During the next period from 2005 and up to 2021, volume of water transport between Svalbard and Franz Josef Land (January–August) and days with storm showed increasing trend only, most likely due to temperature conditions first increased to the maxim in 2015–2016 and decreased after that. Primary production and jellyfish showed increasing trend since 2005. Large fraction of mesozooplankton and jellyfish showed increasing trend before 2005, while decreasing after that. Trends for many of biological parameters (numbers, biomass, length, weight, condition) for capelin, polar cod and herring were increasing during the first period while decreased during the second. Several of biological parameters (length and weight) for cod showed decreasing trend during both periods. Herring, polar cod, haddock, and blue whiting proportion in the cod diet have increased since 1990 and up to 2004, while no trends found since that. Landings showed an increasing trend for haddock (1990–2004) and cod, Greenland halibut and beaked redfish (since 2005) (Table A5.1).

Table A5.1

Order	1990-2004 (148 biotic and abiotic)		2005-2021 (136 biotic and abiotic)	
	Increasing trend	**Decreasing trend**	**Increasing trend**	**Decreasing trend**
1	Area_ArW, Area_IceMax, Storms, NBSO, TempNW, Kola_Sal, Strat_SE, Strat_SW	Area_AW, BSX, Kola_Temp	Storms, NBSO	Area_AW, Area_MW, BSO, BSX, Area_IceMin, Temp_FB_aug, SBSO, TaAnom_West
2			18 PProd_BARENTS	
3, 3.5	Plank_Large_BS, Jellyfish_biomass		Amphipods_TB	Plank_Large_BS, Shrimp_biom
4	CAP_0_N_Keff, CAP_3_L, CAP_3_W, CAP_4_L, CAP_4_W, CAP_5_N, CAP_5_L, CAP_5_W, CAP_5_C, CAP_Mat3, POL_1_N, POL_1_B, POL_2_N, POL_2_B, POL_3_N, POL_3_B, POL_3_L, POL_3_W, POL_4_N, POL_4_B, POL_5_N, POL_5_B, POL_5_L, POL_5_W, POL_TSN, POL_TSB, HER_0_N, HER_0_B, HER_0_L, HER_1-3_B	CAP_0_L, CAP_1_N, CAP_1_B, CAP_2_N, CAP_2_N, CAP_imm_B, CAP_TSB, POL_1_L, POL_1_W		CAP_2_L, CAP _3_N, CAP _3_B, CAP_3_L, CAP_5_L, CAP_5W, CAP_5C, CAP_mat_B, CAP_SSB,CAP_landings, POL_1_L, POL_1_W, POL_2_N, POL_2_B, POL_2_L, POL_2_W, POL_3_N, POL_3_B, POL_3_L, POL_3_W, POL_4_N, POL_4_B, POL_4_L, POL_5_N, POL_5_B, POL_5_N, POL_TSB, HER_0_N, HER_0_B, HER_0_L, HER_1-2_B, HER_1-3_B, BLW_3_N, BLW_4+_N, BLW_TSB,BLW_B_winter
5	GRH_0_N_noKeff, HAD_0_N, HAD_0_B, HAD_F_4-7, HAD_landings, SAI_0_N	COD_0_L, COD_3_W, COD_5_W, HAD_5_W, SEB_0_N_keff, SEB_0_B, SEB_0_L,	COD_Landings, GRH_0_N_noKeff, GRH_Landings, HAD_5_W, SEM_5+cm_indexwinter, SEM_landings	COD_0_L, COD _Rec3, COD_3_W, COD_5_W, COD_8_W, COD _mat7, HAD_0_N, HAD_0_B, HAD_R3, SAI_0_N

		SEM_5+cm_indexwinter, SEM_landings
6		
7	Herring, Polar cod, Haddock, Blue whiting	Other, Redfish, Long rough dab

Flagged observation (FO) detection

To investigate whether the most recent observation follow the recent trend or is away from the trend, three years ahead predictions are calculated in the two periods, 1990–2004 and 2005–2021. The trend in this case is estimated by stochastic trend model. Stochastic trend model is presented by a class of auto-regressive model and is easily set in state space representation. Kalman filter algorithm is applied to estimate trend component and to calculate the prediction. The trend estimates look more fluctuated rather than estimates by polynomial trend using by TREC. This is because of that stochastic trend follows the data variation in each time point. Particularly upwards and downwards trends estimated by stochastic trend model are consistent with the estimated trends by polynomial model. For the period 1990–2004, we run the analysing procedure using the data recording until 2001 and implement the prediction for 2002–2004. For the period 2005–2021, we run the procedure using the data recording until 2018 and implement the prediction for 2019–2021.

Current state of the Barents Sea ecosystem components

Meteorological and oceanographic conditions

By A. Trofimov (PINRO), R. Ingvaldsen (IMR)

The Barents Sea has become substantial colder since 2015–2016. However, its air and water temperatures in 2021 were generally higher than average, being typical of warm years. In autumn, the areas covered by Atlantic (>3°C) and Arctic (<0°C) waters changed insignificantly compared to 2020; the area covered by cold bottom waters (<0°C) increased slightly and turned out to be the largest since 2011. Ice coverage of the Barents Sea has increased since 2016 due to lower temperatures and lower inflow of Atlantic Water, but the ice coverage in 2021 was still below average. Its seasonal maximum occurred in February–March, earlier than usual. There was no ice in the sea from August to October.

The Barents Sea is a shelf sea of the Arctic Ocean. Being a transition area between the North Atlantic and the Arctic Basin, it plays a key role in water exchange between them. Atlantic waters enter the Arctic Basin through the Barents Sea and the Fram Strait (Figure A5.1). Variations in volume flux, temperature and salinity of Atlantic waters affect hydrographic conditions in both the Barents Sea and the Arctic Ocean and are related to large-scale atmospheric pressure systems.

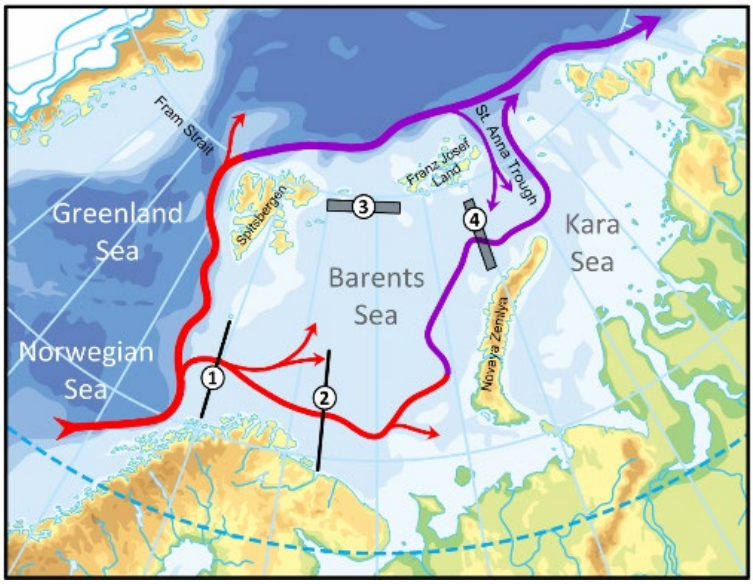

Figure A5.1: The main paths of Atlantic waters in the Barents Sea as well as Fugløya–Bear Island Section (1), Kola Section (2) and boxes in the northwestern (3) and northeastern (4) Barents Sea.

Air pressure, wind and air temperature

In 2021, the winter (December–March) NAO index dropped significantly and reached a negative value of −0.72 (1.79 in 2020), the lowest since 2014. Over the Barents Sea, the number of days with winds more than 15 m/s was higher than or close to the long term mean (1981–2010) all over the year. The storm activity was a record high (since 1981) in the western part of the sea in July, October and November and in the central part in January and May. For the whole year 2021, it was a record high in the western (185 days), central (172 days) and eastern (174 days) parts of the Barents Sea.

Air temperature (http://nomad2.ncep.noaa.gov) averaged over the western (70–76°N, 15–35°E) and eastern (69–77°N, 35–55°E) Barents Sea exceeded the 1981–2010 average for most of 2021 and was close to average only in February in the west and in November–December in the west and east of the sea (Figure A5.2). The largest positive anomalies (>1.5°C) were observed in the west in March, April and June, and in the east in April, June and August. Negative anomalies were only found in May (−0.4°C) in the west and in February (−2.3°C) in the east of the sea. Both air temperature for most of 2021 and the 2021 annual mean air temperature were lower than in 2020 (Figure A5.2).

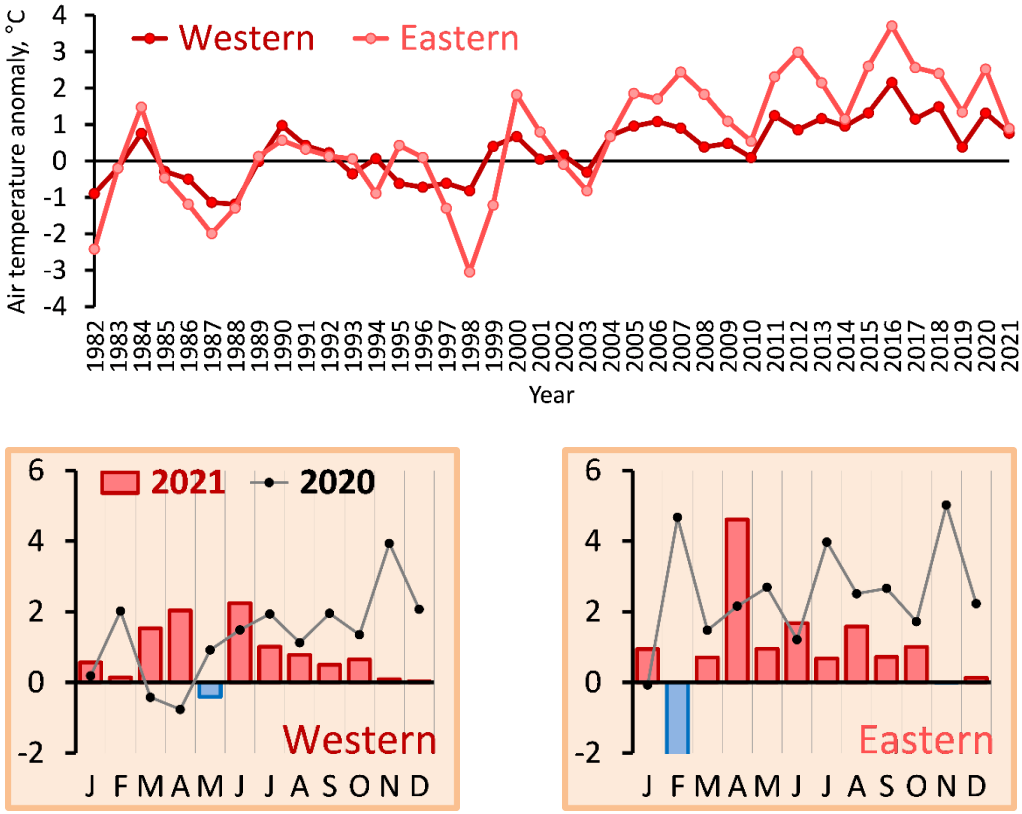

Figure A5.2: Annual (upper) and monthly (lower) air temperature anomalies in the western and eastern Barents Sea.

Ice conditions

In January 2021, the Barents Sea ice coverage (expressed as a percentage of the total sea area) was 32%, i.e. 17% less than the 1981–2010 average (Figure A5.3). In February, it increased significantly (up to 52%) and almost reached its long term mean of 53%. In March, the area covered by ice remained the same (52%, i.e. only 3% below average). Ice melting started in April, a month earlier than usual, and by August, the sea was completely free of ice. In April–July, the ice coverage was 12–16% below average (Figure A5.3). From August to October, there was no ice in the Barents Sea. The first drift ice appeared between the Franz Josef Land and Spitsbergen Archipelagoes at the end of October. In November, the ice coverage was 18%, i.e. 11% less than average. In December, the area covered by ice increased significantly (up to 37%) and almost reached its long term mean of 40%. Overall, the 2021 annual mean ice coverage of the Barents Sea was 9% below average, but 2% more than in 2020.

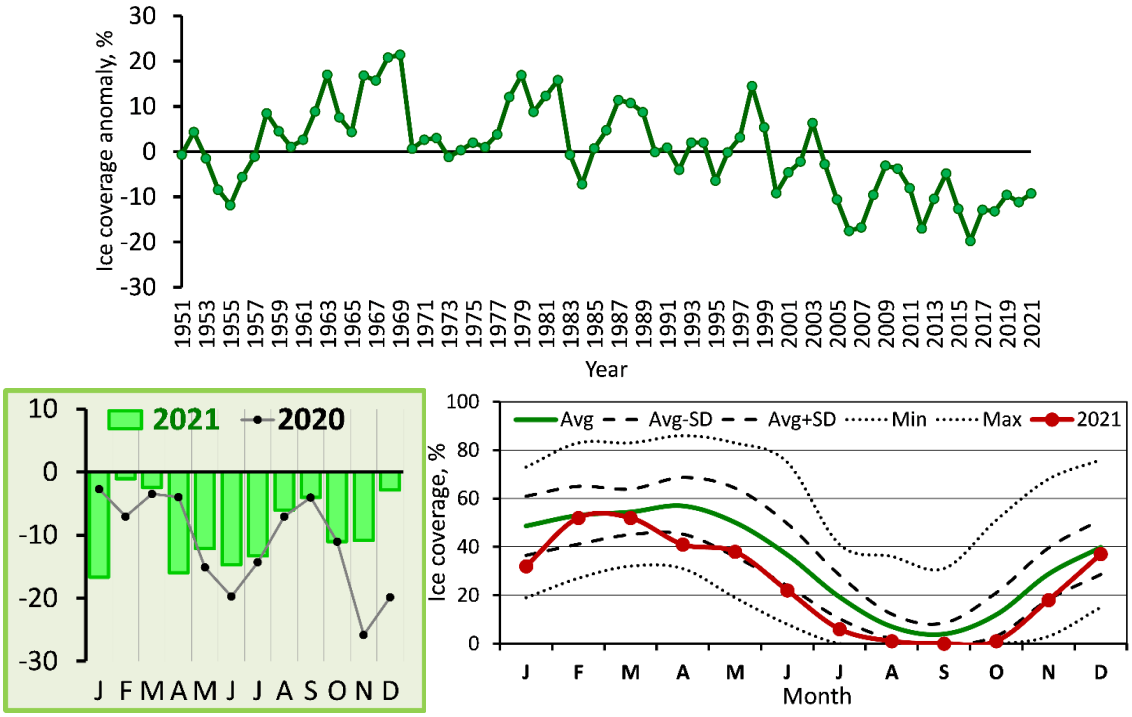

Figure A5.3: Ice coverage (lower right) and its monthly (lower left) and annual (upper) anomalies in the Barents Sea.

Currents and transports

Volume flux into the Barents Sea show now long-term trends but reveal pulses of stronger or weaker inflow (Figure A5.4). The years 2006 and 2015–2016 were extreme years with high inflow during parts of the year. In these years the temperature of the inflowing water also was high. After 2015–2016 the inflow was lower concurring with declining AW temperatures in the inflowing water. Another short pulse of higher winter inflow occurred from December 2019 to February 2020 while the winter inflow of December 2020–February 2021 was low. The time-series currently stop in April 2021.

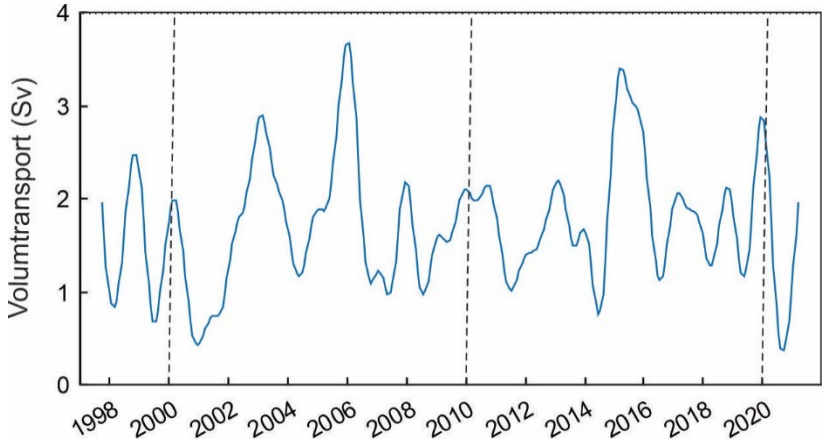

Figure A5.4: Observation-based annual volume flux anomalies (in Sverdrups) through the Fugløya–Bear Island Section from August 1997 to April 2021. The volume flux is calculated for the area 71°15 to 73°45'N, and include all waters flowing inside this area.

Temperature and salinity in standard sections and northern boundary regions

The Fugløya–Bear Island and Vardø–North Sections covers the inflow of Atlantic and Coastal water masses from the Norwegian Sea to the Barents Sea, while the Kola Section covers the same

waters in the southern Barents Sea. Note a difference in the calculation of the temperatures in these sections; in the Fugløya–Bear Island and Vardø–North Sections the temperature is averaged over the 50–200 m depth layer while in the Kola Section the temperature is averaged from 0 to 200 m depth.

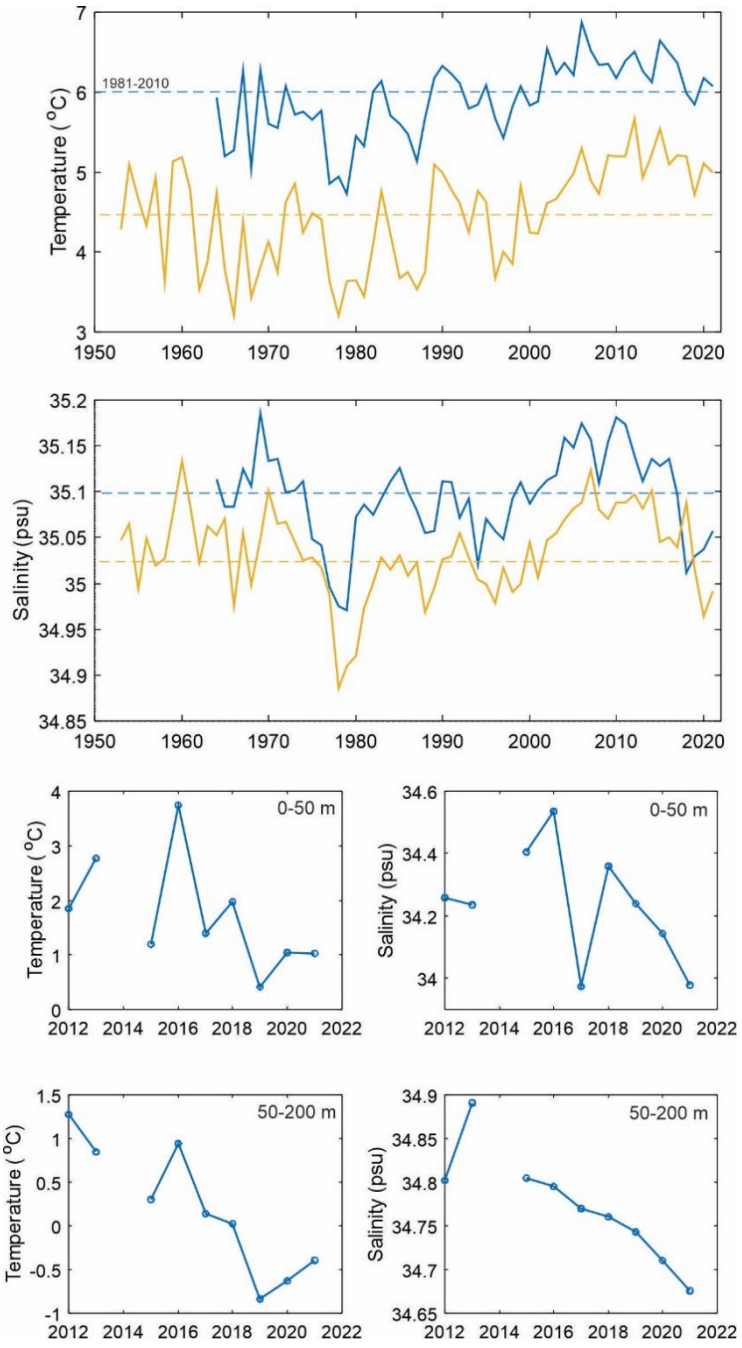

Figure A5.5: Average temperature (top) and salinity (middle) in August–September in the 50–200 m layer in the Fugløya–Bear Island and Vardø–North Sections. Blue lines show Fugløya-Bear Island section, while yellow lines show Vardø–North. Horizontal lines show average over the period 1981–2010. The four lower panels show temperature (left) and salinity (right) at Storbanken (77-78°30N) from the Vardø–North section from 2012.

The inflowing Atlantic Water in the Fugløya-Bear Island and Vardø-North section has warmed by 1.1–1.7°C since the late 1970s, but the warming peaked in 2015–2016 and the temperature has decreased by 0.4–0.5°C after that (Figure A5.5). However, a weak warming was evident in 2020–2021, with temperatures close to, or slightly above, the long term mean (1981–2010). The salinity

in the inflowing Atlantic Water has decreased since 2011, although also salinity has weakly increased in the late few years.

Since 2012, the Vardø-North section has been extended northwards to cover the Barents Sea shelf to 81°N. Time-series calculated for the Storbanken area (77-78°30N) show that this region has cooled considerably in the last years (Figure A5.5). Since the record-warm year of 2016, the temperature at Great Bank has decreased by 2–2.5°C in the surface layer and about 1°C in the 50–200 m water layer.

Temperature of coastal and Atlantic waters in the Kola Section (0–200 m) in 2021 was generally above the long term mean (1981–2010) and typical of warm years (Figure A5.6). At the same time, temperature anomalies decreased northwards from 0.5°C (on average per year) in coastal waters to 0.4°C in Atlantic waters of the Murman Current and to 0.1°C in Atlantic waters of the Central branch of the North Cape Current. Temperature of the Central branch of the North Cape Current in January–May and September–December was close to average, with slightly negative anomalies of −0.1 to −0.2°C in January–March. From early autumn to the end of the year, temperature anomalies were decreasing all over the section. The 2021 annual mean temperature of Atlantic waters (0–200 m) in the Kola Section (central part) was typical of warm years and exceeded the 1981–2010 average by 0.4°C and that in 2020 by 0.1°C (Figure A5.6).

Salinity of coastal and Atlantic waters in the Kola Section (0–200 m) in 2021 was lower than the 1981–2010 average (Figure A5.6). The largest negative anomalies (>0.10 in magnitude) were observed in coastal waters in the first half of 2021, but already in the second half of the year, the salinity approached to the long term mean. In Atlantic waters, salinity anomalies varied insignificantly during the year and equalled −0.07 on average. The 2021 annual mean salinity of Atlantic waters (0–200 m) in the Kola Section (central part) was 0.07 lower than the 1981–2010 average and 0.03 lower than in 2020 (Figure A5.6).

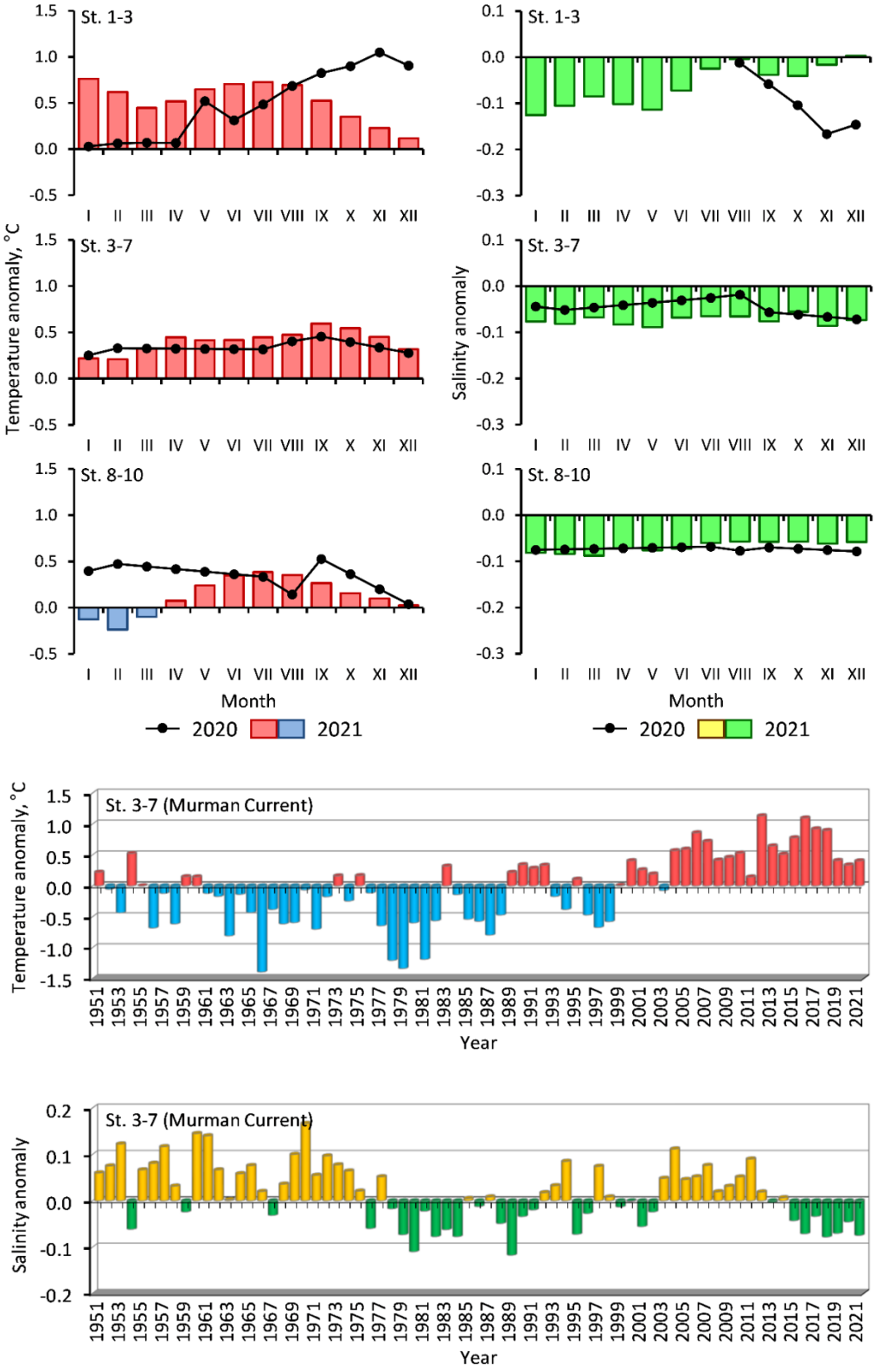

Figure A5.6: Monthly and annual temperature and salinity anomalies in the 0–200 m layer in the Kola Section. St. 1–3 – Coastal waters, St. 3–7 – Murman Current, St. 8–10 – Central branch of the North Cape Current. Annual mean values for 2016–2021 were recovered.

Spatial variation in temperature and salinity (surface, 100 m and bottom)

Sea surface temperature (SST) (http://iridl.ldeo.columbia.edu) averaged over the southwestern (71–74°N, 20–40°E) and southeastern (69–73°N, 42–55°E) Barents Sea was higher than or close to the 1982–2010 average for most of 2021 (Figure A5.7). In the southwest of the sea, significant positive temperature anomalies (0.4–0.8°C) were only observed in January, June, October and November; in the rest of the year, SST was close to average with anomalies of −0.2 to 0.2°C. In the southeast, significant positive anomalies were observed for most of the year with the largest values (>1.0°C) in July–October; SST was close to average only in December and significantly (by 0.6–0.8°C) lower than average in February–March (Figure A5.7). Both SST for most of 2021 and the 2021 annual mean sea surface temperature were lower than in 2020, only in the first half of 2021, SST in the southwestern part of the sea was generally close to that in the previous year (Figure A5.7).

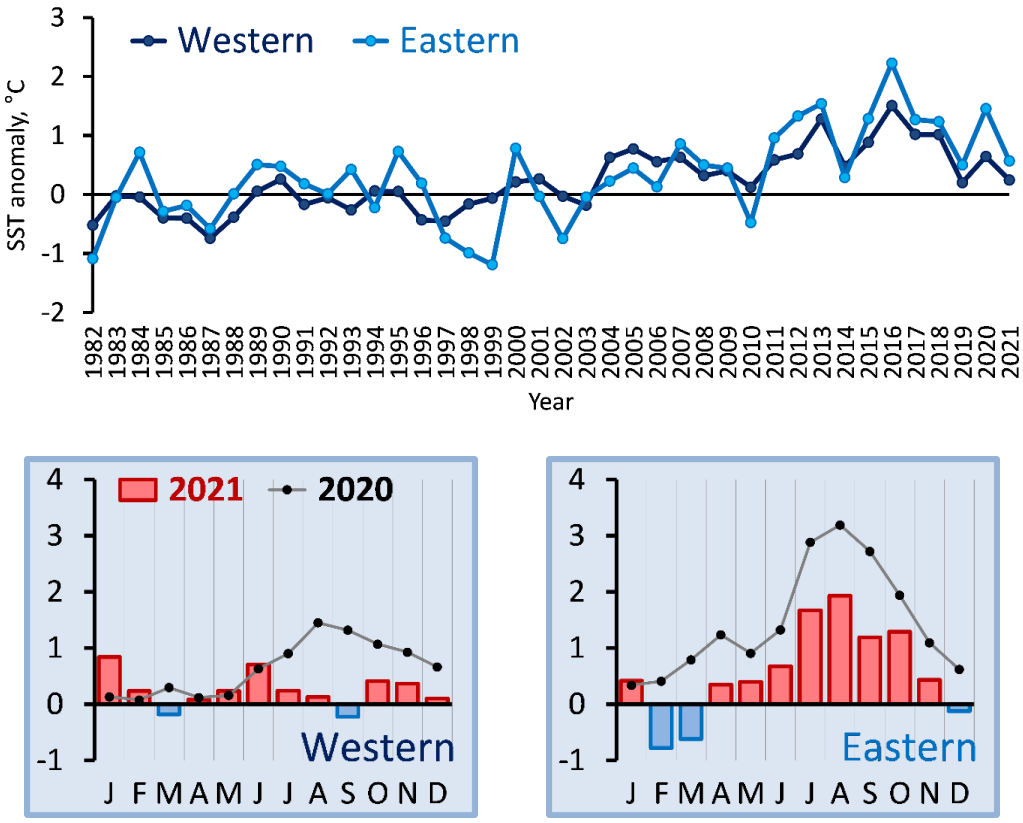

Figure A5.7: Annual (upper) and monthly (lower) sea surface temperature anomalies in the western and eastern Barents Sea.

In August–September 2021, the joint Norwegian-Russian ecosystem survey was carried out in the Barents Sea. Surface temperature was on average 0.7°C higher than the long term mean (1981–2010) in most of the surveyed area (70%), with the largest positive anomalies (>1°C) in the southeastern and northwestern Barents Sea, especially south of the Spitsbergen Archipelago (Figure A5.8). Negative anomalies (about −0.5°C on average) were found in the southwestern and central Barents Sea. Compared to 2020, the surface temperature in 2021 was much lower (by 1.2°C on average) in almost all over the surveyed area (~90%), with the largest negative differences (>2°C in magnitude) in the central and southeasternmost parts of the sea (Figure A5.8). Positive differences in temperature between 2021 and 2020 were found in the northwestern Barents Sea (south of the Spitsbergen Archipelago and around Bear Island).

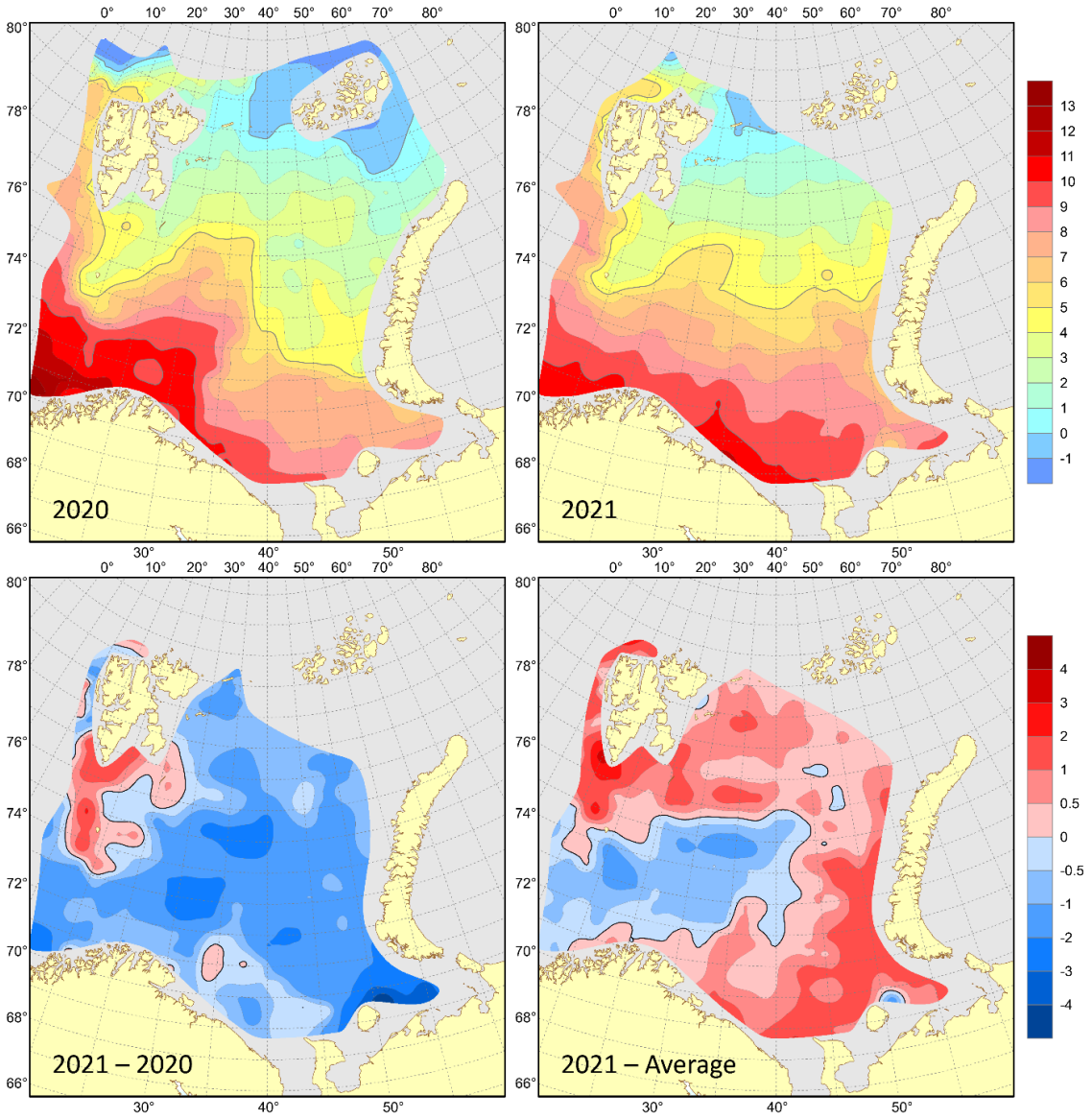

Figure A5.8. Surface temperatures (°C) in August–September 2020 (upper left) and 2021 (upper right), their differences between 2021 and 2020 (lower left, °C) and anomalies in August–September 2021 (lower right, °C).

Arctic waters were mainly found, as usual, in the 50–100 m layer north of 77°N. Temperatures at depths of 50 and 100 m were higher than the long term means (1981–2010) (on average, by 0.8 and 0.5°C, respectively) in about 80% of the surveyed area, with the largest positive anomalies in the east, especially at 50 m depth (Figure A5.9). Negative anomalies (about −0.3°C on average) were mostly found in the northern Barents Sea. Compared to 2020, the 50 and 100 m temperatures in 2021 were higher (on average, by 0.6 and 0.4°C, respectively) in two thirds of the surveyed area; negative differences were observed in some separate areas of the Barents Sea and reached the largest values at 50 m depth (Figure A5.9).

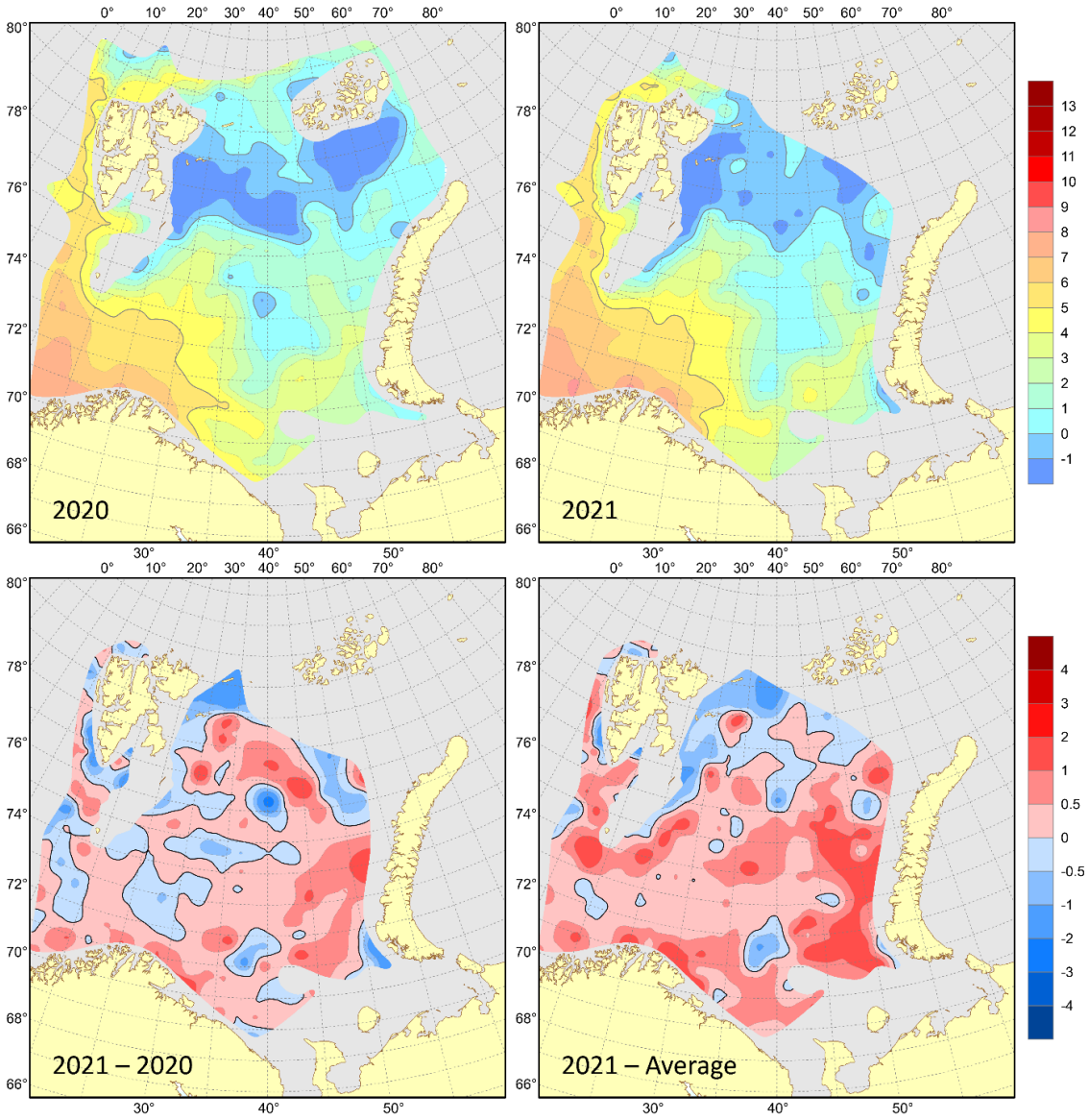

Figure A5.9: 100 m temperatures (°C) in August–September 2020 (upper left) and 2021 (upper right), their differences between 2021 and 2020 (lower left, °C) and anomalies in August–September 2021 (lower right, °C).

Bottom temperature was in general 0.7°C above the 1981–2010 average in three fourths of the surveyed area, with the largest positive anomalies in the southeastern Barents Sea (Figure A5.10). Negative anomalies (−0.5°C on average) were mainly found in the northern part of the sea, especially north of 77°N. Compared to 2020, the bottom temperature in 2021 was on average 0.5°C higher in three fourths of the surveyed area (Figure A5.10). Bottom waters were colder (on average, by 0.5°C) than in 2020 in some separate parts of the sea, with the largest differences in temperature in the southeast.

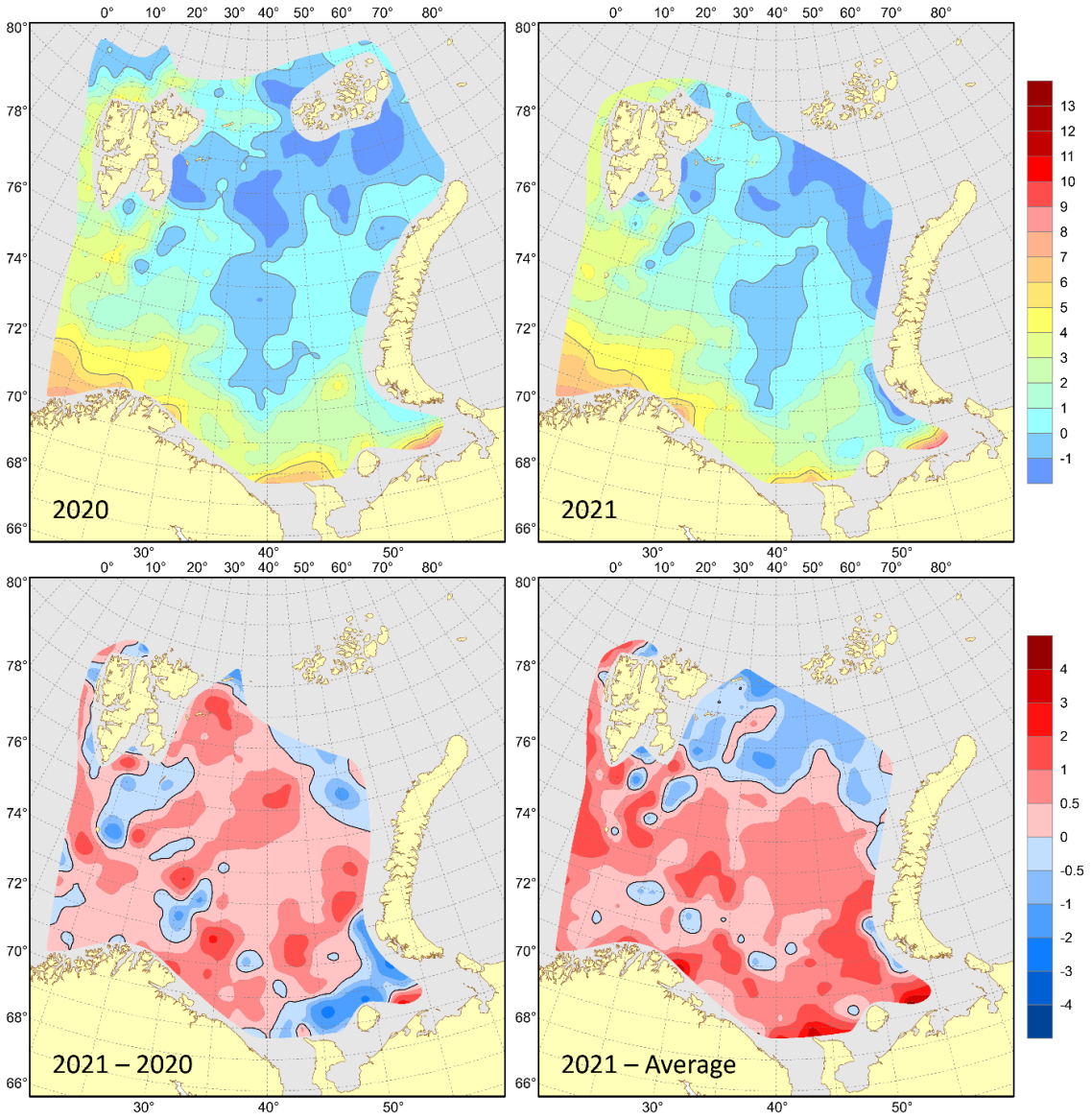

Figure A5.10: Bottom temperatures (°C) in August–September 2020 (upper left) and 2021 (upper right), their differences between 2021 and 2020 (lower left, °C) and anomalies in August–September 2021 (lower right, °C).

Surface salinity was on average 0.3 higher than the 1981–2010 average in 80% of the surveyed area, with the largest positive anomalies (>0.4) in the north and southeast (Figure A5.11). Negative anomalies (–0.1 on average) were observed in the southwestern part of the sea as well as in a small area west of Kolguev Island. In August–September 2021, surface waters were on average 0.2 saltier than in 2020 in about 80% of the surveyed area; they were fresher (on average, by 0.2) mainly in the coastal area of the southwestern Barents Sea as well as east of the Spitsbergen Archipelago and in a small area northwest of Kolguev Island (Figure A5.11).

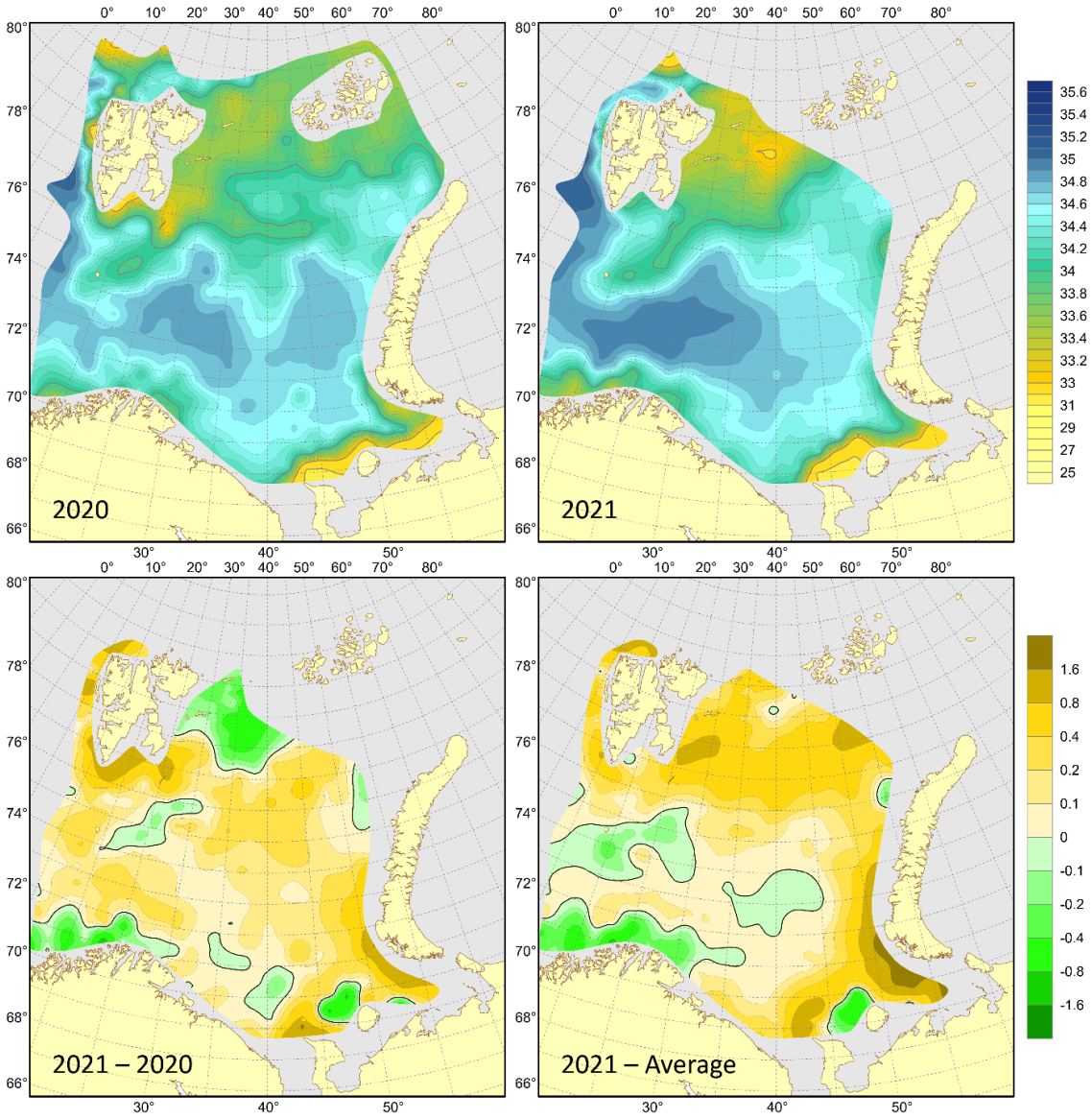

Figure A5.11: Surface salinities in August–September 2020 (upper left) and 2021 (upper right), their differences between 2021 and 2020 (lower left) and anomalies in August–September 2021 (lower right).

Salinity of deeper waters was lower than the 1981–2010 average (by 0.1 on average) in about 60% of the surveyed area at 50 m depth and almost all over the sea (85% of the area) at 100 m depth, with the largest negative anomalies in coastal waters in the southwestern Barents Sea as well as east of Bear Island and around Kolguev Island (Figure A5.12). Positive anomalies were mainly observed in the northwestern part of the sea. In August–September 2021, waters at depths of 50 and 100 m were fresher (by 0.1 on average) than in 2020 in about 55% of the surveyed area, with the largest negative differences in the southeastern Barents Sea and over the Spitsbergen Bank (Figure A5.12). Significant positive differences (>0.1) in salinity between 2021 and 2020 were mainly observed at 50 m depth in some areas between 72 and 76°N. At a depth of 50 m, both positive and negative anomalies and differences were larger than at 100 m depth. At a depth of 100 m, salinity anomalies and differences of less than 0.1 (in magnitude) occupied 88 and 92% of the surveyed area, respectively (Figure A5.12).

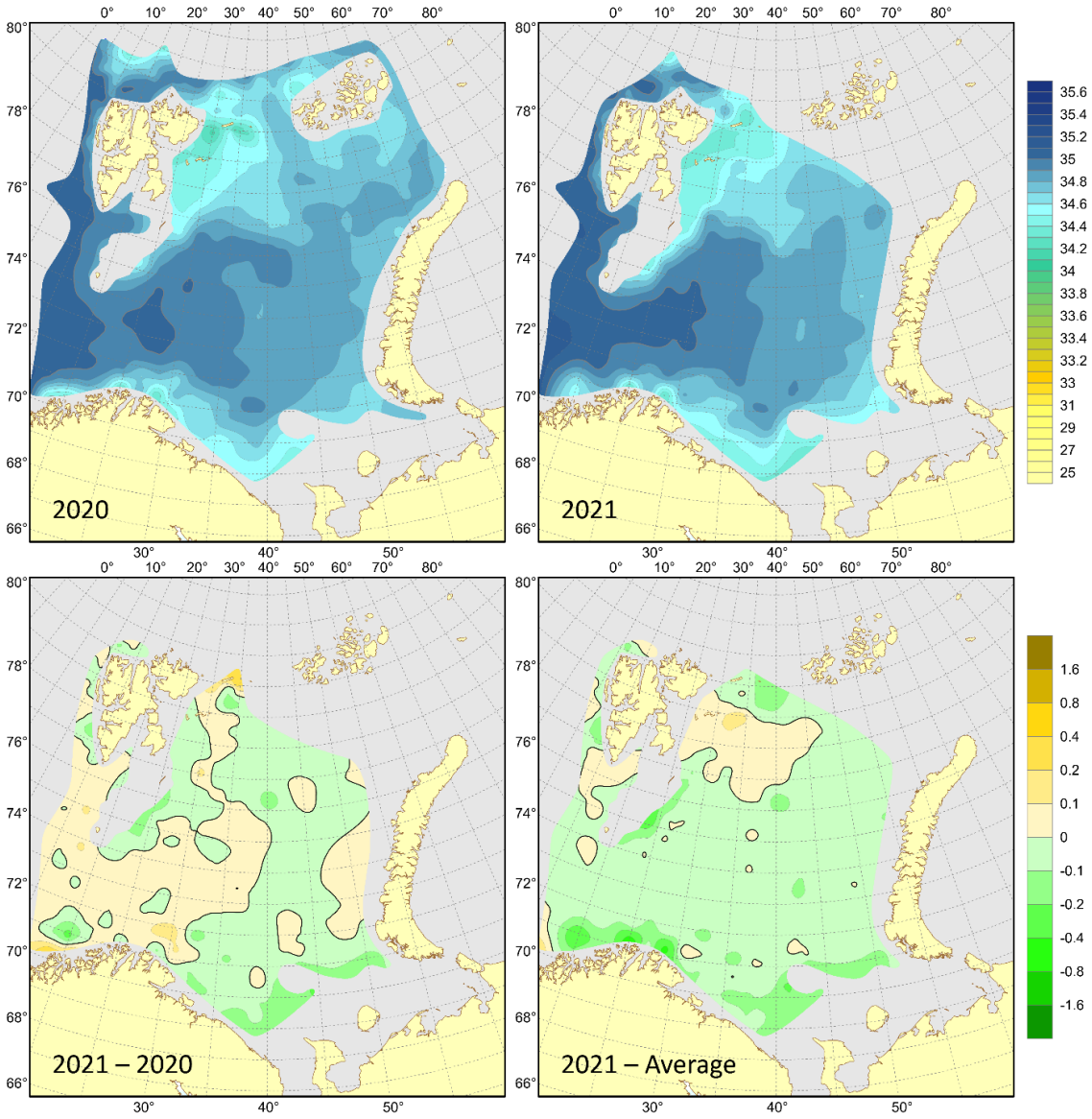

Figure A5.12: 100 m salinities in August–September 2020 (upper left) and 2021 (upper right), their differences between 2021 and 2020 (lower left) and anomalies in August–September 2021 (lower right).

Bottom salinity was slightly lower than the 1981–2010 average almost all over the surveyed area (~90%), with the largest negative anomalies (>0.1 in magnitude) mainly in the northern (some small areas) and southeastern Barents Sea as well as over the Spitsbergen Bank (Figure A5.13). Positive anomalies were found in some areas around the Spitsbergen Archipelago. In August–September 2021, bottom waters were a bit fresher than in 2020 in half of the surveyed area, with the largest negative differences (>0.1 in magnitude) in the southeast (Figure A5.13). These waters were saltier compared to 2020 mainly in the southwestern and eastern Barents Sea as well as east of Bear Island. As a whole, bottom salinity anomalies and differences were small (<0.1 in magnitude) almost all over the surveyed area (83 and 84%, respectively).

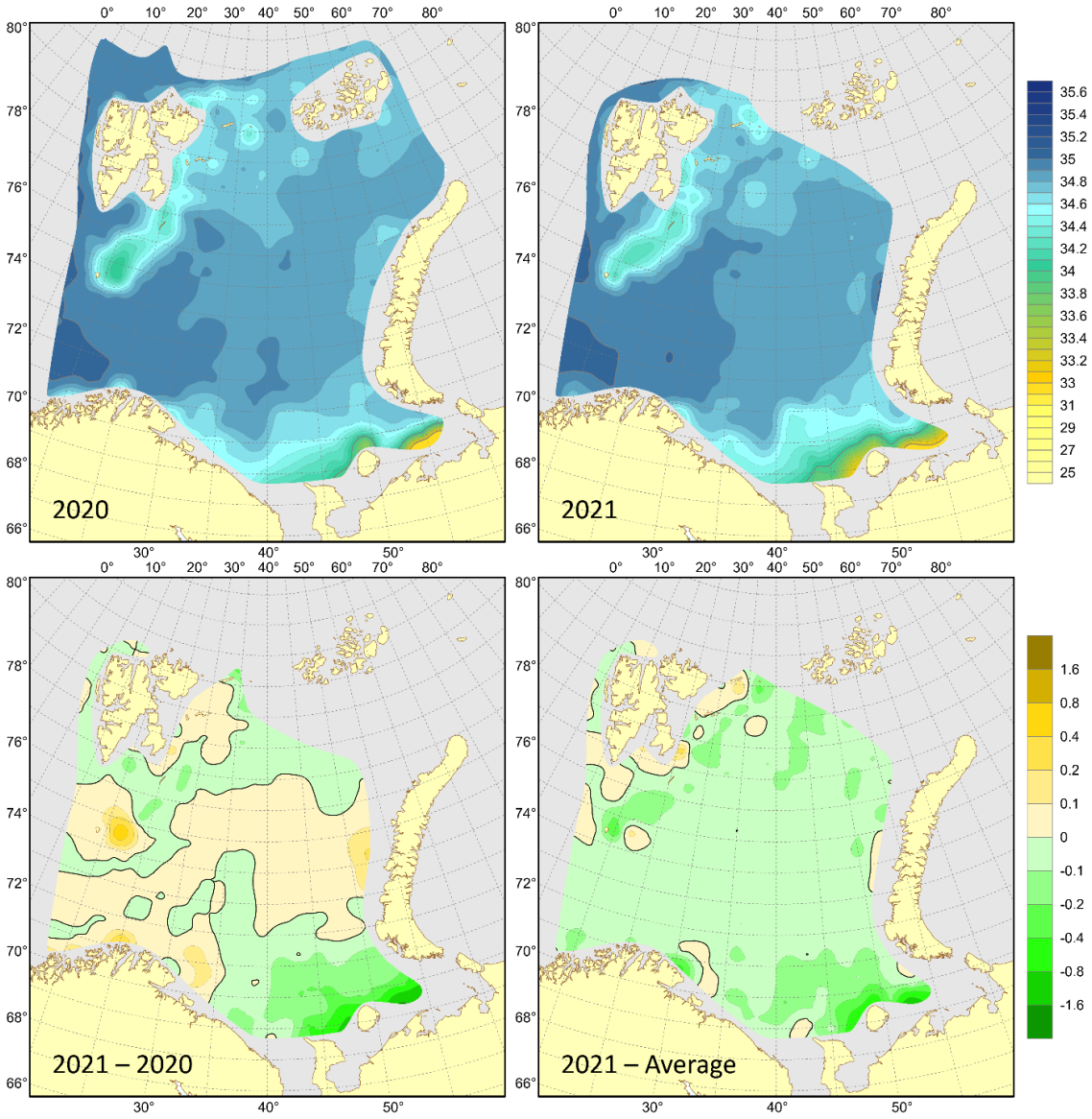

Figure A5.13: Bottom salinities in August–September 2020 (upper left) and 2021 (upper right), their differences between 2021 and 2020 (lower left) and anomalies in August–September 2021 (lower right).

Water masses

In the past decades, the area of Atlantic Waters has increased in the Barents Sea, whereas the area of Arctic Water has decreased (Figure A5.14). The strongest rate of change occurred in the early 2000s, with rapid increases in Atlantic Water area and corresponding reductions in Arctic Water area. The period from 2006–2016 was characterized by a small area of Arctic Water and high variability. After 2016, the Arctic Waters area has increased to comparable amounts as in 2004–2005. The situation in 2021 was much similar as to in 2020. Since 2000, the area covered by cold bottom water was the largest in 2003 and rather small in 2007, 2008, 2012, 2016–2018; in 2016, it reached a record-low value since 1965 and then it has been increasing for the past five years; in 2021, it reached the largest value since 2011 (Figure A5.14).

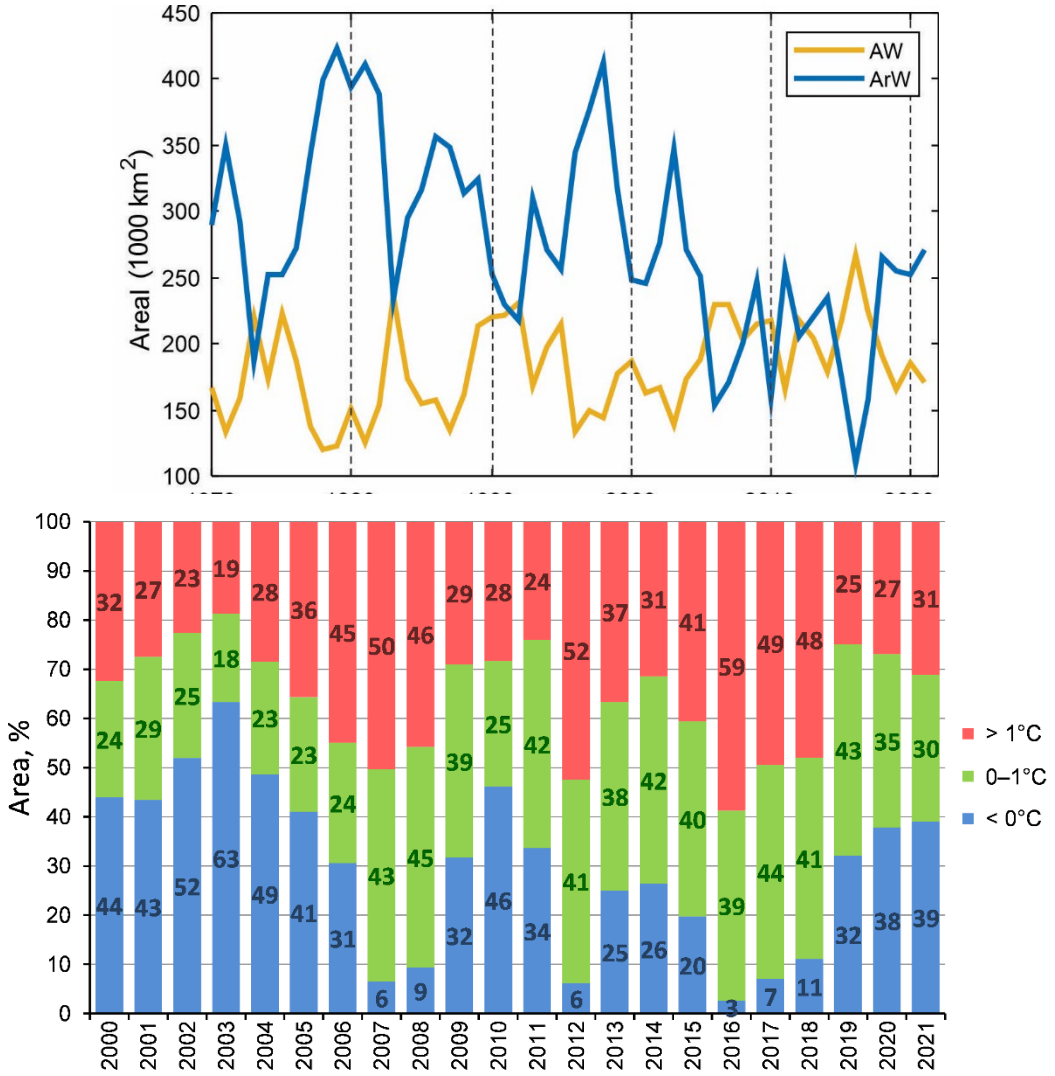

Figure A5.14: Areas covered by Atlantic Water (T>3°C) and Arctic Water (T<0°C) at 50-200 m (72-80°N, 20-50°E) (upper panel), and areas covered by water with different temperatures near the bottom (lower panel) in the Barents Sea (71–79°N, 25–55°E) in August–September 2000–2021.

Phytoplankton and primary production

By Padmini Dalpadado

Although the NPP of the whole Barents Sea showed substantial interannual variability, there was a marked significant increase during the study period, 1998–2021. Average NPP for the whole Barents Sea was much lower in years 1998–2008 than in the more recent decade 2009–2021 (64.8 and 97.1 Tg C, respectively). The NPP in the western and eastern regions of the Barents Sea increased significantly during the study period, the increase in the northeastern region was up to 5 times larger compared to the southwestern region.

The primary production is the foundation of the life in the Barents Sea ecosystem. The rich and diverse plankton community in the ecosystem sustains some of the world's largest demersal fish stocks such as cod (*Gadus morhua*) and haddock (*Melanogrammus aeglefinus*) as well as pelagic stocks such as capelin (*Mallotus villosus*) (ICES, 2018)

Estimated NPP for the Barents Sea demonstrated large interannual variability with the year 2021 showing a decreasing level compared to the two preceding ones. The NPP trends however display a doubling of production during the last 24 years likely related to ice-free conditions leading to more open water area and duration of the production period (updated dataseries from Dalpadado *et al.*, 2020). Concurrently, with the warming conditions in the Barents Sea and related ice loss, the shorter but intense under ice algae production will decrease including associated biological diversity (sympagic fauna).

The phytoplankton development in the Barents Sea is typical for a high latitude region with a pronounced maximum in biomass and productivity during spring. During winter and early spring (January–March), both phytoplankton biomass and productivity are quite low. The spring bloom is initiated during mid-April to mid-May and may vary strongly from one year to another. The bloom duration is typically about 3–4 weeks, and it is followed by a reduction of phytoplankton biomass mainly due to the exhaustion of nutrients and grazing by zooplankton. Later in autumn when the increasing winds start to mix the upper layer and bring nutrients to the surface, a short autumn bloom can be observed. However, the temporal development of this general description can vary geographically. The spring bloom in the Atlantic water domain without sea ice is thermocline-driven, whereas in the Arctic domain with seasonal sea ice, stability from ice-melt determines the timing of the bloom (Skjoldal and Rey 1989, Hunt *et al.* 2012). Thus, the spring bloom at the ice-edge in the Barents Sea can sometimes take place earlier than in the southern regions due to early stratification from ice melting.

Satellite data

Remote sensing data having high spatial and temporal resolution were used in obtaining Chl *a* concentration (mg m^{-3}) and mean daily NPP (g C m^{-2} day^{-1}). Daily net primary production (NPP) and open water area (OWA) were calculated from satellite data as described in detail in Arrigo and Van Dijken (2015). Satellite-derived surface Chl *a* (Sat Chl *a*, Level 3, 8 days binned) was based on SeaWiFS and MODIS/Aqua sensors. SeaWiFS was used in 1998–2002, and MODIS/Aqua in 2003–2021. Data were updated using NASA's latest reprocessing - version R2018.0. For the years where data were available for both sensors (2003–2007), SeaWiFS Chl was consistently higher than MODIS/Aqua Chl. Therefore, we used a correction factor for SeaWiFS Chl to create a comparable 24-year time-series. The values for the Southeast and Pechora polygons were recalculated excluding the regions most influenced by river inflow (18% and 41% of the total area, respectively). The work presented here (c.f. Dalpadado *et al.,* 2020), was made in collaboration with Professor Kevin Arrigo and Gert van Dijken from the Stanford University, USA

Validation of satellite Chl *a* using *in situ* data showed significant correlations between the two variables in the Barents Sea (Dalpadado *et al.* 2014, ICES/WGIBAR 2017) and thus, the NPP model based on satellite data by Arrigo *et al.* (2015) gives reasonable results that compare well with sea ground truthing measurements. Also, estimates of new production from phytoplankton based on nitrogen consumption (seasonal draw-down of nitrate in the water column) for the Fugløya - Bear Island (FB) and Vardø-Nord (VN) sections, representing the western and central Barents Sea respectively, from March to June resulted in values comparable to satellite NPP estimates (Rey *et al.* pers. com.).

Spatial and temporal patterns of Chl a in spring

Remote sensing data, providing good spatial and temporal coverage, were used to explore the seasonal and interannual variability of Chl *a* distribution. Satellite data from the Barents Sea during 2016–2018 showed large interannual variability with the highest Chl *a* concentration

generally observed in May (Figure A5.15). There was much less sea ice in 2016, and a north- and eastward expansion of the Chl *a* distribution. Furthermore, earlier blooming and higher concentrations in the eastern regions in April and May were observed this year. 2017 was a colder year with more ice especially compared to 2016. Chl *a* was much lower during April to July in 2017 compared to the previous year. The ice cover was larger in April 2017 and 2018, than in 2016. Though the Chl *a* in April in 2018 was lower compared to 2016, high concentrations were observed in May for both years.

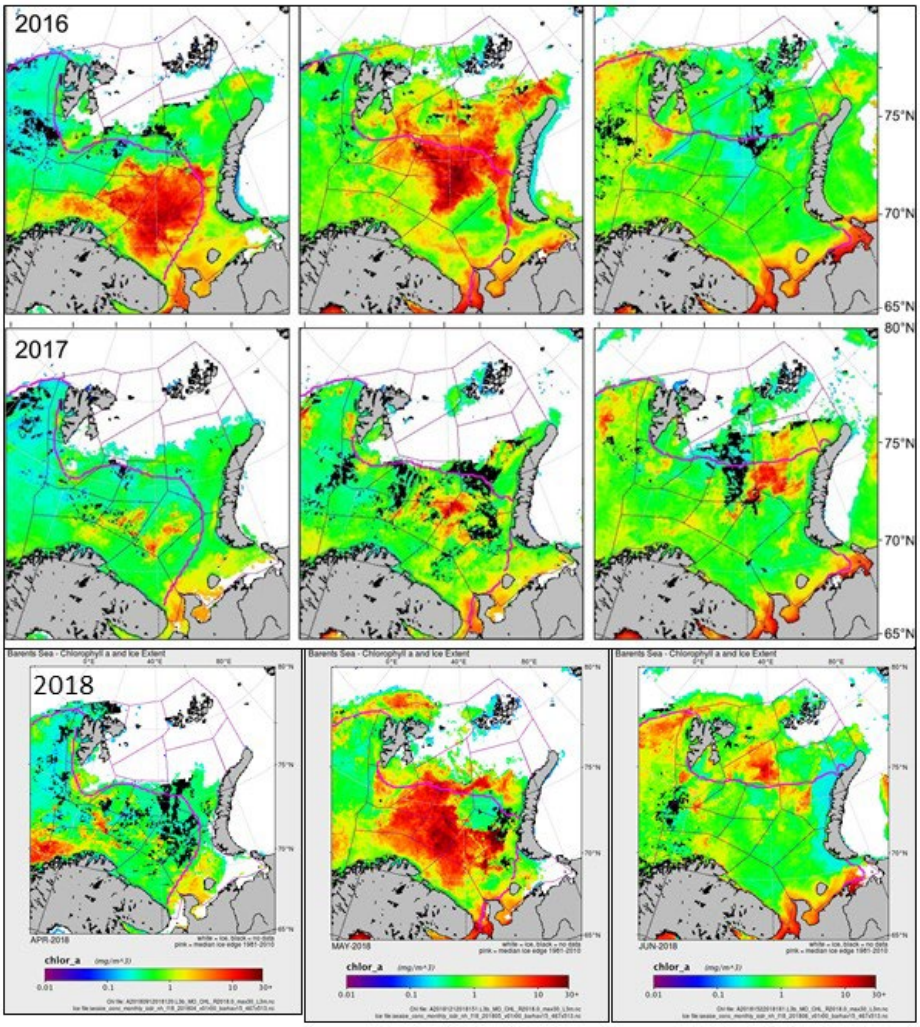

Figure A5.15. Spatial distributions of Chl *a* (mg m^{-3}) in April, May and June for 2016, 2017 and 2018. White areas indicate ice coverage. The black areas indicate no data. The pink lines show the climatological (average 1981–2010) position of the ice edge.

Net Primary Production (NPP)

Although the NPP of the whole Barents Sea showed substantial interannual variability, there was a marked significant increase during the study period, 1998–2021 (Figure A5.16, $p = 0.001$). Average NPP for the whole Barents Sea was much lower in years 1998–2008 than in the more recent decade 2009–2021 (64.8 and 97.1 Tg C, respectively). The NPP in the western and eastern regions of the Barents Sea increased significantly during the study period ($p < 0.01$), the increase in the northeastern region was up to 5 times larger compared to the southwestern region.

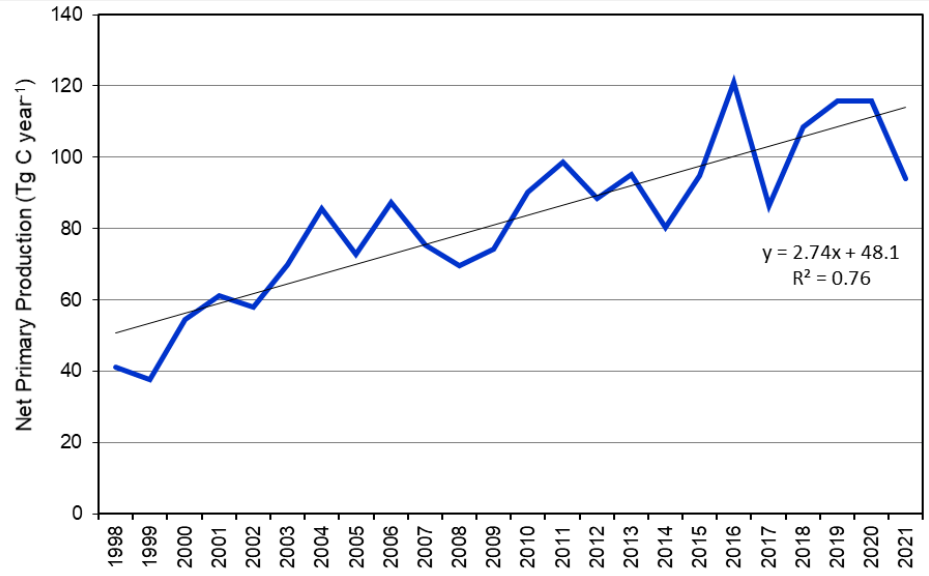

Figure A5.16: Annual net primary production (satellite based NPP) for the whole Barents Sea.

References

Arrigo K.R. and van Dijken G. (2015). Continued increases in Arctic Ocean primary production. Progress in Oceanography 136:60-70

Dalpadado P., Arrigo, A.R., Hjøllo, S., Rey, F. Ingvaldsen R.B., Sperfeld, E. Dijken G.L.V, Olsen, A., Ottersen, G. (2014). Productivity in the Barents Sea - response to recent climate variability. PLoS ONE 9(5):e95273 doi:10.1371/journal.pone.0095273

Dalpadado P, Arrigo KR, van Dijken GL, Skjoldal HR, Bagøien E, Dolgov A, Prokopchuk I, Sperfeld E (2020). Climate effects on temporal and spatial dynamics of phytoplankton and zooplankton in the Barents Sea. Progress in Oceanography 185,102320.

ICES 2018. Report of the Arctic Fisheries Working Group, Ispra, Italy, 16–24 April 2018.

ICES C.M. 2018/ACOM:06, 857pp.

Hunt G.L., Blanchard A.L., Boveng P., Dalpadado P., Drinkwater K., Eisner L., Hopcroft R., Kovacs K.M., Norcross B.L., Renaud P., Reigstad M., Renner M., Skjoldal H.R, Whitehouse A., Woodgate R. A 2012. The Barents and Chukchi Seas: Comparison of two Arctic shelf ecosystems. Journal of Marine Systems: 43-68

Sakshaug E., Johnsen G., Kristiansen S. et al (2009). Phytoplankton and primary production. 2009. In Ecosystem Barents Sea. Eds. Sakshaug E, Johnsen G, Kovacs K. Tapir Academic Press, Norway. pp: 167-208

Skjoldal, H.R., Rey, F., 1989. pelagic production and variability of the Barents Sea ecosystem. In: Sherman, K., Alexander, L.M. (Eds.), Biomass yields and geography of large marine ecosystems, AAAS Selected Symposium, vol. 111. Westview Press, pp. 241–286.

Zooplankton

Mesozooplankton biomass and species abundances

Mesozooplankton biomass – large-scale distributions

By Espen Bagøien (IMR), Irina Prokopchuk (PINRO), Padmini Dalpadado (IMR), Jon Rønning (IMR)

Mesozooplankton play a key role in the Barents Sea ecosystem by transferring energy from primary producers to organisms higher up in the foodweb. Geographic large-scale patterns for mesozooplankton biomass show similarities across years, despite some interannual variability. During August–September 2021, relatively high biomass levels (>10 g dry wt. m^{-2}) were observed just north of the Norwegian mainland at the Bear Island Trench, northeast of Svalbard/Spitsbergen, and in the deeper part of the central-eastern Barents Sea (Figure A5.17). Low biomass levels (<4 g dry wt. m^{-2}) were observed southeast of Svalbard including the Great and Central Banks and the Hopen Deep, as well as in the regions farthest east near Novaya Zemlya and north of the eastern part of Kola (Figure A5.17). The overall large-scale horizontal distribution of plankton in the Barents Sea during August–September 2021 resembled that in 2020.

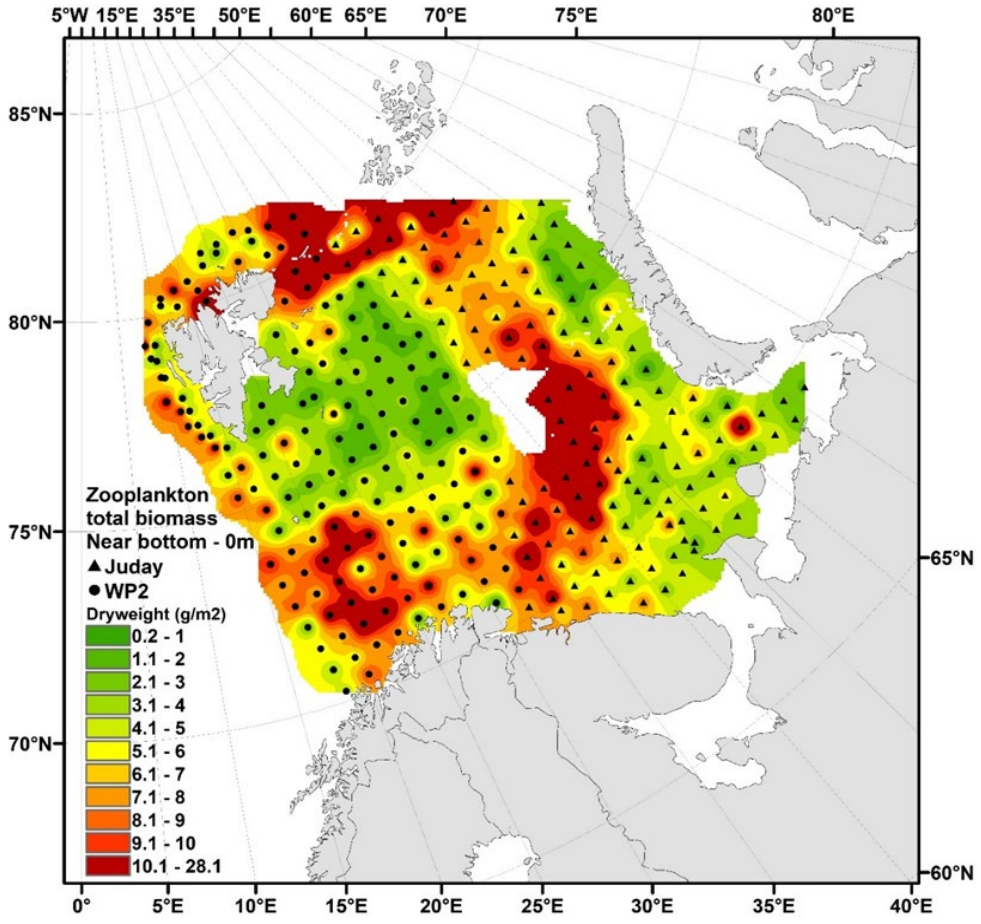

Figure A5.17: Distribution of total mesozooplankton biomass (g dry wt. m^{-2}) from near seabed to surface. Data based on 319 samples collected during BESS from 13. Aug–30. Sep 2021. A WP2 net was applied by IMR and a Juday net by PINRO, both nets with mesh-size 180 µm. Interpolation made in ArcGIS v.10.6.1, module Spatial Analyst, using inverse distance weighting (default settings).

In the Norwegian sector of the Barents Sea, mesozooplankton biomass was size-fractionated by filtering the wet samples through a series of 3 sieves with decreasing mesh-size (2000, 1000, and 180 µm), thereafter dried at 60°C and weighed (see time-series in Figure A5.18). The average biomass for the smallest size-fraction in 2021 (2.1 g dry wt. m^{-2}) was below the 20-year long term average for 2001–2020. (2.5 g dry wt. m^{-2}). Likewise, the average for the intermediate size-fraction in 2021 (2.9 dry wt. m^{-2}) was lower than the 20-year long term average, (3.5 g dry wt. m^{-2}). For the largest size-fraction, the values during the last ca. 13 years have typically been lower than in earlier years. However, no marked differences in biomass were seen when comparing the 2021 value with the 20-year long term average (0.9 vs. 1.0 g dry wt. m^{-2}).

Based only on Norwegian data, average zooplankton biomass (sum of all size-fractions) during August–September 2021 was 5.9 (SD 4.4, N= 171) g dry wt. m^{-2} for the whole western part of the Barents Sea (Figure A5.18 - red filled circles). This estimate is lower than in 2020 (6.7 g dry wt. m^{-2}), and below the long term (2001–2020) average (7.0 g dry wt. m^{-2}). Note that the number of stations west and northwest of Svalbard in 2021 was somewhat higher than usual in earlier years and compared to the rest of survey area.

In the Russian sector, average biomass for the area covered in 2021 was 6.7 (SD 4.5, N=148) g dry wt. m^{-2} (Figure A5.18). This is not directly comparable to the average for the Russian area covered in 2020, 6.8 (SD 3.7) g dry wt. m^{-2}. The reason for this is differences in the geographical sampling areas, including the area around Franz Joseph Land in 2020, where high biomasses are typically observed.

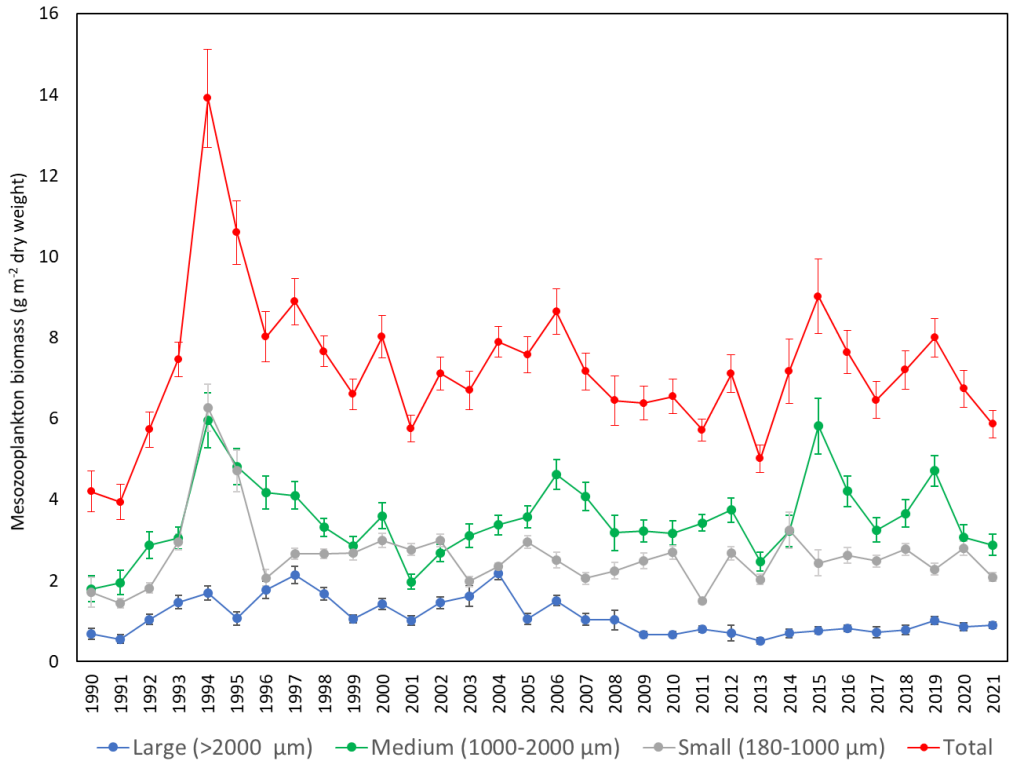

Figure A5.18: Time-series of average annual mesozooplankton biomass (WP2 net, 180 µm) from close to the seabed to surface (g dry wt. m^{-2}) within the western and central Barents Sea (i.e. the Norwegian sector) during the autumn BESS (1990–2021). Standard errors shown as vertical bars.

Zooplankton biomass varies between years and is believed to be partly controlled by predation pressure from pelagic fish, mainly capelin. However, the impact of predation varies geographically. Predation from other planktivorous pelagic fish (herring, polar cod, and blue whiting) and pelagic juvenile demersal fish species (cod, haddock, saithe, and redfish), and larger plankton

forms (e.g. chaetognaths, amphipods and gelatinous plankton) can also affect the mesozooplankton in the Barents Sea. In addition, processes such as advective transport of plankton from the Norwegian Sea into the Barents Sea, changes in primary production and local production of zooplankton are likely to contribute to the variability of zooplankton biomass.

Methodological factors such as differences in geographical survey coverage between years, and to some extent also uneven spatial sampling density, can contribute to the variability of estimated average biomass between years. Hence, time-series on mesozooplankton biomasses within well-defined and consistent subareas (spatial polygons - see Figure A5.19) are evaluated in the following section.

Mesozooplankton biomass in spatial polygons of the Barents Sea

By Padmini Dalpadado (IMR), Espen Bagøien (IMR), Irina Prokopchuk (PINRO)

Zooplankton were collected at 148 stations with Juday net and 171 stations with WP2 (Figure A5.17 and Figure A5.19) during the BESS 2021 survey. Biomass trends were explored region-wise, within the 15 ICES WGIBAR polygons. The WP2 and Juday nets provide comparable results with respect to mesozooplankton biomass and species (Skjoldal *et al.* 2019). The Norwegian biomass samples are dried before weighing, while the Russian samples are preserved in 4% formalin and their wet weight measured. Dry-weight is then estimated by dividing the wet-weight with a factor of 5. The data from WP2 and Juday were grouped together in the following evaluation.

Total zooplankton biomass – based on combined data from IMR and PINRO

Average biomass in 2021 was calculated for each polygon (Figure A5.19). The number of observations in 2021 were between 13 and 42 in 13 out of 15 polygons, while the two remaining polygons had 0 and 4 observations (Table A5.2). Time-series for annual biomass averages within each of four westerly polygons (Southwest, Bear Island Trench, Svalbard South, Hopen Deep), three bank polygons in the central region (Thor Iversen Bank, Central Bank and Great Bank), and four polygons in the eastern Barents Sea (Southeast, Southeastern Basin, Pechora and Northeast) are shown in Figure A5.20.

Since 2002 the biomass for the three western polygons Southwest, Bear Island Trench, and Hopen Deep have mostly fluctuated between ~ 5-15 g dw m^{-2}, with the levels typically being highest for the Bear Island Trench (Figure A5.20, upper panel). The fourth western polygon, Svalbard South, displayed some annual averages somewhat lower than 5 g dw m^{-2}. For the Bear Island Trench, Hopen Deep and Svalbard South polygons, the average biomass was lower in 2021 than 2020, and generally also well below the preceding 5-year and 19-year averages. The Southwest polygon, however, showed a similar biomass in 2021 as 2020, and did not show a clear trend over the 20-year period. The 2021-average for Southwest was lower than the preceding 5-year average but slightly above the preceding 19-year average. During the last two decades, the biomasses within these western polygons have displayed considerable year-to-year variability without consistent long-term trends, although with a tendency of decreased levels for Svalbard South was noted during the last 6 years.

The biomass for the Central Bank, Great Bank and Thor Iversen Bank have shown declining trends since the early 2000s, reaching minima around year 2013 (Figure A5.20, middle panel).

The biomass then increased for all three banks, with the time-series for Thor Iversen and Central Banks displaying maxima during 2017-2019, and thereafter falling to lower levels. On the Great Bank, the biomass remained low somewhat longer, showing a peak value in 2019, and rapidly declining again. Since 2006, the annual average biomass has been higher on Thor Iversen Bank than the Central and Great Banks. For the Thor Iversen and Central Banks, the average biomass in 2021 was somewhat higher than in 2020, while for the Great Bank the biomass was lower in 2021. All three banks showed lower 2021-biomass than for the preceding 5-year and 19-year averages (note that only 4 observations for Thor Iversen Bank in 2016). In the northern polygon Franz-Victoria Trough, just east of Svalbard (not shown in Figure A5.20), the 2021 biomass average was just slightly above the preceding 5-year and 19-year averages (excluding 4 years with very few observations from the latter - see Table A5.2)

For the four eastmost polygons, Southeast, Southeastern Basin, Pechora and Northeast, the biomass has typically shown strong interannual variability but not clear or consistent trends over the last two decades (Figure A5.20, lower panel). Note that for these eastern polygons, some years have few biomass observations (see Table A5.2). The overall picture is that the average biomasses within the polygons Southeast, Southeastern Basin and Pechora in 2021 were similar to the levels observed during the preceding 5 years as well as over the last 19 years (considering only years with $N \geq 5$), while for the Northeast polygon the 2020 and 2021 levels were on the low side compared to earlier years (Figure A5.20, lower panel).

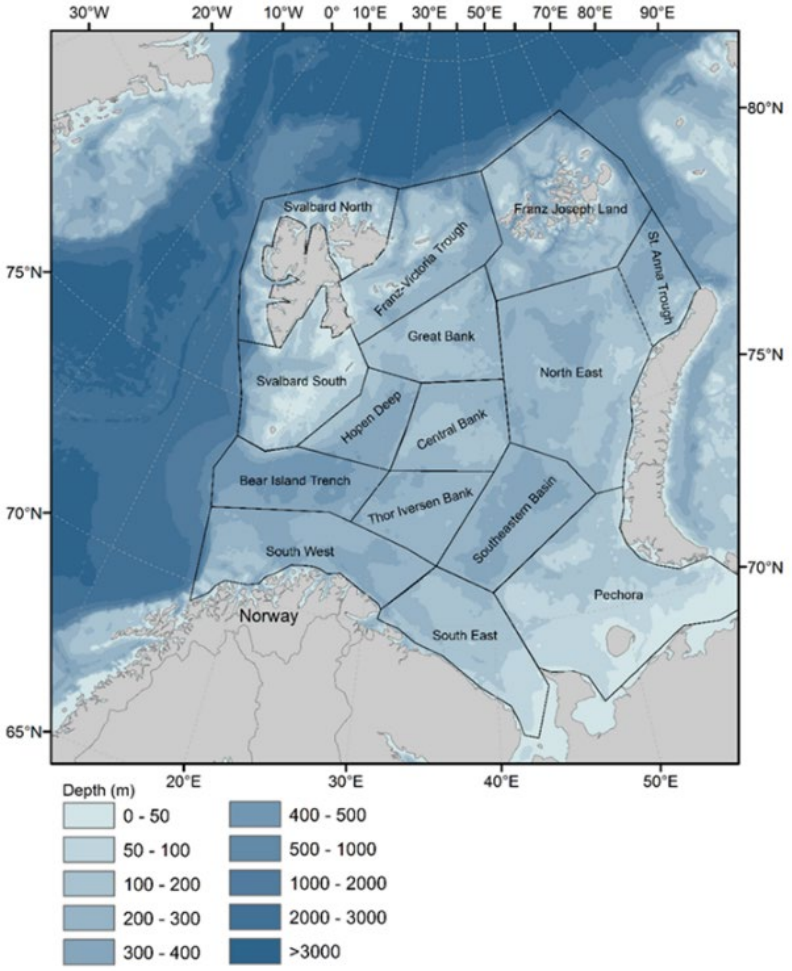

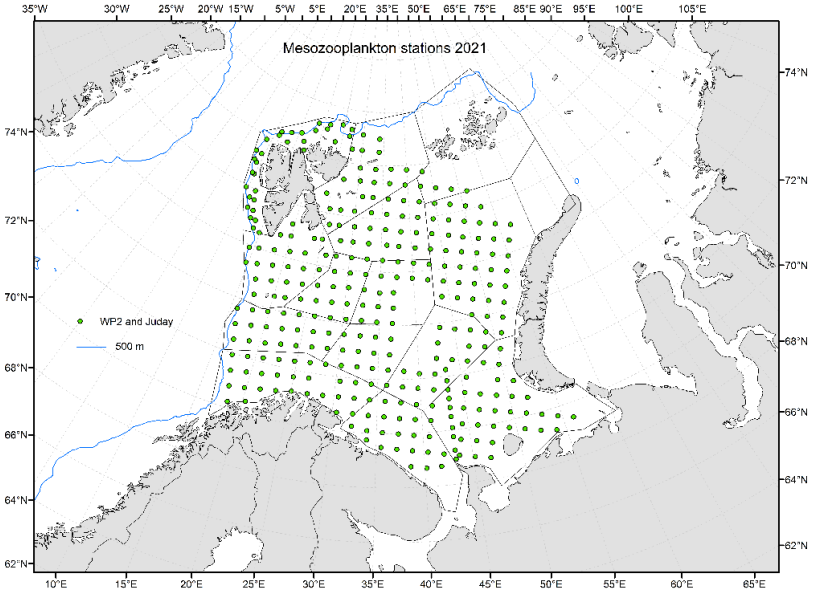

Figure A5.19: Upper panel: The ICES WGIBAR polygons. Lower panel: Zooplankton sampling stations at the joint ecosystem survey in autumn 2021.

Table A5.2. Number of biomass samples per polygon per year. Comprises Norwegian WP2 and Russian Juday nets hauled vertically from near bottom to surface. Based on sampling during the annual joint Norwegian-Russian Barents Sea ecosystem cruise during Aug–early Oct.

	South West	Bear Island Trench	Hopen Deep	Svalb. South	Svalb. North	Thor Iversen Bank	Central Bank	Great Bank	Franz-Victoria Trough	South East	Pechora	South-eastern Basin	North East	Franz Joseph Land	St.Anu Troug
2002	19	15	16	17	0	12	15	20	15	0	14	14	33	1	1
2003	19	11	10	16	0	11	8	5	1	1	0	1	4	0	0
2004	32	24	23	24	2	19	18	30	31	6	18	14	26	1	7
2005	26	19	16	6	0	16	17	13	2	0	0	3	6	1	0
2006	42	26	33	34	0	30	23	34	7	24	0	6	27	0	0
2007	31	16	19	25	0	16	20	17	12	11	11	12	21	8	6
2008	21	11	8	6	0	12	20	15	2	10	21	20	19	9	2
2009	29	17	16	23	30	15	20	21	14	16	4	12	20	5	8
2010	31	21	15	28	11	16	18	23	27	1	21	10	23	12	3
2011	31	18	20	20	15	21	21	22	30	10	23	14	25	5	1
2012	31	22	17	25	12	16	20	23	37	10	21	15	26	7	0
2013	26	20	14	23	19	15	20	21	35	10	19	14	26	12	3
2014	15	11	12	14	26	10	16	17	1	11	21	13	25	6	0
2015	16	9	14	14	13	11	13	24	24	9	19	13	27	6	3
2016	24	16	15	20	17	4	20	21	21	1	25	10	21	4	0
2017	27	19	15	22	18	13	17	17	29	6	17	10	28	8	0
2018	28	19	14	17	11	12	17	15	21	3	2	2	10	2	0
2019	28	19	15	25	19	14	22	18	18	10	20	13	8	2	0
2020	29	19	15	24	37	18	15	20	30	11	16	15	46	25	13
2021	29	19	15	24	32	13	16	19	24	21	42	21	41	4	0

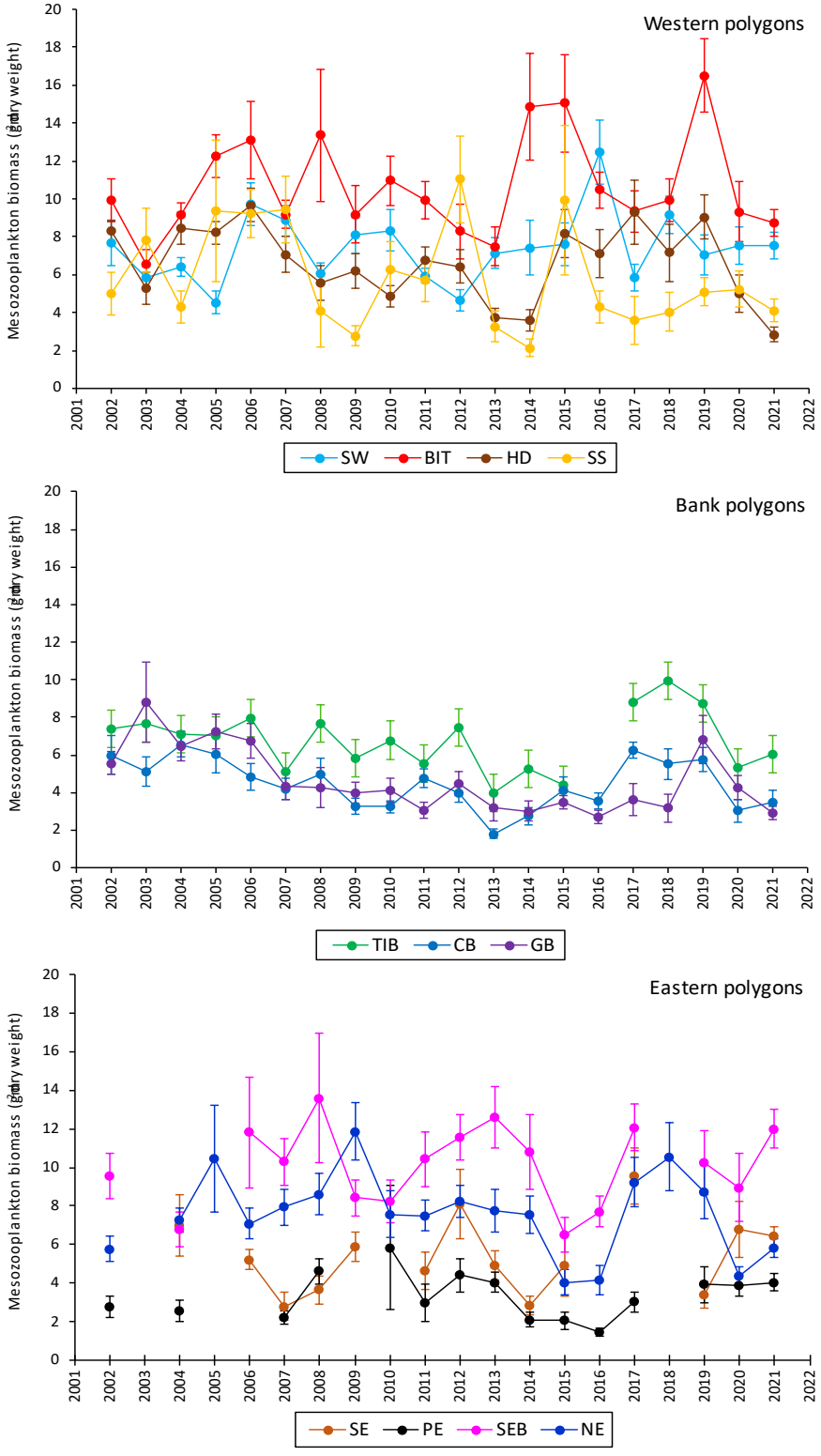

Figure A5.20: Time-series 2002-2021 for annual average zooplankton biomass (g dry wt. m^{-2}) with standard errors within different subareas (spatial polygons) of the Barents Sea. Only averages representing at least 5 observations per polygon per year are shown in the figure – averages representing fewer observations are omitted (see Table A5.2). Upper panel – four subareas in the western Barents Sea: Southwest (SW), Bear Island Trench (BIT), Hopen Deep (HD) and Svalbard South (SS). Middle panel – three subareas in the central Barents Sea: Thor Iversen Bank (TIB), Central Bank (CB) and Great Bank (GB). Lower panel – four subareas in the eastern Barents Sea: Southeast (SE), Southeastern Basin (SEB), Pechora (PE) and Northeast (NE). The results represent total zooplankton biomass from near seabed to surface, as collected with WP2 or Juday plankton nets, both with mesh-size 180 µm.

Zooplankton biomass in size fractions

In the Norwegian part of the Barents Sea, IMR determines zooplankton biomass collected with WP2 net for three size-fractions. In summary, the sieve with mesh-size 2 mm will generally retain large copepods like *Calanus hyperboreus* and *Paraeuchaeta* sp., to some extent older stages of the smaller *Calanus glacialis,* as well as krill, amphipods, large chaetognaths, etc. (Skjoldal 2021). The sieve with mesh-size 1 mm will typically hold back older stages of intermediately sized copepods like *Calanus finmarchicus*, *C. glacialis* and *Metridia* sp. Finally, small copepod species like *Oithona*, *Oncaea*, *Microcalanus* and *Pseudocalanus* and young copepodite stages of intermediately sized copepod species such as *C. finmarchicus* and *C. glacialis,* along with appendicularians and meroplanktonic invertebrates, will mostly be retained on the sieve with the smallest mesh-size (0.18 mm).

Time-series for size-fractioned biomass during August–September 1989–2021 were evaluated for selected polygons representing the western inflow region for Atlantic water, as well as bank areas in the central Barents Sea that are influenced by Arctic water. Here we briefly summarize the highlights, starting with the westmost Atlantic water influenced polygons (trends for size-fractioned biomass on polygon level are not shown). For polygon Southwest, no interannual trends were clear except for the large size-fraction where the biomass is indicated to be lower since about 2008, though with a higher biomass again in 2021. For the Bear Island Trench, a decreasing trend in biomass for the largest size-fraction was observed during about 1998–2014, after which the level has stabilized or increased slightly. However, the biomass for the intermediate size-fraction (typically representing copepods of intermediate size – as older stages of *Calanus finmarchicus*) was notably lower than normal in both 2020 and 2021. For the Hopen Deep polygon, no long-term trends are evident. Still, the biomass for the small as well as large size-fraction were on the low side in 2021, and clearly low for the intermediate size-fraction in both 2020 and 2021. For Thor Iversen Bank, located just east of Bear Island Trench and also influenced by Atlantic water, no consistent strong trends were observed. It is worth mentioning that the biomass for the intermediate size-fraction was rather low in both 2020 and 2021. For the Central Bank and Great Bank, both located in the central Barents Sea and influenced by Arctic water, a considerable year-to-year variation as well as generally decreasing long-term trends for all size-fractions were observed. For the Great Bank, the biomass in 2021 was rather low for the intermediate size-fraction, while for the Central bank the biomass was markedly low for the small and intermediate size-fractions in both 2020 and 2021, and for the large size-fraction in 2021.

Mesozooplankton species-composition along the Fugløya - Bear Island and the Kola transects

By Irina Prokopchuk, Espen Bagøien, Padmini Dalpadado, Jon Rønning

The zooplankton display strong seasonal cycles at high latitudes. The number of individuals and their developmental state will change throughout the year. Hence, the time of sampling in the season is a very important factor when evaluating zooplankton time-series.

The Fugløya - Bear Island (FB) transect, crossing the western entrance to the Barents Sea, is generally monitored by IMR 5–6 timer per year, covering the different seasons. Up to eight stations with fixed positions are sampled during each coverage, although the number may vary depending on weather conditions. Zooplankton samples collected each year during the 1995–2021 period from four fixed locations at different latitudes (70°30′N, 72°00′N, 73°30′N, and 74°00′N) and representing different water masses (Coastal, Atlantic, and mixed Atlantic/Arctic) have been analysed taxonomically. Average annual abundance for each of the species *C. finmarchicus, C.*

glacialis and *C. hyperboreus* is estimated by pooling the four stations throughout the seasonal cycle and summing up the copepodite stages I-VI (Figure A5.21, left). The arcto-boreal species *C. finmarchicus* is, by far, the most common of these three species (Skjoldal *et al*., 2021), and displays some interannual variation in abundance. *C. finmarchicus* tends to be most abundant at the three southernmost stations. A particularly high abundance was recorded during 2010 along most of the transect, except at the northernmost station. Except for 2013, *C. finmarchicus* has generally been abundant along most of the transect until 2019. However, during the two last years, exceptionally low average abundances of *C. finmarchicus* were registered along the Fugløya-Bjørnøya section (Figure A5.21). The 2020 and 2021 averages were the lowest since the time-series was started in 1995. 2020 comprised only 4 coverages of the transect, as the planned March cruise was cancelled due to the COVID-19 situation. Both the May and August abundances of this species in 2020 were very low compared to what is typical for those parts of the season in earlier years. The above-mentioned low *C. finmarchicus* abundances were supported by a remarkably low FB zooplankton biomass (8 stations) in May 2020 compared to this month in other years, while also in August 2020 the biomass was much lower than typical for that month. Only 4 full coverages of the FB section were made in 2021 (March, April, August, and December). The stations closest to the Norwegian coast showed unusually low values in March and April, while all four stations displayed abundances much lower than the average for August. Lack of coverage in May or June, the most productive period, has most likely contributed to the low average estimated for 2021. The FB abundances of *C. finmarchicus* during the next years will be followed closely to see if the low abundances registered these two last years are becoming a recurring feature.

The Arctic species *C. glacialis* has typically been most abundant at the two northern-most stations, representing Atlantic (73°30'N) and mixed Atlantic-Arctic waters (74°00'N). This species also shows some interannual variation in abundance, particularly in the late 1990s (Figure A5.21, left). Abundance of *C. glacialis* along the FB transect has decreased since the initial years of this time-series (1995–1998), with very low abundance recorded in some years since 2005, including 2021. The abundance of the large and Arctic species, *C. hyperboreus*, along the FB transect has been low relative to the abundance of *C. finmarchicus*, but generally also compared to *C. glacialis* throughout the study period. Few individuals of this species have been recorded for some years since 2008, although the levels have not been particularly low during the very last years. The FB time-series of *C. hyperboreus* abundance shows a clear interannual variability (Figure A5.21, left).

Calanus helgolandicus, a more southerly species, is observed regularly at the Fugløya - Bear Island transect, particularly during the December–February period (Dalpadado *et al.,* 2012). Even in winter, the abundance of *C. helgolandicus* along the FB transect seldom surpasses a few hundred individuals per square meter. This species is common in the North Sea but is also observed in the Norwegian Sea off mid-Norway, particularly in autumn (Continuous Plankton Recorder survey, Strand *et al.* 2020). Our FB time-series provides no evidence of an increase over the years, neither of the proportion or absolute abundance of *C. helgolandicus.*

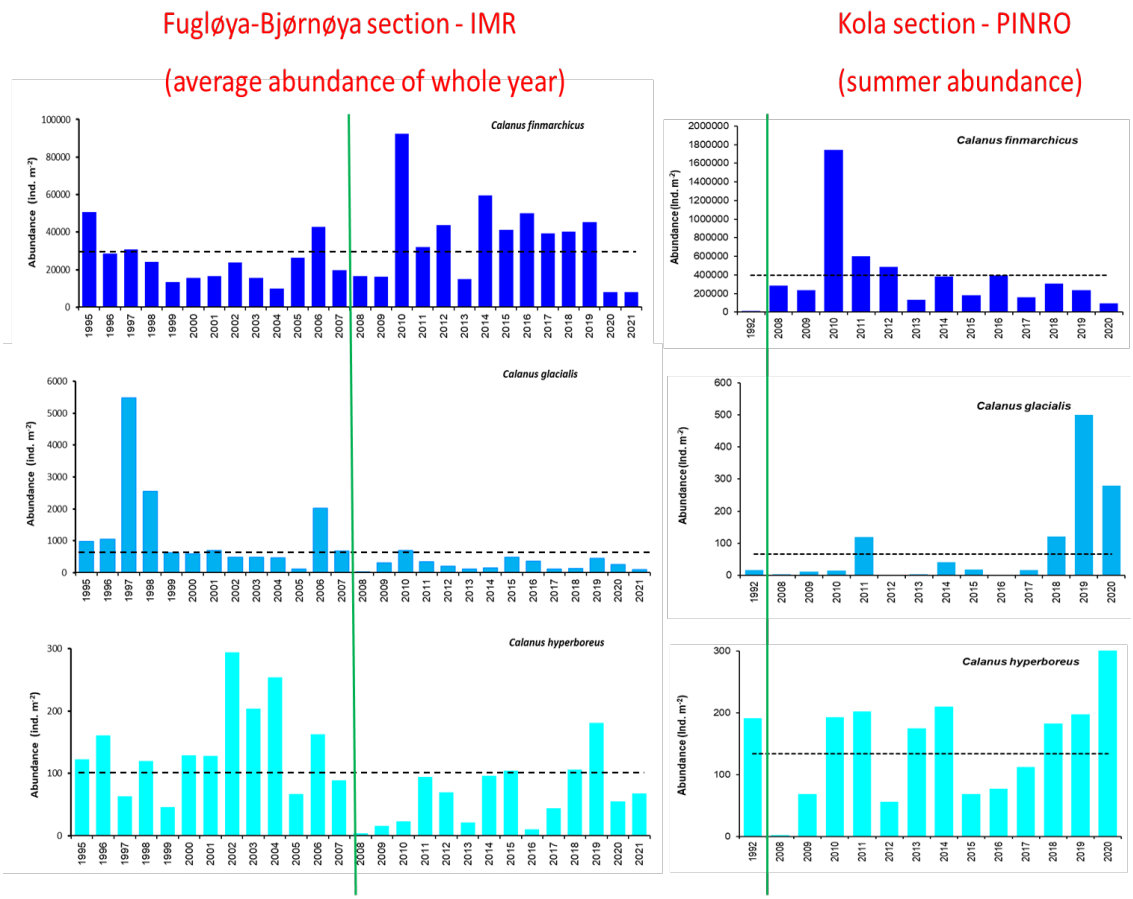

Figure A5.21: Time-series of abundances (ind. m^{-2}) of *Calanus finmarchicus, C. glacialis,* and *C. hyperboreus* along the Fugløya-Bjørnøya (1995–2021) (left) and Kola (1992, 2008-2020) (right) transects. Note that for the FB transect, each bar represents the annual average for 4 stations and mostly 5–6 coverages per year, while for the Kola transect the data show early-summer abundances – hence these data are not directly comparable. Also, be aware of the strongly differing scales for abundances between the two transects and the species. The right-hand sides from the vertical green lines show the same years for the two transects. Dotted horizontal lines indicate the long term averages for the different species, 1995–2021 for the FB section and 1992, and 2004–2020 for the Kola section. *Calanus finmarchicus* was present in low abundances at the Kola section in 1992 even if this is hard to see in the figure.

Russian (PINRO) investigations along the Kola section in July 2020 showed copepods as the dominant group of zooplankton at that time, comprising on average 87% in abundance and 81% in biomass, and *C. finmarchicus* as the dominant species. Average abundance of *C. finmarchicus* in 2020 was ca. 41% of 2019 value, and ca. 25% of the long term average (Figure A5.21, right). The highest abundance of *C. finmarchicus* was observed at 70º30'N, 72°00'N and 72°30'N at the stations influenced by Atlantic waters, while its lowest abundance was observed at the station at 73°00'N. In the *C. finmarchicus* population, individuals belonging to copepodite stages CIV-CV dominated at all the stations, while copepodite stages CI-CIII were present at the three northern stations.

The abundance of the Arctic species *C. glacialis* showed a considerable increase since 2018. However, its average abundance in 2020 was ca. 56% of the 2019 estimate, but 4.2 times higher than the long term average (Figure A5.21, right). Previously, *C. glacialis* mainly occurred at the most northern stations, while in 2020 it was observed at 8 stations, and its abundance increased northwards. Only copepodites of stage CV were observed for this species.

Average abundance of the arctic species *C. hyperboreus*, the largest *Calanus* species in the Barents Sea, in 2020 was 1.6 times higher than in 2019 and exceeded the long term average by a factor of 2.3 (Figure A5.21, right). A gradual increase in *C. hyperboreus* abundance has been observed since

2015. The highest abundance of this species in 2020 was observed at 73°30′ N and 74°00′ N, the two northernmost stations of the transect, and the population was represented by copepodites CIV-CVI.

Species composition from the autumn ecosystem cruise

By Irina Prokopchuk

PINRO investigations of mesozooplankton conducted by the BESS during August–September 2019 showed that in the Russian part, copepods dominated both in abundance (79.5%) and biomass (69.5%) (Figure A5.22). Total zooplankton abundance in the southern (south of ca. 75°N) Barents Sea was higher than in the northern part (north of ca. 75°N) of the sea (2 190 and 1 725 ind. m^{-3}, respectively), while the total zooplankton biomass was about twice as high in the northern as the southern Barents Sea (286.9 and 143.9 mg m^{-3}, respectively). However, the results from the northern Barents Sea are not quite comparable with previous years as only 13 stations were conducted in the northern part of the sea in 2019.

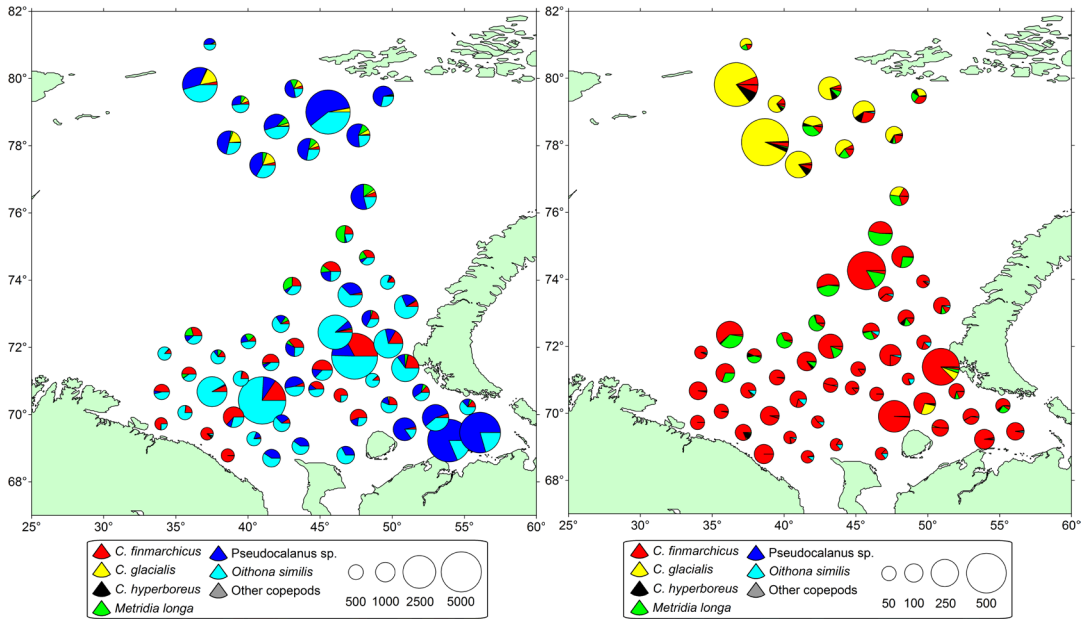

Figure A5.22: Abundance (ind. m^{-3}) (left) and biomass (wet-weight, mg m^{-3}) (right) of the most numerous copepod species (surface to sea floor) in the Barents Sea (based on the PINRO samples from the BESS during August-September of 2019)

In the southern Barents Sea, total zooplankton abundance and biomass in 2019 had increased by factors 1.7 and 1.1, respectively, compared with 2018. Copepods dominated both abundance and biomass (76.8 and 70.6%, respectively). Among other groups, the most important were chaetognaths comprising 16.6% of total zooplankton biomass, while their abundance was very low (0.2%). Considering species composition of copepods, *Oithona similis*, *C. finmarchicus* and *Pseudocalanus* sp. were the most abundant (43.4, 23.2 and 15.9% of total copepod abundance, respectively), and *Metridia longa* comprised 3.5% (Figure A5.22). However, in terms of copepod biomass, *C. finmarchicus* (63.7%), *Pseudocalanus* sp. (14.4%) and *M. longa* (9.4%) were the most important species, while *O. similis* comprised only 3.0% (Figure A5.22). In 2019, abundance of *C. finmarchicus*, *O. similis* and *Pseudocalanus* sp. had increased compared to 2018, while increase of biomass was observed only for *Pseudocalanus* sp. and *O. similis*. It is necessary to point out, in 2019 plankton was collected on 46 stations, while in 2018 only on 9 stations, so that the results for 2018 and 2019 should be compared with caution.

In the northern Barents Sea, total zooplankton abundance in 2019 was ca. 87% of the 2018 value, while total biomass increased by a factor of 1.2 in 2019 compared with 2018. Copepods were the most abundant (89.2% of total zooplankton abundance) zooplankton group. Regarding total zooplankton biomass, copepods (64.7%) also represented the most important group during 2019, while chaetognaths and pteropods comprised 15.6 and 11.2%, respectively. In the northern Barents Sea, the small copepods *Pseudocalanus* sp. and *O. similis* were the most abundant (42.6 and 31.7% of total copepod abundance, respectively) (Figure A5.22). Total copepod biomass consisted mainly of larger *C. glacialis* (56.8%) and *M. longa* (15.8%), and of small *Pseudocalanus* sp. (12.8%) (Figure A5.22). Abundance and biomass of *C. glacialis* have been increasing since 2015. Abundance and biomass of *C. finmarchicus*, *M. longa* and *Pseudocalanus* sp. increased in the period from 2016 to 2018 and in 2019 it decreased. At the same time, the abundance and biomass of *O. similis* have been decreased from 2016 to 2018, and its increase was observed in 2019.

References

Strand E, Bagøien E, Edwards M, Broms C, Klevjer T (2020). Spatial distributions and seasonality of four *Calanus* species in the Northeast Atlantic. Progress in Oceanography. 185, 102344.

Dalpadado P, Ingvaldsen RB, Stige LC, Bogstad B, Knutsen T, Ottersen G, Ellertsen B (2012). Climate effects on Barents Sea ecosystem dynamics. – ICES Journal of Marine Science, 69: 1303-1316.

Skjoldal HR, Prokopchuk I, Bagøien E, Dalpadado P, Nesterova V, Rønning J, Knutsen T (2019). Comparison of Juday and WP2 nets used in joint Norwegian-Russian monitoring of zooplankton in the Barents Sea. Journal of Plankton Research 41:759-769.

Skjoldal HR (2021). Species composition of three size fractions of zooplankton used in routine monitoring of the Barents Sea ecosystem. Journal of Plankton Research, Vol. 43: 762–772.

Macroplankton biomass and distribution

Krill

Krill (euphausiids) represents the most important group of macrozooplankton in the Barents Sea, followed by hyperiid amphipods. Krill plays a significant role in the Barents Sea ecosystem, facilitating transport of energy between different trophic levels. There are mainly four species of krill in the Barents Sea; *Thysanoessa inermis* primarily associated with the Atlantic boreal western and central regions, whereas the neritic *Thysanoessa raschii* mainly occurs in the southeastern Barents Sea. These two species can reach 30 mm in length. *Meganytiphanes norvegica,* the largest species (up to 45 mm) is mainly restricted to typical Atlantic waters. The smallest of the species, the oceanic *Thysanoessa longicaudata* (up to 18 mm), is associated with the inflowing Atlantic water.

Winter distribution and abundance

By Irina Prokopchuk (PINRO), Ksenia Zaytseva (PINRO), Anna Mikhina (PINRO), Andrey Dolgov (PINRO)

Figures by Ksenia Zaytseva (PINRO) and Irina Prokopchuk (PINRO)

The PINRO long-term dataseries on euphausiids was initiated in 1959 and terminated in 2016 (Figure A5.23). A new time-series on euphausiids has been launched in February–March 2015 in the course of the Joint Barents Sea winter survey.

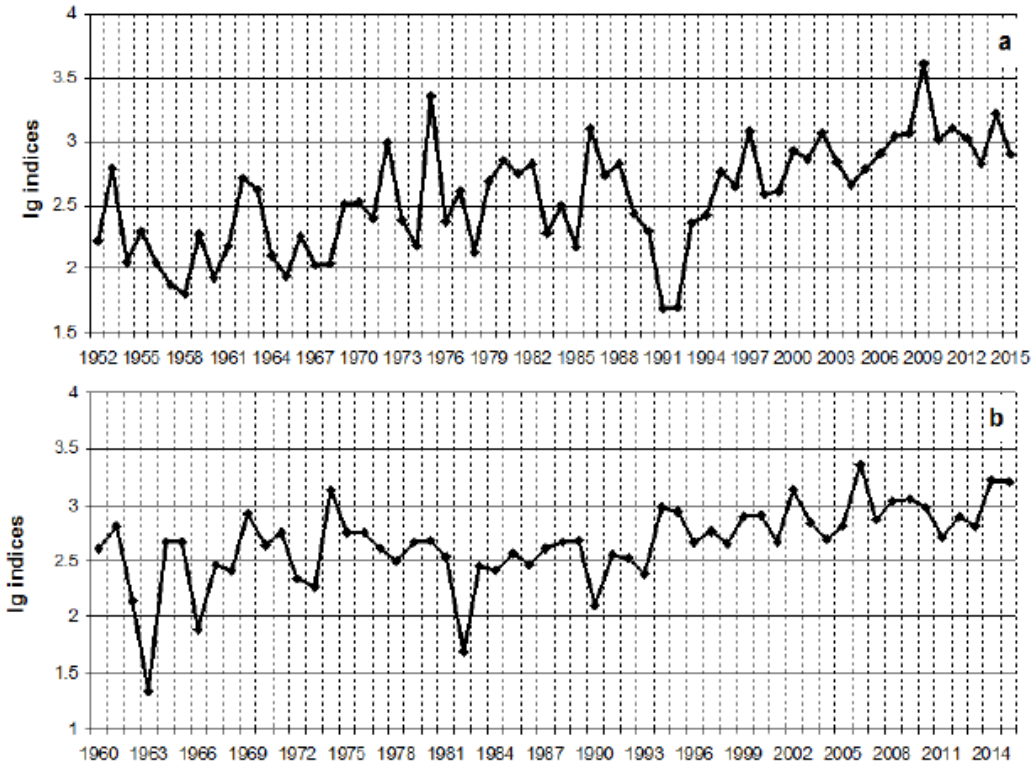

Figure A5.23: Abundance-indices of euphausiids (log10 of number, ind. 1000 m^{-3}) based on trawl-attached plankton net catches in the near–bottom layer of the Barents Sea from the Russian winter survey during October–December 1959–2015. a) Southern Barents Sea; and b) Northwestern Barents Sea. Note that these dataseries were discontinued in 2016 but are presented here to show the general trends since the early 1950s and 1960s.

Euphausiids were collected in the southeastern Barents Sea in February 2021 during the Russian-Norwegian winter survey using a trawl-attached plankton net. Since in a course of the survey different areas were covered in different years (2015–2020), comparison with previous years requires caution.

Distribution of euphausiids in the southeastern Barents Sea in February 2021 is presented in Figure A5.24. Total abundance of euphausiids in 2021 had decreased to ca. 41% of the 2020 abundance. Average abundance of euphausiids in 2021 (755 ind. 1000 m^{-3}) was lower than in previous years (2015–2020 average – 1212 ind. 1000 m^{-3}). In 2021, the average euphausiid abundance decreased in all the subareas. However, at one station of the eastern subarea the extremely high total euphausiid abundance of 18440 ind. 1000 m^{-3} was observed. This resulted in an increased average abundance, making interannual comparison difficult, and thus this extreme value was excluded from the analysis.

Euphausiids were traditionally represented by local species *Thysanoessa inermis* and *T. raschii*, as well as by Atlantic species *Meganyctiphanes norvegica* and *T. longicaudata*. Two last-mentioned species penetrate into the Barents Sea with warm Atlantic waters from the Norwegian Sea. Another warm-water species *Nematoscelis megalops*, which had been regularly registered in the coastal, western and central areas since 2003, except 2020, was again observed in four subareas of the Barents Sea in 2021. *T. inermis* is the most numerous species and comprised 60–70% of total euphausiid abundance in the southeastern Barents Sea and in 2021 *T. inermis* comprised 74% of total euphausiid abundance. In 2021, the abundances of *T. inermis*, *T. raschii* and *T. longicaudata* had decreased considerably compared to 2020, while that of *M. norvegica* had increased.

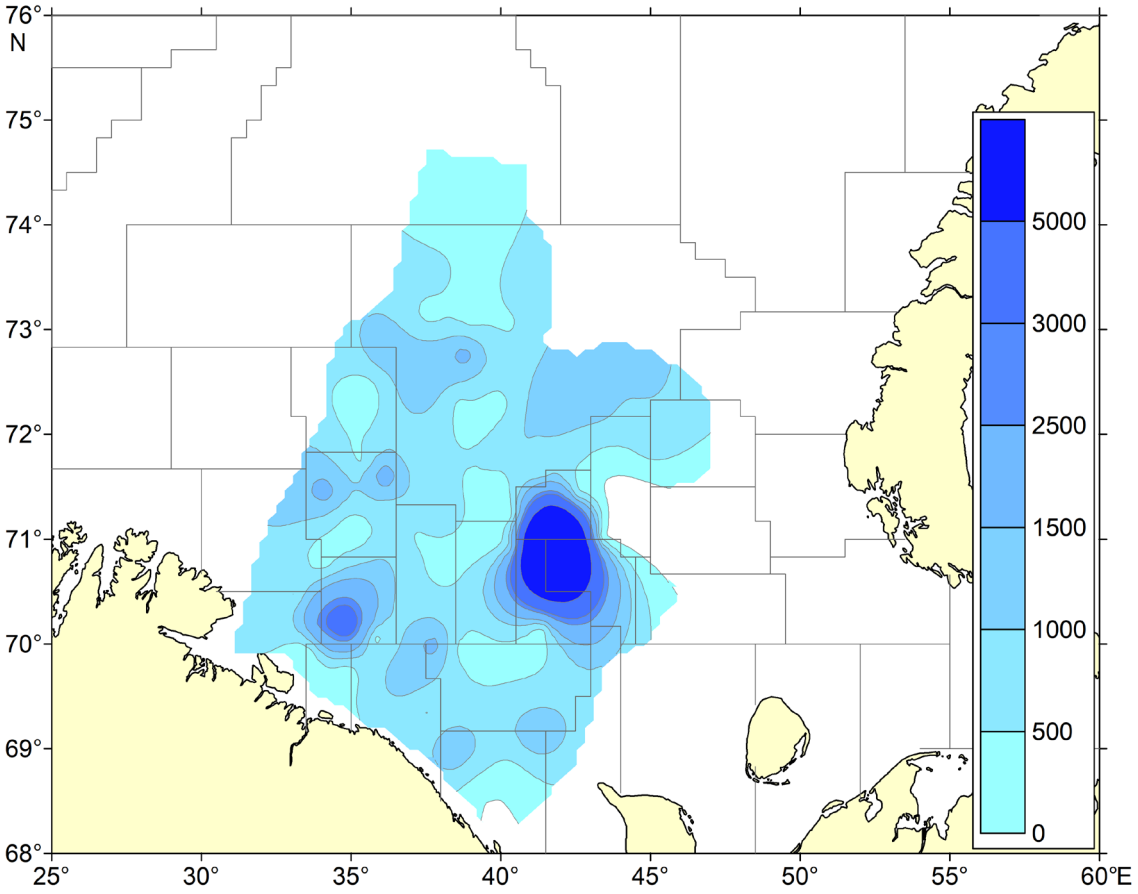

Figure A5.24: Euphausiid abundance (ind. 1000 m^{-3}) based on trawl-attached plankton net catches in the near-bottom layer of the southeastern Barents Sea from the Russian-Norwegian winter survey in February 2021.

Summer–autumn distribution and biomass

Area coverage and estimations

In 2021, coverage of the macroplankton was suboptimal due to lack of coverage in some areas in the southeastern and eastern parts of the Barents Sea (Figure A5.25).

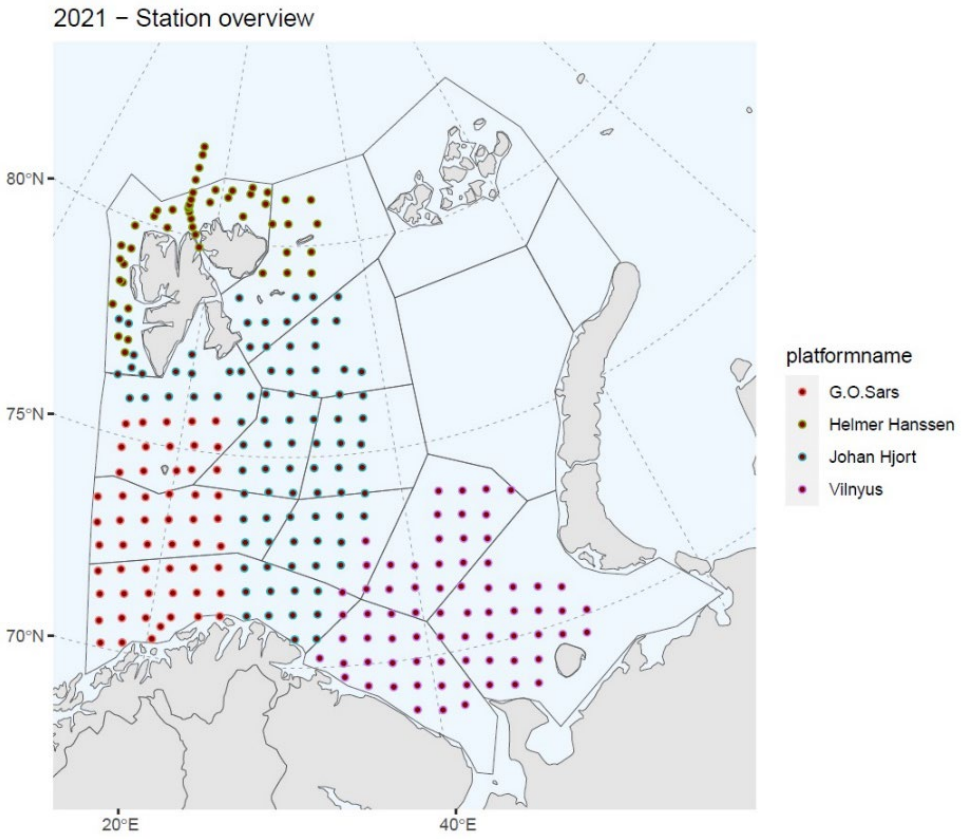

Figure A5.25: Spatial coverage during the BESS in 2021.

Euphausiids biomass indices have been calculated in Excel for the period 1980–2017 based on methods described in Eriksen and Dalpadado 2011. In 2021, R scripts (R is a free software environment designed for data organization, statistical analyses and visualization (R Core Team, 2021) for estimation of macroplankton (both euphausiids and amphipods) biomass estimates were developed and tested. During the night, most of krill migrate to upper water layer for feeding, and therefore it is more available for the pelagic trawl. Pelagic amphipods stay at upper water column and therefore catches not varied between day and night. New biomass indices based on euphausiids night catches and amphipods both day and night catches, that were taken by pelagic Harstad trawl. The catch weights were standardized for trawled distance, volume of filtered water and covered depths layer (mainly upper 60 m) and presented as biomass (grammes wet weight per square meter, g/m2). These biomasses were later averaged for each of 15 WGIBAR-subareas (Figure A5.26). Two datasets representing annual biomass indices as calculated by Excel and R were compared and found to be similar (Pearson correlation analysis, r=0.56). Differences in indices could be related to differences in calculation of sun elevation, defining night and day catches, and coverage area.

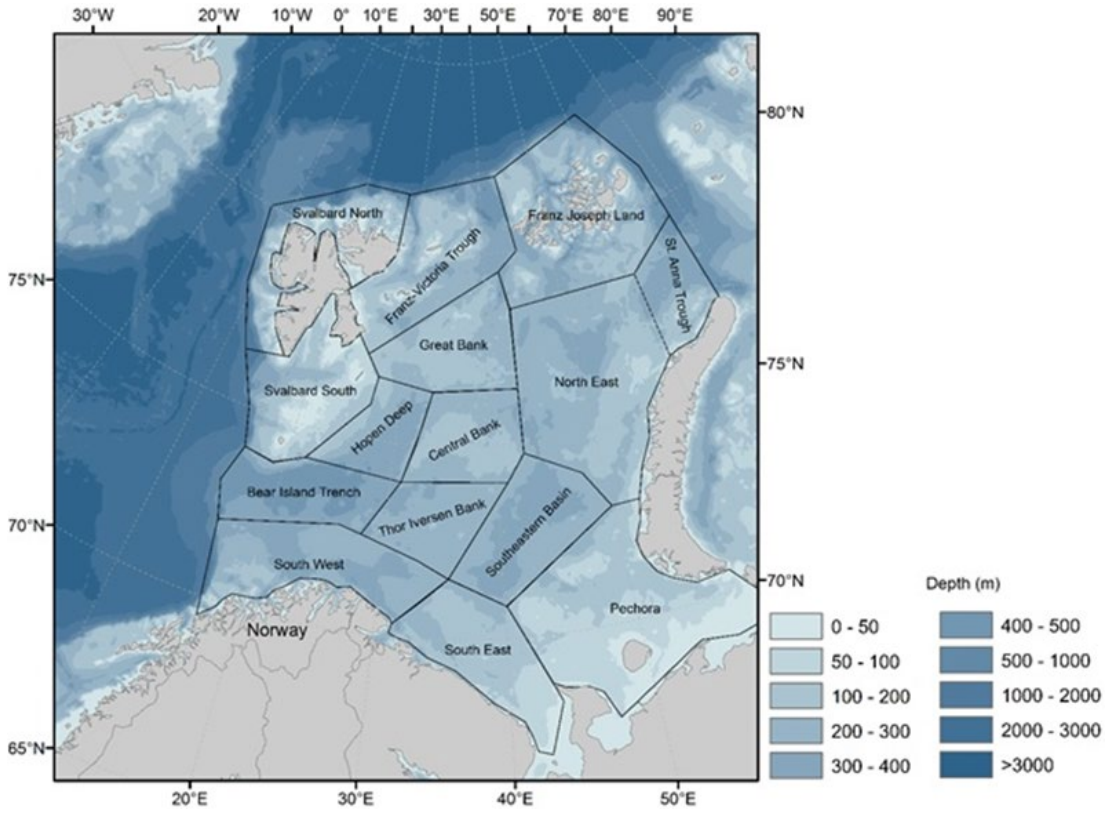

Figure A5.26: Map showing subdivision of the Barents Sea into 15 WGIBAR-subareas (regions) used to calculate estimates of 0-group abundance based on the BESS.

Here, we presented biomass time-series for euphausiids, and amphipods calculated by R for the period 2003–2021. Note, that most of macroplankton were recorded to higher taxonomic lever at the beginning, and since 2014, training of personnel and help from plankton experts improved the identification of macroplankton.

Distribution and biomass indices of krill

by E. Eriksen, B. Husson, T. Prokhorova and A. Dolgov

Figure by S. Karlson and B. Husson

Distribution of krill and biomass

In 2021, the euphausiids (krill) taken by standard pelagic trawl in upper 60 m were identified to species level at most of stations. Some parts of the eastern Barents Sea were not covered in 2021 (see above).

In 2021, traditionally krill were widely distributed in the Barents Sea (Figure A5.27). The catch weights were standardized for trawled distance, volume of filtered water and covered depths layer (mainly upper 60 m) and biomass calculated for each station and presented as grammes wet weight per square meter (g/m^2). The night catches were higher (8.79 g/m^2) than day catches (3.87 g/m^2) and long term mean (2003–2021, 5.08 g/m^2).

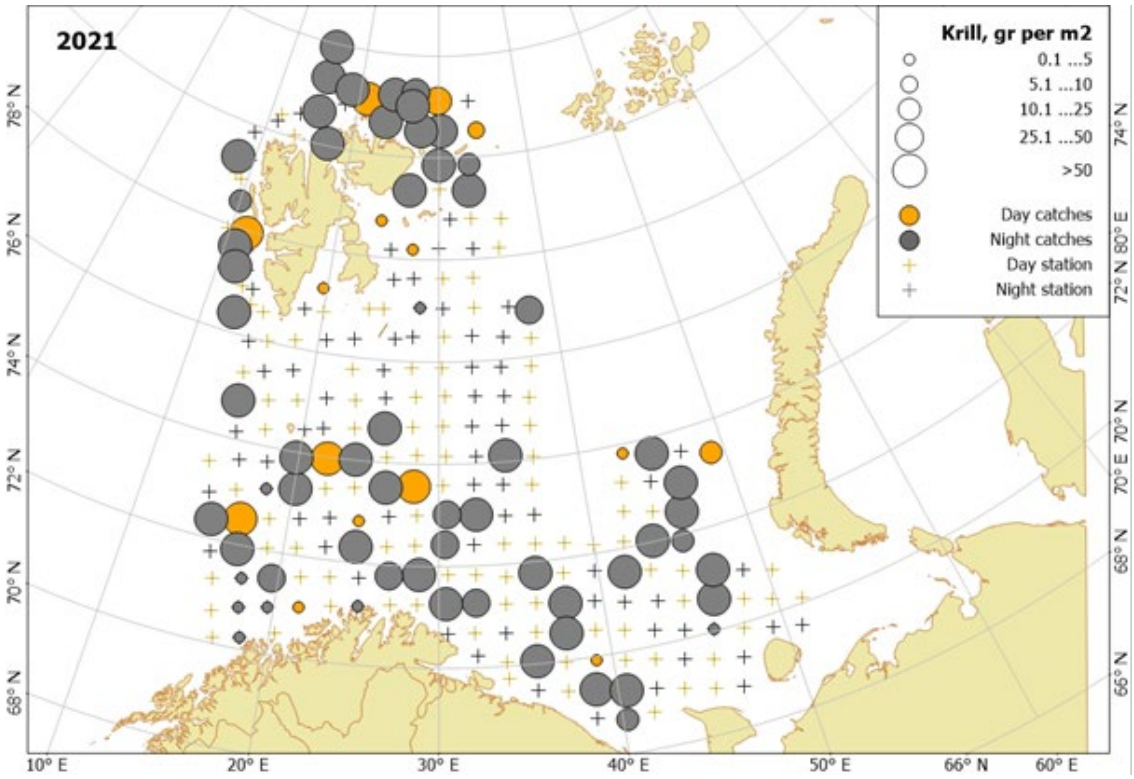

Figure A5.27: Krill distribution, based on pelagic trawl stations covering the upper water layers (0-60 m), in surveyed area of the Barents Sea in August–October 2021.

In 2021, a total of 107 night stations and 185 day stations were taken. During the night, most of krill migrate to upper water layer for feeding, and therefore it is more available for the trawl. Higher night biomasses with an average of 52 g/m^2 were observed in Bear Island polygon.

Based on the euphausiid species identification in 2021, large warm-water *Meganyctiphanes norvegica* were widely distributed in the Barents Sea, what is typical for recent warm period. *M. norvegica* were mostly restricted to the Atlantic waters in the central and southern areas with one additional catch in the west. In contrast, local cold-water *T. inermis* and *T. raschii* were mainly found in the southeastern and northern Barents Sea. Two catches of warm-water *Thysanoessa longicaudata* were taken in the western area. The smaller *T. longicaudata*, and juvenile euphausiids are not representative caught for their distribution due these small organisms escape through the mesh of the pelagic trawl during hauling (see length distribution of captured krill from trawl catches in ICES WGIBAR 2020).

In 2021, the total biomass of krill was estimated about 8.4 million tonnes wet weight for the covered area (Figure A5.28). It is the highest value since 2016 and the long term mean level of 5.5 million tonnes. The biomass is relatively high considering heavy predation by quite large capelin stock and other planktivorous fish during the 2021 feeding summer season. High biomass of krill suggests that satisfactory feeding conditions for planctivorous fishes can be expected in 2022.

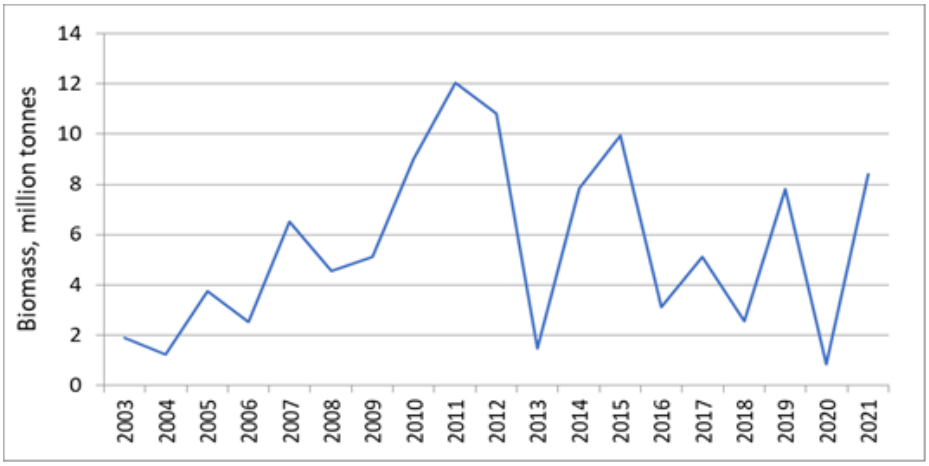

Figure A5.28. Krill species distribution, based on trawl stations both day and night, covering the upper water layers (0–60 m), in surveyed area of the Barents Sea in August–October 2021. The proportions are based on wet weights.

Distribution and biomass indices of amphipods (mainly Hyperiids)

by E. Eriksen, B. Husson, T. Prokhorova and A. Dolgov

Figure by S. Karlson and B. Husson

In 2021, the amphipods taken by standard pelagic trawl were identified to species level at most of stations. Some part of the eastern Barents Sea was not covered in 2021 (see above). The catch weights were standardized for trawled distance, volume of filtered water and covered depths layer (mainly upper 60 m) and presented as biomass (grammes wet weight per square meter, g/m^2).

In 2021, the amphipods were generally found in traditional area with low water temperature – north of the Svalbard/Spitsbergen archipelago, and some catches were taken in the southwestern and eastern areas (Figure A5.29). Total biomass of hyperiids was 271 thousand tonnes in 2021, that was lower than in 2020 (665 thousand tonnes), while slightly higher than long term mean (242 thousand tonnes).

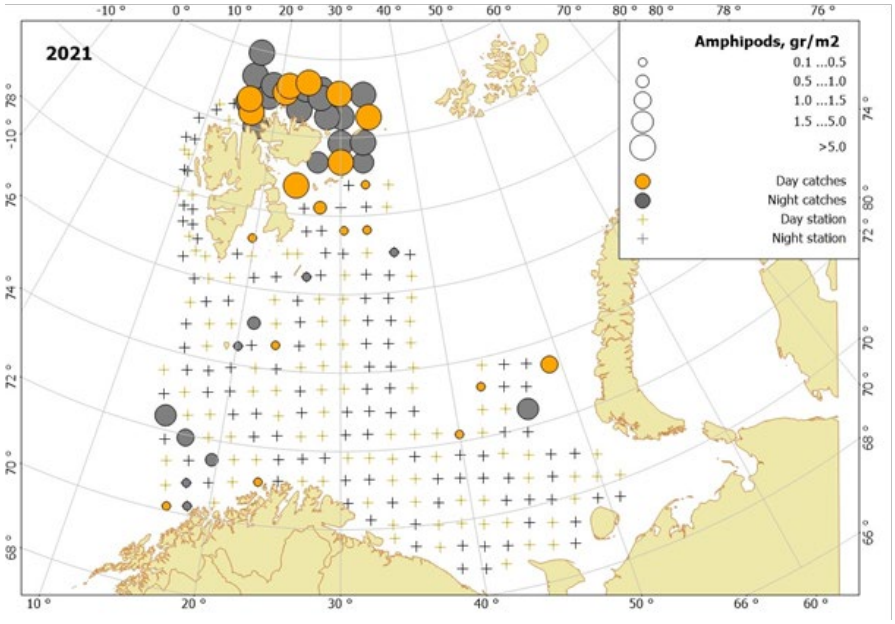

Figure A5.29: Amphipods distribution, based on pelagic trawl stations covering the upper water layers (0–60 m), in surveyed area of the Barents Sea in August–October 2021.

The Arctic *Themisto libellula* is a dominant pelagic amphipod, which is carnivorous and has copepods as important parts of the diet. The highest *T. libellula* catches were taken in the Svalbard North polygon in 2017 and 2018 and were 10.1 and 11.6 gr/m^2 respectively. In 2021, catches were lower with an average of 3.6 g/m^2.

Jellyfish

Area coverage and estimations

Area coverage see above and figure A5.25. Biomass of gelatinous zooplankton has been calculated by use of different softwares during the last for decades: SAS (for the new 23 fisheries subareas, 1980–2017) and MatLab (for the new 15 WGIBAR-subareas (1980–2018, WGIBAR 2018) and R (for the new 15 WGIBAR-subareas (2003–2021). Due to SAS-software upgrading which led to challenges with the running of scripts and limited personnel resources with respect to programming in MatLab, we decided to develop R-scripts. R is a free software environment designed for data organization, statistical analyses and visualization (R Core Team, 2021) for estimation of biomass indices for 15 WGIBAR-subareas. Two datasets representing annual biomass indices as calculated by R and SAS were compared and found to be very similar (Pearson correlation analysis, r=0.97).

Mean catches and total biomass were also estimated for groups: large jellyfish (*Cyanea capillata* and *Cyanea lamarckii*) and small jellyfish (*Aurelia aurita* and Ctenophora species) and others.

Here, we presented time-series for biomass indices calculated by SAS (1980–2017) and by R (2018–2021). Spatial biomass indices calculated by R for 2003–2021.

Distribution and biomass indices of jellyfish

By E. Eriksen (IMR), T. Prokhorova (VNIRO), A. Dolgov (VNIRO) and S. Karlson (IMR)

In August–October 2021, lion's mane jellyfish (*Cyanea capillata*; Scyphozoa) was the most common and widely distributed jellyfish species, both with respect to occurrence (found at 238 stations) and weight (average catch of 19.8 kg/nm^2, corresponding to 9.1 tonnes per sq nm) (Figure

A5.30). Large catches (corresponding to > 10 tonnes per sq nmi) were made in the central and southeastern Barents Sea. Moon jellyfish, *Aurelia aurita,* was found at 33 stations in the southern Barents Sea with an average biomass of 356 kg/nm². Single specimens of blue stinging jellyfish, *Cyanea lamarckii*, were found at 21 stations in the western Barents Sea with average biomass 30 kg/nm². *C. lamarckii* has been regularly observed in the Barents Sea in recent years and the presence of this warm-temperate species may be linked to the inflow of Atlantic water masses. Ctenophores were found at 13 stations in the central, northern, and southeastern Barents Sea with an average biomass of 18 kg/nm² (Figure A5.31).

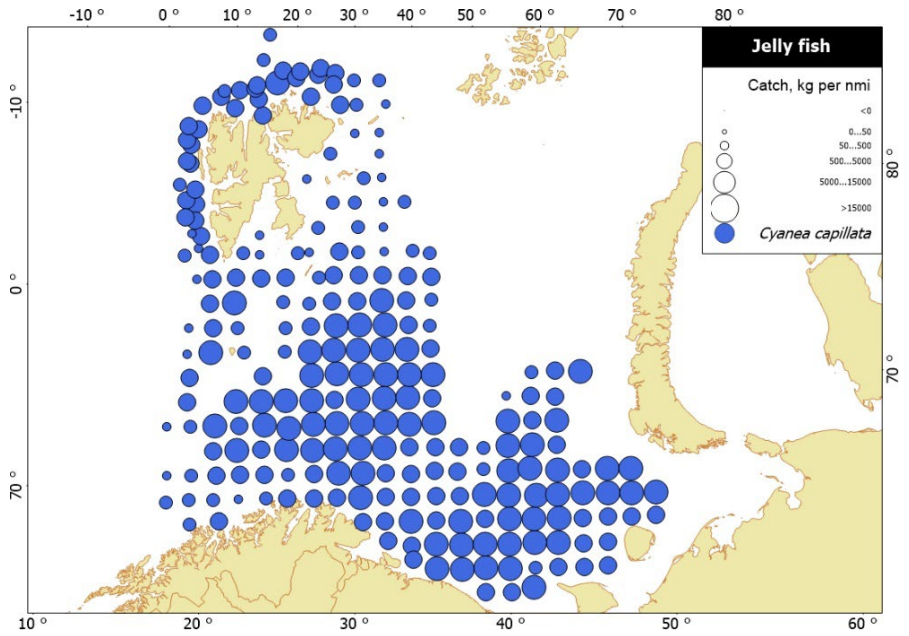

Figure A5.30. Distribution of *Cyanea capillata* (wet weight; kg per square nautical mile) in the covered area of the Barents Sea, August–October 2021. Catches both day and night from standard pelagic trawl 0–60 m depth

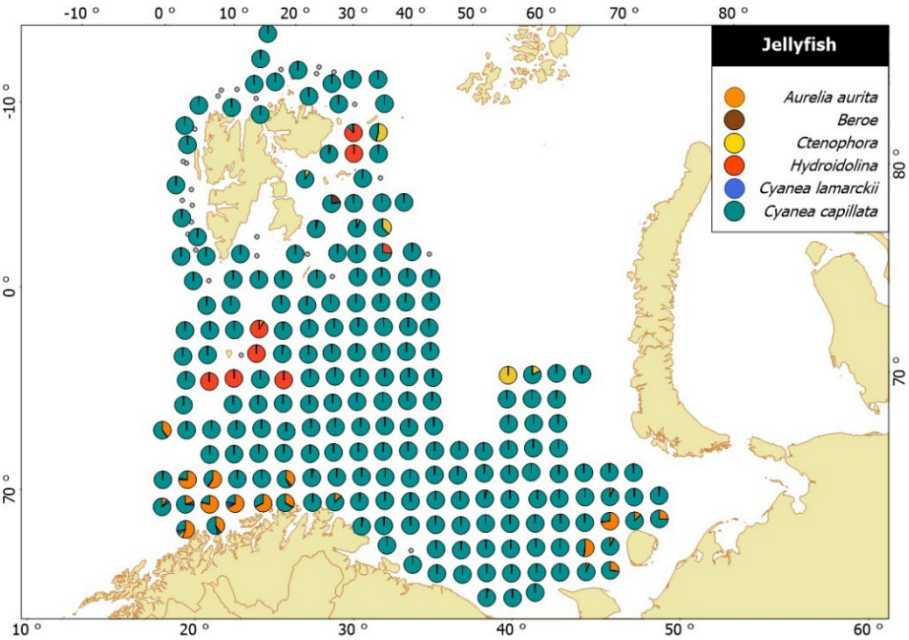

Figure A5.31: Jellyfish composition in catches in the surveyed area in August–October 2021. Note that all circles are of the same size and do not size of catch. Colours within the circles indicate species-composition.

Geographical distribution of jellyfish, mainly *C. capillata*, has shown an increase in central, southern, eastern, and northern areas since 2013 with the widest distribution in 2017, when biomasses reached almost 5 million tonnes for the covered area of the Barents Sea (Figure A5.32).

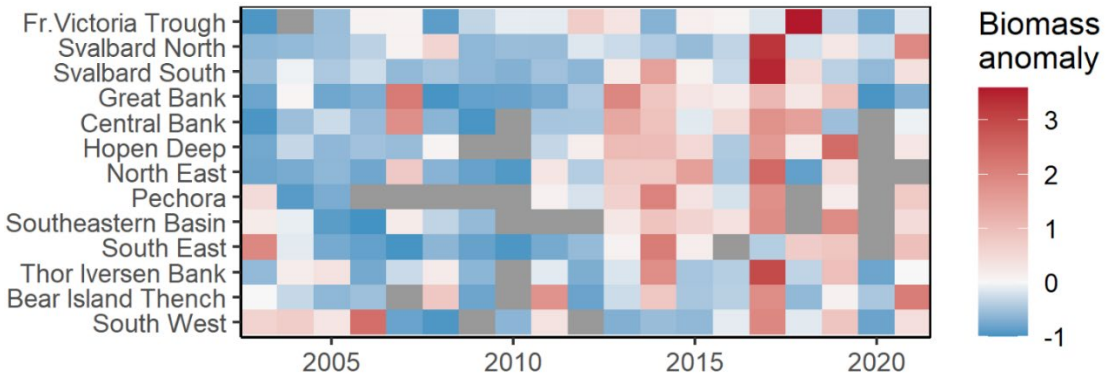

Figure A5.32: Spatial anomalies of jellyfish biomasses, mainly *C. capillata*, in covered area of the Barents Sea in August–September 2003–2021. The names refer to the Barents Sea polygons used in ICES WGIBAR.

Biomass indices were calculated for the total of all jellyfishes for the period 1980–2003. In addition to the total biomass for all jellyfishes, the biomasses for large jellyfish (dominated by *C. capillata*), small jellyfish (dominated by *A. aurita*), and other jellyfish (found occasionally) were also calculated for the period 2004–2021. In 2021, total jellyfish biomass for the covered area of the Barents Sea was 2.7 million tonnes (Figure A5.33). Biomasses were dominated by *C. capillata* (2.6 million tonnes).

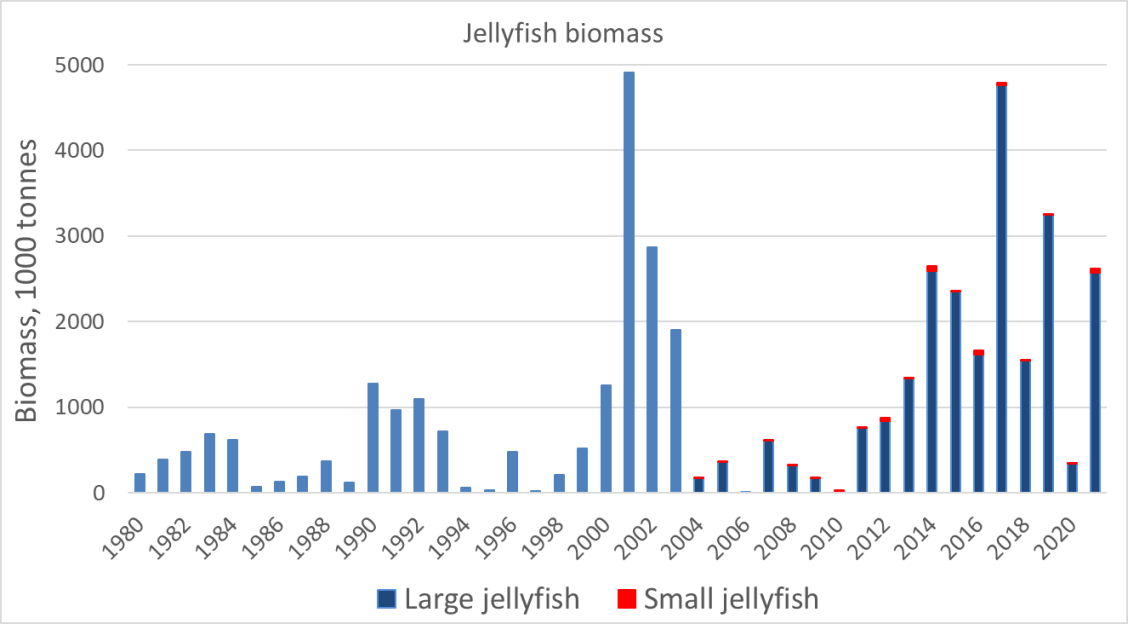

Figure A5.33. Total biomass of jellyfish in covered area of the Barents Sea in August-September 1980–2021. Large jellyfish (dominated by *C. capillata)*, small jellyfish (dominated by *A. aurita)*, and other jellyfish (found occasionally). NB: small and other jellyfish were recorded from 2004 only (indicated by darker blue). Biomass estimates in 2018 and 2020 were underestimated due to lack of complete coverage.

References

R Core Team (2021). R: A language and environment for statistical computing. R Foundation for Statistical Computing, Vienna, Austria. https://www.R-project.org/.

Benthos and shellfish

Benthos

N.A. Strelkova (VNIRO), L.L. Jorgensen (IMR), A.S. Kudryashova, D.V. Zakharov (VNIRO)

The distribution of megabenthos biomass shows relative stable large-scale patterns. Biomass and number of taxa was above long term mean, while abundances were below. High biomass particularly in the southwest; and another, but much more variable, high biomass in the northeast and northwest. In the southeast king crabs increased the biomass north of Kapp Kanin. Fluctuation of total biomass of megabenthos is positive correlated with the water temperature on the Kola Sections, but with a time-lag of about 7 years

The status of megabenthos in 2021

The area where benthos was identified from bottom trawls (benthic stations) in 2021 is shown in figure A5.34, and the main results of the BESS 2021, compared with 2020 and long term average value, are given in table A5.3. Four vessels with a total of nine benthic experts (two experts onboard of Russian vessel and seven experts onboard of Norwegian vessels) were involved in this work. No benthic experts were onboard the Norwegian RV "Johan Hjort" during the first part of cruise, which resulted in a total number of surveyed stations being below average (Table A5.3) and no benthic data from a large area in the middle part of the sea (Figure A5.34).

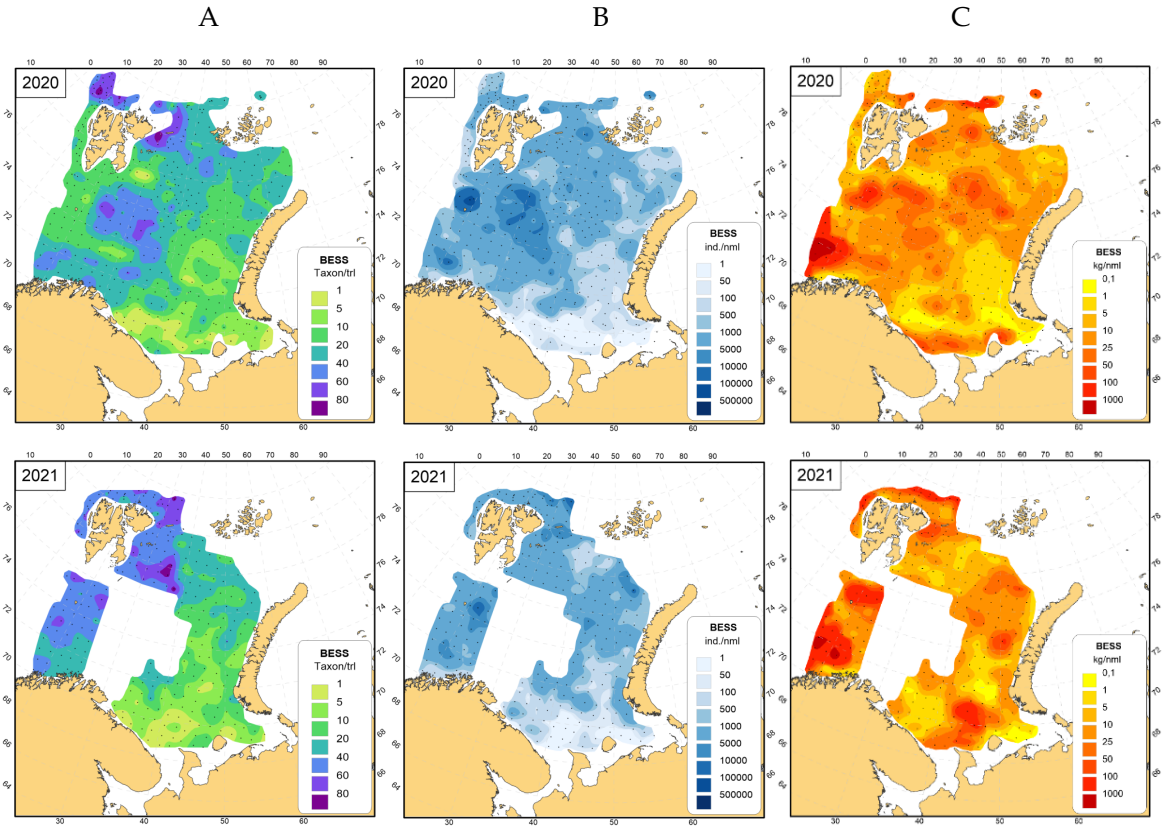

Figure A5.34: The A) number of taxa per station, B) number of individuals, and C) biomass per nautical mile according to BESS 2020 (upper row) and 2021 (lower row). The northern shrimp *Pandalus borealis* (a semi-pelagic species) are excluded (but see the chapter below on "State of selected benthic species" in this annex).

Table A5.3: The main characteristics of the megabenthic bycatches (excluding *Pandalus borealis*) during BESS 2020, 2021, and average long-term values for the period 2005–2020; the minimum-maximum / average±standard error

Characteristics	long term average**	2020	2021
Number of stations	165-637 / **372.9**±30.9	429	254
Total number of taxa	218-621 / **444.1**±31.8	611	572
Total number of species	142-427 / **298.2**±22.0	401	384
Number of taxa per station;	14.8-38.6 / **24.4**±1.8	1-135 / 26.8±1.4	1-94 / 29.7±1.4
Number of individuals per station	421-7967 / **2 485**±450	1-265 775 / 1 488±870	2-17 113 / 842±102
Number of individuals per n.ml*	522-9832 / **2 950**±538	1-288 572 / 1 733±945	2-22 204 / 1 077±131
Biomass per station (kg)	10.0-95.7 /**37.6**±5.1	0.002-1 254 / 20.3±5.6	0.003-1 623 / 40.0±10.3
Biomass per n.ml (kg)	12.7-125.5 / **48.2**±6.7	0.002-2 416 / 30.4±10.5	0.004-2 074 / 50.6±12.9

*** n.ml – nautical mile**

**** calculated as the interannual average value of interstation mean values for each year during 2005–2020**

Due to fewer stations in 2021 were the total number of benthic invertebrate taxa and species slightly lower that in 2020 (Table A5.3). However, this does not indicate a reduced taxonomic quality or decreased biodiversity because the average number of taxa per station and percentage of benthic invertebrates identified to species was higher. The spatial distribution of the number

of taxa per station in 2021 was generally the same as the long-term pattern. Large numbers of taxa were recorded in the northwestern part of the sea, while small numbers were in the south-east (Figure A5.34A).

The number of individuals per nautical mile or station in 2021 is lower, while the biomass is higher than in 2020. The average values in 2021 are within the range of long-term variation for both number and biomass (Table A5.3).

Long-term trends in spatial and temporal megabenthos distribution

The species diversity

Despite the number of processed benthic stations showing some negative trends, the number of annually recorded species has increased nearly twice over the period from 2005 to 2021 (Figure A5.35).

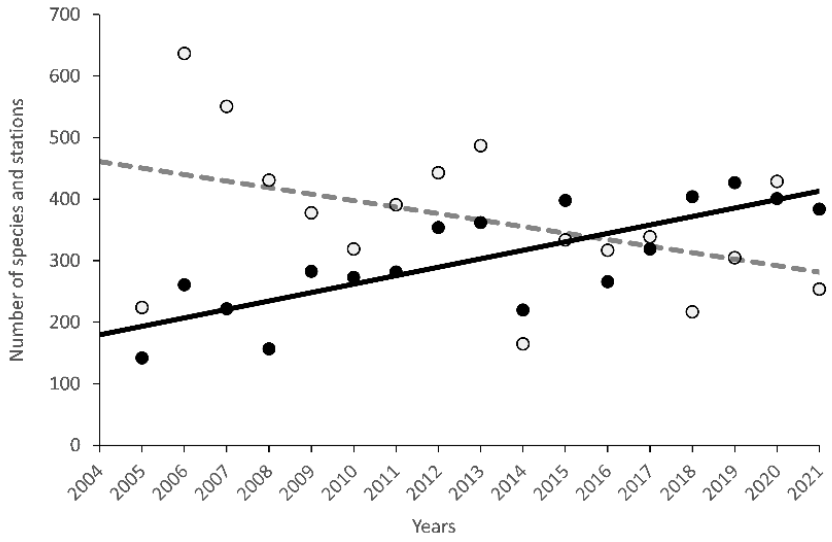

Figure A5.35: Number of trawl stations where benthos was identified (open circles and dotted line) and number of identified species (black circles and solid line) during the BESS 2005–2021.

This is the direct result of the join Russian-Norwegian efforts to improve the field guides of megabenthos species and the growing skills of experts involved in the BESS.

During the BESS 2005–2017, 694 megabenthic species (1058 taxa) have been recorded in the Barents Sea and adjacent water of the shelf and upper bathyal (Zakharov *at al*., 2020).

From 2005–2021 the BESS cruise recorded several new benthic species for the Barents Sea; finding of some of them could be a result of spreading of new species toward the north due to long warming period (Zakharov, Jørgensen, 2017; Golikov *et al.,* 2013, 2014).

In 2021, ten new species were recorded for the first time since 2005 in the Norwegian part of the Barents Sea: bryozoans *Alcyonidium diaphanum*, polychaetes worm *Aphrodita hastata*, crab *Atelecyclus rotundatus*, sea cucumber *Bathyplotes natans*, hydroid polyp *Laomedea angulata*, ascidians *Polycarpa pomaria* and *Synoicum incrustatum*, and soft corals of the Nephteidae family *Gersemia mirabilis*, *Duva multiflora*, and *Pseudodrifa racemosa* (Figure A5.36). With the exception of two ascidians (*S. incrustatum* and *P. pomaria*) which have earlier been recorded in the Svalbard water (Gulliksen *et al*., 1999), all listed species are the new for the Barents Sea fauna.

Two species (crab *A. rotundatus* and sea cucumber *B. natans*) recorded in the southwestern part of the Barents Sea shelf, could likely be a result of their spreading to the north due to long warming period.

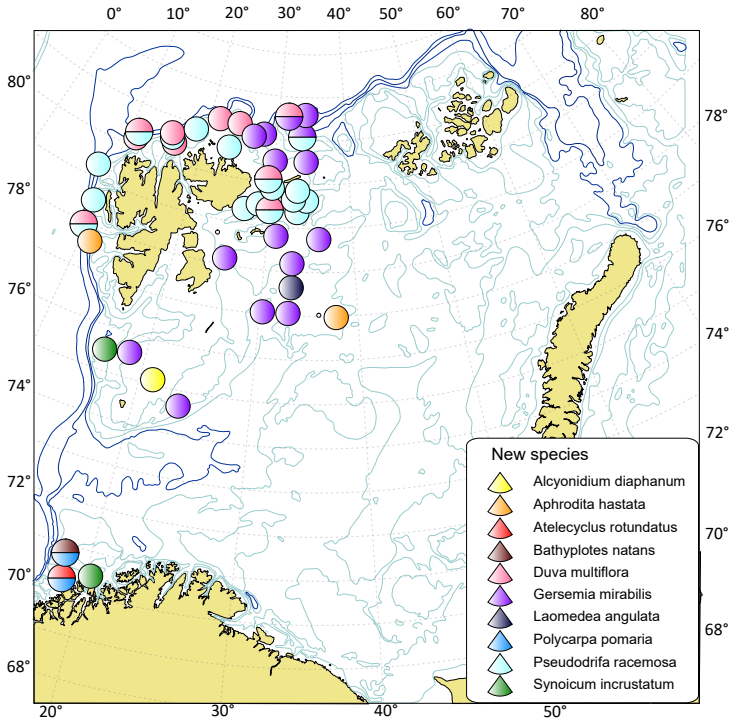

Figure A5.36: Megabenthic species recorded for the first time in 2021 in the Barents Sea and adjacent water since BESS started in 2005.

Spatial distribution and temporal variation of megabenthic biomass

Because colonial and fragmented species (like e.g. sponges) are difficult to count, the biomass is more frequently used when detecting long-term BESS variations in megabenthic communities.

Spatial distribution

Despite the interannual differences in area covered by stations, the monitoring series of the megabenthos biomass-distribution shows relative stable large-scale patterns (Figure A5.37).

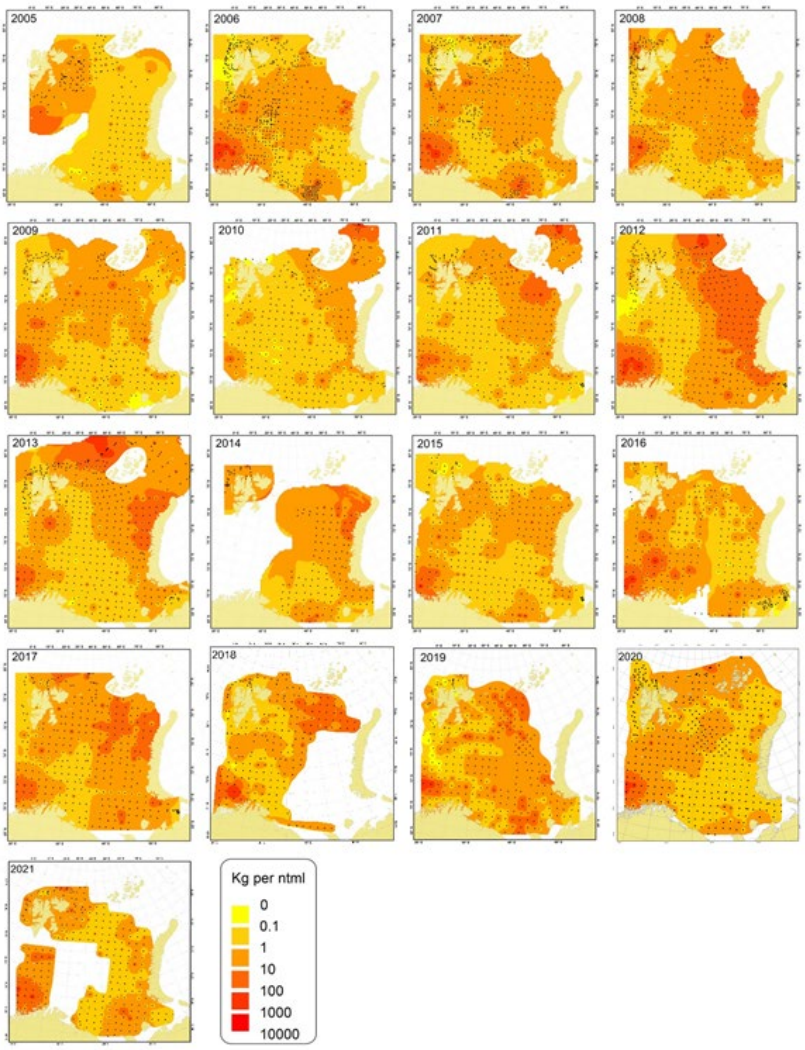

Figure A5.37. Distribution of the megabenthos biomass (excluding Pandalus borealis) in the Barents Sea from 2005 to 2021.

In the southwestern part of the Barents Sea shelf and in its west and north margins, has dense sponge aggregations (mostly formed by species of *Geodia, Stryphnus* and *Steletta* genus) been recorded during the entire megabenthos monitoring period. Biomass of bycatches in these areas can reach up to several tonnes per trawling. Local biomass hot spots in the Spitsbergen Bank includes dense aggregations of sea cucumber *Cucumaria frondosa*, sea urchin of *Strongylocentrotus* genus and sea squirts. High biomass records are also observed within the red king crab area near Kanin Nos peninsula. The biomass hot spot in the Novaya Zemlya shallows coincides with the area of dense snow crab population. The central Barents Sea is highly variable in biomass but does never reach the highest or lowest recorded values in the Barents Sea.

Figure A5.37 also illustrates the deficiency and fault in the megabenthos assessment in several of the survey years. In 2005, 2014, 2018 and 2021 there were a lack of station coverage in the Norwegian or Russian areas. In 2019, the northeastern part of the sea was incompletely covered. In 2014, 2015, 2016 and 2019 the Loophole area was not sampled because a commercial snow crab fishery. In 2012 and probably 2017 the biomass was overestimated in the Russian zone due to technical issues with the trawl tuning. Such lack of coverage and non-standardized processing should be considered when analysing the megabenthic time-series.

Interannual fluctuation of the mean values of the megabenthos biomass

To make an estimation of the long-term megabenthos dynamics, interannual changes of the mean biomass were calculated for the total Barents Sea (Figure A5.38A), and thereafter expressed for four separate areas of the sea – southwest and northwest (Figure A5.38B), southeast and northeast (Figure A5.38 C). Moreover, with the aim of standardization of interannual data, the biomass of *Pandalus borealis* and all catches more than one tonne are excluded from calculations.

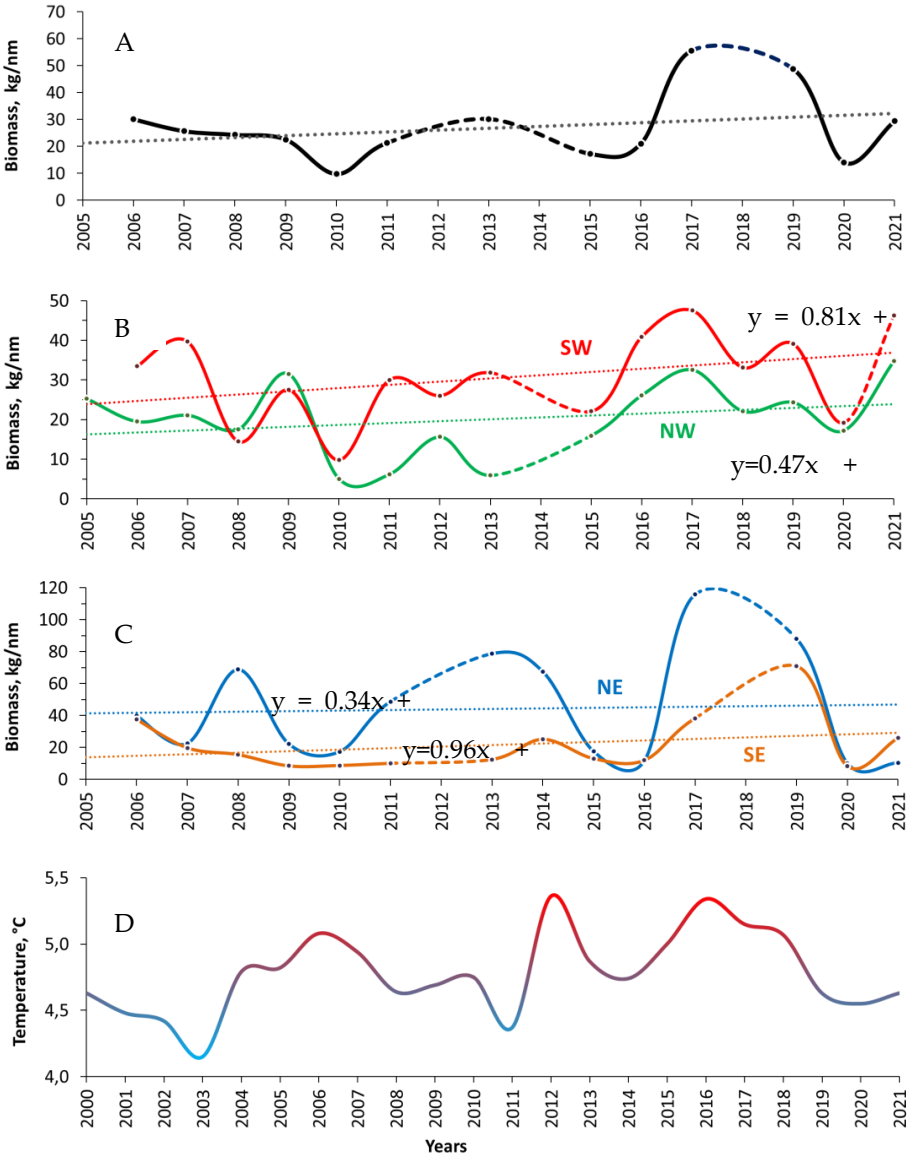

Figure A5.38: Interannual variations of the mean megabenthos biomass in total Barents Sea (A) and in it western (B) and eastern (C) sections and fluctuation of the average annual temperature in the water layer 0–200 m in the 3–7 stations of the «Kola Section» Meridian(D). Biomass of *Pandalus borealis* and all catches more than 1 tonne are excluded. The dotted lines in the plots A, B, and C are no reliable data of mean biomass. The point lines in the plots A, B, and C are linear trend lines. Area restrictions: Total Barents Sea – 68-80°N, 15-62°E; southwestern sector (SW) – 68-74°N, 15-40°E; northwestern sector (NW) – 74-80°N, 15-40°E; southeastern sector (SE) – 68-74°N, 40-62°E; northeastern sector (NE) –74-80°N, 40-62°E.

The sixteen years of monitoring (though inconsistent in area-coverage and quality of sampling) reveal a moderate, positive trend of increasing megabenthic biomass during the period 2006–2021 when calculated for the "total Barents Sea"(Figure A5.38A).

According to indexes ("a" and "b") of the linear trend line equations (y=ax+b), the highest level of megabenthic biomass is observed in the northeast of the Barents Sea (NE, b=41.13), followed

by southwest sector (SW, b=23.05), northwest (NW, b=15.81) and southeast (SE, b=13.02). The positive trend of biomass dynamic is most pronounced in the southeast (SE, a=0.96) and southwestern (SW, a=0.81) parts of the Barents Sea shelf, followed by northwest sector (NW, a=0.47) and minimal in the northeast part of the sea (NE, a=0.34) (Figure A5.38B and A5.38C). Such pattern well reflects both the difference in the reaction of benthos to warming in different parts of the Barents Sea (boreal, subarctic and arctic) and negative impact of the bottom-trawl fishery to megabenthos.

On the background of this trend, there are strong interannual variations of average megabenthic biomass values both for the total Barents Sea (Figure A5.38A) and for its separate sectors (Figure A5.38B and A5.38C). Despite the significant uncertain of this parameter due to its sensitivity to the area-coverage by stations and quality of sampling, weak positive correlation (r = 0.59 for "total") between dynamic of megabenthic biomass and fluctuation of the water temperature on the «Kola Section» Meridian (Figure A5.38D), with a time-lag of about 7 years, have been shown (ICES, 2019, 2020).

A similar response to change of environmental conditions was documented for the Barents Sea macrobenthos, but with a delay in approximately four years (Lubina *et al*., 2012, 2016; Denisenko, 2013). The difference in duration of the time-lag between macro- (grab's) and mega- (trawl's) benthos can be caused by different mean size and longevity of the lifespan of these size groups of benthic organisms causing a faster life-turnover for small organisms.

In 2021 mean biomass both for the total Barents Sea (Figure A5.38B) and for all four sectors (Figure A5.38C and A5.38D) slightly increased, which support the hypothesis of a 7-year time-lag correlation between megabenthic biomass and water temperature. According to this hypothesis, increasing of biomass in 2021 can be the result of the increasing temperature during 2014–2015.

Vulnerable habitats and distribution of their species-indicators

According to the criteria of NAFO (Kenchington *et al*., 2019) and a few recent publications (Buhl-Mortensen *et al*., 2019; Burgos *et al*., 2020), three groups of the Barents Sea megabenthic species can be characterized as indicators of vulnerable habitats: sponge ground, coral gardens, and sea pens fields.

Sponge ground

Sponges are widely distributed on the Barents Sea shelf. Results obtained during the period of 2005 to 2020 shows that sponge aggregations larger than 500 kg/n.ml were mostly recorded in the southwestern part of the shelf and in the northern margin (Figure A5.39, left). These dense sponge aggregations are largely comprised of the *Geodia* genus (*G. barretti*, *G. atlantica*, *G. macandrewii, G. phlegrae*, *G. parva*, and *G. hentsheli*), *Stelette rhaphidiophora* and *Stryphnus panderosus.* In the central and eastern part of the Barents Sea the sponge biomass does not usually exceed one kilogramme per nautical mile of trawling (Figure A5.39).

In 2021, dense aggregations of sponges (more than a tonne per trawling) were recorded in three stations in the southwestern part of the shelf, at 263 to 334 m depth. These sponge grounds were dominated by *Geodia barretti*, and *G. macandrewii*. Dense aggregations of sponges with biomass 500 to 1000 kg/n.ml were recorded on southwestern part of the shelf at 327 m depth (dominated by *G. barretti*) and to the north of Spitsbergen at 147 m depth (dominated by *G. macandrewii*) (Figure A5.39, right).

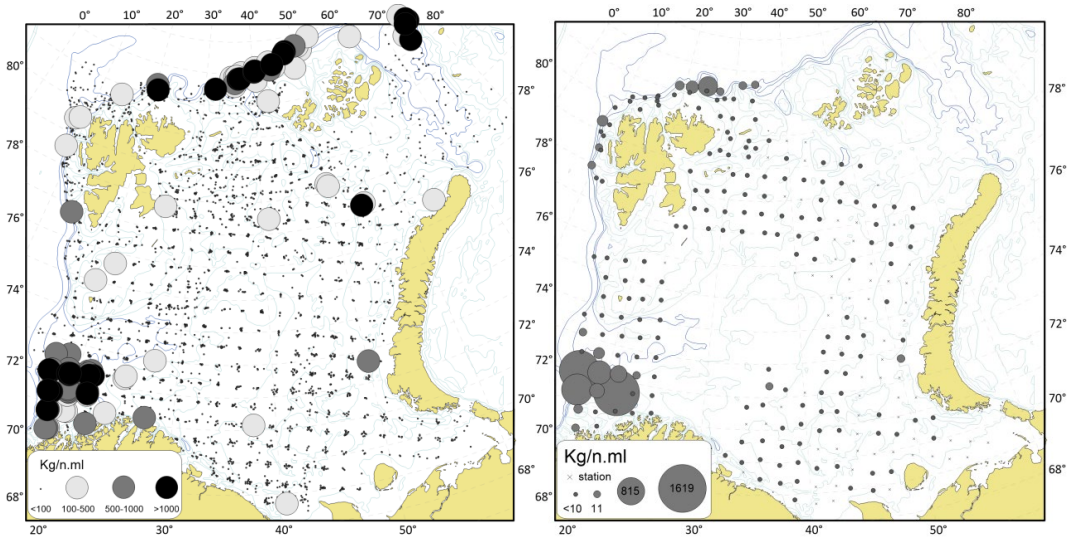

Figure A5.39: Distribution of sponges within the Barents Sea shelf according to BESS 2005–2020 (left) and in 2021 (right).

Coral gardens

The 2005 to 2020 monitoring series also revile on the Barents Sea shelf the five anthozoans species indicators of "coral gardens": stony cup coral *Caryophillia smithii* and *Flabellum* sp., and gorgonian corals *Isidella lofotensis, Radicipes* sp., and *Paragorgia arborea* (Figure A5.40, left).

In 2021, stony cup corals identified as *Flabellum* sp. (79-439 g/n.ml) were found in the southwestern part of the shelf at 226 to 393 m depth (Figure A5.40, right).

One individual of the nonbranched gorgonian coral *Radicipes* sp. (less than 1 gramme) and a few fragments of the *Isidella lofotensis* (20 g/n.ml) were recorded at one station in the upper part of continental slope north of Spitsbergen archipelago at 773 m depth (Figure A5.40, right).

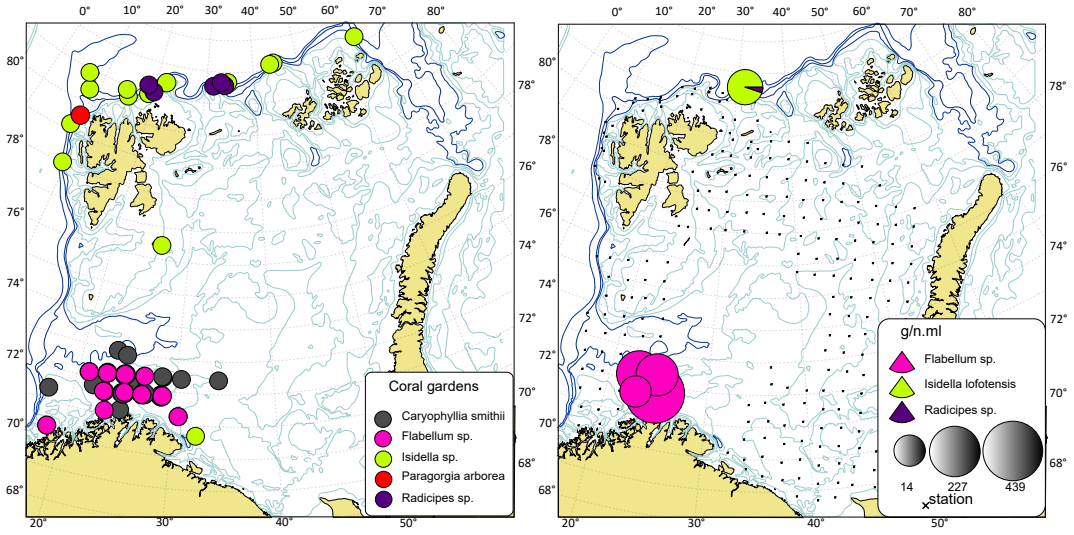

Figure A5.40: Stony cup corals and gorgonian corals sites within the Barents Sea shelf according to observations from the BESS 2005–2020 (left) and in 2021 (right)

Sea pens fields

Three species of sea pens (Pennatulacea) were found within the Barents Sea shelf: *Umbellula encrinus*, *Funiculina quadrangularis* and *Virgularia mirabilis* (Figure A5.41 left). Among these species, only *U. encrinus* forms quite dense aggregations that can be characterized as vulnerable habitat "sea-pen fields". The main fields of *U. encrinus* are located in the north margin of the Barents Sea

shelf within the depth 109–1334 m (in the main deeper 200–300 m). The densest concentrations of *Umbellula* were recorded in the Yermak Plateau and in the water around the Franz Josef Land archipelago where its biomass reached more than 100 kg/n.ml. *F. quadrangularis* and *V. mirabilis* were recorded only at a few stations (few grammes and few individuals per nautical mile).

In 2021 *U. encrinus* was recorded at three stations north of Spitsbergen archipelago at 114–773 m depth (20 individuals; 2–136 g/n.ml). Three small individuals of sea pen *Virgularia* sp. (~1 gramme) were recorded at one station north of Spitsbergen archipelago (Figure A5.41 right).

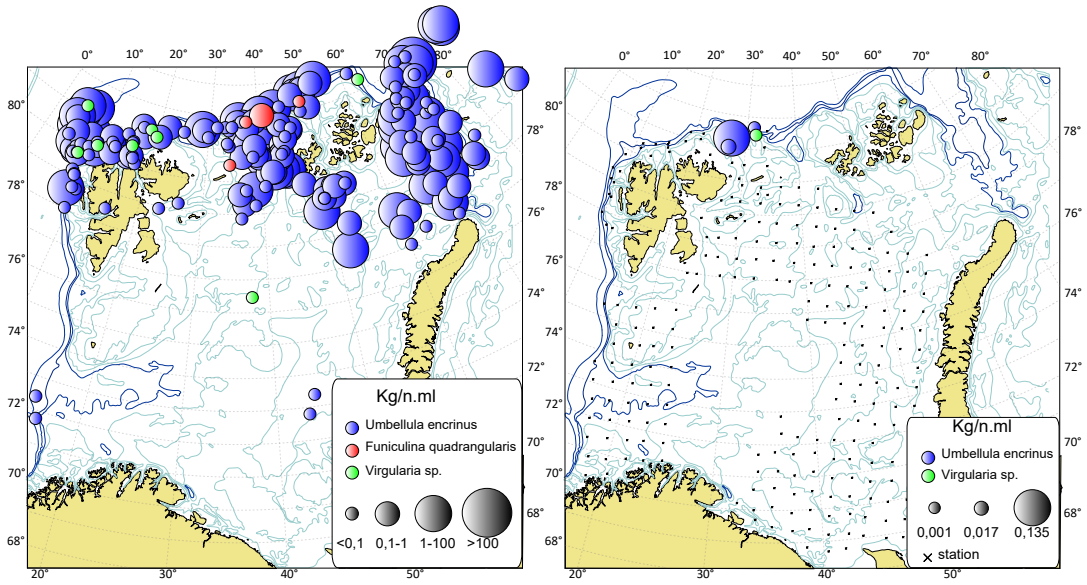

Figure A5.41: Biomass (kg/n.ml) distribution of sea pens within the Barents Sea shelf according to the BESS 2005–2020 (left) and in 2021 (right).

Large upraised and fragile megabenthos taxa in the Barents Sea

Several other megabenthic species, widely distributed in the Barents Sea shelf, fit the criteria of taxa, vulnerable for the bottom trawling: fragility and upraising (Jørgensen *et al.*, 2016). Among them are the soft corals of Nephtheidae family, large brittle stars of the genus *Gorgonocephalus*, and upraised and fragile non stalked sea lilies of the order Comatulida.

According to BESS 2005–2020 four valid species of the **Nephtheidae family soft corals** are widely distributed within the entire shelf of the Barents Sea: *Drifa glomerata*, *Duva florida*, *Gersemia fruticosa*, and G. *rubiformis* (Figure A5.42). The frequency of occurrence of the soft corals during BESS 2005–2021 is 45%, while the total biomass reach 92 kg/n.ml (average 0.69 kg/n.ml).

In 2021 seven species of the soft corals belonging to the family Nephtheidae were found during BESS (Figure A5.42, right), among which *Gersemia mirabilis, Duva multiflora* and *Pseudodrifa racemosa* are new for the fauna of the Barents Sea. The recording of these species is a result of using a new detailed identification guide of Nephtheidae family species on the Norwegian vessels during the BESS 2021.

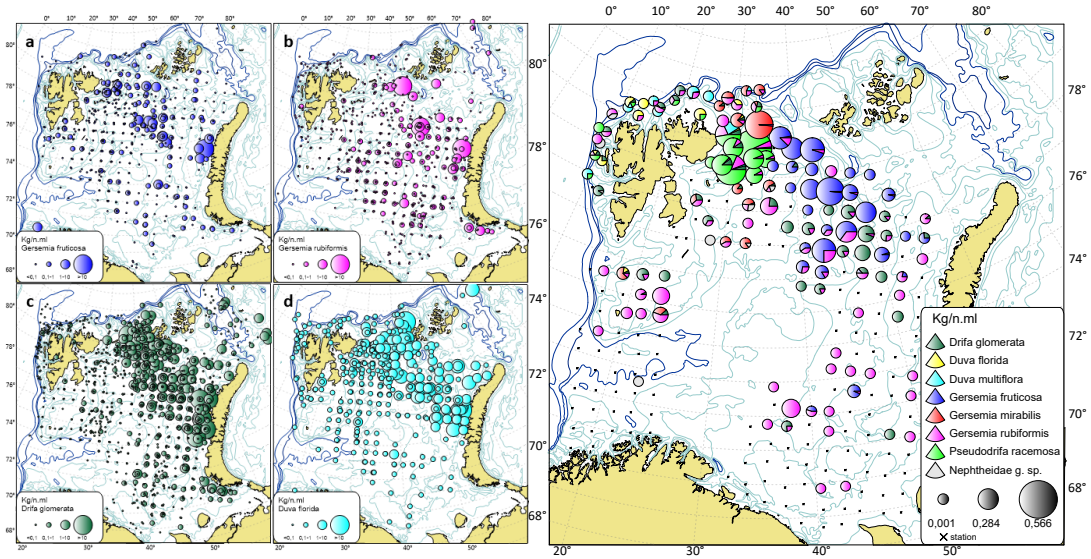

Figure A5.42: Biomass (kg/n.ml) distribution of soft corals (a – *Gersemia fruticosa*, b – *G. rubiformis*, c – *Drifa glomerata*, d – *Duva florida*) within the Barents Sea shelf according to BESS 2005–2020 and in 2021 (e).

The distribution of the largest among brittle stars species of **the genus *Gorgonocephalus*** (with a 10 cm disk diameter and an arm span up to a few dozen cm) is closely associated with populations of the soft corals. Some data suggests that embryos of *Gorgonocephalus* genus ophiuroids develop inside the polyps of soft coral (e.g. the genus *Gersemia*). After leaving the polyps, the young *Gorgonocephalus* clings to the surface of the soft coral before they leave the colony to attach themselves to an adult gorgonocephalus ophiurids. After some time they eventually assume an independent existence (Fedotov, 1924; Patent, 1970). The general pattern of the soft corals and basket stars distribution within the Barents Sea shelf indicates a strong dependence of each other. Both taxa are most abundant in the northeast part of the Barents Sea (Figure A5.42 and A5.43).

According to BESS 2005–2020 three valid species of *Gorgonocephalus* genus were found in the Barents Sea shelf (*G. arcticus*, *G. eucnemis* and *G. lamarckii*) among which *G. arcticus* and *G. eucnemis* are widely distributed within the main part of the sea, while *G. lamarckii* was recorded in the southwestern part of the shelf (Figure A5.43). The frequency of the basket stars occurrence during 2005 to 2021 is 31%, with a biomass up to 264 kg/n.ml (average 7.0 kg/n.ml).

In 2021, three species of the basket stars were recorded within the Barents Sea shelf: *G. arcticus*, *G. eucnemis*, and *G. lamarckii*. The most abundant of them are *G. arcticus*, followed by *G. eucnemis.* The *G. lamarckii* were only recorded on four stations in the Norwegian part of the survey to east of Spitsbergen archipelago (Figure A5.43, bottom). Basket stars were recorded at 84 out of 254 stations of BESS, from 44 to 773 m depth, and a total biomass of the *Gorgonocephalus* brittle stars ranging from 0.001 to 62.2 kg per nautical mile of trawling (average of 3.7 kg).

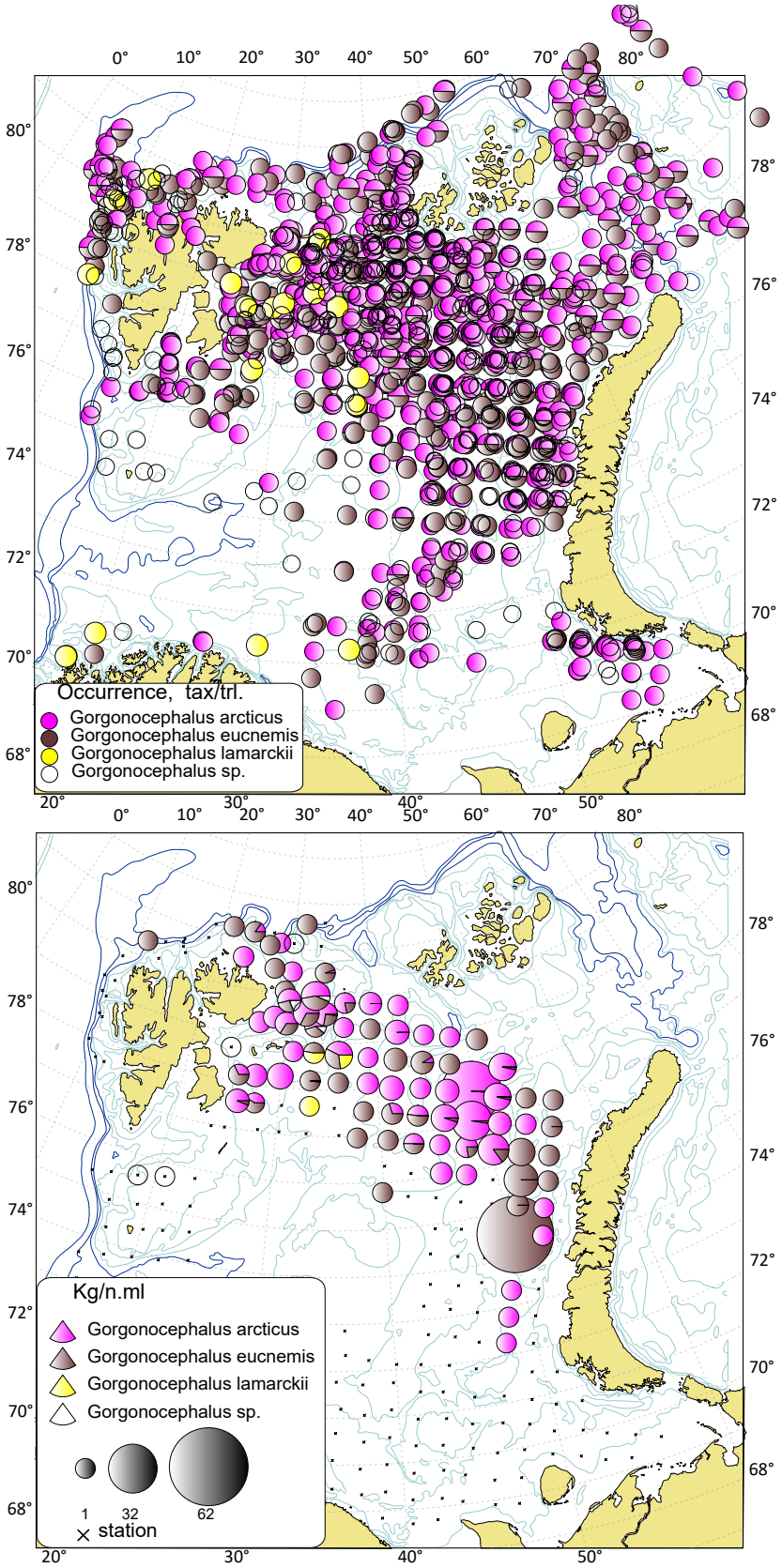

Figure A5.43: Occurrence of the brittle stars of genus *Gorgonocephalus* (*G. arcticus*, *G. eucnemis*, *G. lamarckii*) within the Barents Sea shelf according to BESS 2005–2020 (top) and their biomass (kg/nm) distribution in 2021 (bottom).

Another species that is abundant in the Barents Sea is the large, upraised and fragile **comatulid sea lilies** that obviously fit the criteria of vulnerable taxa. Two species of the order Comatulida (non-stalked crinoid) are distributed on the shelf of the Barents Sea. The bigger and more abundant in the north and central part of the Barents Sea is *Heliometra glacialis* followed by the smaller and less abundant *Poliometra prolixa,* having its main distribution in the water north and east of the Spitsbergen archipelago (Figure A5.44, left).

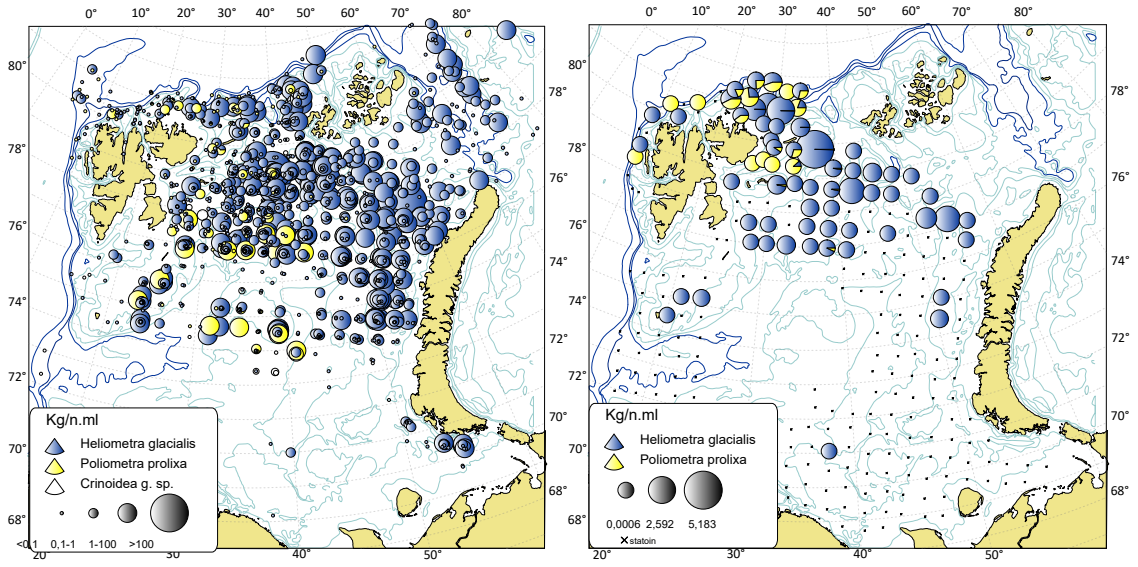

Figure A5.44: Biomass (kg/nm) distribution of the Comatulidae crinoids *Heliometra glacialis* and *Poliometra prolixa* within the Barents Sea shelf according to BESS 2005–2020 (left) and 2021 (right).

In 2021 non-stalked crinoids were recorded at 68 out of 254 stations of BESS, from 47 to 773 m depth, and with a total biomass ranging from 0.001 to 5.1 kg/nm per nm of trawling (average of 0.4 kg/nm) (Figure A5.44, right).

References

Buhl-Mortensen L., Burgos J., Steingrund P., Buhl-Mortensen P., Ólafsdóttir S., Ragnarsson S. (2019). Vulnerable Marine Ecosystems (VME) Coral and Sponge VMEs in Arctic and Sub-Arctic Waters-Distribution and Threats. TemaNord 2019:519. Nordic Council of Ministers, 144. https://issuu.com/nordic_council_of_ministers/docs/tn2019519_web

Burgos JM, Buhl-Mortensen L, Buhl-Mortensen P, Ólafsdóttir SH, Steingrund P, Ragnarsson SÁ, Skagseth Ø (2020) Predicting the Distribution of Indicator Taxa of Vulnerable Marine Ecosystems in the Arctic and Sub-arctic Waters of the Nordic Seas. Front. Mar. Sci. 7:131. doi: 10.3389/fmars.2020.00131

Denisenko S.G.(2013). Biodiversity and bioresources of macrozoobenthos in the Barents Sea. Structure and long-term changes. Saint Petersburg: Nauka. 284 pp. (In Russian).

Fedotov D. M. (1924). Einige Beobachtungen tiber die Biologie und Metamorphose von Gorgonocephalus. Zool. Anz., 61: 303-331.

Golikov A.V., Sabirov R.M., Lubin P.A., Jørgensen L.L. Changes in distribution and range structure of Arctic cephalopods due to climatic changes of the last decades // Biodiversity. 2013. Vol. 14. No 1. P. 28–35.

Golikov A.V., Sabirov R.M., Lubin P.A., Jørgensen L.L., Beck I.-M. The northernmost record of Sepietta oweniana (Cephalopoda: Sepiolidae) and comments on boreo-subtropical cephalopod species

occurrence in the Arctic // Marine Biodiversity Records. 2014. Vol. 7, e58 (4 pages). doi:10.1017/S1755267214000645.

Gulliksen B., Palerud R., Brattegard T., Sneli J.A. 1999. Distribution of marine benthic macro-organisms at Svalbard (including Bear Island) and Jan Mayen. Figures and tabulated catalogues of species-distributions, literature and synonyms. Research Report for DN 1999-4. Directorate for Nature Management, p. 148.

Jørgensen L.L, Planque B, Thangstad TH, Certain G (2016). Vulnerability of megabenthic species to trawling in the Barents Sea. ICES Journal of Marine Science, 73: i84-i97. DOI: 10.1093/icesjms/fsv107.

Kenchington, E., Lirette, C., Murillo, F.J., Downie, L. Beazley1, A.-L. Downie (2019) Vulnerable Marine Ecosystems in the NAFO Regulatory Area: Updated Kernel Density Analyses of Vulnerable Marine Ecosystem Indicators. Serial No. N7030 NAFO SCR Doc. 19/058.

Lyubina O.S., Frolova E.A., Dikaeva D.R. (2012). Current zoobenthos monitoring at the Kola Transect in the Barents Sea. Berichte zur Polarforschung, 640: 177-189.

Lyubina O.S., Strelkova (Anisimova) N.A., Lubin P.A., Frolova E.A., Dikaeva D.R., Zimina O.L., Akhmetchina O.Yu., Manushin I.E., Nekhaev I.O., Frolov A.A., Zakharov D.V., Garbul E.A., Vyaznikova V.S. (2016). Modern quantitative distribution of zoobenthos along the transect Kola Section / Transactions of the Kola Science Centre. Series 3 Oceanology, 2/2016 (36): 64-91. (In Rusian).

Patent D.H. (1970). Life history of the basket star, Gorgonocephalus eucnemis (Müller & Troschel) (echinodermata; ophiuroidea), Ophelia, 8:1, 145-159. http://dx.doi.org/10.1080/00785326.1970.10429556

Zakharov D.V., Jørgensen L.L. (2017). New species of the gastropods in the Barents Sea and adjacent waters // Russian Journal of the Biological Invasions (Российский Журнал Биологических Инвазий) № 2, 2017: 38-45 (In Russin).

Zakharov D.V., Jørgensen L.L., Manushin I.E., Strelkova N.A. (2020). Barents Sea megabenthos: spatial and temporal distribution and production / *Marine Biological Journal*, 5(2): 19-37. (*Морской биологический журнал*, 2020, том 5, № 2, с. 19–37). https://mbj.marine-research.org; doi: 10.21072/mbj.2020.05.2.03

State of selected benthic species

By Aleksei Stesko, Sergey Bakanev (PINRO), Ann Merete Hjelset, Carsten Hvingel (IMR)

Snow crab

The snow crab (*Chionoecetes opilio*) is a newly established species in the Barents Sea and was first recorded in May 1996 on the Goose Bank area (Strelkova, 2016). Since then, it has increased in both distribution and abundance. In 2012 commercial harvesting of the snow crab started.

Annual monitoring of the snow crab population began with the Norwegian and Russian Barents Sea Ecosystem Survey (BESS) in 2004. While new dedicated snow crab surveys are under development BESS hold the longest time-series on snow crab population status in the Barents Sea.

The snow crab data from BESS are quite variable but indicate that the snow crab population is still developing both in distribution and abundance (Table A5.4 and Figure A5.45).

Table A5.4: The total and mean catches (per nautical mile) of snow crab during BESS in 2005–2021.

Year	Total number of stations	Number of stations with snow crab	Total catch, ind.	Total catch, kg	Mean abundance, ind./nm	Mean biomass, kg/nm
2005	649	10	14	2.5	1	0.3
2006	550	28	68	11	3	0.5
2007	608	55	133	18	3	0.4
2008	452	76	668	69	11	1.2
2009	387	61	276	36	6	0.8
2010	331	56	437	22	10	0.5
2011	401	78	6219	154	99	2.4
2012	455	116	37072	1169	395	12.6
2013	493	131	20357	1205	210	12.7
2014	304	78	12871	658	206	10.5
2015	335	89	4245	378	57	5.2
2016	317	84	2156	137	26	1.9
2017	376	159	25878	1422	147	10.0
2018*	217	61	19494	846	393	16.7
2019*	323	87	15523	608	145	6.6
2020	461	141	4403	436	38	3.7
2021	341	105	1705	110	20	1.2

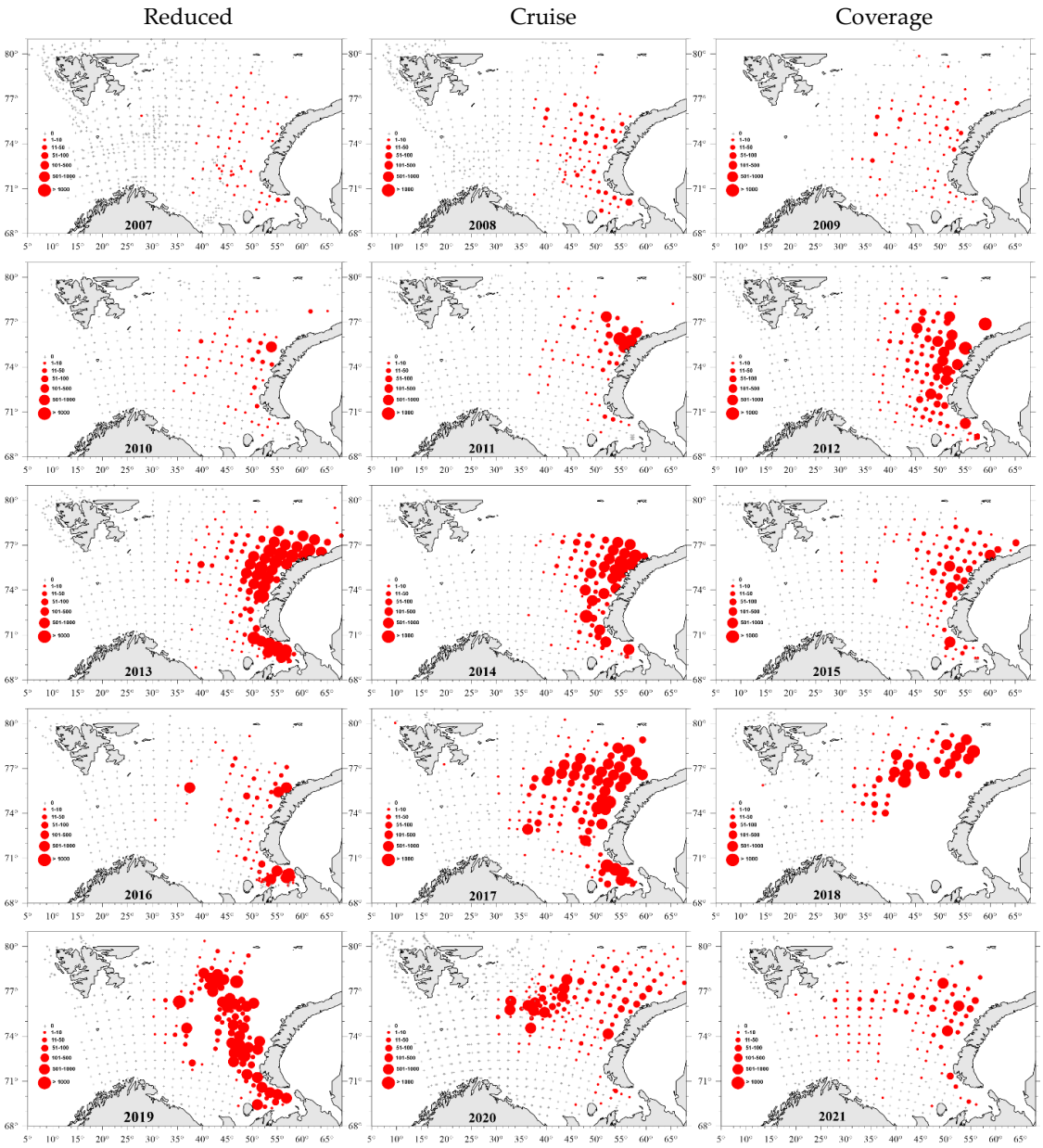

Figure A5.45: Catches of snow crab in the Barents Sea derived from the Barents Sea ecosystem survey (BESS) data from 2007 to 2021. Snow crab density is expressed as the number of crabs per nautical mile. Reduced cruise coverage in 2018 and 2019.

In 2021 Northeastern part of the Barents Sea wasn't covered by the survey, but most likely distribution of snow crab in this area is unchanged compared with the distribution in 2020 (Figure A5.46).

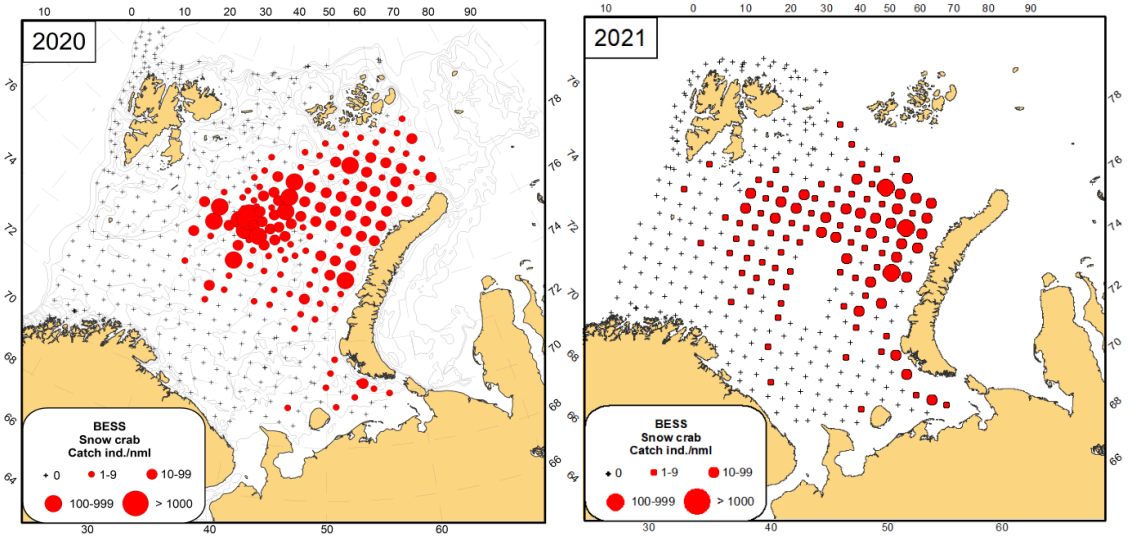

Figure A5.46: Catches of snow crab (*Chionoecetes opilio*) in the Barents Sea in August–October 2020–2021 (BESS data). The catches can also represent the distribution of snow crab in the Barents Sea.

Size structure of the snow crab population indicate variable recruitment pulses. During the ecosystem survey period, abundant generations were recorded with 3 years' interval - in 2009, 2012, and 2015–2016, 2017–2020 (Figure A5.47, Bakanev and Pavlov 2021, 2022).

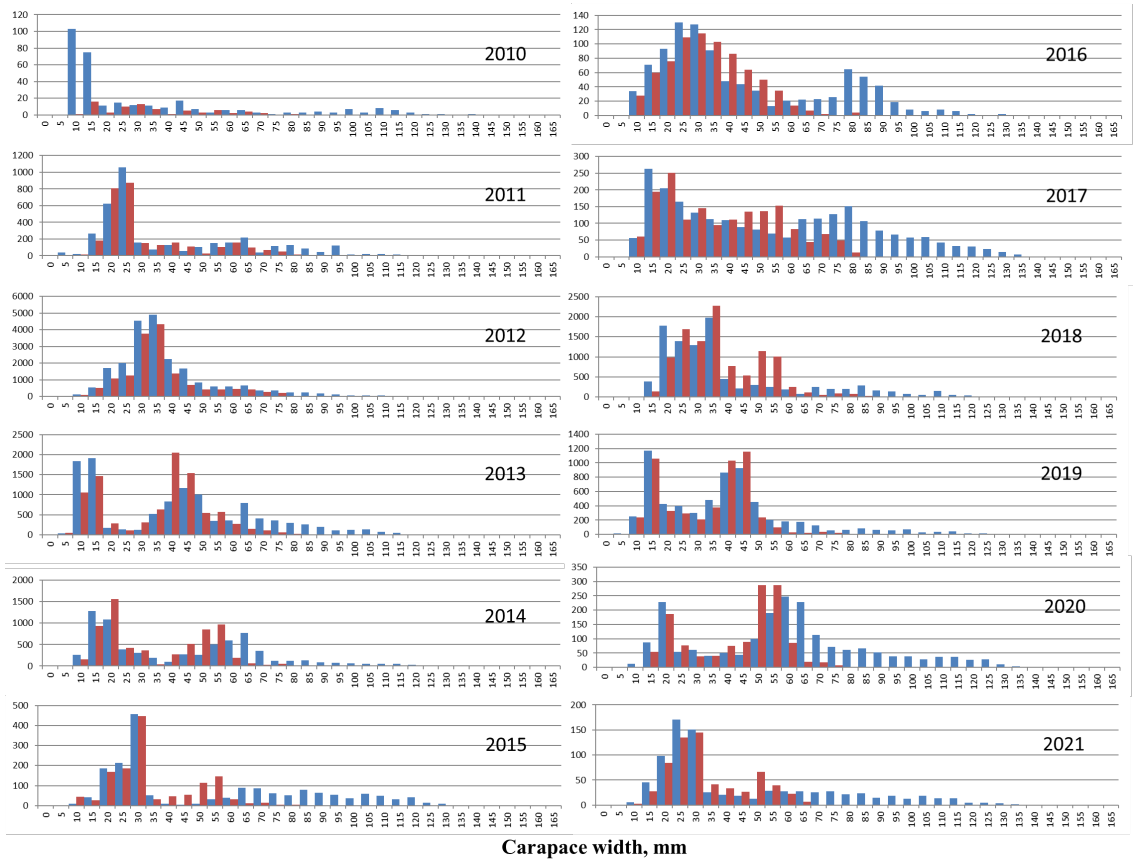

Figure A5.47: The sex and size structure of the snow crab population from 2010–2021 (Bakanev and Pavlov, 2021, 2022, with editions), number of individuals on the *y-axis*.

Since 2003, snow crabs in the eastern part of the Barents Sea, have been recorded in stomachs of demersal fish species (cod, haddock, catfish, and thorny skate). A study by Holt *et al.* (2021)

shows that the snow crab is a new prey item for cod. However, it does not represent an important component of their diet, less than <10% in the period examined (2003–2018).

Northern shrimp

Northern shrimp (*Pandalus borealis*) is common and widely distributed in the Barents Sea, with the highest densities on muddy flats at a bottom depth of 250–350 m and temperatures between -0,5 – 1,5°C (Figure A5.47).

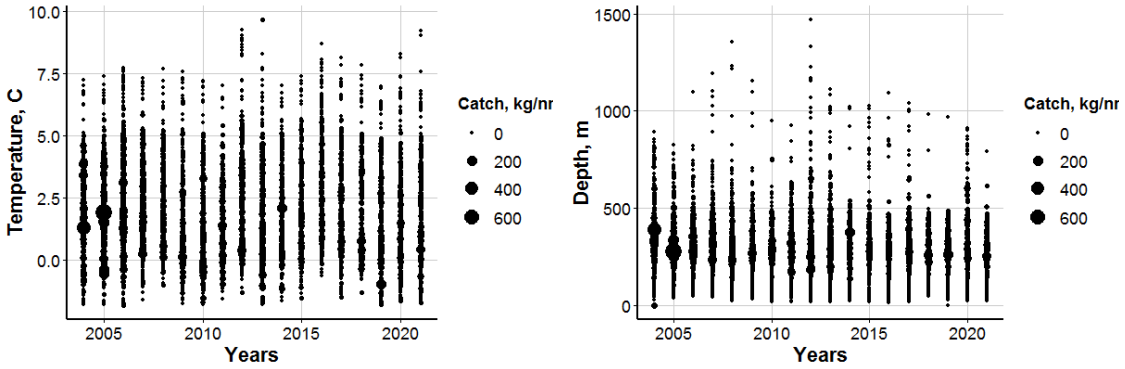

Figure A5.47: Mean biomass (kg per nautical mile) per bottom temperature (C°) and depth (m) in the Barents Sea during BESS 2005–2021 (S.V. Bakanev, C. Hvingel, 2022, in print).

During the survey in 2021 341 trawl hauls were completed – 275 of them contained northern shrimp. The biomass of shrimp varied from several grammes to 129.1 kg/nml with an average catch of 6.2±0.7 kg nml (Figure A5.48).

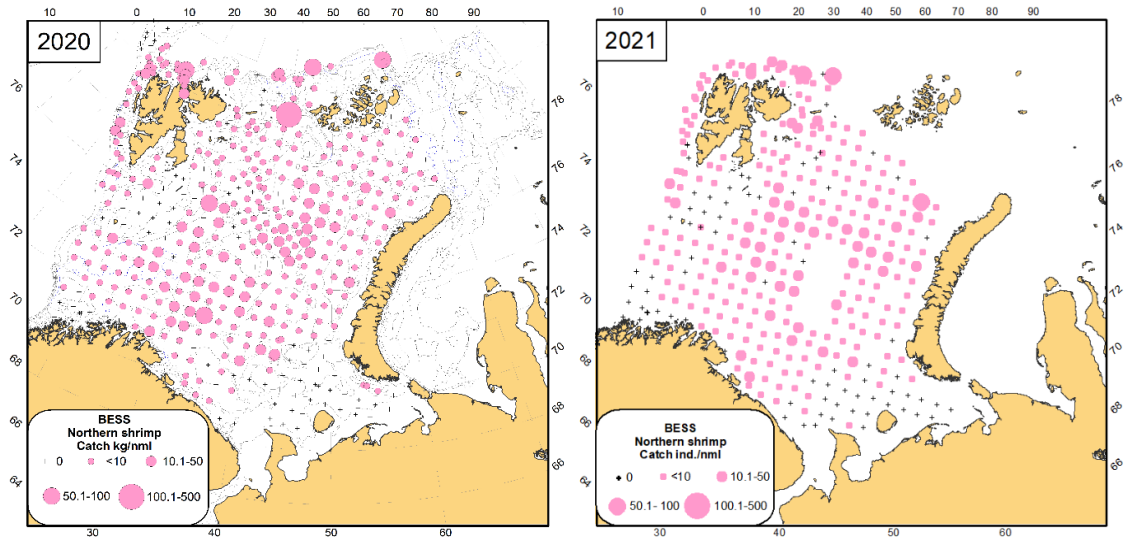

Figure A5.48: Distribution of the Northern shrimp (*Pandalus borealis*) in the Barents Sea, August–October 2020 and 2021 (S.V. Bakanev, C. Hvingel, 2022, *in print)*.

During the BESS 2006–2020 average catches of the shrimp varied from 4 to 11 kg (Figure A5.49), all stayed stable around the average level. Some of the observed variation may related to inconsistencies in survey coverage.

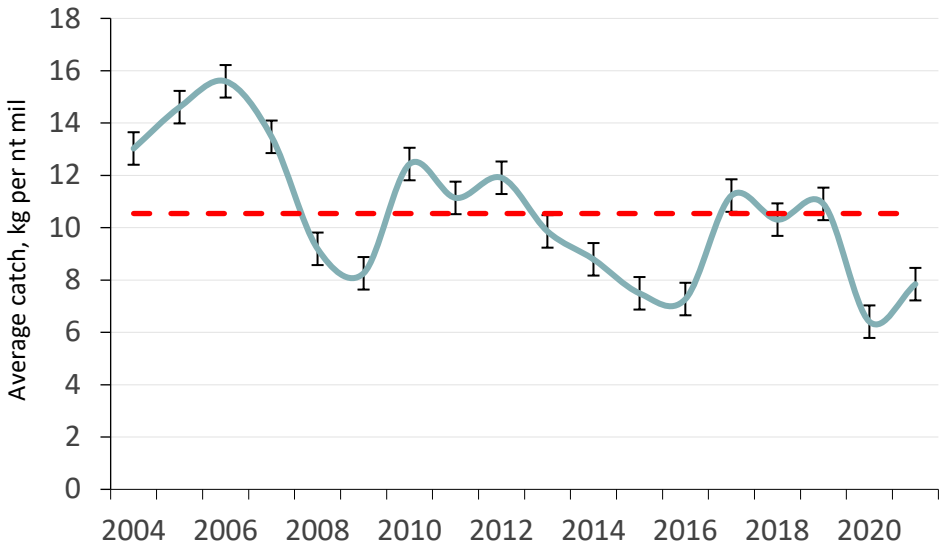

Figure A5.49: Mean catches of the Northern shrimp (*Pandalus borealis*) in the Barents Sea during the BESS 2006–2018. The red line shows mean value over all years.

Biological analyses of the northern shrimp population in the eastern part of the BESS were conducted in 2018 by Russian scientists. Similar to 2017, the bulk of the population consisted of younger individuals: males of 12–27 mm carapace length; and females of 17–30 mm carapace length (Figure A5.50).

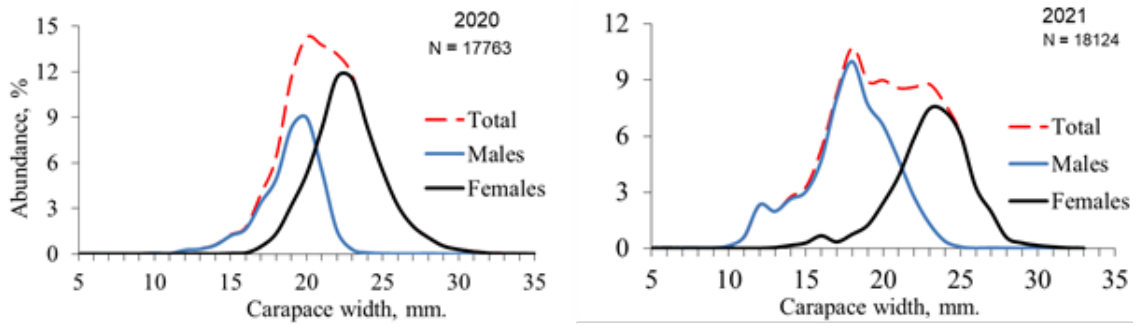

Figure A5.50: Size and sex structure of catches of the Northern shrimp (*Pandalus borealis*) in the eastern Barents Sea, August–October 2020–2021 (S.V. Bakanev, C. Hvingel, 2022).

References

Holt, R. E., Hvingel, C., Agnalt, A. L., Dolgov, A. V., Hjelset, A. M., and Bogstad, B. 2021. Snow crab (*Chionoecetes opilio*), a new food item for North-east Arctic cod (*Gadus morhua*) in the Barents Sea. Ices Journal of Marine Science, 78: 491-501.

Bakanev S.V, Pavlov V.A. Snow crab. State of biological resources of the Barents and the White seas and the North Atlantic in 2020, 2021

Bakanev S.V, Pavlov V.A. Snow crab. State of biological resources of the Barents and the White seas and the North Atlantic in 2021, 2022 – in print

Bakanev S. V., C. Hvingel. Northern shrimp (Pandalus borealis) in: Survey report from the joint Norwegian/Russian ecosystem survey in the Barents Sea and the adjacent waters August-October 2021 / D. Prozorkevich, G.O. Johansen, A. Trofimov, R. Ingvaldsen [et al.]; ed.: D. Prozorkevich, G.I. van der Meeren ; IMR, PINRO. - Bergen: IMR, 2022. – in press

Pelagic fish

By D. Prozorkevich (PINRO), E. Eriksen (IMR), B. Bogstad (IMR), T. Prokhorova (PINRO), H. Gjøsæter (IMR), G. Skaret (IMR)

Total biomass

Zero-group fish are important consumers of plankton and are prey for predators (larger fish, seabirds and marine mammals) and, therefore, are important for transfer of energy between trophic levels in the ecosystem. Estimated total biomass of 0-group fish species (cod, haddock, herring, capelin, polar cod, and redfish) varied from a low of 44 thousand tonnes in 1987 to a peak of 2.91 million tonnes in 2004 with a long term average of 1.2 million tonnes (Figure A5.51). In 2021, estimated total biomass of 0-group fish species was close to 1 million tonnes, which is slightly below the long term mean. In 2021, the biomass of 0-group fish was higher than in 2018–2020 and was dominated by cod, haddock and herring. The biomass of polar cod and capelin were underestimated due to lack of coverage (see above) and were very low in 2021. For more information about re-calculation of 0-group abundance and biomass indices see "Fish Recruitment" by Eriksen *et al.* 2022 in the BESS survey report.

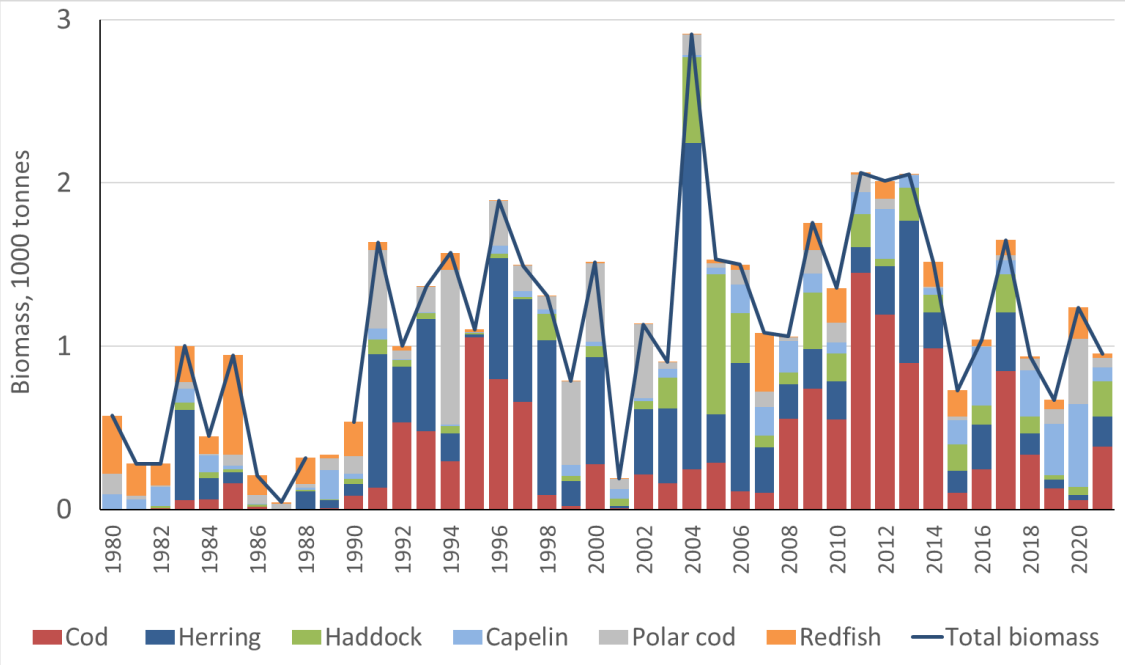

Figure A5.51: Biomass of 0-group fish species in the Barents Sea, August–October 1980–2021.

Capelin, young herring (age 1–4), and polar cod constitute the bulk of pelagic fish biomass in the Barents Sea. During some years (e.g. 2004–2007 and 2015–2016), blue whiting (*Micromesistius poutassou*) also had relatively high biomass in the deeper, western parts of the Barents Sea. Total biomass of the main pelagic species during 1986–2021 fluctuated between 0.5 and 9 million tonnes; largely driven by fluctuations in the capelin stock (Figure A5.52). During 2014–2020, the cumulative biomass of capelin, herring, polar cod, and blue whiting was below the long term average, while in 2021 the cumulative biomass was above the average, and at the same level as in the period 2004–2013.

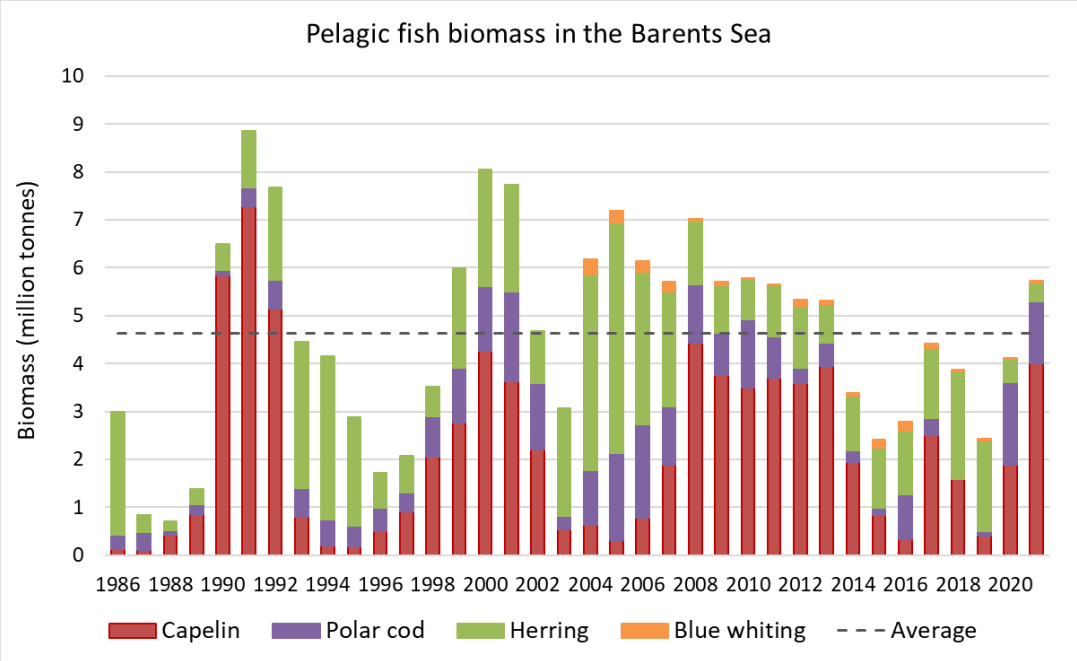

Figure A5.52: Total biomass of pelagic fish component (excluding 0-group) in the Barents Sea in 1986–2021.

Capelin

Young-of-the-year

Estimated abundance of 0-group capelin varied from 958 million in 1993 to 1.5*1012 individuals in 2019 with a long term average of 366*109 individuals for the 1980–2021 period (Figure A5.53). A record strong year class of capelin occurred in 2019, followed by less strong (2020) and intermediate (2021) year classes. In 2021, the total abundance index for 0-group capelin was slightly below the long term mean, and estimated biomass of 0-group capelin was 82 thousand tonnes. In 2021, the eastern Barents Sea was not fully covered, where 0-group capelin were also found, and thus abundance and biomass indices were slightly underestimated.

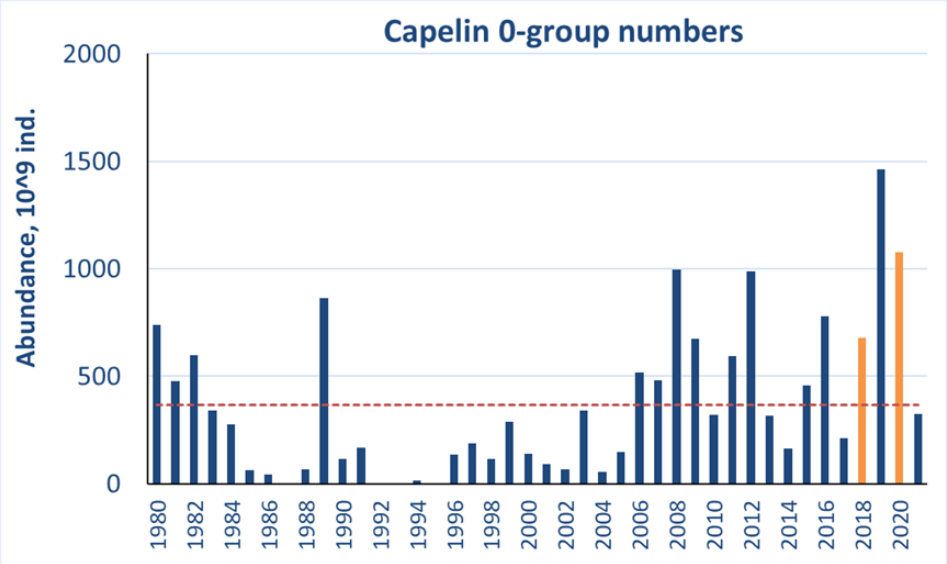

Figure A5.53: 0-group capelin abundance estimates corrected for Keff (blue columns). Red dotted line shows the long term average, while orange columns showed indices that were corrected for lack of coverage.

The highest abundance per strata were found in the north central (Great Bank, $81*10^9$ ind.) and western (Bear Island Trench, $64*10^9$ ind.) areas.

The 0-group capelin body length varied from 1 to 7.5 cm in 2021, while most of capelin were medium size with body length of 3.5 to 5.4 cm. Larger individuals (with an average length above 5 cm) were found mainly in central, western, and southern areas. Small individuals (< 3 cm) were found in the Franz Victoria Trough, Svalbard South and Svalbard North. The smallest (< 3 cm) capelin in the northern areas most likely came from summer spawning. Small capelin (< 3 cm) from summer spawning were also found in the Pechora polygon, where summer offspring have been commonly observed.

Adult capelin

The BESS survey covered well the capelin distribution in 2021 except for the loophole (International waters), and the coverage was synoptical. The geographical distribution of capelin recorded acoustically is shown in Figure A5.54. Capelin had a more northerly distribution in 2021 than in 2020, and concentrations were larger. The more northern distribution likely reflects a higher proportion of bigger capelin in the population (2-year-olds) in 2021 than in 2020 when 1-year-olds were dominating. Like in previous years, the main concentrations were found to the southwest of Svalbard (Spitsbergen) between 76°N and 78°N, which is historically the most typical distribution area for feeding capelin at this time of the year. There were also significant concentrations on the eastern part of the Great Bank where little was found in 2020.

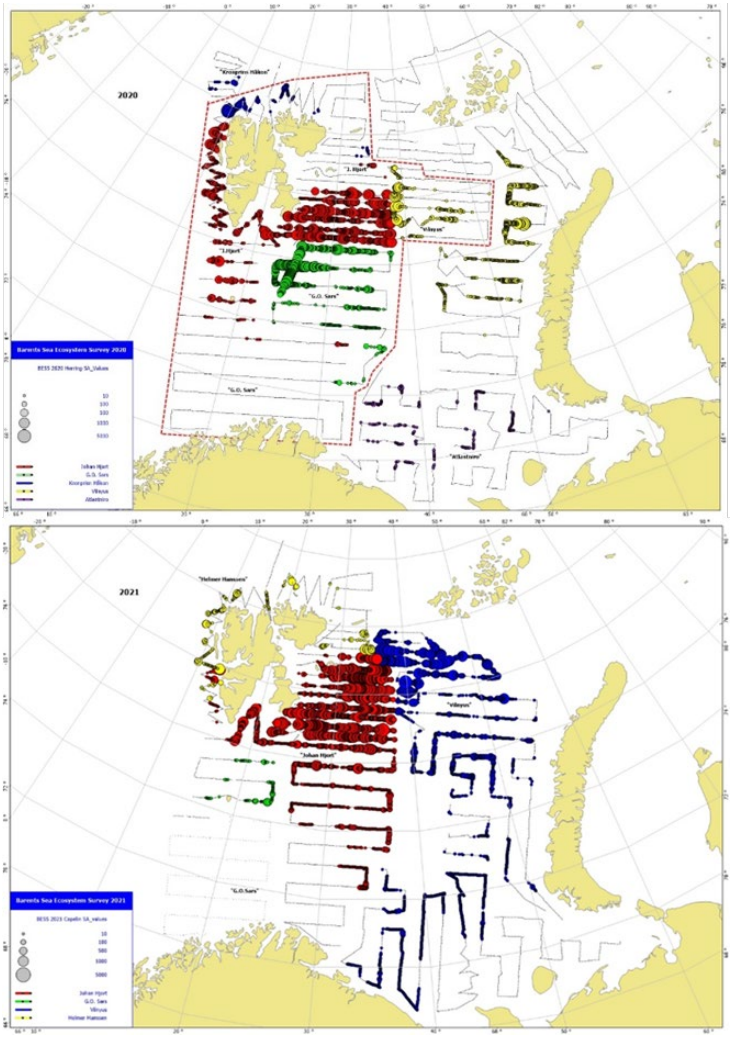

Figure A5.54: Geographic distribution of capelin in 2021 (top panel) and 2020 (bottom panel). Circle size corresponds to s_A (nautical area backscattering coefficient) values per nautical mile. The red dashed line in the figure from 2020 marks the area which had been covered by the time of the capelin assessment on 8 October 2020 before the entire survey had been completed.

Average weight at age was lower than in previous years for all age groups 1, 2 and 3 (Figure A5.55). In particular, it was low for the 2-year-olds which are dominating the capelin biomass. This 2019 year class is the strongest since 2000, and the low growth is likely due to density-dependent effects where the growth goes down due to competition for food (see chapter on trophic interactions).

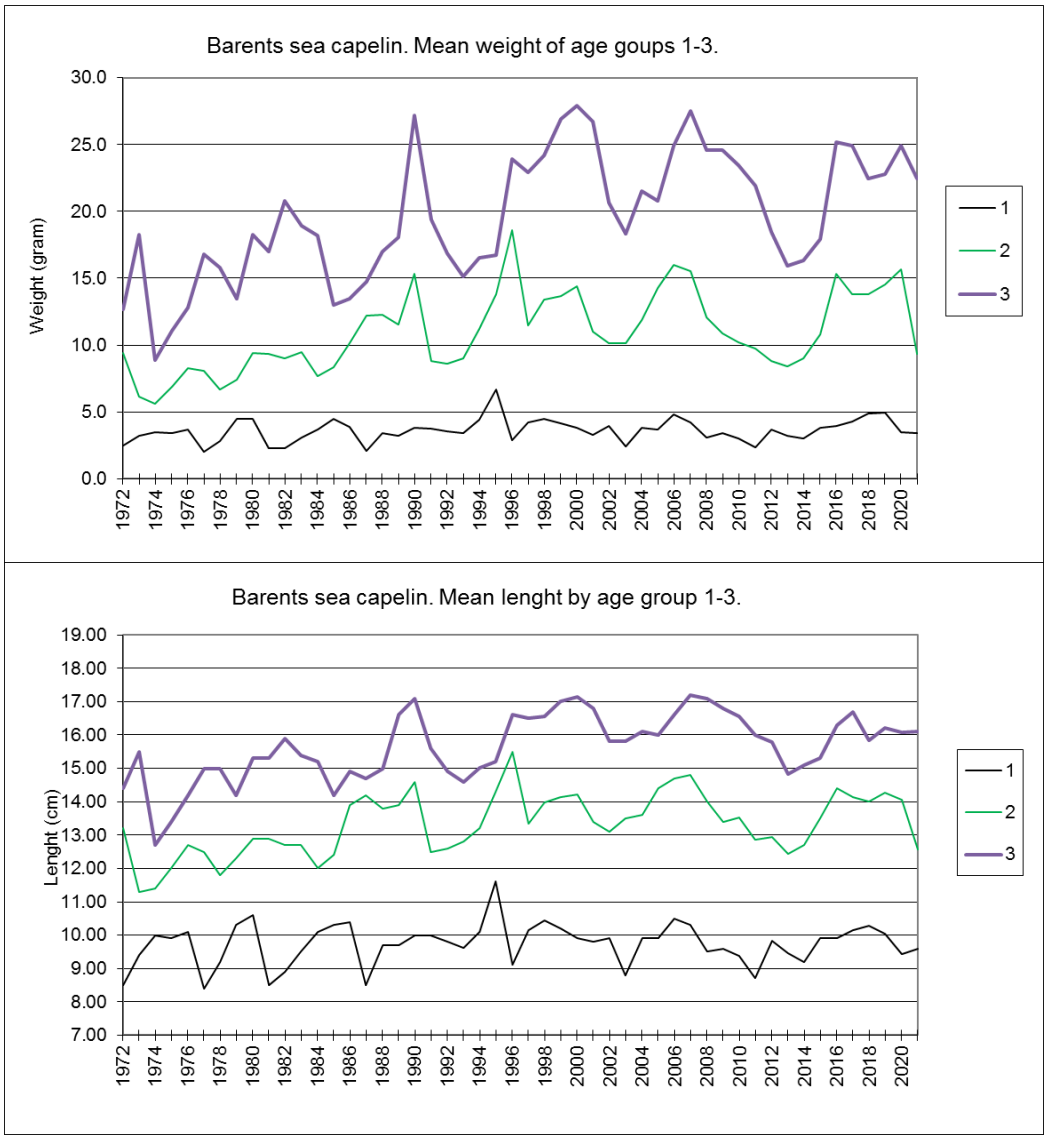

Figure A5.55: Weight (upper) and length (lower) at age for capelin during August–September 1972–2021.

The total stock was estimated to about 4 million tonnes, which is the highest estimated biomass since 2008 and above the long term average level (2.8 million tonnes) (Figure A5.56). About 36% (1.438 million tonnes) of the 2021 stock had length above 14 cm and was therefore considered to be maturing. 2-year old capelin (2019 year class) dominated in the capelin stock both in abundance and biomass, and the abundance of 2-year-olds was the highest since 1991 (Figure A5.57). This agrees well with the observed high abundances of 0-group capelin in 2019 and 1-group in 2020.

Age 1 capelin (2020 year class) were also more abundant than the long term average, which means that there has been two consecutive years of good recruitment after 6 years of poor recruitment.

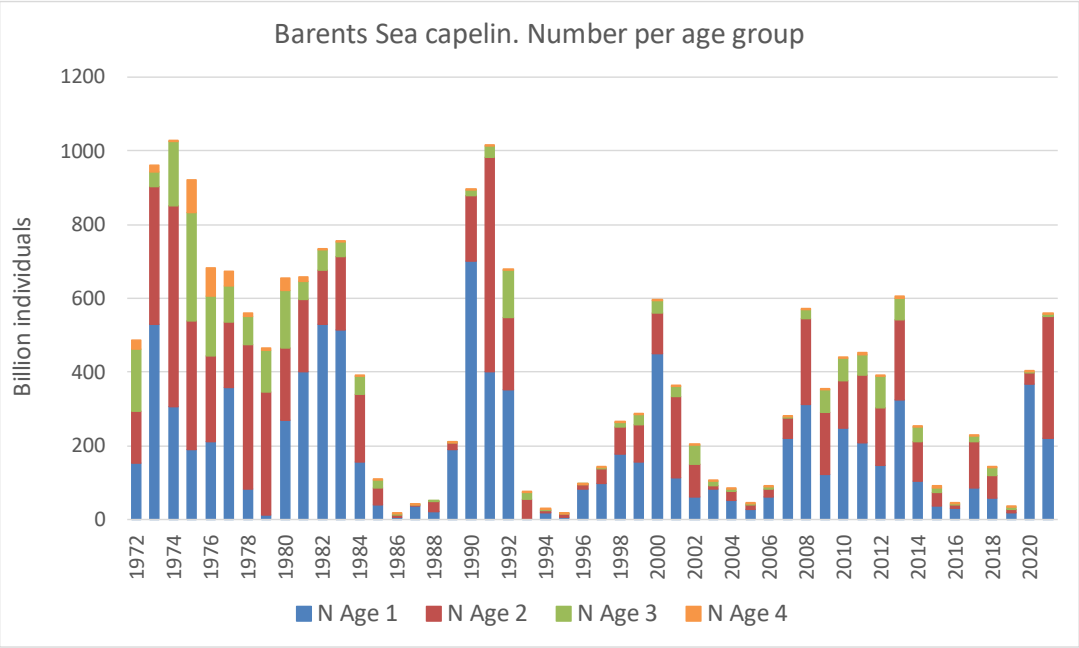

Figure A5.56: Age composition of the capelin stock (age 1–4) during 1972–2021. (Note: abundance of age 5 and older are negligible and have been removed).

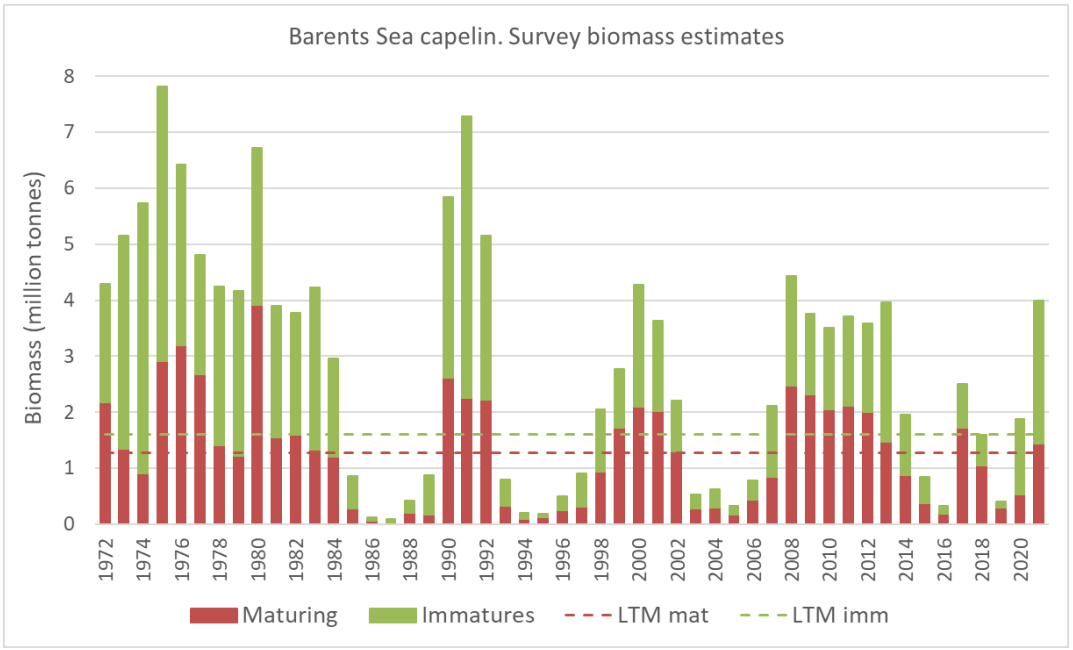

Figure A5.57: Capelin biomass based on the 1972–2021 acoustic survey data: biomass of maturing and immatures, total stock biomass and long term means.

Due to near total spawning mortality, the natural mortality of capelin can be estimated indirectly only. Since fishing mortality for ages 1 and 2 is absent or very small, it can be assumed that the total mortality for these age groups is natural. Figure A5.58 shows natural mortality (M) estimated from the autumn survey as the change in abundance of age 1 capelin in year N to age 2 capelin in year N+1. In some years, negative mortality values were obtained most likely due to underestimation of age 1 fish in the survey showing that there is high uncertainty associated with the method. Negative values are not shown in the plot. This shows that the natural mortality rate has been decreasing in recent years.

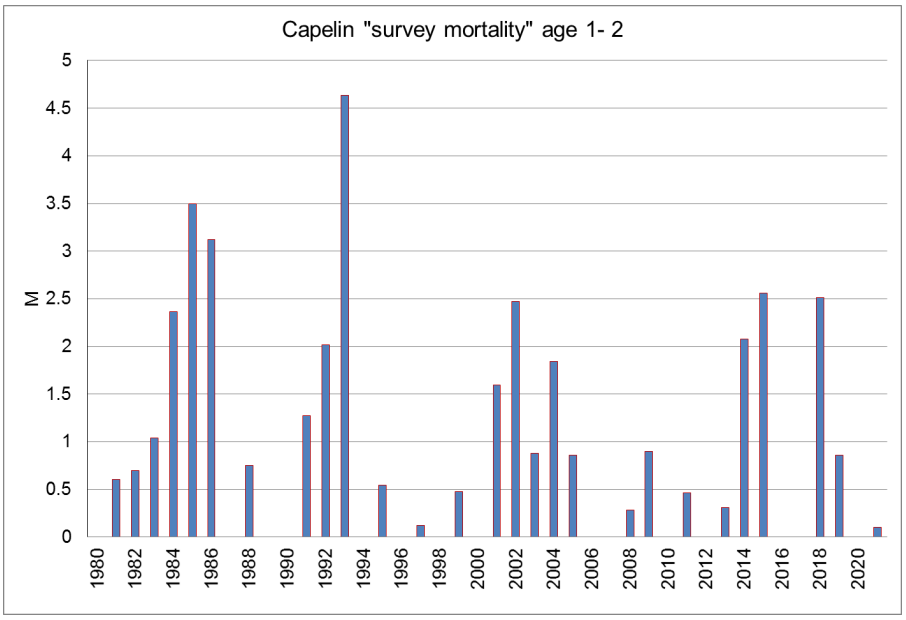

Figure A5.58: Capelin survey mortality from age 1 to age 2 estimated from acoustic survey data. (Negative mortality values are not shown).

Spatial distribution of capelin in the Barents Sea during the feeding period depends on the environment and the composition and size of the stock. Important factors are position of the ice edge, distribution of zooplankton, and capelin stock size and age composition (Ingvaldsen and Gjøsæter 2013). In years with a large stock, capelin is distributed widely. Juvenile capelin is distributed further south than adults. During the 1972 to 1979 period, the capelin stock was large and widely distributed. During 1980 to 1989, the stock size decreased, and distribution was more southward. Since the 2000s, capelin feeding area expanded north- and eastwards. During 2010 to 2017, the stock was in good condition and feeding area expanded significantly northwards into ice-free waters (Figure A5.59). This represented a northward shift in feeding area of 60 to 80 nautical miles compared to the 1970s. During 2018 to 2019, capelin stock size decreased, and the area of distribution decreased correspondingly (Figure A5.60). In 2020 to 2021, the capelin stock size has again increased due to good recruitment, and the distribution has again expanded northwards. In general, during periods of warming in the Barents Sea, capelin move further north and northeastwards to find feeding grounds with high plankton biomass. But at low stock levels and hence lower intraspecific competition for food, shorter migrations are needed for adequate food supply.

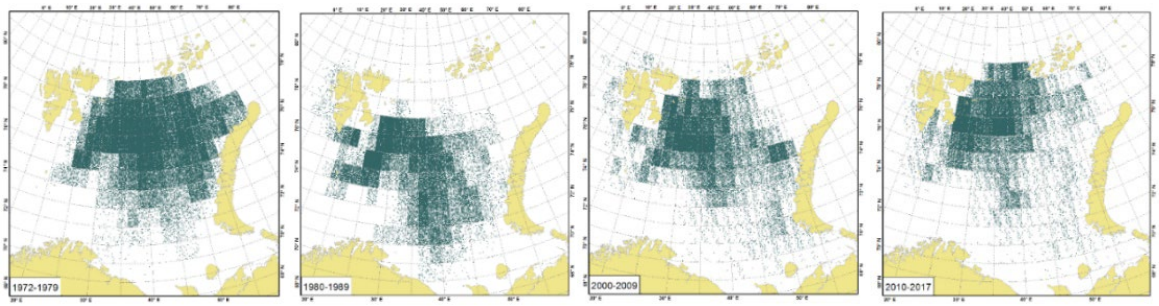

Figure A5.59: Distribution of capelin during August–September by decade (1970s, 1980s, 2000s, and 2010s). Biomasses presented for World Meteorological Organization (WMO) squares system of geocodes which divide areas into latitude-longitude grids (1° latitude by 2° longitude). One dot is equal to 500 tonnes.

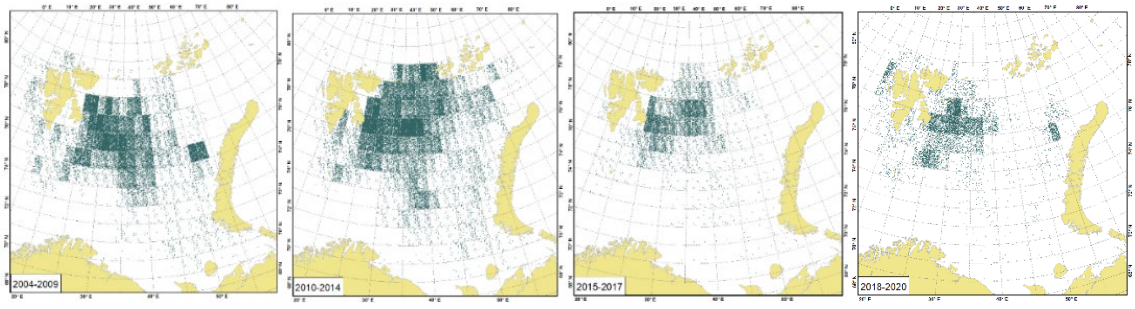

Figure A5.60: Distribution of capelin during August–September for recent periods of high temperature condition and cod stock size. Note that cod abundance peaked in 2013 and that temperature decreased in 2018–2019. Time periods are further broken down into sub-periods (2004–2009, 2010-2014 and 2015–2017 and 2018–2020). Biomass is presented for WMO squares. One dot is equal to 500 tonnes.

Herring

Young-of-the-year

Estimated abundance of 0-group herring varied from $37*10^6$ individuals in 1981 to $774*10^9$ individuals in 2004 with a long term average of $155*10^9$ individuals for the 1980-2021 period (Figure A5.61). In 2021, the total abundance index for 0-group herring was higher to the long term mean and was $209*10^9$ individuals (Figure A5.61). Therefore, the 2021-year class of herring seemed to be intermediate. Estimated biomass of 0-group herring was 184 thousand tonnes. In 2021, the eastern Barents Sea was not fully covered, however zero border of herring distribution were found in the east, and thus it will not influence abundance and biomass indices estimates.

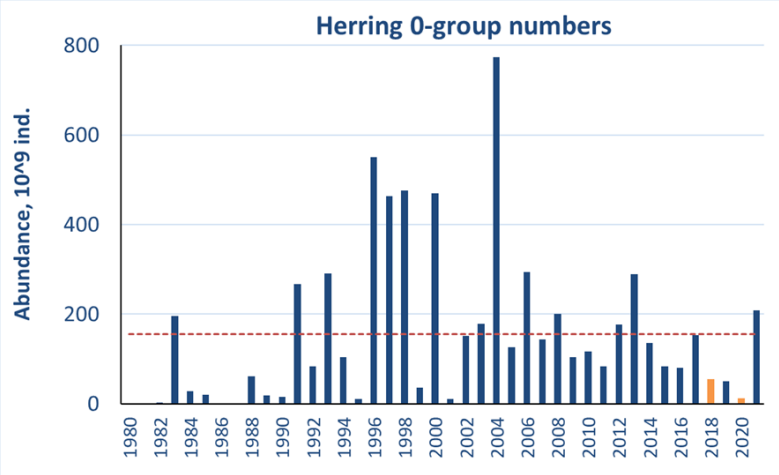

Figure A5.61: 0-group herring abundance estimates corrected for Keff (blue columns). Red dotted line shows the long term average. Abundance of herring in 2018 and 2020 were somewhat underestimated due to lack of coverage in the eastern Barents Sea.

0-group herring were found in the southern Barents Sea. The highest average herring abundance per polygon ($116*10^9$ individuals) of average fish size (5.6 cm) were found in the Southwest polygon.

0-group herring length distribution had two peaks (3.5–4.5 cm and 5.0–5.9 cm) in 2021. Larger individuals were observed in the Bear Island Trench, Hopen Deep and Central Bank with average length of 6.0 cm, while smallest in the southeastern areas. This could indicate less sufficient feeing conditions in the southeastern Barents Sea.

Herring age 1 and older

Figure A5.62 shows biomass estimates of age 1 and 2 herring combined in the Barents Sea based on the last ICES assessment for age 2+ herring, assuming M=0.9 for age 1. During 2013–2017, biomass of young herring in the Barents Sea was relatively stable. It increased from 2017 to 2018 mainly due to contribution of the strong 2016 year class, and then decreased to a lower level in 2019–2020 and for 2021 it was estimated to be the lowest since 1988. Figure A5.63 shows herring distribution in 2021 and 2020 with highest amounts in the southwest.

The 2020 estimate was dominated by the 2016 year class (age 4 herring). This year class had decreased drastically in 2021, but since the biomass of other age groups was very low, the 2016 year class still had the highest biomass of the age groups. Neither the abundance of age 1–2 as shown in Figure A5.62 nor the abundance estimates from the surveys (June survey and BESS) carried out on young herring give a coherent picture. The estimates from the assessment depend heavily on the assumption of M and also it varies between years whether or not also age 3 herring is present in the Barents Sea. On the other hand, there are not survey data for all years, and they are often inconsistent between years (e.g. the abundance of the 2016- and 2017 year classes in 2020 was higher than the estimates of those year classes in 2019). Thus, an analysis to determine a time-series for young herring abundance in the Barents Sea, taking all data sources into account, should be given high priority.

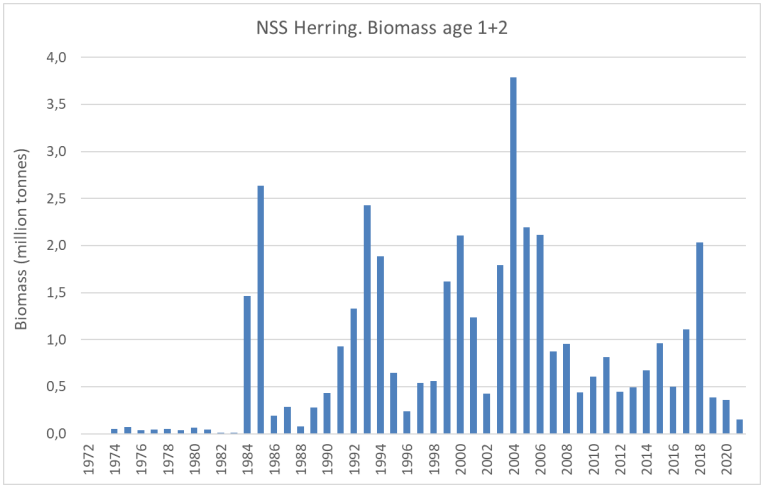

Figure A5.62: Estimated biomass of Norwegian Spring-spawning herring Age 1 and 2 in the Barents Sea – based on Working Group on Widely Distributed Stocks (WGWIDE) assessment (ICES 2021).

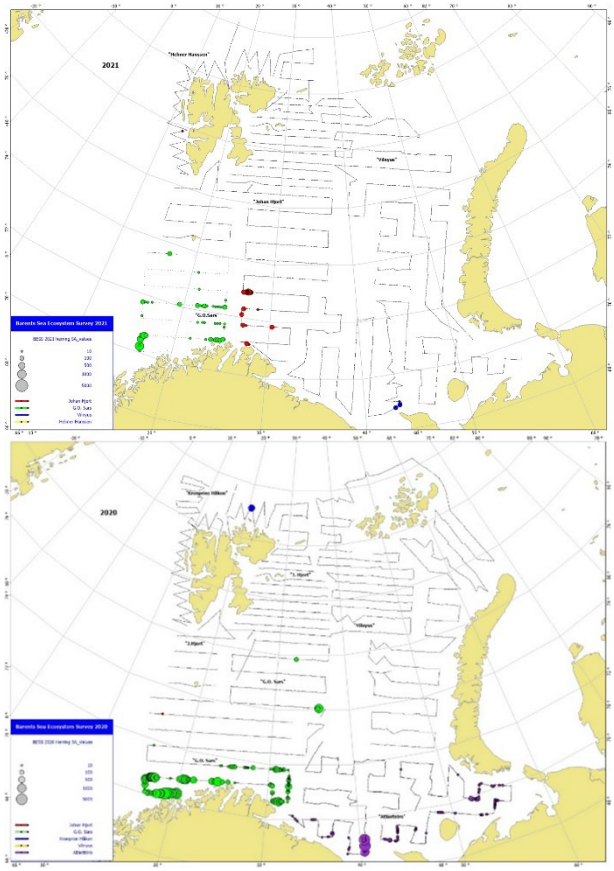

Figure A5.63: Estimated distribution of herring in August–October in 2021 (top panel) and 2020 (bottom panel). Circle sizes correspond to s_A (nautical area backscattering coefficient) averaged over 1 nautical mile.

Polar cod

Polar cod is an Arctic species with a circumpolar distribution. Historically, the world's largest population of this species has been observed in the Barents Sea. In recent years, there have been significant fluctuation of the polar cod stock size.

Young-of-the-year

Estimated abundance of 0-group polar cod varied from 201*10^6 million in 1995 to 2189*10^9 individuals in 1994 with a long term average of 315*10^9 individuals for the 1980 to 2021 period (Figure A5.64). In 2021, the total abundance index for 0-group polar cod was lower than the long term mean and was 136*10^9 individuals (Figure A5.64). The eastern component has been dominated in abundance and biomass during 1980, 1990 and early 2000s. Low abundance of 0-group cod in the traditional core area, southeastern Barents Sea, is most likely due to redistribution of spawning sites out of the Barents Sea and into the western part of Kara Sea. This is indirectly confirmed by 2019 to 2020 studies in the Kara Sea, where a significant amount of the mature polar cod was found.

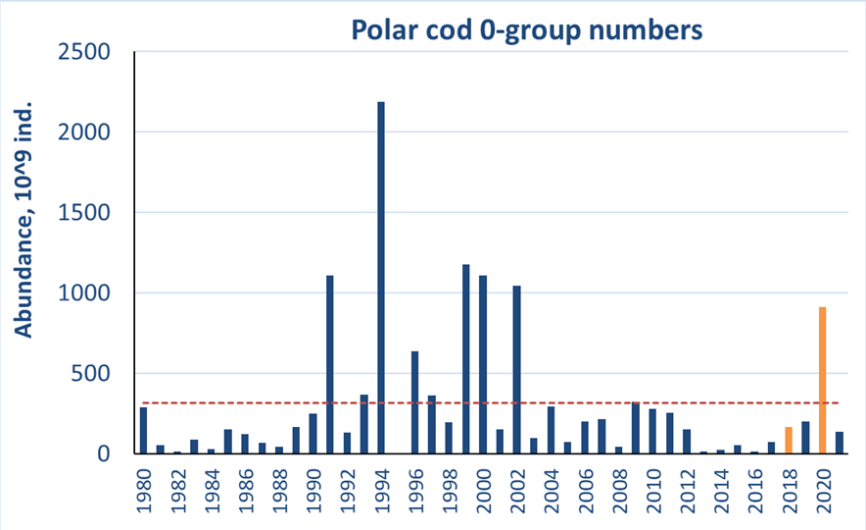

Figure A5.64: 0-group polar cod abundance estimates corrected for Keff for the period 1980–2021 (blue columns). Red horizontal line shows the long term average, while orange column shows indices that were corrected for lack of coverage.

Polar cod were found around the Svalbard (Spitsbergen) archipelago in 2021. Coverage of the 0-group polar cod was not complete, especially in the northern and eastern parts of the Barents Sea, and thus southeastern component of polar cod could not fully be presented here.

The largest polar cod with an average length of 5.4 cm were observed in the Svalbard North polygons, while smallest with an average length of 2.9 cm were observed in the Pechora polygon. Polar cod, like herring, had most likely a worse feeding condition in the southeastern Barents Sea.

Adult polar cod

From 2010 to 2019 there seemed to be a general decrease in biomass of polar cod in the Barents Sea (Figure A5.65). In particular, the abundance of age groups >1 seemed to decrease, but the strong year class of 2015 gave a short-term increase in polar cod stock biomass in 2016, before the stock size decreased again. In 2020, there was a strong increase in polar cod abundance, and abundance of 1-year-olds and overall abundance were the highest on record. Also, in 2021, the overall abundance was high, with high abundance of 1-year-olds and 2-year-olds. The Barents Sea Ecosystem Survey is not designed to cover the entire population of polar cod, so changes in abundance and biomass can result from changes in abundance and/or changes in distribution. In 2020, the survey covered a larger area than normal, extended further north and further east and was also conducted later in the season. But the main concentrations of polar cod were found within the standard coverage area (Figure A5.66). In 2021, the survey coverage was similar as in years prior to 2020, so there is no doubt that the increase in polar cod abundance in the Barents Sea in the recent two years is real, and not an artefact of survey coverage. The main distribution

of polar cod was found in the northeastern parts of the survey area around Franz Josef Bank which is typical, but polar cod were also abundant west of 35°E, to southeast of Svalbard (Spitsbergen), which was observed also in 2020, but not for a long time before that.

The total stock was estimated to be 1299 thousand tonnes. The biomass was dominated by 2-year-olds, but abundance of 1-year-olds was above average and similar to the abundance of 2-year-olds. The 2020 polar cod biomass estimate was one of the highest on record, and also the 2021 estimate was above average. It should be noted that in 2020, most of the sea in the northeast was surveyed.

There is a high variability in polar cod recruitment (Figure A5.64 and Figure A5.65) which affects polar cod biomass. The polar cod recruitment is linked to temperature and sea ice conditions (Huserbråten *et al.* 2019; Bouchard *et al.* 2017). A decrease in recruitment is expected with decreasing ice coverage, but a transient period of increasing biomass was predicted by Bouchard *et al.* (2017) for polar cod in Canadian waters due to earlier ice break-up and enhanced larval survival. Variability in cod distribution and consumption of polar cod may also influence polar cod population size.

It is obvious that polar cod populations of the Barents Sea and Kara Sea are linked. The distribution of the 0-group polar cod in the Barents Sea shows that it is very likely that the 0-group polar cod from spawning grounds in the southwest part of Kara Sea are brought into the Barents Sea through the Kara strait. Thus, the polar cod population in the Barents Sea may be replenished by "Kara Sea recruits". The last investigation of polar cod in the Kara Sea (Figure A5.67) shows that the TSB of polar cod increased and was estimated at 304 thousand tonnes (Anon, 2019) and the total number of fish aged 3 years and more was 78%.

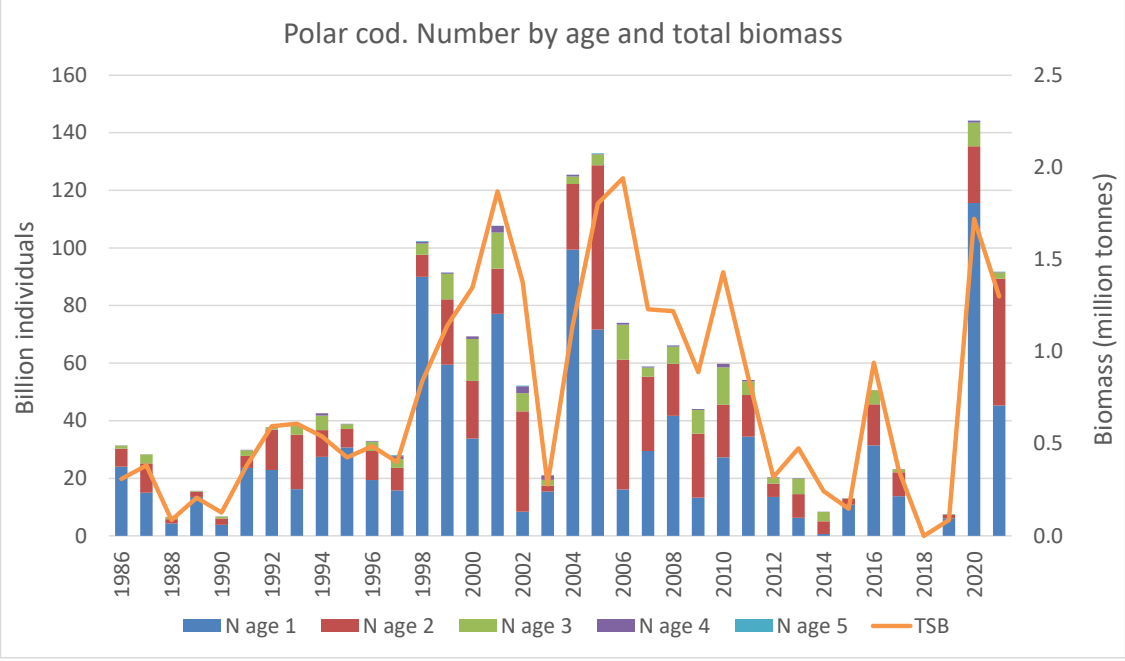

Figure A5.65: Total abundance in billions (coloured bars / left axis) and biomass in millions of tonnes (orange line / right axis) of polar cod in the Barents Sea (acoustic survey and BESS data) collected in August–September during 1986–2021. (For 2003 the values are based on VPA due to poor survey coverage. A reliable estimate is not available for 2018).

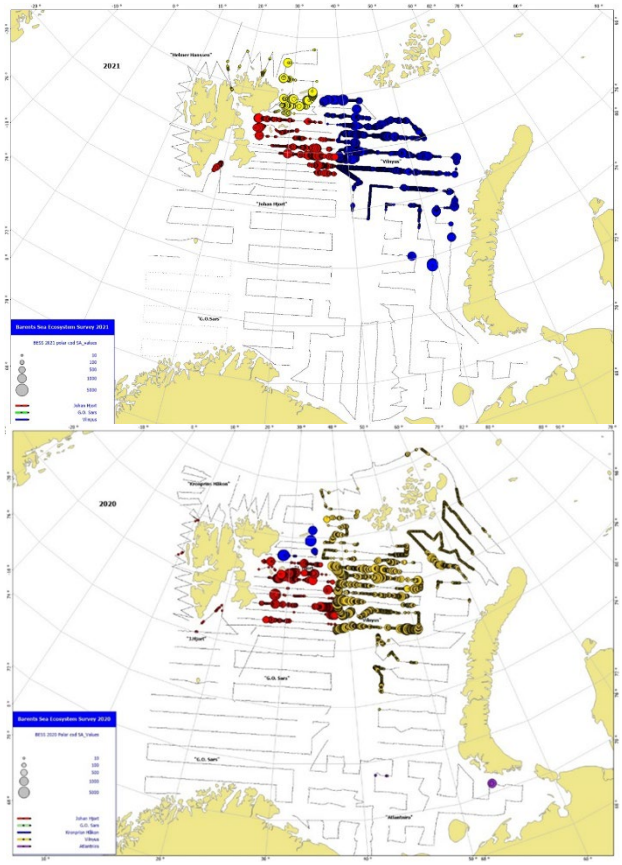

Figure A5.66: Estimated distribution of polar cod during August–October 2021 (top panel) and 2020 (bottom panel). Circle size corresponds to s_A (nautical area backscattering coefficient) values per nautical mile.

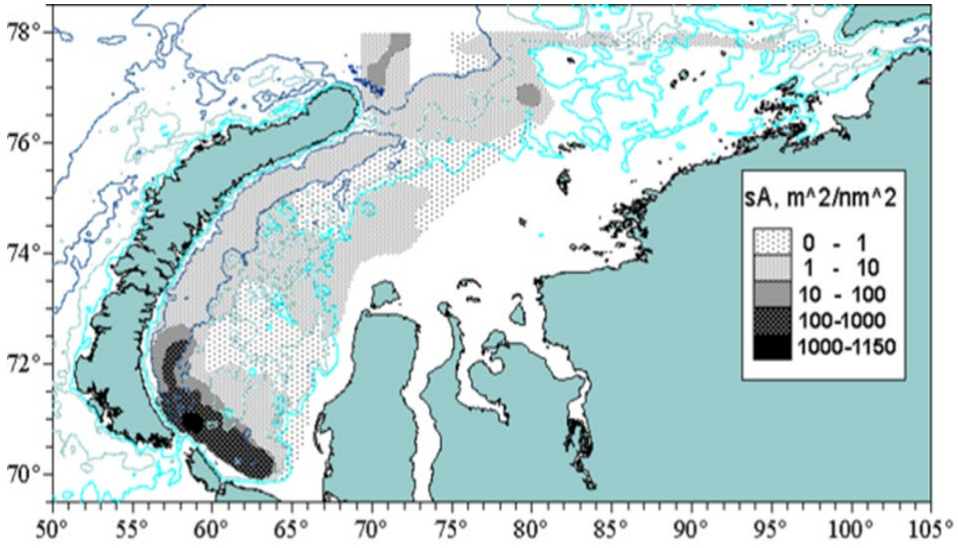

Figure A5.67: Estimated distribution of polar cod in the Kara Sea. Survey RV "Professor Levanidov" 15-29 September 2019. Background area colour correspond to s_A (nautical area backscattering coefficient) averaged over 1 nautical mile.

Blue whiting

Acoustic estimates for the proportion of the blue whiting stock present in the Barents Sea have been made since 2004. In 2017, the BESS data time-series were recalculated using a newer target

strength equation (Pedersen *et al.*, 2011), and a standardized area. The revised estimates were on average about one third of the previous estimates. During 2004 to 2007, estimated biomass of blue whiting in the Barents Sea was >200 000 tonnes (Figure A5.68) but decreased abruptly in 2008 and remained low until 2012. In 2012 and 2013 the strong 2011 year class contributed to an observed increased abundance of blue whiting and in 2015 and 2016 the even stronger 2014 year class contributed largely to the total estimated biomasses >150 000 tonnes in 2015 and 2016 (Figure A5.69). With strong year classes the young blue whiting is abundant along the shelf break to the Norwegian Sea and partly distribute into the Barents Sea. In 2018 to 2020 the blue whiting abundance in the Barents Sea was very low, but abundance increased slightly in 2021 mostly due to the 1-year-olds.

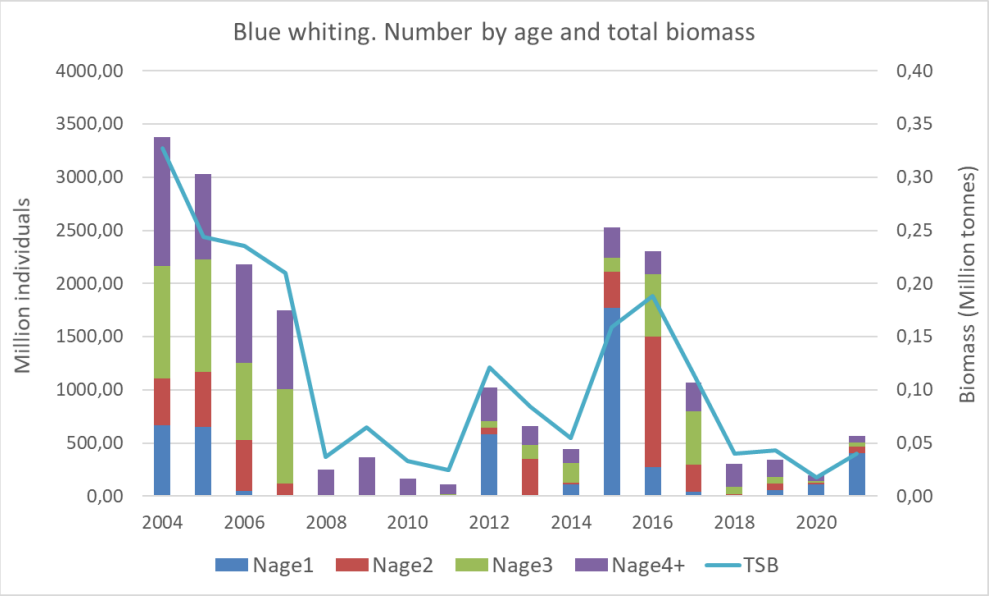

Figure **A5.68: Total abundance in billions (coloured bars / left axis) and biomass in millions of tonnes (blue line / right axis) of blue whiting in the Barents Sea (BESS data revised in 2017) collected in the period August–September during 2004–2021.**

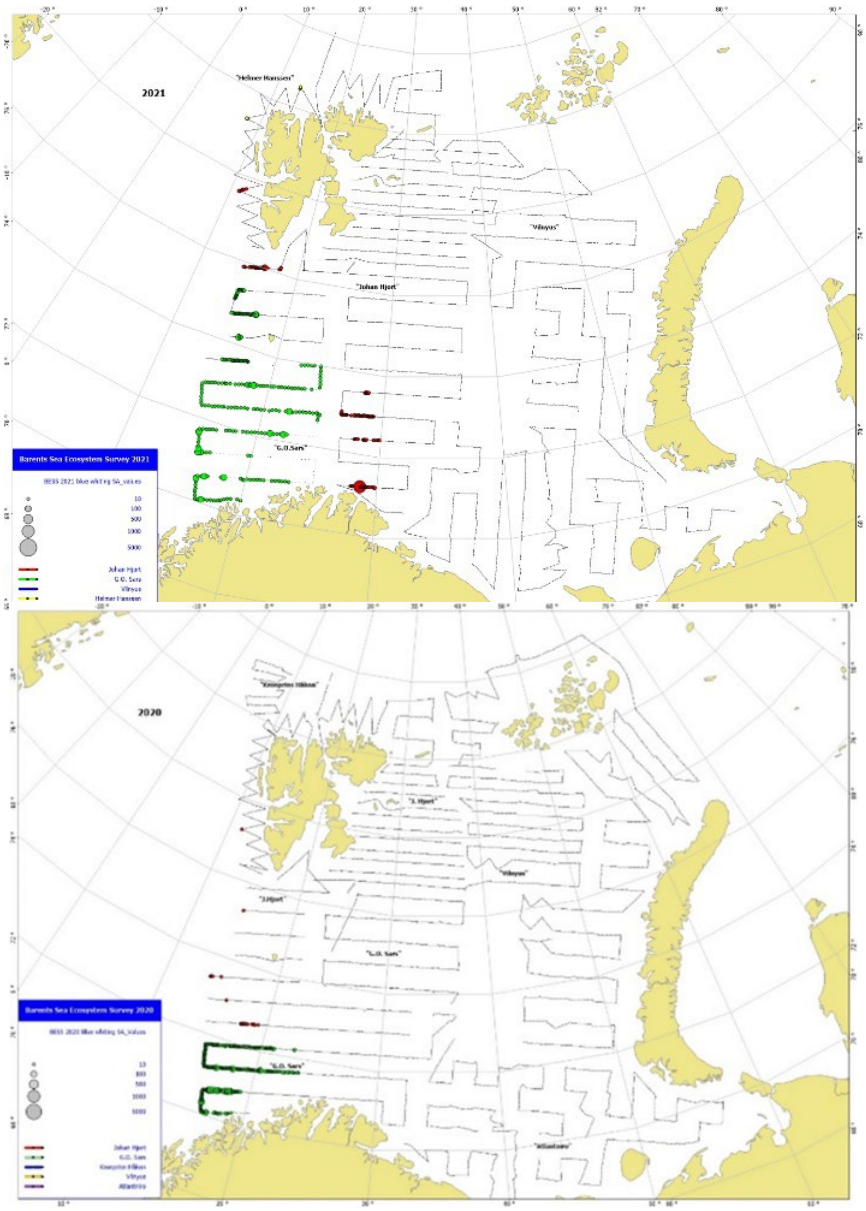

Figure A5.69. Estimated distribution of blue whiting during August–October 2021 (top panel) and 2020 (bottom panel). Circle size corresponds to s_A (nautical area backscattering coefficient) averaged over 1 nautical mile.

References

ICES 2021. 06 Working Group on Widely Distributed Stocks (WGWIDE) Report 2021 - 04 NSSH (Clupea harengus). ICES Scientific Reports. 3:95. 78 pp.

Ingvaldsen, R., Gjøsæter, H., 2013. Responses in spatial distribution of Barents Sea capelin to changes in stock size, ocean temperature and ice cover. *Marine Biology Research*, 9, 867-877.

Pedersen, G., Godø, O. R., Ona, E., and Macaulay, G. J. 2011. A revised target strength–length estimate for blue whiting (*Micromesistius poutassou*): implications for biomass estimates. – ICES Journal of Marine Science, 68: 2222–2228.

Survey report on the multipurpose research of aquatic biological resources on the RV "Professor Levanidov" in the East Siberian, Laptev and Kara Seas during the Transarctic expedition from July 06 to October 02. Moscow 2019. (In Russian.)

Demersal fish

B. Bogstad (IMR), D. Prozorkevich (PINRO), E. Eriksen (IMR), T. Prokhorova (PINRO), A. Russkikh (PINRO), A. Filin (PINRO), E. Johannesen (IMR), P. Krivosheya (PINRO) and Yu. Kovalev (PINRO)

Most Barents Sea fish species are demersal (Dolgov *et al.*, 2011); this fish community consists of about 70 to 90 regularly occurring species, which have been classified into zoogeographic groups. Approximately 25% are either Arctic or mainly Arctic species. The commercial species are boreal or mainly boreal species (Andriashev and Chernova, 1995), except for Greenland halibut (*Reinhardtius hippoglossoides*) that is classified as either Arcto-boreal (Mecklenburg *et al.*, 2013) or mainly Arctic (Andriashev and Chernova, 1995).

Abundance estimates are available for commercial species that are assessed routinely at the ICES AFWG. Figure A5.70 shows such biomass estimates for cod, haddock, beaked redfish and Greenland halibut calculated in 2021. Total biomass of these three species peaked in 2010 to 2013 but remain higher than in the period prior to 2007. Saithe occurs mainly along the Norwegian coast and along the southern coast of the Barents Sea; few occur farther offshore in the Barents Sea itself. The biomass of *Sebastes norvegicus* is fairly low and so we have omitted it from the overview. Other than these main commercial stocks, long rough dab is the demersal stock with the highest biomass. Overall, cod is the dominant demersal species.

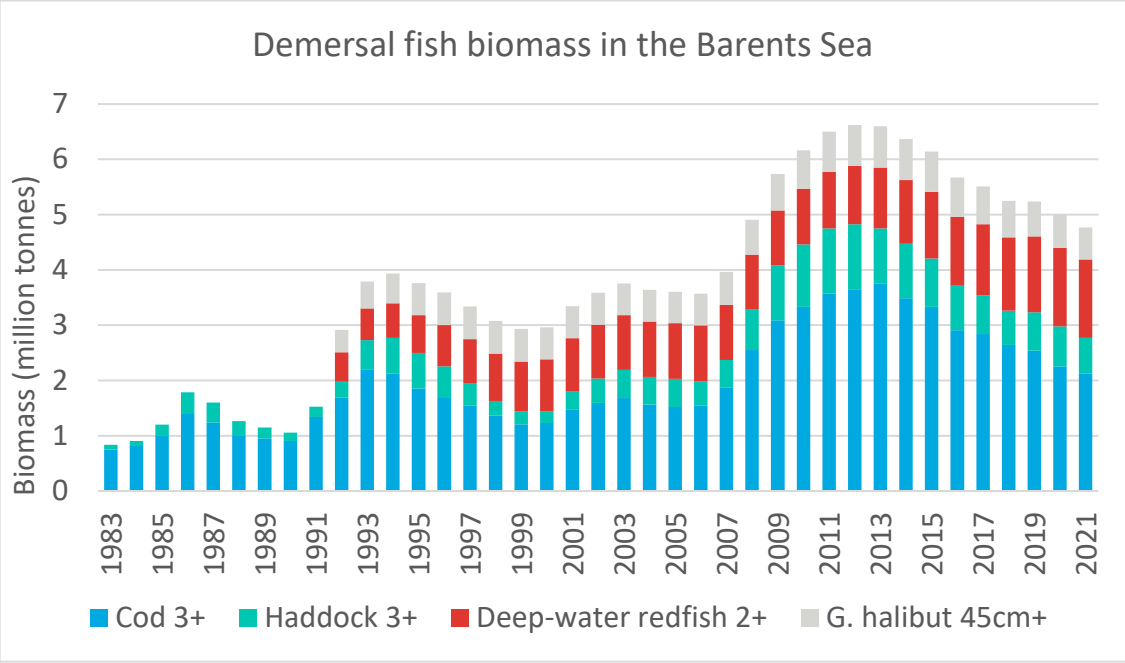

Figure A5.70: Biomass estimates for cod, haddock (1983–2021), beaked redfish and Greenland halibut (1992–2021) from AFWG 2021 (ICES 2021).

Cod

Young-of-the-year

Estimated abundance of 0-group cod varied from 276 $*10^6$ in 1980 to 464$*10^9$ individuals in 2014 with a long term average of 115$*10^9$ individuals for the 1980–2021 period (Figure A5.71). In 2021, the total abundance index for 0-group cod was above the long term mean and was 207$*10^9$

individuals. Cod estimated biomass in 2021 (385 thousand tonnes) was higher than the long term mean for 1980–2021 (340 thousand tonnes).

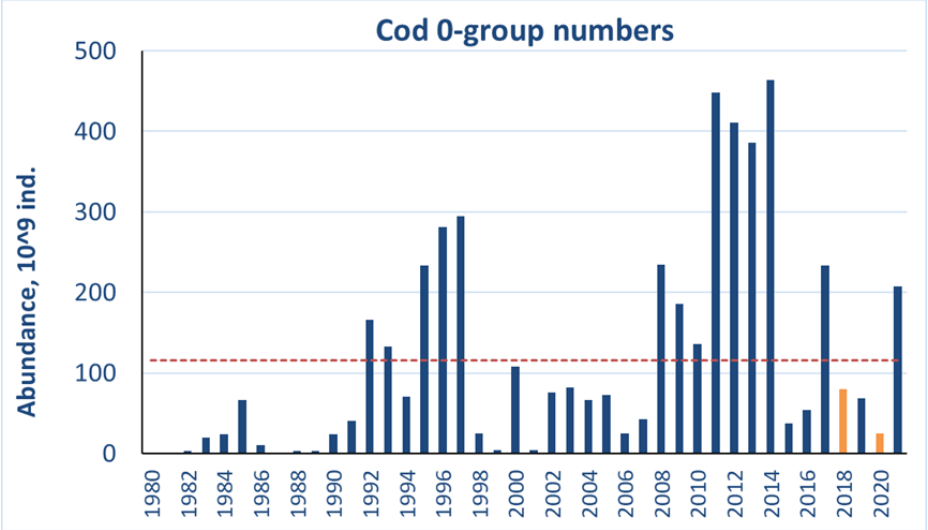

Figure A5.71: 0-group cod abundance estimates corrected for Keff (blue columns). Red dotted line shows the long term average, while orange columns showed indices that were corrected for lack of coverage.

The highest average abundance per polygon were found in the southern (Southeast, $85*10^9$ ind., and Southwest, $53*10^9$ ind.) areas. In 2021, the eastern Barents Sea was not fully covered, where 0-group cod were also found.

In 2021, 0-group cod were dominated by fish of 5.5–7.5 cm length. The largest cod (with an average length > 10.0 cm) were observed in the Southwest followed by fish (with an average length of 8.5–10.0 cm) observed in the Bear Island Trench, while smallest cod (with an average length < 6.0 cm) were found mainly in the Southeast polygons.

Cod one year old and older

The northeast Arctic cod stock is currently in good condition, with average total stock size, and high spawning-stock biomass (Figure A5.72). 0-group abundance was very high in the beginning of the last decade (2011–2014); but this has not resulted in strong year classes, as seen from the recruitment time-series (Figure A5.73) and the updated stock-recruitment plot shown in Figure A5.74.

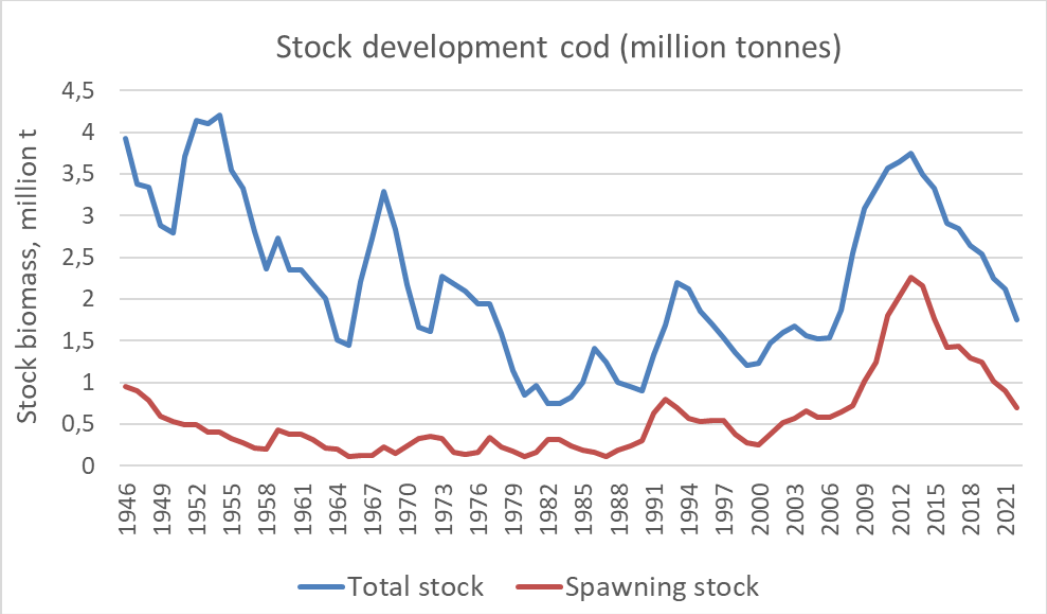

Figure A5.72: Cod total stock and spawning-stock biomass during the 1946–2021 period, including forecast for 2022. From AFWG (ICES 2021).

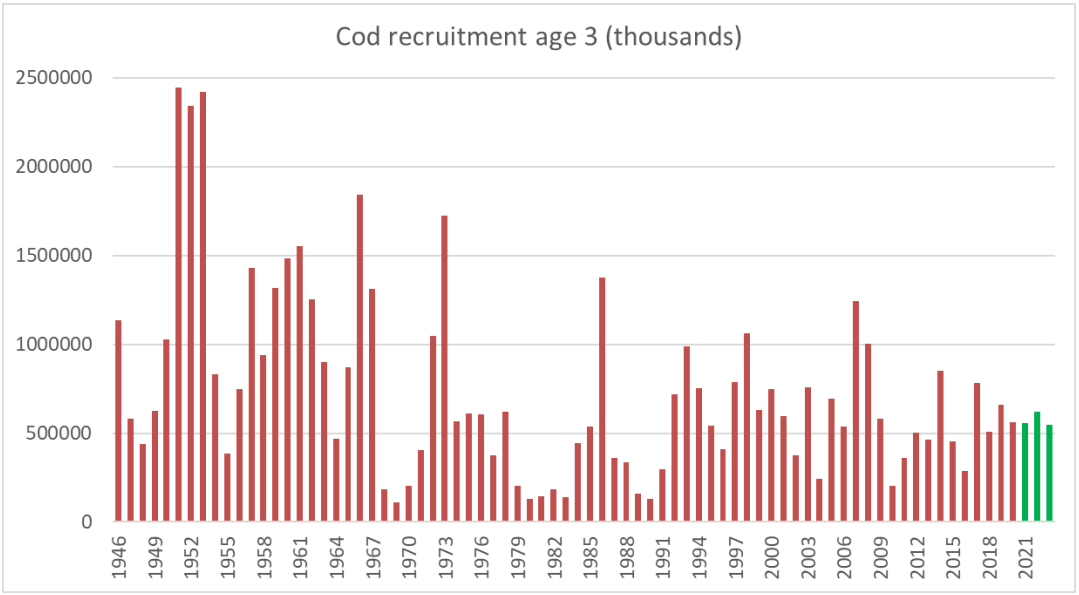

Figure A5.73: Cod recruitment at age 3 during the 1946–2020 period and forecast (green) for 2021–2023 (AFWG, ICES 2021).

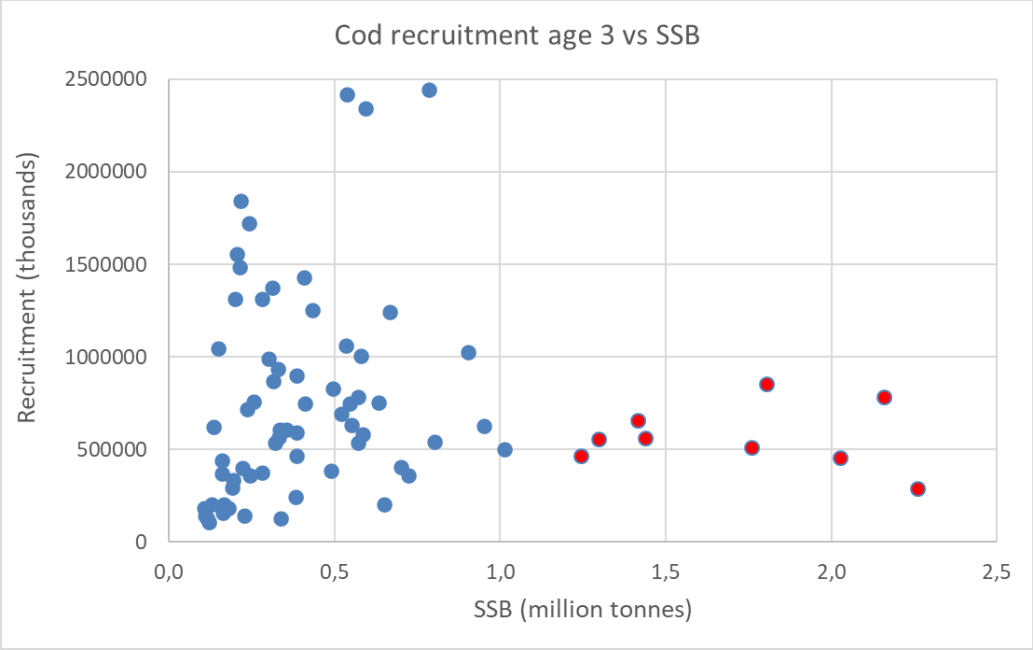

Figure A5.74: Spawning stock-recruitment plot for cod cohorts 1946–2018. Cohorts 2010–2018 shown as red dots.

Strong 2004- and 2005-year classes have, together with a low fishing mortality, led to rebuilding of the cod stock's age structure to that observed in the late 1940s (Figure A5.75).

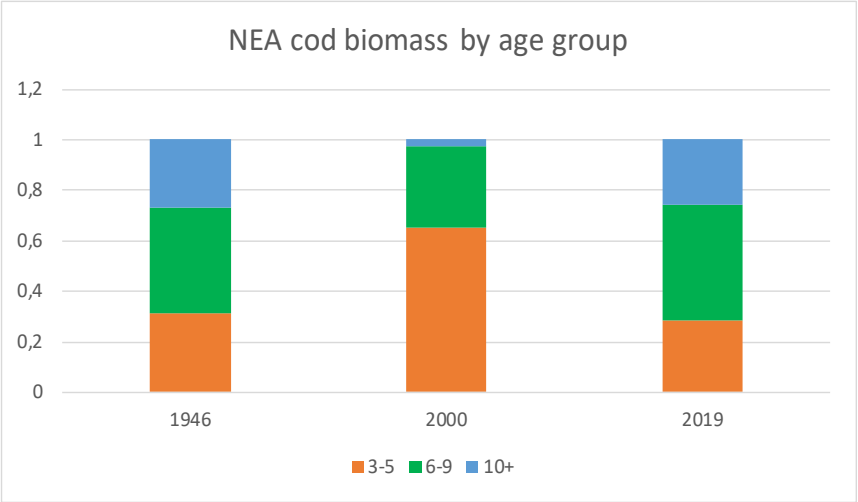

Figure A5.75: Age composition of the cod stock (biomass) in 1946, 2000 and 2019. From stock assessment in ICES 2019.

Cod expanded its distribution area to the north and northeast during the period from 2004 to 2013, while the northern limit of the distribution area in the Barents Sea has shifted considerably southwards again since 2013 (Figure A5.76). This change is likely both related to decreased stock size (Figure A5.72) and lower temperature in the area (Fig A5.10). However, the distribution area along the western and northern coast of Svalbard was stable despite temperature decrease also in this area. The reason for the difference in development between the areas is likely that in the northern Barents Sea the temperature has now fallen below 0°C, while it is still above 0°C NW of Svalbard.

Maps showing the average distribution in three periods (2004–2009, 2010–2014, 2015–2019) are given in last year's report.

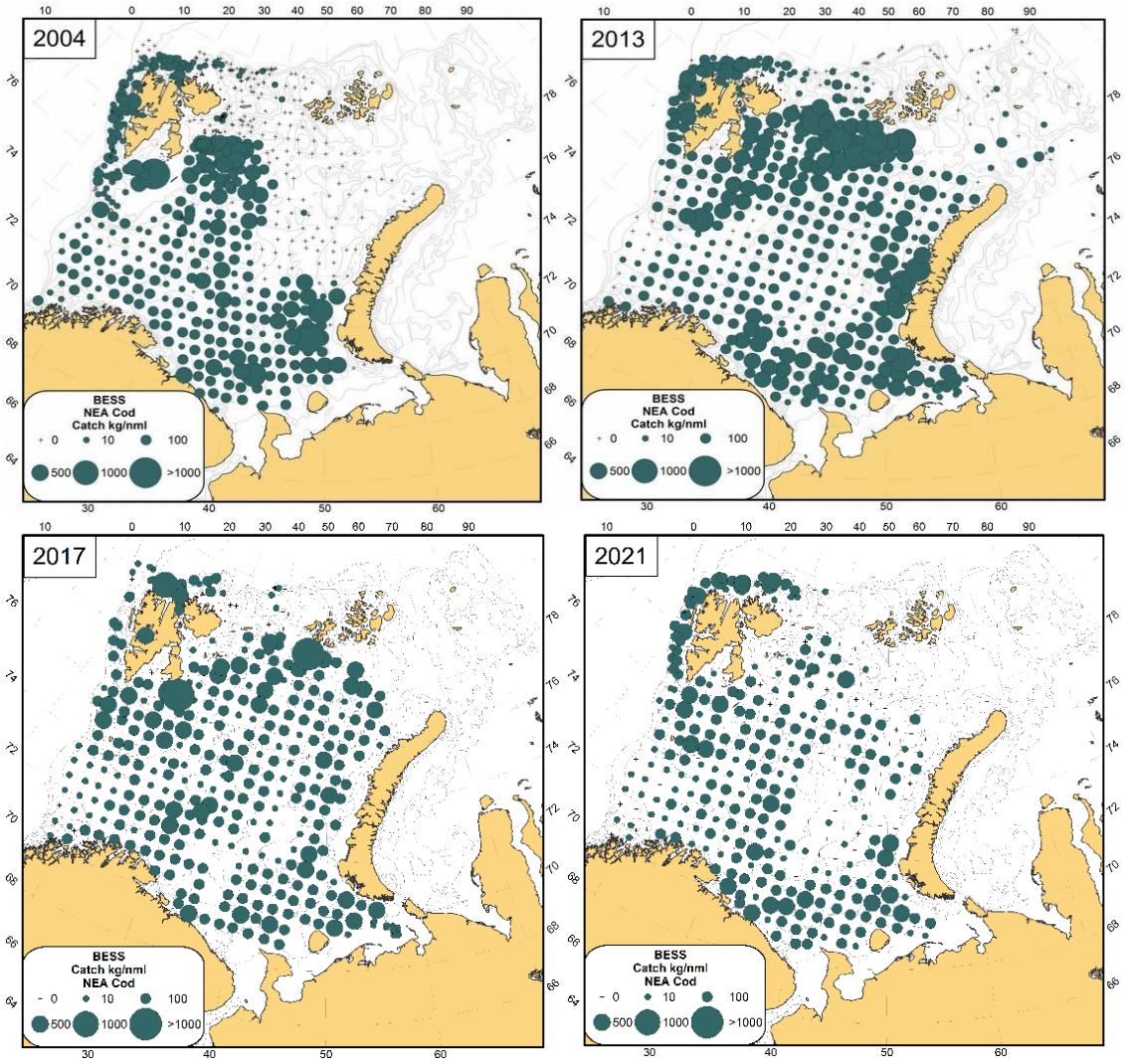

Figure A5.76: Distribution of cod catches (kg/nm) during August–September; for the years 2004, 2013, 2017 and 2021.

Figure A5.77 shows the distribution of cod ≥ 50 cm based on data from the winter survey (January–March during 2008, 2011, and 2021. Note: the survey area was extended northwards in 2014 and coverage is often limited by ice conditions. Cod distribution observed during this survey increased throughout the period, but it is unknown when cod began to inhabit areas north of Bear Island and west of Svalbard during winter.

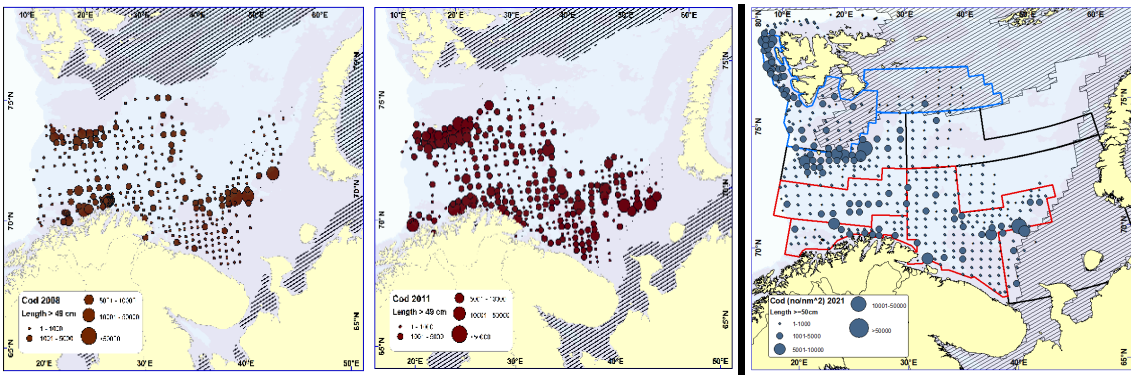

Figure A5.77: Distribution of cod ≥50 cm during winter 2008, 2011, and 2021.

NEA haddock

Young-of-the-year

Estimated abundance of 0-group haddock varied from 75 *10^6 ind. in 1981 to 92*10^9 individuals in 2005 with a long term average of 12*10^9 individuals for the 1980–2021 period (Figure A5.78). In 2021, the total abundance and biomass were higher than in 2020 and the long term mean and was 26*10^9 individuals and 216 thousand tonnes respectively. Thus the 2021-year class may be characterized as strong. Half of the haddock abundance were found in the Southwest polygon and was as high as 16*10^9 ind.

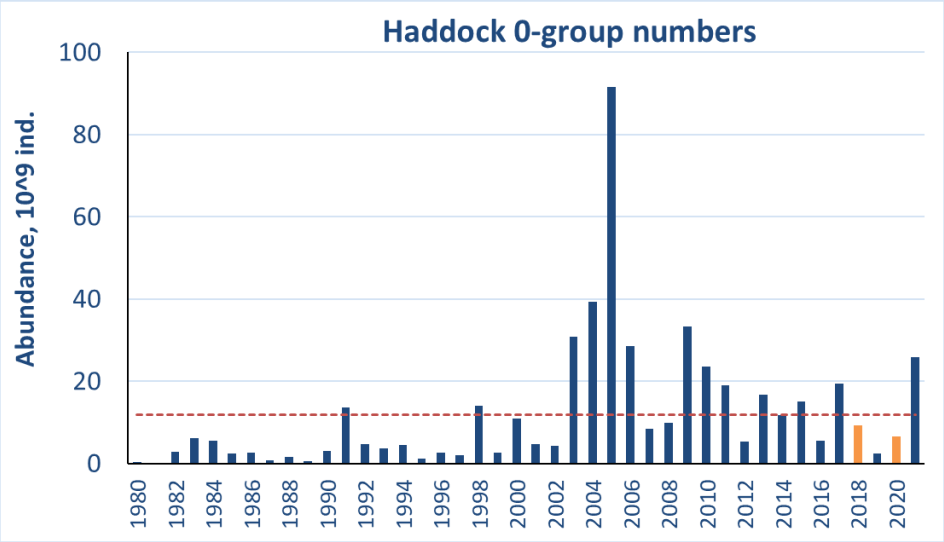

Figure A5.78: 0-group haddock abundance estimates and fluctuation 1980–2021. Orange line shows the long term average; the blue columns indicate abundance; orange columns indicate corrected indices.

In 2021, 0-group haddock dominated by fish of 7.5 to 10.0 cm length. The largest haddock (with an average length > 9.0 cm) were observed in the central areas (Hopen Deep and central Bank). The smallest 0-group haddock, like 0-group of cod and other species were found in the south-eastern Barents Sea (see above).

Haddock one year old and older

The Northeast Arctic haddock stock reached record high levels in 2009 to 2013, due to very strong 2004-2006-year classes. Subsequent recruitment has normalized and ten became very poor in the recent 3 years. The stock remains at a relatively high level and the decline in total stock in recent years was halted to the abundant 2016-year class, but the forecast for 2022 predict a further decline in total stock biomass while spawning-stock biomass is predicted to be stable. (Figure A5.79 and A5.80). The large spawning stock did not, until 2016, result in strong year classes (Figure A5.81).

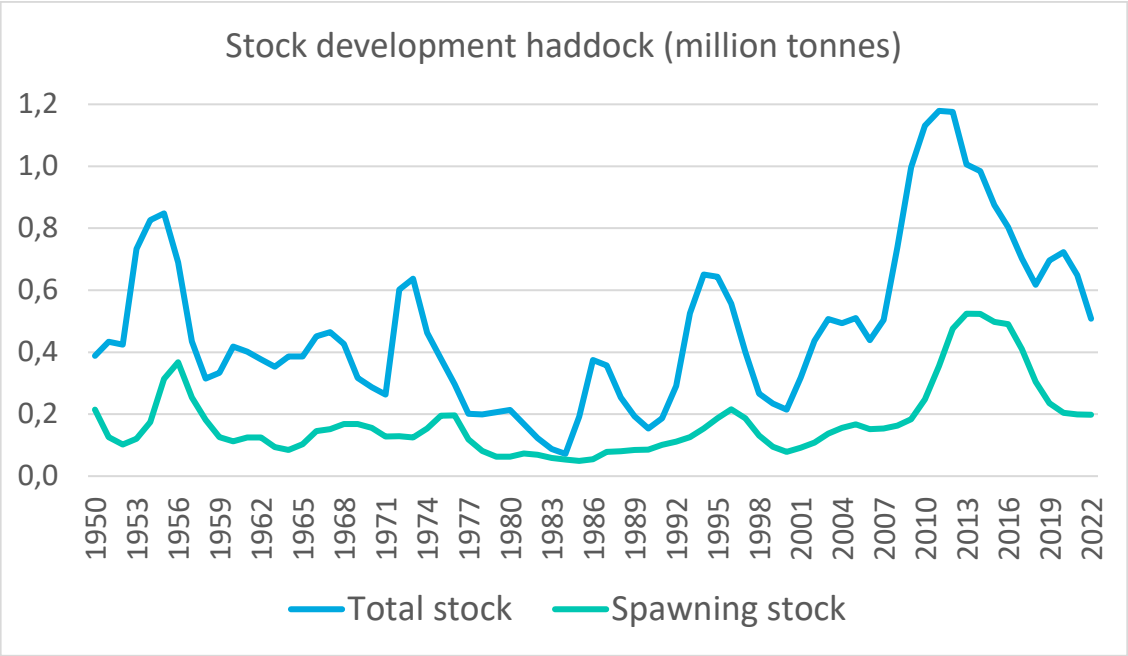

Figure A5.79: Haddock total stock and spawning stock development during the 1950–2021 period and forecast for 2022 from AFWG (ICES 2021).

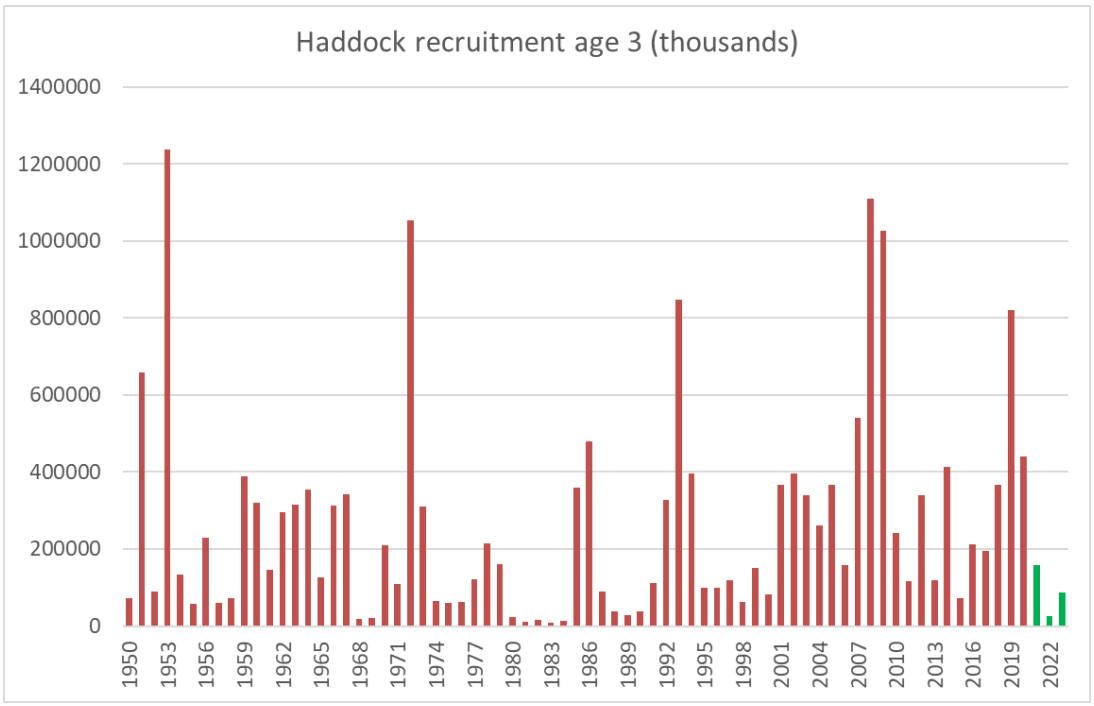

Figure A5.80: Recruitment of haddock during the 1950–2020 period (red) and forecast for 2021–2023 (green) from AFWG (ICES 2021).

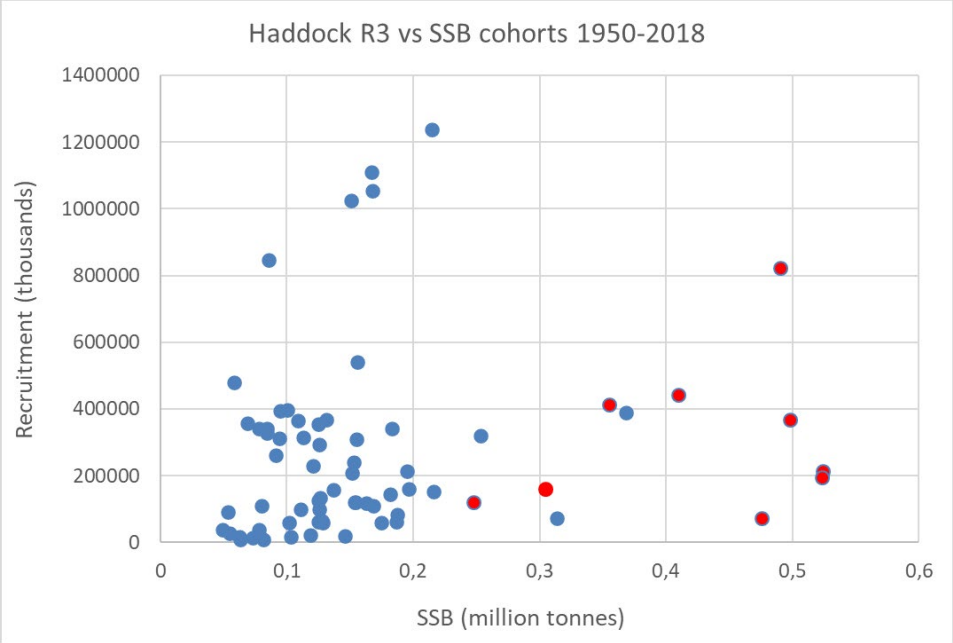

Figure A5.81: Spawning stock-recruitment plot for haddock cohorts 1950–2018. Cohorts 2010–2018 shown as red dots.

Due to low indices from the ecosystem survey 2020 and winter survey 2021, and also low commercial catches, the haddock stock was revised down compared to the prognosis used in quota advice for 2021. The decline in indices in two different surveys suggests a stock decline related to higher mortality or migration. The ecosystem drivers are unknown. The maps of the distribution in August–September 2019–2021 (Figure A5.82) show that haddock has disappeared from the Novaya Zemlya bank area.

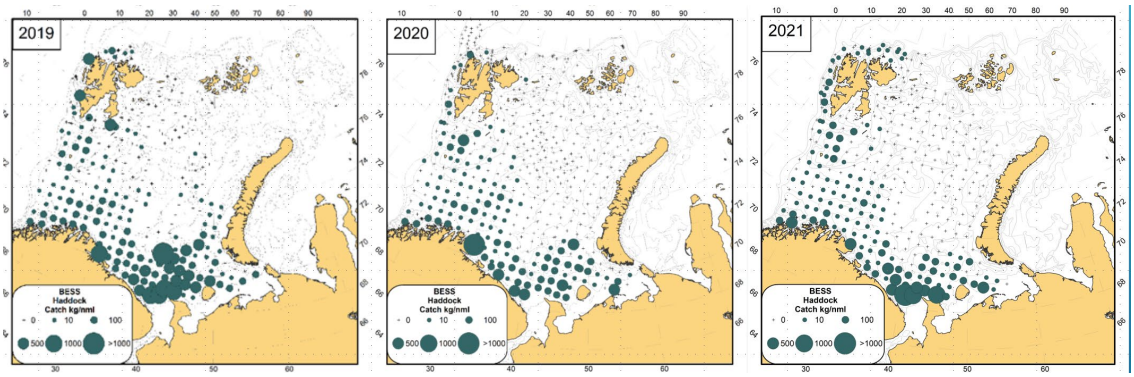

Figure A5.82: Distribution of haddock during the ecosystem survey 2019–2021.

Long rough dab

Young of the year

Estimated abundance of 0-group long rough dab was low in 2013 and very high in 1986 (Figure A5.83). In 2021, the total abundance index for 0-group fish were 128.6 million individuals that was lower than in 2020 and long term mean (571 $*10^6$ individuals). Thus the 2021-year class of long rough dab may be characterized as a weak.

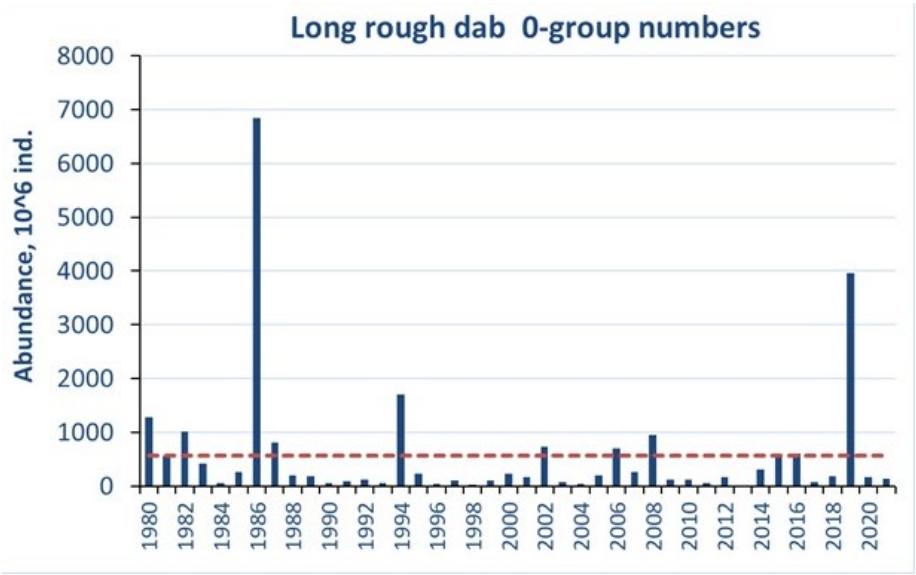

Figure A5.83: 0-group long rough dab abundance in the Barents Sea during the 1980–2021 period. Red dotted line shows the long term average; the blue columns indicate fluctuating abundance.

In 2021, 0-group long rough dab were mainly distributed north, south and east of Svalbard (Spitsbergen), and the southwestern and southeastern corner of the Barents Sea. In 2021, the eastern Barents Sea was not covered well, but probably long rough dab was not distributed here numerously.

Larger long rough dab were found in the northern polygons (Great bank, Svalbard North, and Fr. Victoria Trough) with an average of 4 cm, while smallest long rough dab were found in the Southwest polygon with an average of 1.6 cm.

Older long rough dab

Older long rough dab (LRD) (age 1+) is widely distributed in the Barents Sea. Usually, major concentrations of long rough dab are distributed in the central, northern, and eastern parts of the Barents Sea. LRD is a very numerous species. The total number of LRD in the Barents Sea can be more than $5 \cdot 10^9$ individuals (Figure A5.84). Long rough dab abundance estimates based on results from the BESS time-series (August–September) have been relatively stable during the current decade. Many small fish were observed in trawl catches especially in eastern areas during the 2015 to 2017 BESS. The 2018 index was not calculated due to limited survey coverage in the eastern region of the Barents Sea and in 2019 to 2021 the index was estimated somewhat above the mean for the period 2004-2021 (Figure A5.84).

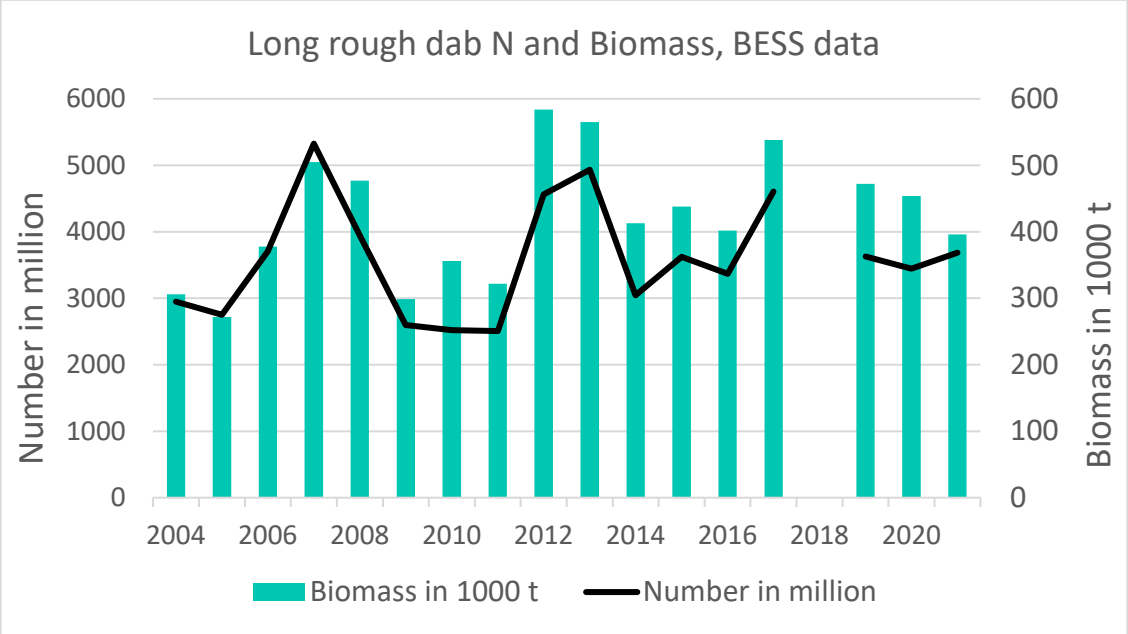

Figure A5.84: Stock numbers and biomass of long rough dab based on BESS data during the 2004–2021 period, calculated using bottom trawl estimated swept-area from BESS.

Greenland halibut

Young of the year

In 2021, the total abundance index for 0-group fish were 53.6 million individuals, that was higher than the long term mean of 29 million individuals (Figure A5.85).

0-group Greenland halibut was distributed west, north, and south of Svalbard (Spitsbergen) in 2021 like distribution in 2018 to 2020. 0-group Greenland halibut length varied from 3.0 to 8.9 cm. Larger fish were found in the Svalbard North and Svalbard South polygons, and fish length were with an average of 6.8 cm, while slightly smaller fish were found in the Fr. Victoria Trough with an average of 6.3 cm.

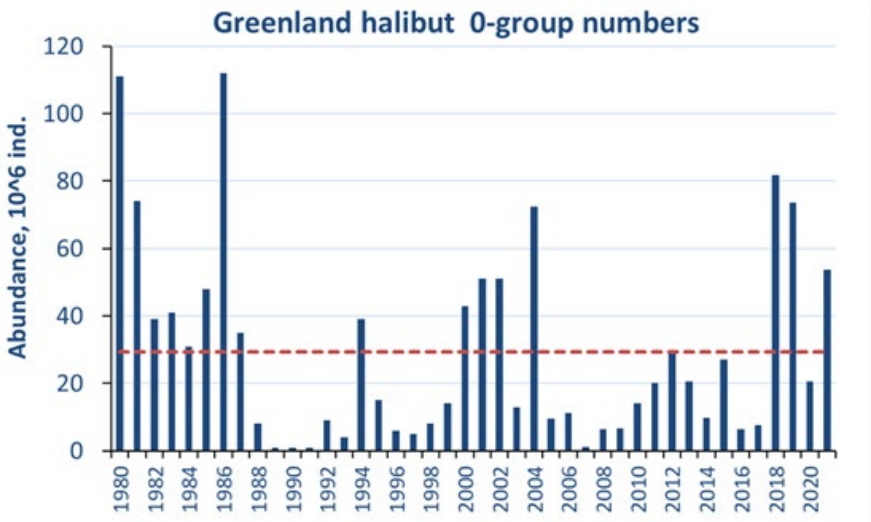

Figure A5.85: 0-group Greenland halibut abundance estimates were not corrected for Keff (blue column). Red dotted line shows the long term average.

0-group Greenland halibut is distributed mainly in the Svalbard (Spitsbergen) fjords and close to the seabed, therefore, abundance indices in the open sea areas may not represent year class strength but give some indication about recruitment dynamics.

Older Greenland halibut

The adult component of the stock is mainly distributed outside the ecosystem survey area, i.e. on the slope. In recent years, an increasing number of large Greenland halibut has been captured in deeper waters of the area surveyed by the BESS (Figure A5.86). Northern and northeastern areas of the Barents Sea serve as nursery grounds for the stock. Greenland halibut are also relatively abundant in deep channels running between the shallowest fishing banks.

The fishable component of the stock (length ≥45 cm) increased from 1992 to 2012 and then stabilized before decreasing slightly in the most recent years (Figure A5.87). The harvest rate is low but increasing.

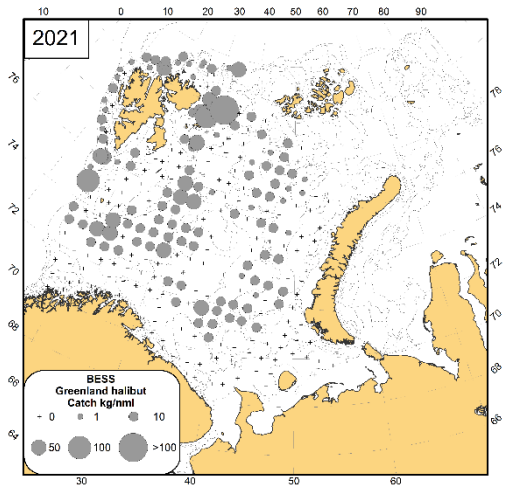

Figure A5.86: Greenland halibut distribution (specimens/nautical mile) during August–September 2021 based on the BESS data.

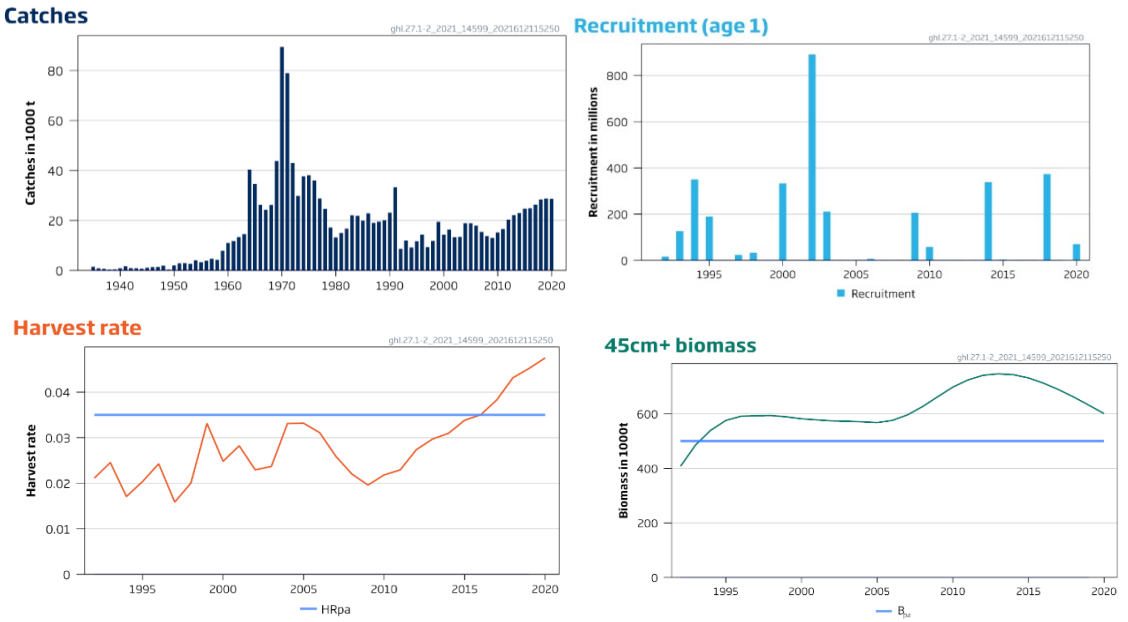

Figure A5.87. Northeast Arctic Greenland halibut: catches, recruitment, harvest rate and biomass of 45+ cm Greenland halibut as estimated by the GADGET model during the 1992–2020 period (ICES 2021).

Deepwater redfish (*S. mentella*)

Young-of-the-year

Estimated abundance of 0-group deepwater redfish varied from $23*10^6$ million individuals in 2001 to $1.6*10^{12}$ ind. in 1985, and the long term average abundance was $222*10^9$ ind. for the 1980-2021 period (Figure A5.88). In 2021, the total abundance index for 0-group deepwater redfish was very low and was $41.4*10^9$ ind., which is much lower than the long term mean. Thus the 2021-year class may be characterized as a weak. Estimated biomass was also low (96 thousand tonnes) in 2021.

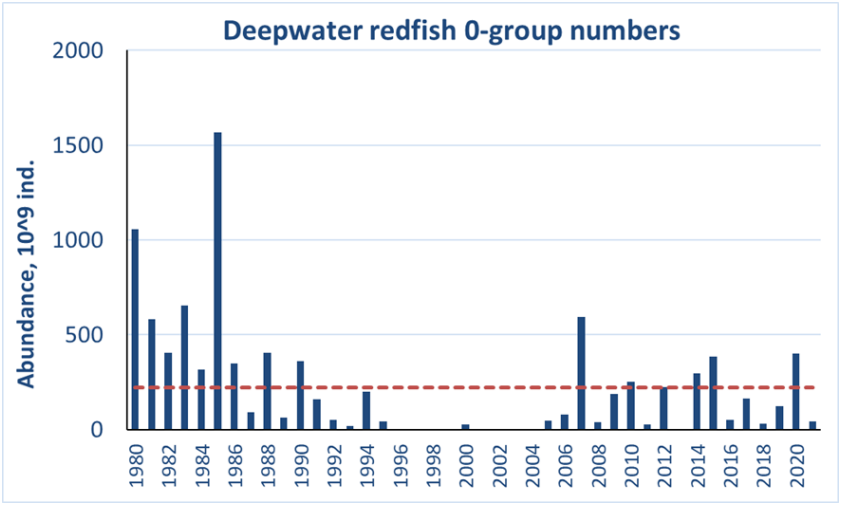

Figure A5.88: 0-group deepwater redfish abundance corrected for Keff (blue column). Red dotted line shows the long term average.

0-group redfish was distributed from north of Norwegian coast to the northwest of Svalbard (Spitsbergen) archipelago in 2021. The densest concentrations and the largest fish with an average of 3.7 cm were found in the Svalbard North polygon.

Deepwater redfish one year old and older

In 2020, deepwater redfish were widely distributed in the Barents Sea. During the BESS and the winter survey, the largest concentrations were observed, as usual, in western and northwestern parts of the Barents Sea. Biomass was higher during 2013–2021 than in preceding years. Geographic distribution of deepwater redfish during the 2021 BESS is shown in Figure A5.89. Most of the adult fish are observed in the Norwegian Sea. Stock development trends from the latest ICES AFWG assessment are shown in Figure A5.90. During the last decade, the deepwater redfish spawning-stock biomass has remained relatively stable around 800 000 tonnes.

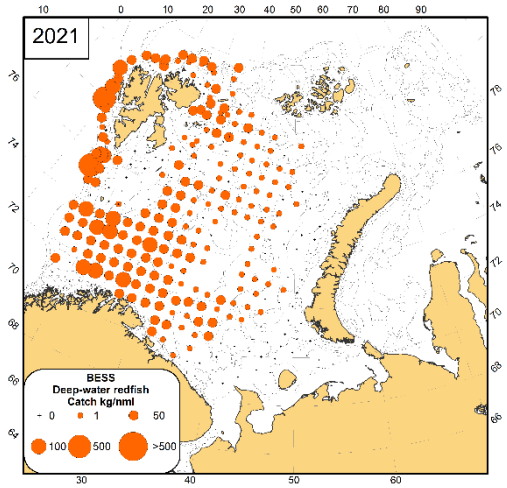

Figure A5.89. Geographic distribution of deepwater redfish during the 2021 BESS survey.

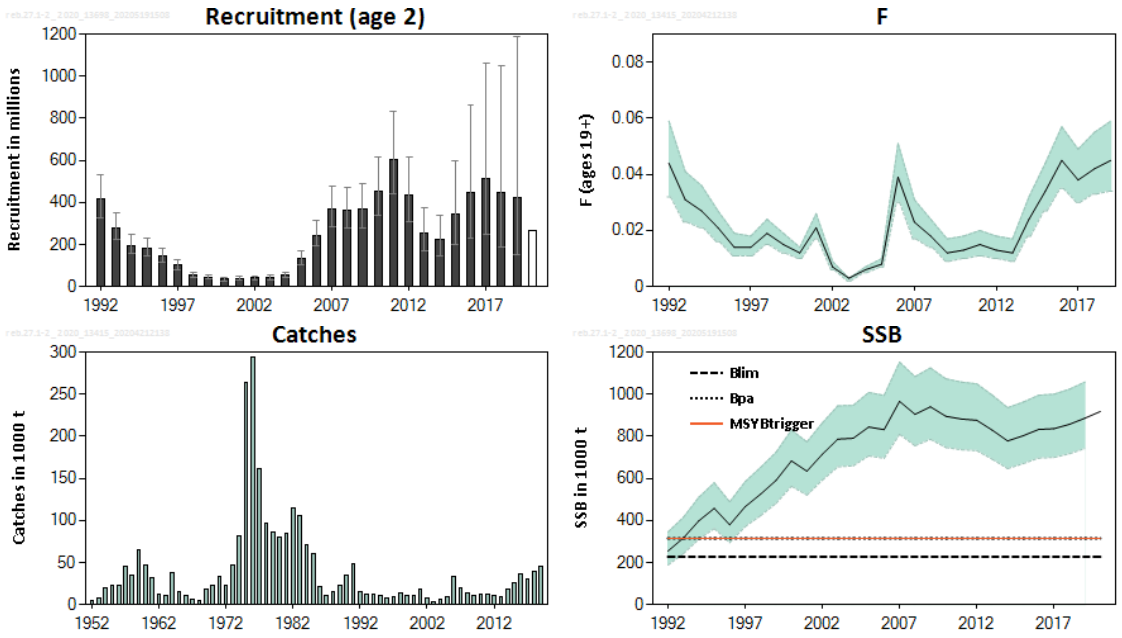

Figure A5.90. Catches, recruitment, harvest rate and biomass for *S. mentella* in ICES Subareas 1 and 2 (ICES, 2020).

Zoogeographical groups of non-commercial species

Distribution of zoogeographical fish groups

By E. Johannesen (IMR), T. Prokhorova (PINRO) and B. Husson (IMR)

During the 2021 ecosystem survey 90 species from 29 families were collected. It is 5 species less than in 2020. The northeastern part between Franz-Joseph Land and Novaya Zemlya was not covered, so less Arctic habitat were covered compared to last year (Figure A5.91). The highest number of species belongs to the families Zoarcidae (14 species), Gadidae (10 species) and Pleuronectidae (10 species). Among the analysed species most belong to the Arctic (29.9%), mainly boreal (26.1%) and boreal (20.9%) zoogeographic groups. Median and maximum catches decreased for all, except mainly boreal and boreal species. Distribution of the groups have not changed since the previous year. As usual boreal and mainly boreal species occurred mainly in the southern and southwestern part of the Barents Sea, while arctic and mainly arctic species in the northern and northeastern part. Arctic-boreal species were found in the central and northern part of the area (Figure A5.91).

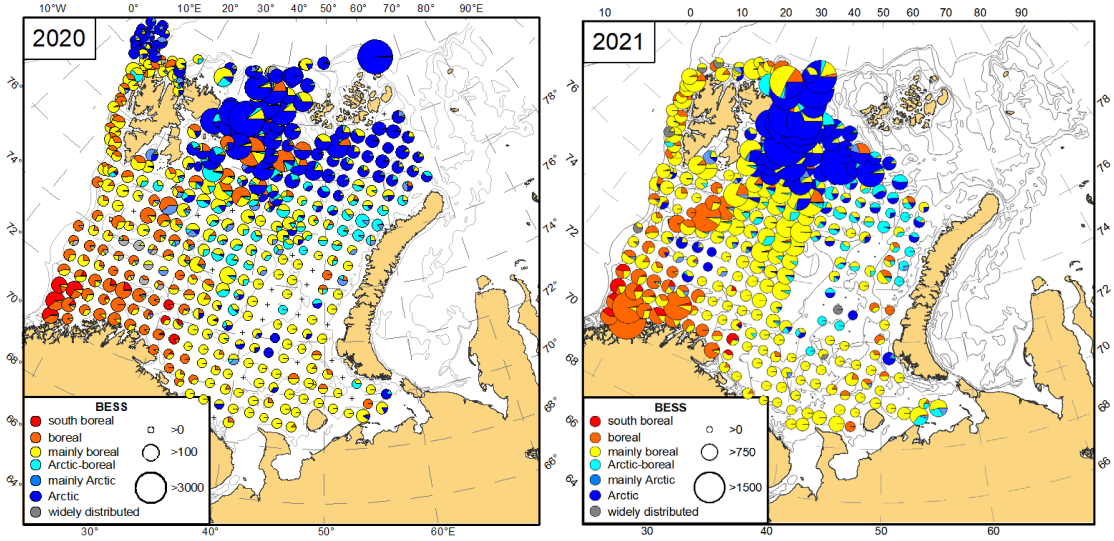

Figure A5.91: Distribution of non-commercial fish species from different zoogeographic groups during the ecosystem survey 2020 (left) and 2021 (right). The size of circle corresponds to abundance (individuals per nautical mile, only bottom trawl stations were used, both pelagic and demersal species are included), commercial species excluded.

There is no trend in spatial distribution changes of species of each zoogeographical group in recent years (Figure A5.92).

The median catch of species of the boreal zoogeographic group in 2021 was the highest since 2004, while those of the Arctic-boreal and mainly Arctic zoogeographic group in 2021 were the lowest since 2004 (excluding 2010 when they were at about the same level) (Figure A5.93). There is no clear trend in the other zoogeographic groups. It should be noted however, that variation in survey coverage each year might influence the results (for more detail see section 1.6 Progress report on ToR (f) in this report).

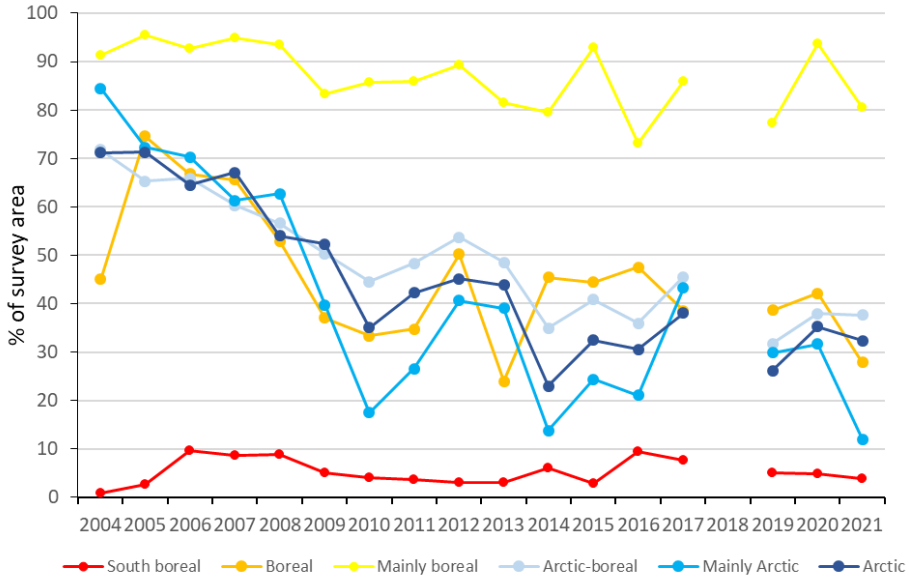

Figure A5.92: The area occupied by species of different zoogeographical groups (% of total survey area calculated for each year). Only bottom-trawl catches of non-commercial fish were used, both demersal and pelagic species are included. 2018 – are not included due to the poor coverage of the Russian Zone).

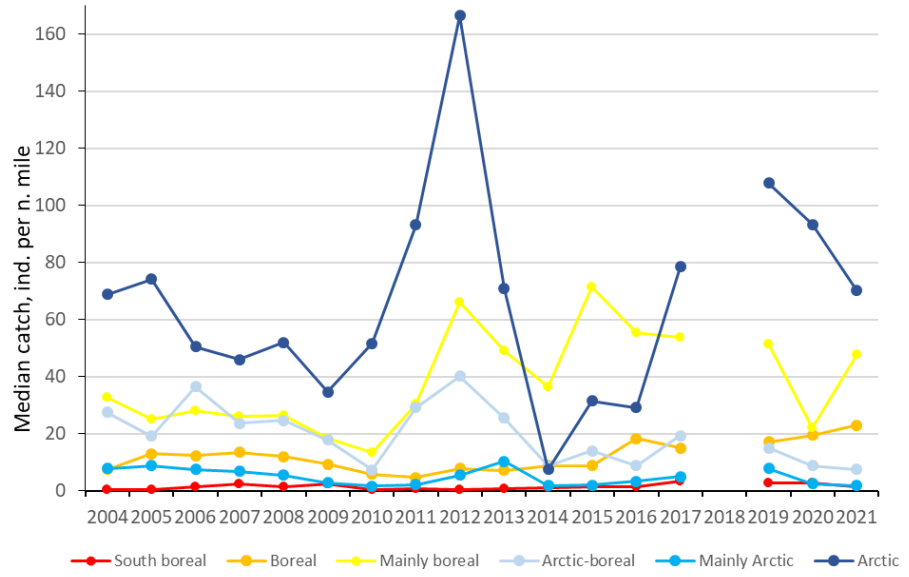

Figure A5.93. Median catch (individuals per nautical mile) of non-commercial fish from different zoogeographic groups (only bottom-trawl data were used, both pelagic and demersal species are included) (2014 – investigation area was limited in the north due to ice coverage, 2018 – are not included due to the poor coverage of the Russian Zone).

A biogeographic score was assigned for all species according to their zoogeographic affiliation (Andriashev and Chernova, 1995). This index was averaged per trawl, weighed by the relative abundance of each species in the trawl. Maps of the "arcticness" of the catches is plotted in Figure A5.94, This shows a decrease in proportion of arctic species in trawls until 2008/2010, then a stabilization of the situation.

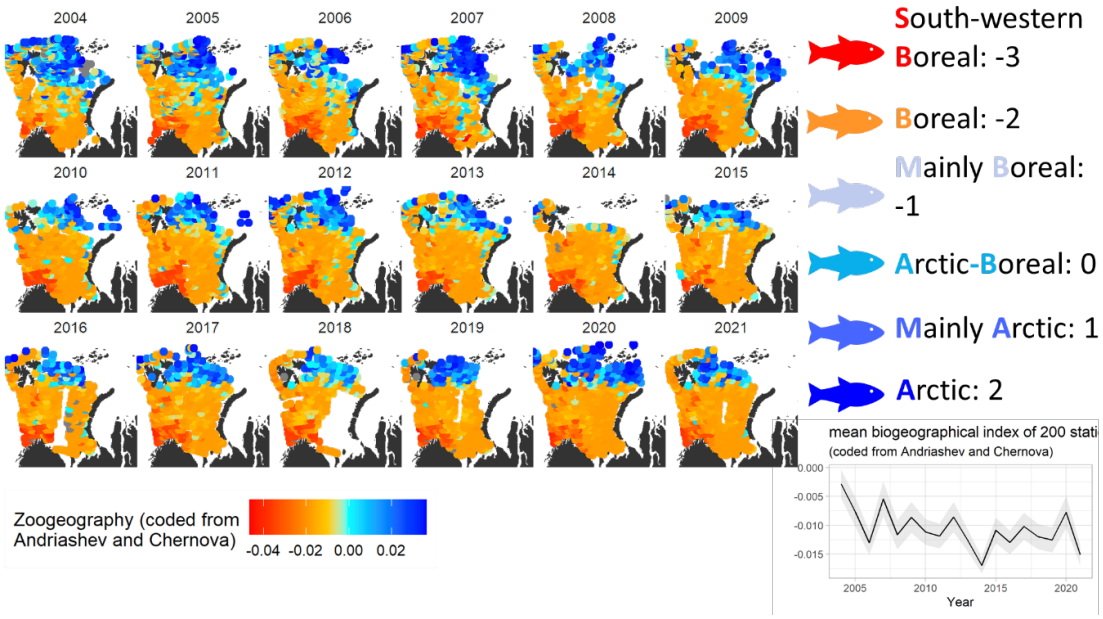

Figure A5.94: "Arcticness" index maps by years 2004–2021, the color goes from red (low arcticness) to blue (high arcticness). All species were assigned a score according to their zoogeographic affiliation, then given weight according to their relative abundance in the trawl. The graph shows the yearly averages, but please note the variable coverage, e.g. in 2014 when ice restricted access to the northern Barents Sea. Commercial species (Cod, haddock, Greenland halibut, deepwater redfish, herring, polar cod, capelin, blue whiting) were excluded.

Abundance of small non-commercial fish species

By E. Eriksen, T. Prokhorova, and A. Dolgov

Despite the distribution and biology of the non-commercial fish species and their role in the Barents Sea ecosystem being investigated since mid-1990s, their distribution patterns, abundance and biomass is poorly studied. Since 2012 abundance and biomass of pelagically distributed juveniles of fish species from the families Agonidae, Ammodytidae, Cottidae, Liparidae, Myctophidae and Stichaeidae (called "small fishes" here) were calculated presented in the Survey report.

In 2021, the total biomass of small fishes (764 tonnes for all these families) was the lowest since 2008. Total biomass of small fish was dominated by species from families Stichaeidae, Liparidae and Ammodytidae. Composition of small fish biomasses varied between polygons, the southeastern and southwestern polygons dominated by Ammodytidae, the northern and central polygons dominated by Stichaeidae and Liparidae (Figure A5.95).

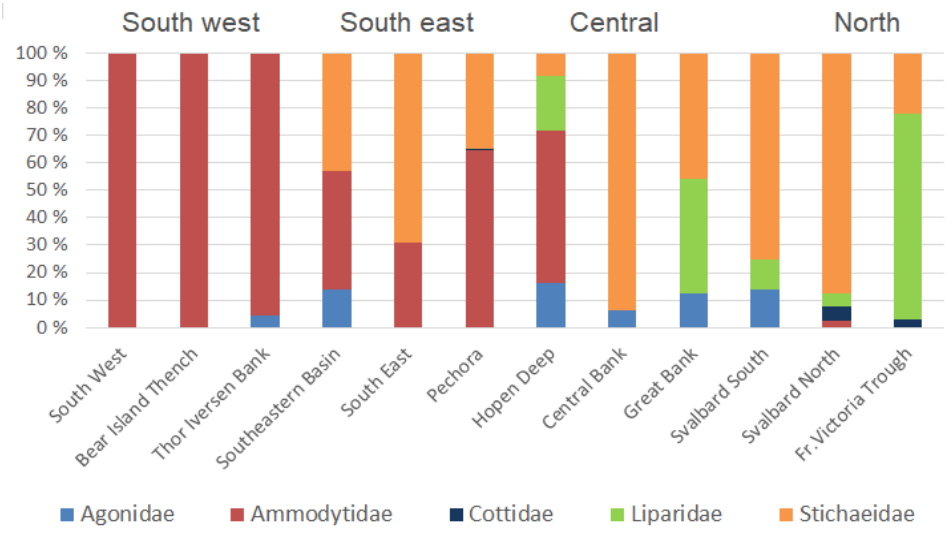

Figure A5.95: Spatial distribution of small-fish biomasses in the WGIBAR-subareas (polygons) in August–September 2021.

Abundance and biomass of **Agonidae** were calculated in R for the period of 2003 to 2021 for 15 WGIBAR-polygons. The highest densities of Agonidae were found in the Northeast during 2004–2007, 2009, and 2011, in the Great Bank in the 2013, 2016–2017 and in 2021, and in the Central Bank 2008, 2015, 2018–2020 (Figure A5.96).

Total abundance and biomass of **Ammodytidae** calculated in R for the period of 2003–2021 for 15 WGIBAR-polygons. The highest densities of Ammodytidae were found in the Pechora during 2003, 2009, 2011, 2013, 2021, in the Thor Iversen Bank during 2004, 2008, 2012, in the Southeast during 2005–2006, in the Bear Island Trench during 2007, 2014, 2018, in the Svalbard South during 2015–2017, 2020, and in the Svalbard North during 2019 (Figure A5.96).

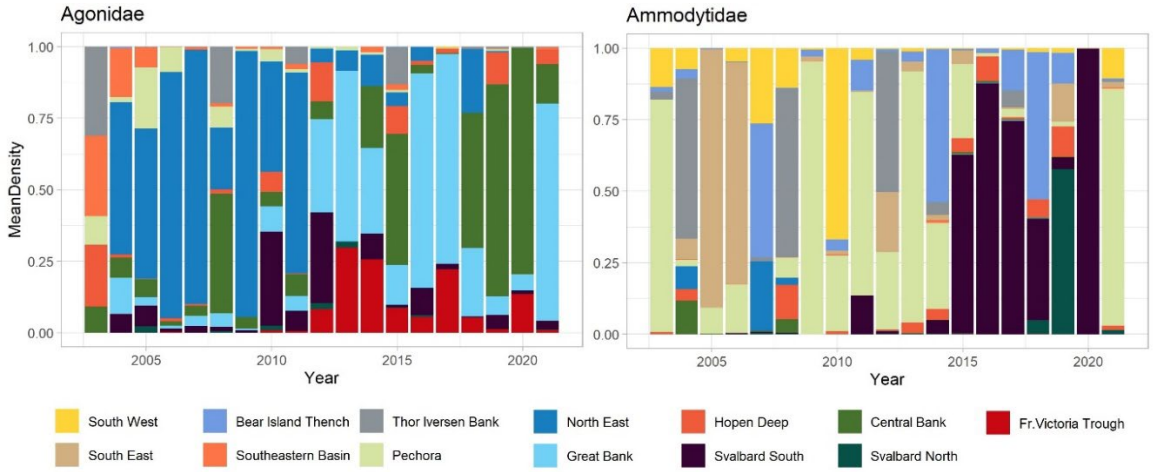

Figure A5.96: Spatial distribution of mean polygon densities of Agonidae and Ammodytidae in August–September 2004–2021.

References

Andriyashev, A.P. and Chernova, N.V. 1995. Annotated list of fish-like vertebrates and fishes of the Arctic Seas and adjacent waters. Journal of Icthyology, 34: 435-456.

Marine mammals and seabirds

Marine Mammals

Summer distribution of marine mammals

By Nils Øien (IMR), Roman Klepikovskiy (PINRO)

The summer abundance of minke whales in the Barents Sea has recently increased from a stable level of about 40 000 animals to around 70 000 animals. Also, humpback whales have increased their summer abundance in the Barents Sea from a low level prior to year 2000 to about 7000 animals in recent years. The other cetacean populations have remained stable in numbers. In 2020, 4159 individuals of twelve species of marine mammals were sighted during the Barents Sea Ecosystem Survey (BESS) in August–October 2020. The baleen whales had aggregated distributions East of Bear Island area and west, north and east of Hopen in the area between 76°N and 78°N.

During the BESS 2021, marine mammal observers were onboard all Norwegian and Russian RVs. In total, 2168 individuals of 10 marine mammal species were observed during the BESS, of these 153 individuals were not identified to species level. The observations are presented in Table A5.5 and distributions in the Figure A5.97 (toothed whales) and Figure A5.98 (baleen whales).

As in previous years, white-beaked dolphin (*Lagenorhynchus albirostris*) was one of the most abundant and widely distributed species. A larger number of dolphins were recorded north of 74°N, as in the previous year.

Besides white-beaked dolphin other toothed whales included sperm whale (*Physeter macrocephalus*), harbour porpoise (*Phocoena phocoena*) and killer whale (*Orcinus orca*) were observed. Sperm whales were observed in the western areas (west of 30°E) of the Barents Sea and at deeper waters along the continental slope. The harbor porpoises were recorded mainly in the southeastern coastal areas. Killer whales were recorded in Svalbard South and Southeastern Basin regions.

Table A5.5: Numbers of marine mammal individuals by species observed during BESS 2021.

Name of species	Total	%
Fin Whale	246	11.4
Humpback Whale	157	7.2
Minke Whale	175	8.1
Sei whale	12	0.6
Blue whale	2	0.1
Unidentified whale	79	3.6
White-beaked dolphin	1 375	63.4
Harbour Porpoise	20	0.90
Killer Whale	4	0.20
Sperm Whale	22	1.00

Unidentified dolphins	70	3.2
Walrus	2	0.1
Unidentified marine mammal	4	0.20
Total sum	**2 168**	**100**

The baleen whale species minke (*Balaenoptera acutorostrata*), humpback (*Megaptera novaeangliae*), fin (*Balaenoptera physalus*), sei whales (*Balaenoptera borealis*) and blue whales (*Balaenoptera musculus*) were also abundant in the BS in 2021.

Minke whale were widely distributed in the BS. The densest aggregation of minke whale were overlapping with capelin concentrations and in the western areas and southwest of Svalbard (Spitsbergen).

The humpback whale were recorded mainly in the northcentral areas. The higher densities of humpback whales were recorded in areas of high aggregations of mature capelin, and often together with fin and minke whales.

Fin whale was widely distributed in the research area, and was recorded to about 50°E. The densest aggregations of fin whale were recorded in the north and southwest of Svalbard.

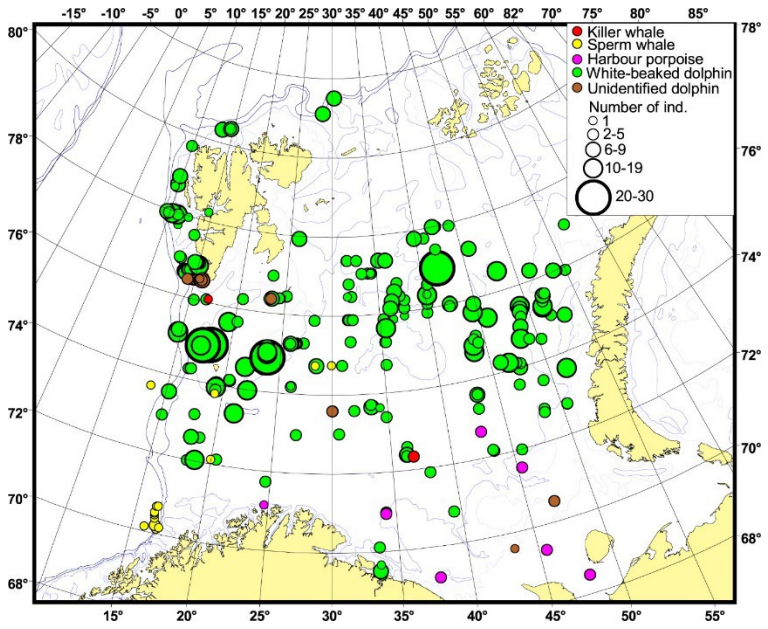

Figure A5.97: Distribution of toothed whales in August–September 2021.

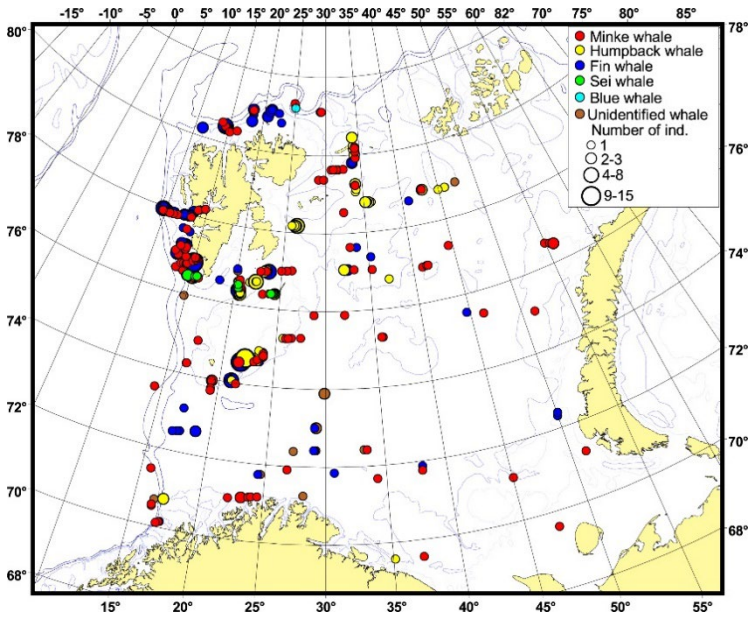

Figure A5.98: Distribution of baleen whales in August–September 2021.

In 2021, 12 individuals of sei whales were recorded south of Svalbard, they were not observed there earlier. Two blue whales were recorded north of Svalbard. In 2021, the pinnipeds of walrus (*Odobenus rosmarus*) only were observed. Two animals were registered at Svalbard. Harp seal (*Pagophilus groenlandicus*), bearded seal (*Erignathus barbatus*), ringed seal (*Phoca hispida*) and polar bears (*Ursus maritimus*) were not observed during the survey, likely due to lack of ice in the survey area.

Since the late 1980s Norway has conducted visual sighting surveys in the Northeast Atlantic with minke whales as target species to estimate summer abundance of this species and other cetacean species. The surveys have been run as mosaic coverages of the total survey area over six-year periods. In the Barents Sea the species most often observed during these surveys have been the minke whale, followed by white-beaked dolphins, harbour porpoises, humpback whales and fin whales. The impression is that minke whales are abundant in the northern and eastern areas during summer. Harbour porpoises are mostly observed in the southern parts of the area and we know that they are associated with the coastal areas along Kola and the fjord systems. Humpback whales are mainly sighted in the northwest and associated with the capelin distribution. The white-beaked dolphins are observed in the southern and central parts of the survey area, especially over the Central Bank. From these surveys a series of abundance estimates can be compiled to illustrate the status over a period of nearly 30 years. Over the period from about 1995 to 2018 the summer abundance of minke whales has been quite stable but has recently shown a considerable increase to the present 68 000 animals (Figure A5.99). Also, humpback whales have shown a large increase in summer abundance in the Barents Sea from very small numbers prior to year 2000 to around 7000 animals recently (Figure A5.100). Other cetacean species have shown relatively stable abundances within the Barents Sea over the survey period.

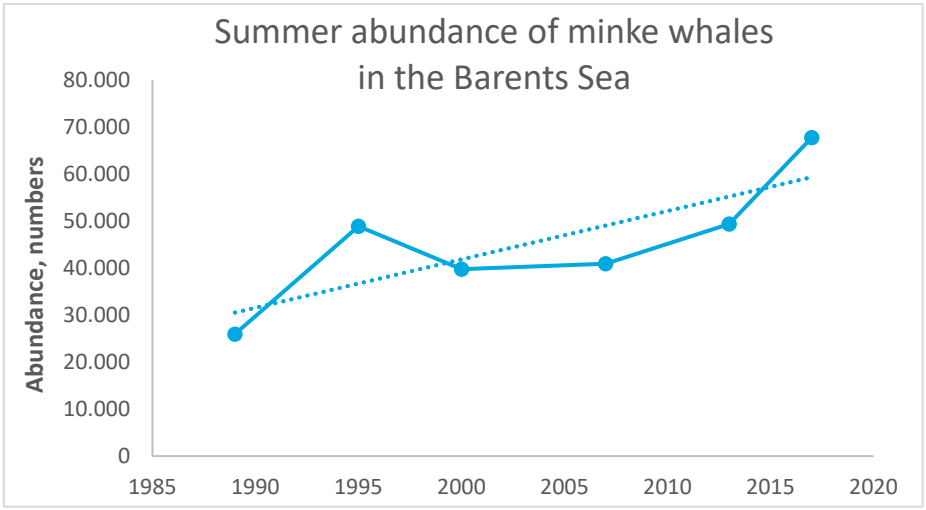

Figure A5.99: Summer abundance of minke whales in the Barents Sea over the past 30 years.

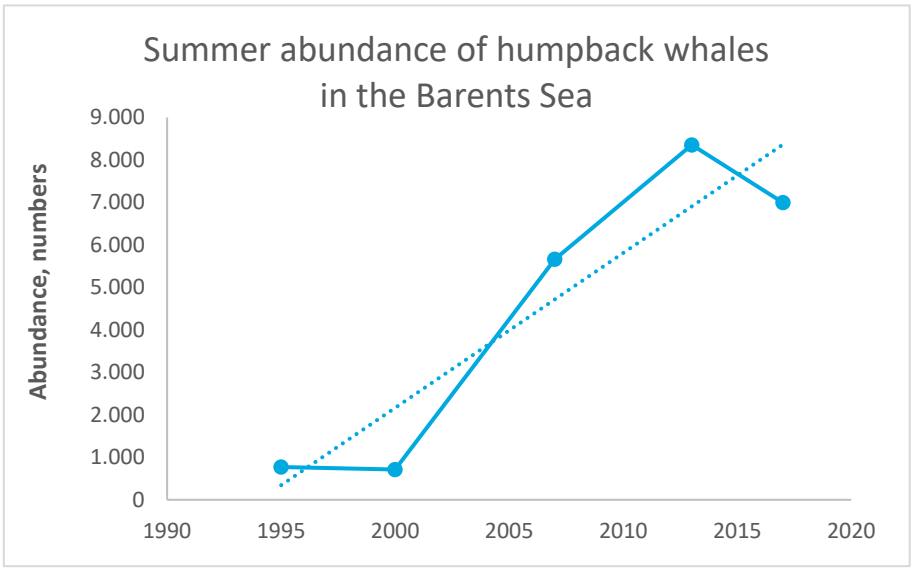

Figure A5.100. Summer abundance of humpback whales in the Barents Sea over the past 20 years.

Marine mammal frequency of occurrence during 2004 to 2021

By Roman Klepikovskiy (PINRO)

The Barents Sea is a productive ecosystem and an important feeding ground for marine mammals during summer and autumn. During the joint Norwegian-Russian ecosystem survey (BESS), marine mammals have been observed visually from the vessels by experts. Frequency of occurrence (FO, number of observations, not number of observed marine mammals) were estimated based on the BESS data for the period 2004–2021 and showed in Figure A5.101. Three peaks of FO of marine mammals were observed in 2007, 2010 and 2017–2021. Note, that lack of marine mammal observers in the western part (2004, 2005, 2008, 2009 and 2014), and lack of full coverage in the eastern parts of the Barents Sea in 2016, 2018 and 2020 may influence the result.

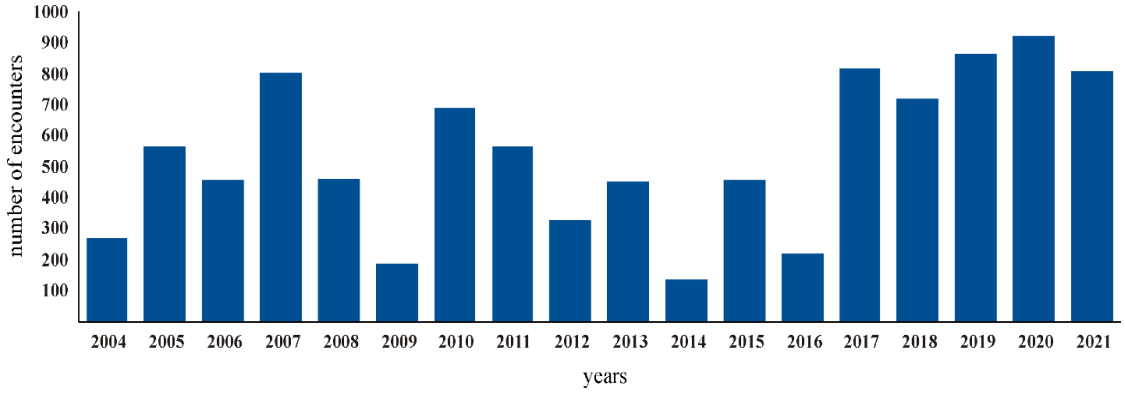

Figure A5.101: Frequency of occurrence of marine mammals (number of observations) in the Barents Sea, during BESS in 2004–2021.

The BESS cover open sea and thus more than 90% of observations of all marine mammals' observations belongs to Cetacea. The most frequently occurrent species during the BESS were white-beaked dolphin (*Lagenorhynchus albirostris*), minke whale (*Balaenoptera acutorostrata*), fin whale (*Balaenoptera physalus*) and humpback whale (*Megaptera novaeangliae*) (Figure A5.102).

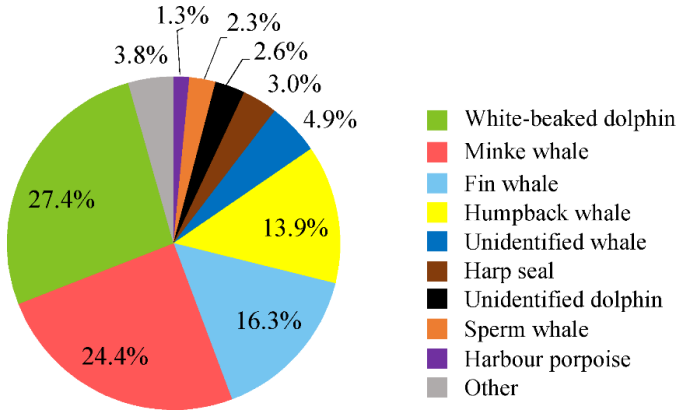

Figure A5.102: Species composition of marine mammals' observations, and their proportion in the Barents Sea, during BESS in 2004–2021.

The Barents Sea were divided in to four (western, Svalbard or Spitsbergen, southeastern and northeastern) regions (Figure A5.103) and FO's were calculated for each region.

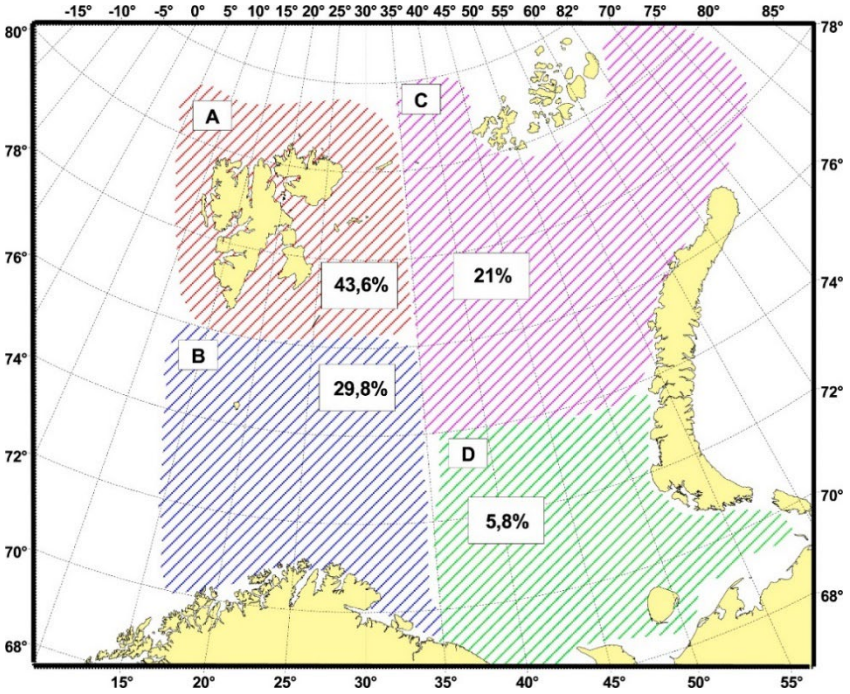

Figure A5.103: Frequency of occurrence of marine mammals (%) in the four regions in Barents Sea during BESS in 2004–2021: A – Svalbard/Spitsbergen, B – Western, C – Northeastern, D – Southeastern.

A. The Svalbard area is located between 76°N and 82°N and between 5 °E and 35 °E. The highest frequency of occurrence of marine mammals (43.6% of all observations) were observed in the area. Additionally, the largest number of species (16) were also observed in the area. This area, especially east of Svalbard is a main capelin area. Capelin are an important prey for many of marine mammals and overlap between highest numbers of observations and species and main mature capelin observations most likely link to important feeding ground (first of all capelin, but also euphausiids). Minke whale, fin whale, humpback whale and white-beaked dolphin were most frequently observed in the area (Figure A5.103A).

B. The western area is located between 76°N and the Norwegian and Russian coasts and between 5°E and 35°E. Almost one third part of all observation were observed in the area. Totally, 14 species of marine mammals (next largest number of species recorded in the BS) were observed and observation dominated by white-beaked dolphin, minke whale, fin whale, sperm whale (*Physeter macrocephalus*), humpback whale (Figure A5.103B). The western area is also productive area with highest concentrations of euphausiids and juvenile fish such as haddock, cod, herring, redfish and capelin. Immature capelin and herring also observed here.

C. The northeastern area is located between 74°N and 82°N and between 35°E and 70°E. The number of observed marine mammals was lesser and consisted 21% of all observations. Totally, 13 species were observed and white-beaked dolphin, humpback whale, minke whale, fin whale, and harp seal (*Pagophilus groenlandicus*) were frequently observed (Figure A5.103C). This area is dominated by polar cod, cod and capelin. Polar cod is an important prey for harp seals.

D. The southeastern area is located between 74°N the Russian coast and between 35°E and 70°E. During BESS, the lowest numbers of marine mammals' observations were found here (5.8% of all observations). However, 10 different species were recorded, and white-beaked dolphin, minke whale, harbour porpoise (*Phocoena phocoena*) and fin whale were most frequent observed (Figure A5.103D). This area dominated by polar cod, cod and herring.

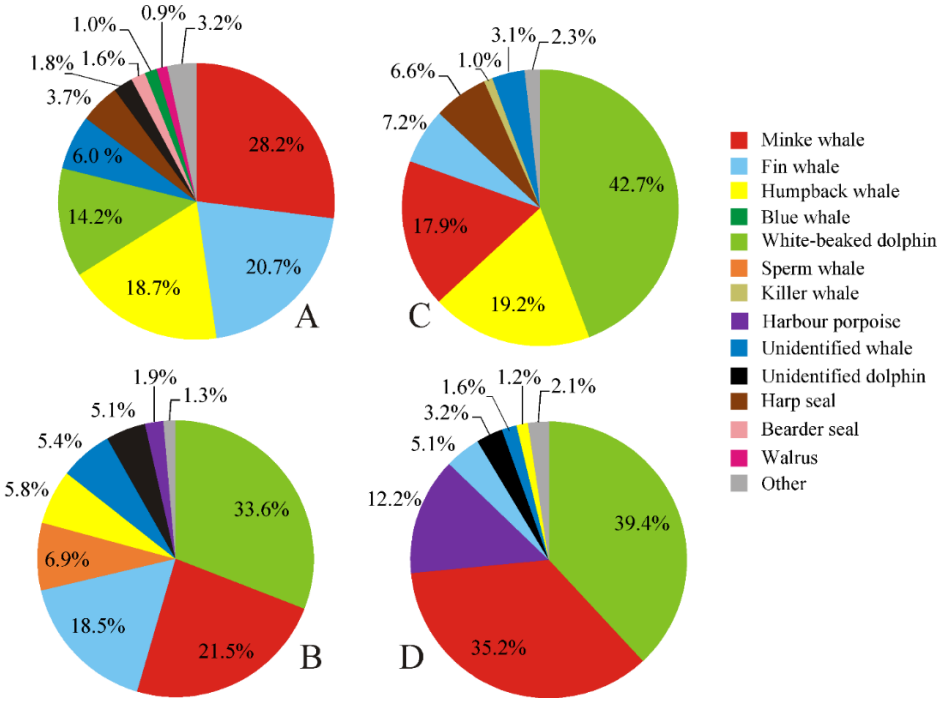

Figure A5.103: Frequency of occurrence of marine mammals and species composition (%) in different areas (A - Svalbard, B – Western, C – Northeastern, D – Southeast) in the Barents Sea during BESS in 2004–2021.

Figure A5.104 shown frequency of occurrence of marine mammals in these four areas in different years. Svalbard or Spitsbergen was most of all other areas visited by marine mammals and number of their observations increased from 2004 to 2021. During last five years marine mammals were observed about 400 times and more in the Svalbard area. Next highest visited area was the western area, which was most likely used as migration corridor for some whales. Largest numbers of observations were observed during 2005–2007, 2010 and 2019–2021. The frequency of occurrence and species composition varied between these four areas of the Barents Sea. The Svalbard, inhabiting by capelin, polar cod and macroplankton such as euphausiids and amphipods, were visited more frequently and by a higher number of species, and thus had highest predation pressure. The western area, inhabiting by 0-group fishes and macroplankton, experienced next highest predation pressure, but this differ between years.

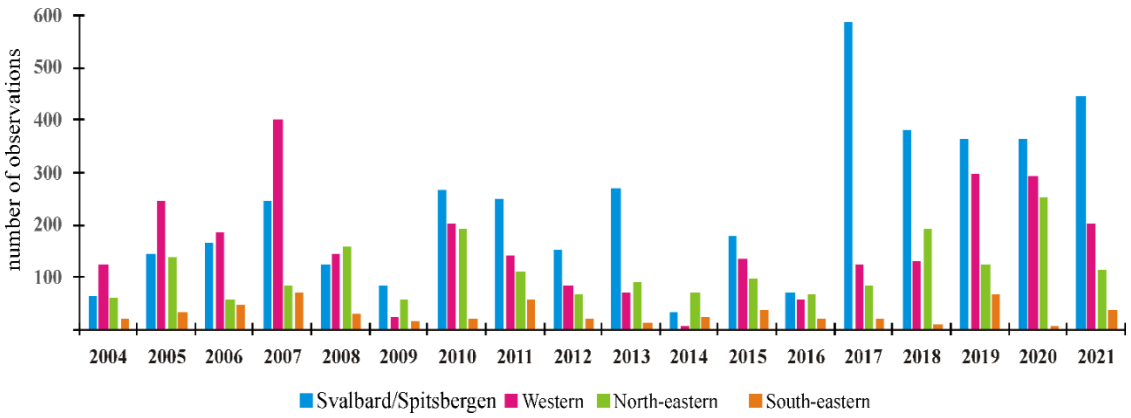

Figure A5.104: Frequency of occurrence of marine mammals in four areas of the Barents Sea during 2004–2021.

Ice associated marine mammals

By Jon Aars (NPI), Hanne Johnsen (NPI), Christian Lydersen (NPI), and Kit M. Kovacs (NPI)

Sea ice habitat loss due to a warming climate is a serious threat to all ice-associated marine mammals. Declines in Arctic sea ice and associated environmental changes have been linked to shifts in species distribution. The Norwegian Polar Institute (NPI) conduct regular monitoring of walruses and polar bears in Svalbard updated through MOSJ (environmental monitoring of Svalbard and Jan Mayen) as well as research on species not covered by regular monitoring.

Walruses (*Odobenus marinus*) were once highly abundant in the Svalbard archipelago, but 350 years of unregulated harvest brought them to the brink of extinction before they were protected in 1952. The population remains Red Listed as "vulnerable" today and following several decades of protection one can now see a clear growth in the population (Figure A5.105).

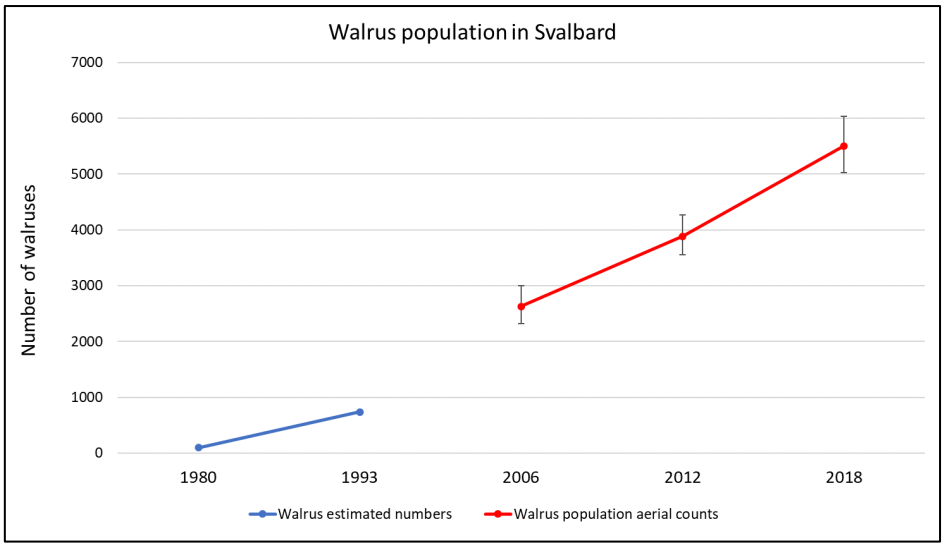

Figure A5.105: In the 1980s and 1990s, estimates were made from observations from land or ships, spread out over weeks or months. Data from 2006 and 2012 are based on the number of animals on designated aerial surveys, and counts are corrected for the proportion of animals at sea at the time of the survey. Source: https://www.mosj.no/en/fauna/marine/walrus-population.html

The first systematic abundance survey of walruses in Svalbard, also included in MOSJ, was conducted in 2006 (Lydersen *et al.* 2008). Before that, crude "guestimates" were made from observations from land or ships, spread out over weeks or months. The walruses in Svalbard are part of a shared population with Franz Josef Land, we only survey the Svalbard fraction. The survey in 2006 covered all known terrestrial haul-out sites within Svalbard (79 in total) during a tight time window in August. 17 haul-out sites were occupied by animals when the survey was flown. The photographs of the active sites revealed 657 animals. An extensive behavioural dataset from satellite-relay-data-loggers was used to correct for animals that were in the water at the time of the survey. The resulting estimate was 2629 (95% CI: 2318–2998). With updates approximately every five years, the second survey in this MOSJ time-series was flown in 2012 (Kovacs *et al.* 2014). The new estimate was 3886 (95% CI: 3553–4262) and covered 91 haul-out sites of which 24 were occupied during the survey. Nine of the active sites contained females with calves, in contrast to only one site in the 2006 survey. The most recent survey in this time-series was carried out in 2018. At the time of the survey, 5503 (95% CI: 5031-6036) walrus were estimated in the Svalbard area (https://www.mosj.no/en/fauna/marine/walrus-population.html). This is a 41.6% increase since the previous survey in 2012. Animals were present at 19 of the visited haul-out sites, and calves were observed at seven of these. In 2018, there were 98 terrestrial walrus haul-out sites in the database for Svalbard. The next update in this time-series is planned for 2023.

The intensive hunting of polar bears (*Ursus maritimus*) in Svalbard began around 1870, and the population was at low levels when the species was protected from 1973. In the following years the population probably increased considerably, and newer data indicates that the population has not likely been reduced the last 10 to 15 years, despite a large reduction in available sea ice in the same period. In August 2004 the Barents Sea population of polar bears was estimated to around 2650 (95% CI ~ 1900-3600) animals (Aars *et al.* 2009), a number assumed to reflect a significant increase following the protection in 1973 (Aars *et al.* 2009; Derocher 2005). This means that currently the population is not likely threatened by the effects smaller populations may be affected by, such as loss of genetic diversity or random demographic processes. A study on genetic diversity do however show a slight loss of genetic diversity among Svalbard bears, and increased between-area structure within the archipelago, best explained by restricted movement of bears due to less sea ice that work as a substrate for movement (Maduna *et al.* 2021).

The Barents Sea area inhabits one of the total nineteen assumed Arctic sub populations of polar bears with a high genetic exchange towards neighbouring populations in the east and west (Peacock *et al.* 2015). The availability of sea ice habitat has in recent years been reduced much faster for the Barents Sea population than for other polar bear populations (Stern and Laidre 2016) and reproducing females are increasingly prevented from reaching important denning areas east of Svalbard (Aars 2013; Derocher *et al.* 2011).

The monitoring includes number of dens and sea ice coverage at Kongsøya and at Hopen, and recruitment of cubs and yearlings using data from the annual capture-recapture program. The occurrence of dens on Hopen and Kongsøya clearly shows that few females reach these islands in autumn if the ice arrives late, sometime after the first part of November. It is unclear whether this means that the proportion of females in the subpopulation having cubs is declining. One assumes that a higher proportion of adult females now den in the Russian Arctic (Franz Josef Land). A model on the availability of denning areas (that all are on land) shows that while Franz Josef land is still reachable from the hunting areas at the marginal ice zone, late in this century all the denning areas may be unavailable for the pelagic bears (Merkel and Aars 2022). Habitats have also shifted much further north following the ice edge which is the area where most polar bears hunt for a large portion of the year (Lone *et al.* 2018). Data from the annual tagging program shows a weak decline in litter size over the years, but there is no significant decrease. Further, there is no significant change over time in the number of cubs per adult female, or in the proportion of females with yearlings. It appears that the local population at Svalbard has remained at around 300 bears from 2004 to 2015, and the total number in the Norwegian Arctic has not been declining, and possibly been increasing (Aars *et al.* 2017). There are no signs that the condition (i.e. fat storage) of the monitored polar bears has decreased over time (Figure A5.106). Although the loss of sea ice has been evident around Svalbard in recent years, and is expected to continue in the coming decades, the size of the subpopulation may still be below the carrying capacity. It is therefore not surprising that it looks as if the subpopulation is likely growing, or at least seems to be stable, although the availability of habitats has become poorer for much of the year.

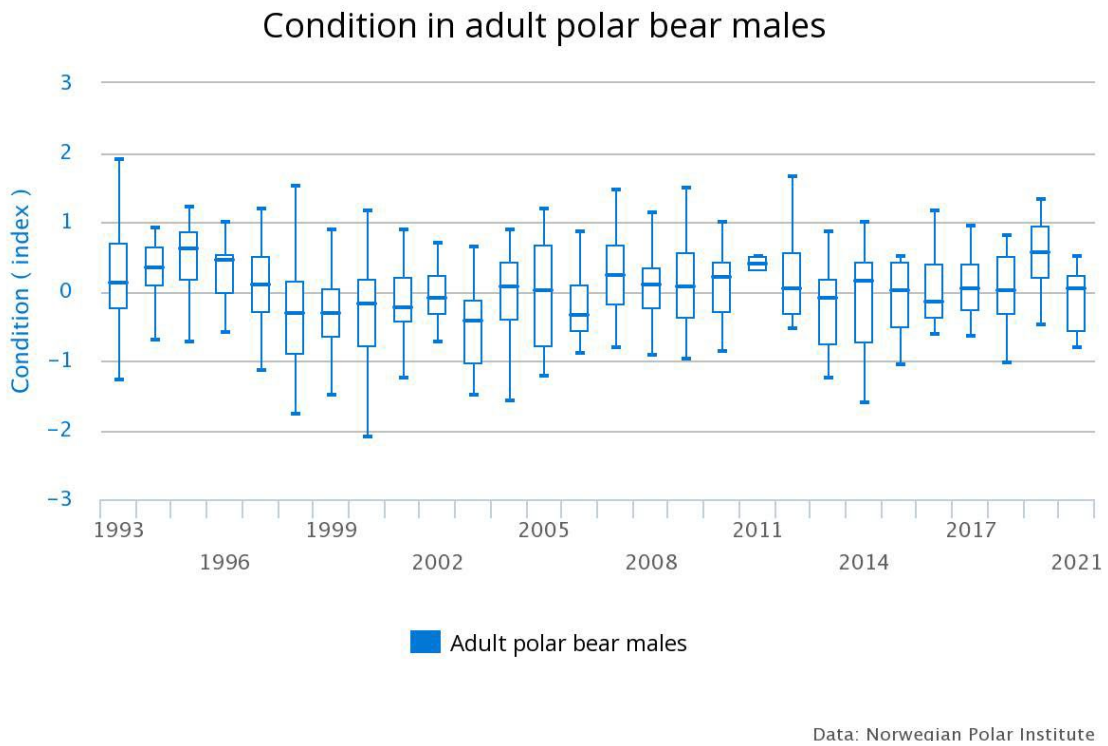

Figure A5.106: Body condition index of adult male polar bears caught in spring (March–May) in the period 1993–2021 (no data for 2020). The lines in the middle of each box show the median value, and the box segments and lines above and below the median each cover ca 25% of the data points. There is no significant trend over time. Source: https://www.mosj.no/en/fauna/marine/polar-bear.html.

Climate change is affecting different species at different rates. The sudden sea ice decline in 2006 had an impact on the spatial overlap and the predator–prey relationship between polar bear and ringed seal (*Pusa hispida*) (Hamilton *et al.* 2017). Following the reduction in sea ice, polar bears spent the same amount of time at tidal glacial fronts during spring, but less time during summer and autumn. Since ringed seals did not change their glacier front association during summer, this led to a decrease in spatial overlap values between these two species in the coastal areas of Svalbard. During summer polar bears are now moving greater distances daily and spend more time close to ground-nesting bird colonies, where bear predation can have substantial local effects. This study shows the importance of considering multiple species when exploring the impacts of climate change.

Other ice-associated marine mammals

NPI also do research and publish data on species of ice associated marine mammals not covered by MOSJ. Among these species are bearded seal (*Erignathus barbatus*), ringed seals, white whales (*Delphinapterus leucas*), bowhead whales (*Balaena mysticetus*) and narwhals (*Monodon monoceros*).

The rapid warming of the Arctic and consequential loss of sea ice represent a serious threat to ice-associated species in the region. In 2015, an aerial survey was carried out to estimate the abundance of Arctic endemic whale species in the marginal ice zone north of Svalbard. The survey was performed from the Russian/Norwegian border and westwards (i.e. in Norwegian waters). In an area of just over 52 000 km^2 no white whales were seen, but an estimated 343 (95% CI: 136-862) bowhead whales and 837 narwhals (95% CI: 314-2233) was estimated to have occurred in the study area (Vacquié-Garcia *et al.*, 2017). The bowhead whales were generally found close to the ice edge, while the narwhals were found deep into the ice all the way to the end of

the survey lines (suggesting that their distributional area likely expanded north of the surveyed area). This study highlights that the sea ice represents an important habitat for these species in late summer in this region and clearly documents that aircrafts are required to conduct surveys of bowhead whales and narwhals.

Passive acoustic monitoring (PAM) is an efficient method for studying marine mammals that are vocally active in areas that are difficult to access on a year-round basis. PAM data from the Fram strait suggests that bowheads and narwhal are present inside the ice all year-round (Stafford *et al.* 2012, Ahonen *et al.* 2017,2019). Satellite tracking data from 13 bowhead whales from the Spitsbergen population (Kovacs *et al.* 2020) showed that the whales spread across the entire region thought to be the historical range for this species regionally – extending from East Greenland far into Russian territories, east of Franz Josef Land. The data showed that the whales dispersed southward from wintering grounds in the northernmost parts of their range during spring, returning northward again in autumn; a pattern opposite all other bowhead whale populations. They occupied areas with particularly cold sea surface temperatures and spent most of their time inside the ice edge, including areas classified as being 90-100% ice cover. Tagging of bowheads from the Spitsbergen population thus revealed that they do not migrate in the classical sense like other bowhead populations. In addition, a recently published study on genetics based on analyses of skin samples from the satellite tagged individuals, revealed that these animals are parts of the original Spitsbergen stock, and not individuals that have immigrated from other stocks due to lighter ice conditions as speculated (Bachmann *et al.* 2021).

White whales are the most frequently observed whale species around Svalbard where it stays close to the coast and glacier fronts during the ice-free time of year (Lydersen *et al.* 2001; Vacquié-Garcia *et al.* 2018). In 2018 the first aerial survey of white whales covering the entire Svalbard area was conducted (Vacquié-Garcia *et al.* 2020) and the stock size was estimated to 549 individuals (95% CI: 436–723). Given that the species is one of the most frequently observed cetaceans in the area the estimate was surprisingly low. It does however reflect on the previous difficulties in finding animals in white whale tagging programs. These data are important in providing a baseline for comparison with future estimates of this species very much affected by environmental changes.

Ringed seal is the principal prey of polar bears and is a key Arctic species that is closely associated with the sea ice for most of its life cycle. The Svalbard ringed seals have two different strategies following breeding and molting. The first is to migrate northwards to the marginal ice zone (Hamilton *et al.* 2015) while the other is to stay coastbound mainly close to glacier fronts (Hamilton *et al.* 2016). It is mostly younger animals that migrate north while adult animals remain by the coast. Satellite tracking of ringed seals before and after the marginal ice zone moved north show change in behaviour in that they spend more time swimming and diving and less time at the surface or resting on the ice compared to before (Hamilton *et al.* 2015). The data shows that they must work harder to locate food which ultimately could affect the condition of the animals with possible consequences for reproduction and survival (Hamilton *et al.* 2015). For the adult ringed seals that live along the coast of Svalbard, satellite tracking shows that these remain very connected to glacier fronts – more in the current situation than before the ice conditions changed in the fjords on the west side of Svalbard (Hamilton *et al.* 2016, 2019). Now there are individuals that stay in front of the same glacier front throughout the tracking period. Also, for these adult seals, there is a verified change in diving behaviour which indicates that they must work harder to locate food (Hamilton *et al.* 2016). In recent years, there have also been several reports of ringed seals resting on land, which has previously been uncommon for this very ice-dependent species. There have even been registrations of ringed seals grouped together with harbour seals (*Phoca vitulina*) on land, which is a development no one had anticipated in connection with climate change and the lack of sea ice for this species (Lydersen *et al.*, 2017).

Bearded seals are one of the least studied Arctic marine mammals. Tracking studies of adult animals in Svalbard revealed large individual variation in diving, movement and activity patterns (Hamilton *et al.* 2018). Bearded seals depend heavily on sea ice for giving birth and then use it as nursing and resting platforms for the pups. The reduction of sea ice in Svalbard did not affect the growth rate of pups since most females shifted from first-year ice floes to pieces of glacier-ice for birthing and nursing their offspring (Kovacs *et al.* 2020). However, this is a short-term solution since retraction of tidal glaciers eventually will end up on land, eliminating this replacement birthing and nursing strategy.

Identifying marine mammal hotspots and areas of high species richness is essential to help guide management and conservation efforts. A recent major study (Hamilton *et al.* 2021) summarizes the deployment of 585 satellite transmitters on 13 species of marine mammals in the Greenland- and northern Barents Seas from the period 2005 to 2018 and shows that parts of the study area, especially the northernmost parts, are to be regarded as "hot spot" areas for these marine mammal species (Figure A5.107). The marginal ice zone (MIZ) of the Greenland Sea and northern Barents Sea, the waters surrounding the Svalbard archipelago and a few Northeast Greenland coastal sites were identified as key marine mammal hotspots and areas of high species richness in this region.

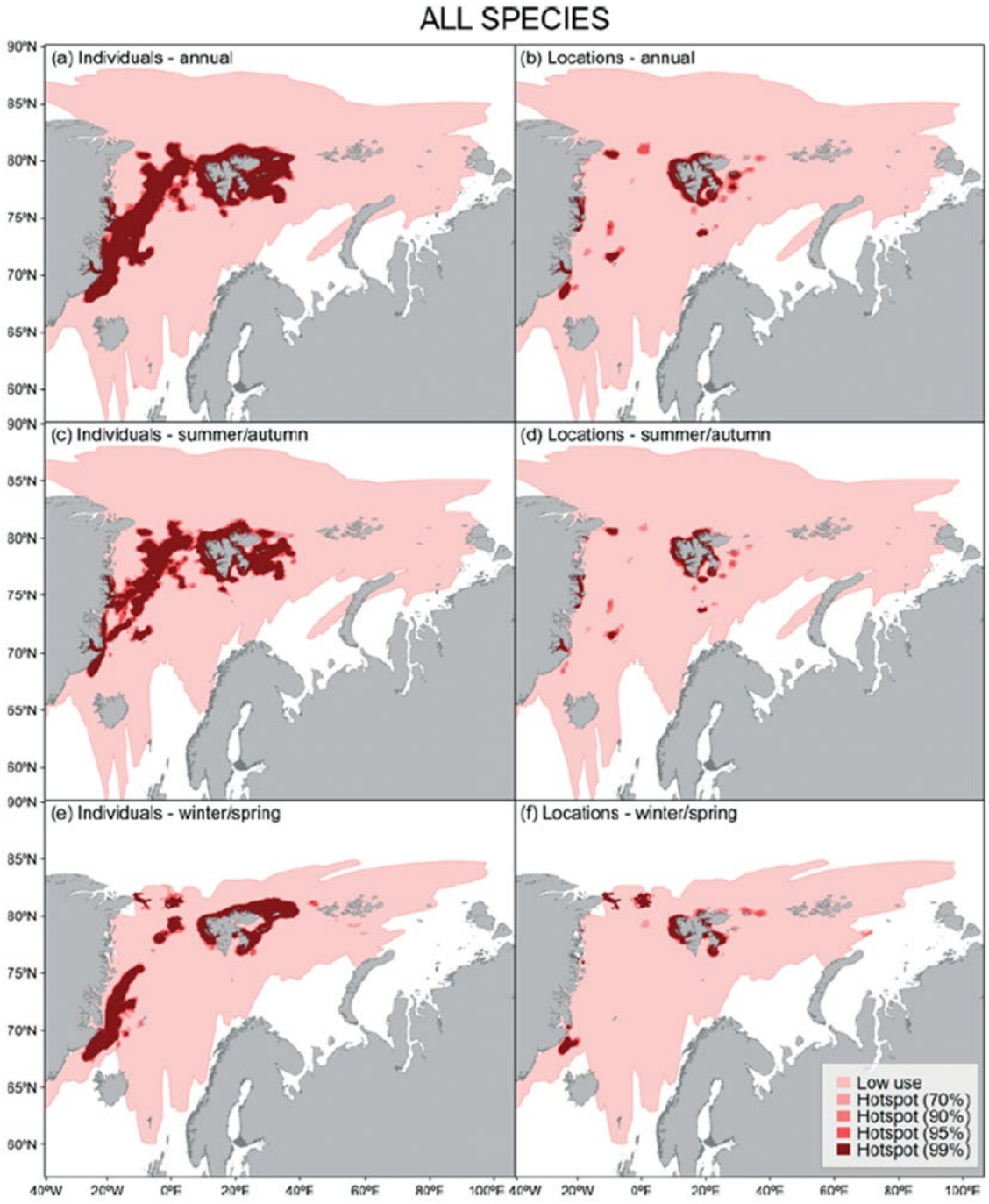

Figure A5.107: (a,c,e) individual hotspots and (b,d,f) location hotspots for the 13 species tagged around Svalbard and Northeast Greenland over (a,b) the entire year, (c,d) during summer/autumn and (e,f) during winter/spring. Increasing intensities of red indicate hotspots of different levels of statistical significance. Hamilton *et al.*, 2021.

References

Aars J. 2013. Variation in detection probability of polar bear maternity dens. Polar Biology 36(8):1089-1096.

Aars J., Marques T.A., Buckland S.T., Andersen M., Belikov S., Boltunov A., Wiig O. 2009. Estimating the Barents Sea polar bear subpopulation size. Marine mammal science 25(1): 35–52.

Aars J., Marques T.A., Lone K., Andersen M., Wiig Ø., Fløystad I.D.B., Hagen S.B., Buckland S.T. 2017. The number and distribution of polar bears in the western Barents Sea. Polar Research 36(1)

Ahonen H., Stafford K.M, de Steur L, Lydersen C., Wiig O, Kovacs K.M. 2017. The underwater soundscape in western Fram Strait: Breeding ground of Spitsbergen's endangered bowhead whales. Marine Pollution Bulletin 123(1-2):97-112.

Ahonen H., Stafford K.M, Lydersen C., de Steur L., Kovacs K.M. 2019. A multi-year study of narwhal occurrence in the western Fram Strait - detected via passive acoustic monitoring. Polar Research 8.

Bachmann L., Cabrera A. A., Heide-Jørgensen M. P., Shpak O. V., Lydersen C., Wiig Ø., Kovacs K. M. 2021. Mitogenomics and the genetic differentiation of contemporary Balaena mysticetus (Cetacea) from Svalbard. Zool. J. Linn. Soc. 191: 1192-1203.

Derocher A.E. 2005. Population ecology of polar bears at Svalbard, Norway. 47(3): 267–275.

Derocher A., Andersen M., Wiig Ø., Aars J., Hansen E., Biuw M. 2011. Sea ice and polar bear den ecology at Hopen Island, Svalbard. Marine Ecology Progress Series 441: 273–279.

Hamilton C.D., Kovacs K.M., Ims R.A., Aars J. and Lydersen C. 2017. An Arctic predator-prey system in flux: climate change impacts on coastal space use by polar bears and ringed seals. Journal of Animal Ecology. 86: 1054-1064.

Hamilton C. D., Kovacs K.M., Lydersen C. 2018. Individual variability in diving, movement and activity patterns of adult bearded seals in Svalbard, Norway. Scientific Reports 8(1):16988.

Hamilton C.D., Lydersen C., Aars J., Biuw M., Boltunov A.N., Born E.W., Dietz R., Folkow L.P, Glazov D.M., Haug T., Heide-Jørgensen M.P., Kettemer L.E., Laidre K.L., Øien N., Nordøy E.S., Rikardsen A. H., Rosing-Asvid A., Semenova V., Shpak O.V., Sveegaard S., Ugarte F., Wiig Ø., Kovacs K.M. 2021. Marine mammal hotspots in the Greenland and Barents Seas. Marine Ecology Progress Series. 659:3-28.

Hamilton C. D., Lydersen C., Ims R.A., Kovacs K.M. 2015. Predictions replaced by facts: a keystone species' behavioural responses to declining arctic sea-ice. Biology Letters 11(11).

Hamilton C. D., Lydersen C., Ims R.A., Kovacs K.M. 2016. Coastal habitat use by ringed seals *Pusa hispida* following a regional sea-ice collapse: importance of glacial refugia in a changing Arctic. Marine Ecology Progress Series 545:261-277.

Hamilton C. D., Vacquié-Garcia J., Kovacs K.M., Ims R.A., Kohler J., Lydersen C. 2019. Contrasting changes in space use induced by climate change in two Arctic marine mammal species. Biology Letters15(3):20180834

Kovacs K.M., Aars J., Lydersen C. 2014. Walruses recovering after 60+ years of protection in Svalbard, Norway. Polar Research 33: 26034.

Kovacs K. M., Krafft B.A., Lydersen C. 2020. Bearded seal (*Erignathus barbatus*) birth mass and pup growth in periods with contrasting ice conditions in Svalbard, Norway. Marine Mammal Science 36(1):276-284.

Lone K., Merkel B., Lydersen C., Kovacs K.M. Aars J. 2018. Sea ice resource selection models for polar bears in the Barents Sea subpopulation. Ecography, 41: 567-578.

Lydersen C., Aars J., Kovacs K.M. 2008. Estimating the number of walruses in Svalbard from aerial surveys and behavioural data from satellite telemetry. Arctic 61: 119–128.

Lydersen C., Martin A., Kovacs K.M., Gjertz I. 2001. Summer and autumn movements of white whales *Delphinapterus leucas* in Svalbard, Norway. Marine Ecology-progress Series. 219:265-274.

Lydersen C., Vaquie-Garcia J., Lydersen E., Christensen G.N., Kovacs K.M. 2017. Novel terrestrial haulout behaviour by ringed seals (*Pusa hispida*) in Svalbard, in association with harbour seals (*Phoca vitulina*). Polar Research 36(1):1374124.

Maduna S. N., Aars J., Fløystad I., Klutsch C. F. C., Zeyl Fiskebeck E. M. L., Wiig Ø., Ehrich D., Andersen M., Bachmann L., Derocher A., Nyman T., Eiken H. G., Hagen S. B. 2021. Sea ice reduction drives genetic differentiation among Barents Sea polar bears. Proc. R. Soc. B 288: 20211741.

Merkel B., Aars J. Shifting polar bear Ursus maritimus denning habitat availability in the European Arctic. Polar Biology, https://doi.org/10.1007/s00300-022-03016-5.

Peacock E., Sonsthagen S.A., Obbard M.E., Boltunov A., Regehr E.V., Ovsyanikov N., Aars J., Atkinson S.N., Sage G.K., Hope A.G., Zeyl E., Bachmann L., Ehrich D., Scribner K.T., Amstrup S.C., Belikov S., Born E.W., Derocher A.E., Stirling I., Taylor M.K., Wiig Ø., Paetkau D., Talbot S.L. 2015. Implications of the Circumpolar Genetic Structure of Polar Bears for Their Conservation in a Rapidly Warming Arctic. PLoS One 10(1):e112021

Stafford K. M., Moore S.E., Berchok C.L., Wiig Ø., Lydersen C., Hansen E., Kalmbach D., Kovacs K.M. 2012. Spitsbergen's endangered bowhead whales sing through the polar night. Endangered Species Research 18(2):95-103.

Stern H. L., Laidre K.L. 2016. Sea-ice indicators of polar bear habitat. The Cryosphere 10(5):2027-2041.

Vacquié-Garcia J., Lydersen C., Ims R.A., Kovacs K.M. 2018. Habitats and movement patterns of white whales *Delphinapterus leucas* in Svalbard, Norway in a changing climate. Movement Ecology 6(1):21.

Vacquié-Garcia J., Lydersen C., Marques T.A., Aars J., Ahonen H., Skern-Mauritzen M., Øien N. Kovacs K.M. 2017. Late summer distribution and abundance of ice-associated whales in the Norwegian High Arctic. Endangered Species Research 32:59-70.

Vacquié-Garcia J., Lydersen C., Marques T., Andersen M., Kovacs K.M. 2020. First abundance estimate for white whales *Delphinapterus leucas* in Svalbard, Norway. Endangered Species Research 41:253-263.

Seabirds

By Per Fauchald (NINA)

About six million pairs from 36 seabird species breed regularly in the Barents Sea (Barrett *et al.* (2002), Table A5.6). Allowing for immature birds and non-breeders, the total number of seabirds in the area during spring and summer is about 20 million individuals. Ninety percent of the birds belong to only 5 species: Thick-billed murre, little auk, Atlantic puffin, northern fulmar and black-legged kittiwake. The distribution of colonies is shown in Figure A5.108. Colonies in the high-Arctic Archipelago are dominated by little auks, thick-billed murres and kittiwakes. These birds utilize the intense secondary production that follows the retreating sea ice. Little auks feed mainly on lipid rich Calanus species, amphipods and krill while thick-billed murres and black-legged kittiwakes feed on polar cod, capelin, amphipods and krill. The seabird communities, as well as their diet change markedly south of the polar front. In the Atlantic part of the Barents Sea, the seabirds depend more heavily on fish, including 0-group fish, capelin, I-group herring and sandeels. The shift in diet is accompanied by a shift in species composition. In the south, thick-billed murres are replaced by its sibling species, the common murre. Large colonies of Atlantic puffins that largely sustain on the drift of fish larvae along the Norwegian coast, are found in the southwestern areas.

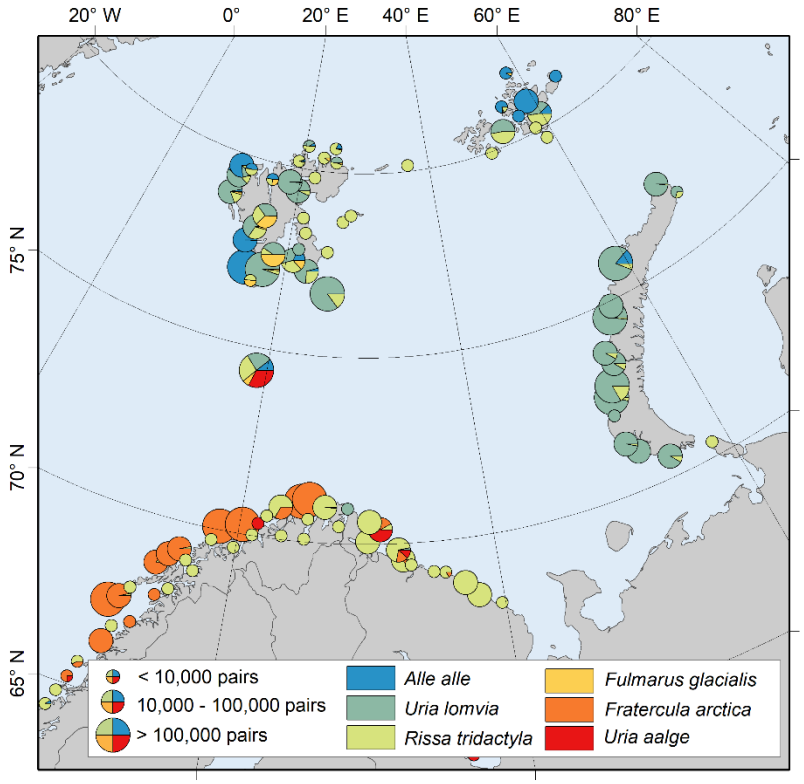

Figure A5.108: Major seabird colonies in the Barents Sea. Data compiled from SEAPOP (www.seapop.no), Fauchald *et al.* (2015) and The Seabird Colony Registry of the Barents and White Seas.

Table A5.6: Seabirds in the Barents Sea sorted by breeding population size in decreasing number. Breeding pairs are from Strøm *et al.* (2009). Observations on BESS 2020 are the observations from Norwegian and Russian vessels during the ecosystem survey in 2021*.

Species name	Scientific name	Breeding pairs	Observations on BESS 2021
Thick-billed murre	Uria lomvia	1 250 000	2 326
Little auk	Alle alle	>1 010 000	0
Atlantic puffin	Fratercula arctica	910 000	349
Northern fulmar	Fulmarus glacialis	500 000–1 000 000	9 795
Black-legged kittiwake	Rissa tridactyla	682 000	6 517
Common eider	Somateria mollisima	157 000–159 000	7
Herring gull	Larus argentatus	122 600	504
Common murre	Uria aalge	104 000	91
Arctic tern	Sterna paradisaea	65 000	84
Black guillemot	Cepphus grylle	58 000	0
Great black-backed gull	Larus marinus	22 930	225
Razorbill	Alca torda	19 600	4

Mew gull	Larus canus	14 200	0
Glaucous gull	Larus hyperboreus	9 000–15 000	111
Great cormorant	Phalacrocorax carbo	11 570	3
European shag	Phalacrocorax aristotelis	6 350–6 400	0
European storm-petrel	Hydrobates pelagicus	1 000–10 000	0
Lesser Black-backed gull	Larus fuscus	3 500	6
Ivory gull	Pagophila eburnea	2 200–3 750	0
Northern gannet	Morus bassanus	1 900–2 150	47
Arctic skua	Stercorarius parasiticus	1 150	72
King eider	Somateria spectabilis	1 000	0
Common tern	Sterna hirundo	>1 000	0
Heuglin’s Gull	Larus heuglini	600–1 100	191
Great skua	Stercorarius skua	540–1 100	61
Leach‘s storm petrel	Oceanodroma leucorhoa	100–1 000	0
Steller‘s eider	Polysticta stelleri	10–100	0
Sabine's gull	Xema sabini	1–10	0
Great northern diver	Gavia immer	0–3	1
Long-tailed duck	Clangula hyemalis	?	0
Black scoter	Melanitta nigra	?	2
Velvet scoter	Melanitta fusca	?	0
Red-breasted merganser	Mergus serrator	?	0
Black-throated loon	Gavia arctica	?	1
Long-tailed skua	Stercorarius longicaudus	?	6
Pomarine skua	Stercorarius pomarinus	?	792
Sooty shearwater	Puffinus griseus	0	18
Ross's gull	Rhodostethia rosea	0	0

***The Norwegian part of the survey in 2021 was restricted to the western and southern part of the Barents Sea.**

Population monitoring in Norway and Svalbard has revealed a downward trend for several populations the last 30 years, including black-legged kittiwakes (Figure A5.109A) and Atlantic puffin (Figure A5.109E) on the Norwegian mainland and thick-billed murres (Figure A5.109F) on Svalbard. The population of common murre was decimated in the 1980s mainly due to a collapse in the capelin stock combined with low abundance of alternative prey. The populations on Bjørnøya

and some colonies on the Norwegian mainland have increased since then (Figure A5.109C and D). The status and trends of the populations of seabirds in the Eastern Barents Sea is less known.

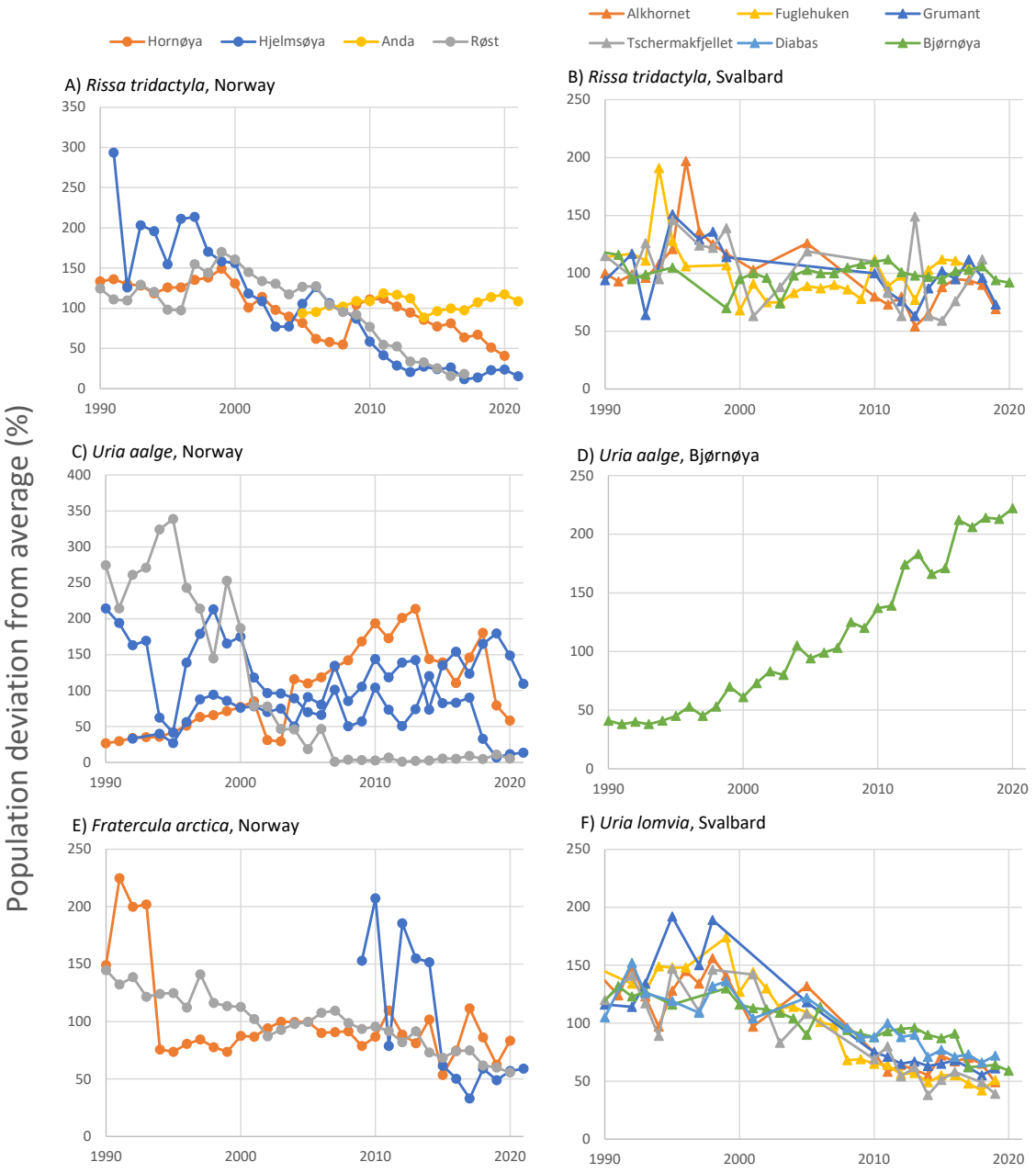

Figure A5.109: Seabird population fluctuations in SEAPOP monitoring sites on the Norwegian mainland (left panel) and Svalbard (right panel). Data sources: Miljøovervåking Svalbard og Jan Mayen -MOSJ (www.mosj.no, updated 2022), SEAPOP (www.seapop.no, updated 2022).

In addition of being an important breeding area for seabirds, data from recent tracking studies (Fauchald *et al.* 2021) show that the Barents Sea is a "hot spot" for Northeast Atlantic seabirds from March to October and in particular an important feeding area for seabirds in early autumn. Accordingly, the number of pelagic seabirds reaches a maximum of approximately 10 million individuals in August, just after breeding (Figure A5.110). This peak is mainly due to Atlantic puffins, Northern fulmars, common murres and black-legged kittiwakes migrating from colonies around the Norwegian Sea into the Barents Sea to feed. This period, from August to September, is also the period when the auk species moult and become flightless for several weeks. After the feeding period, parts of the populations of Atlantic puffin, thick-billed murre, black-legged

kittiwakes, Northern fulmar and little auks leave the Barents Sea. Thus, the number of birds reaches a minimum in the darkest period from December to January with about 5 million birds (Figure A5.110). In general, populations from the western colonies leave the Barents Sea earlier (September–October) and return later (March–April) than birds from the eastern colonies, and a larger proportion of the eastern populations tend to stay in the Barents Sea throughout winter. Migrating birds overwinter in large ocean areas in the northwest and north-central part of the North Atlantic, including the coastal areas off southern and western Greenland, around Iceland, in the Denmark Strait and in the Irminger and Labrador Seas. Common murres from Bjørnøya, Murman and Finnmark stay in the southern Barents Sea throughout the non-breeding period. The seabirds return gradually to the colonies and adjacent areas in early spring from February to April.

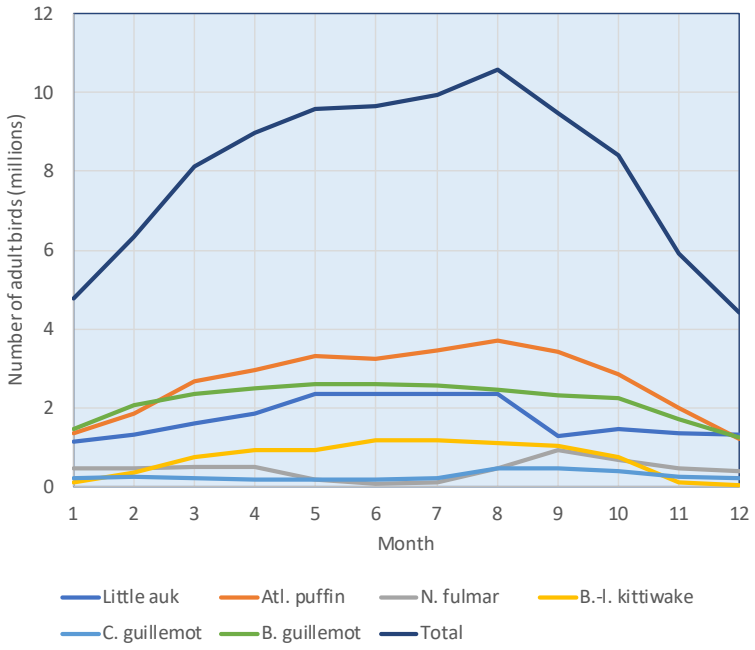

Figure A5.110: Estimated number of adult breeding seabirds present in the Barents Sea area during the annual cycle. Estimates are based on population size and year-round tracking of different populations by the SEATRACK program (see Fauchald *et al*. 2021).

Broadly, the spatial distribution of seabirds during the ecosystem survey in September reflects the climatic gradient from a boreal Atlantic climate with common murres, puffins, herring and black-backed gull in the south and west, to an Arctic climate with little auks, thick-billed murres and kittiwakes in the north and east (Figure A5.111). Seabirds have been surveyed uninterruptedly on Norwegian vessels in the western part of the Barents Sea since 2004, however, the first years and 2021 did not cover the northern areas. Based on the minimum annual survey extent from 2009 to 2020, the abundance (Figure A5.112) of different species and the centre of gravity of the spatial distribution (Figure A5.113) was calculated for each year.

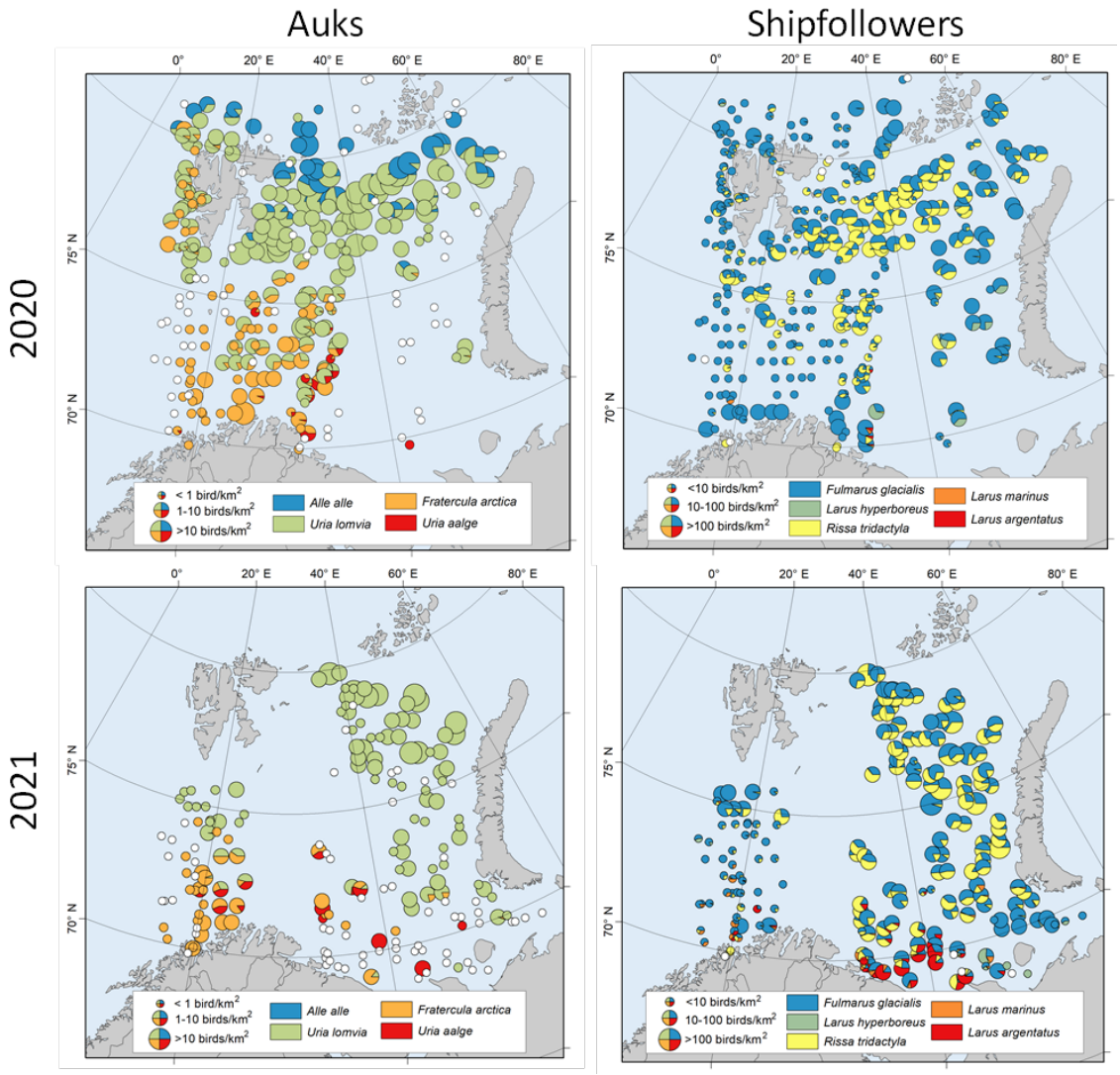

Figure A5.111: Density of seabirds during the Barents Sea ecosystem surveys in 2020 (top) and 2021 (bottom). Left panel is the distribution of auks (little auk, thick-billed murre, Atlantic puffin and common murre). Right panel is the distribution of shipfollowers (northern fulmar, glaucous gull, black-legged kittiwake, black-backed gull and herring gull). Note that the Norwegian survey in 2021 was restricted to the western and southern part of the study area.

Abundance estimates indicate relatively large fluctuations in the number of seabirds at-sea (Figure A5.112). Northern fulmar, black-legged kittiwake and herring gull have decreased significantly in abundance the last ten years. These changes do not necessarily reflect the observed population trends from the colonies (cf. Figure A5.109) since the at-sea abundances also are influenced by annual differences in migration pattern. Note that the ship-followers are attracted to the ship from the surrounding areas and individual birds are therefore likely to be counted several times. Accordingly, the estimated numbers of ship-followers are probably grossly overestimated. Analyses of the centres of gravity show a northward displacement for several species the last ten years (Figure A5.113). The centres of gravity of little auks, thick-billed murre, glaucous gull, black-legged kittiwake, northern fulmar and black-backed gull have moved from 150 to 500 km northward from 2008 to 2019, suggesting that seabirds have been displaced toward the north following a period of warming. Although longer time-series might be warranted, this result could be an early signal of a "borealization" (Fossheim *et al.* 2015) of the seabird communities in the Barents Sea. This result is corroborated by a recent study of the population dynamics of breeding seabirds on Svalbard, suggesting a borealization of the seabird colonies (Descamps and Strøm 2021). The analyses of the Svalbard populations found a general decrease in Arctic species (ivory gull, glaucous gull, little auk and thick-billed murre), while the more boreal species

(common murre, northern fulmar, black-legged kittiwake, northern gannet and great skua) have generally been stable or increasing.

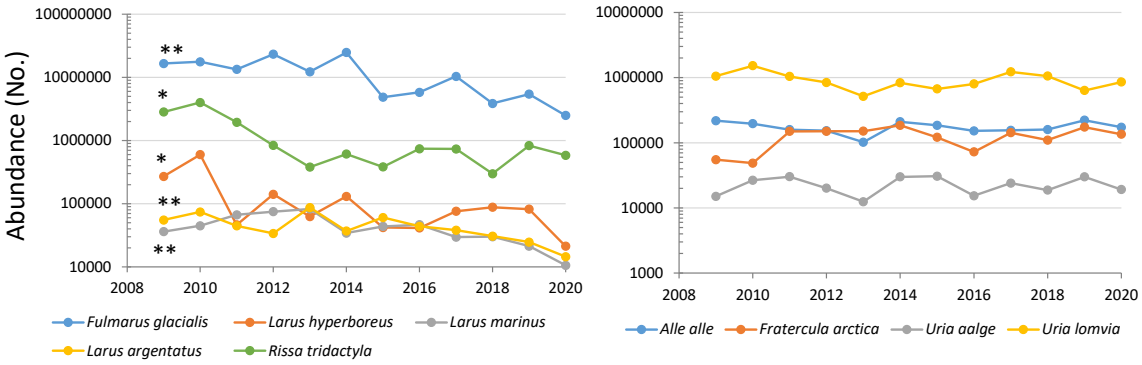

Figure A5.112: Abundance of auks (left) and ship-followers (right) in the Western Barents Sea during the ecosystem surveys 2009–2020. Note that the numbers of ship-followers are systematically overestimated. Asterisks indicate significant negative trends in the abundance estimates (* *P* < 0.05, ** *P* < 0.001).

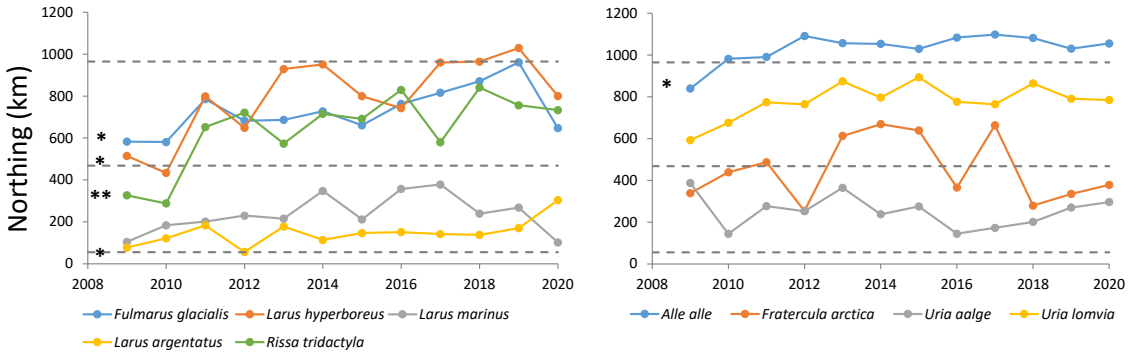

Figure A5.113: Centre of gravity in the north direction of the distribution of auks (left) and shipfollowers (right) in the Western Barents Sea during the ecosystem surveys 2009–2020. Hatched lines indicate the positions of Hammerfest (Norwegian coast), Bjørnøya and Ny Ålesund (Spitsbergen). Asterisks indicate significant positive linear trends in the position of the centre of gravity (* *P* < 0.05, ** *P* < 0.001).

References

Anker-Nilssen, T., Bakken, V., Strøm, H., Golovkin, A.N., Bianki, V.V. and Tatarinkova, I.P. 2000. The Status of Marine Birds Breeding in the Barents Sea Region. Norsk Polarinstitutt Rapportserie, 113. 213 pp.

Barrett, R.T., Anker-Nilssen, T., Gabrielsen, G.W. and Chapdelaine, G. 2002. Food consumption by seabirds in Norwegian waters. - ICES Journal of Marine Science, 59: 43-57.

Descamps, S., Strøm, H. 2021. As the Arctic becomes boreal: Ongoing shifts in a high-Arctic seabird community. Ecology: e03485.

Fauchald, P., Ziryanov, S. V., Strøm, H. and Barrett, R. T. 2011. Seabirds of the Barents Sea. Pages 373-394 in Jakobsen T, Ozhigin VK (Eds) The Barents Sea. Ecosystem, Resources, Management. Tapir Academic Press, Trondheim, Norway.

Fauchald, P., Anker-Nilssen, T., Barrett, R., Bustnes, J. O., Bårdsen, B. J., Christensen-Dalsgaard, S., Descamps, S., Engen, S., Erikstad, K. E., Hanssen, S. A., Lorentsen, S.-H., Moe, B., Reiertsen, T., Strøm, H. and Systad, G. H. (2015). The status and trends of seabirds breeding in Norway and Svalbard. NINA report 1151: 84 pp.

Fauchald, P., Tarroux, A., Amélineau, F., Bråthen, V. S., Descamps, S., Ekker, M., Helgason, H. H., Johansen, M. K., Merkel, B., Moe, B., Åström, J., Anker-Nilssen, T., Bjørnstad, O., Chastel, O., Christensen-

Dalsgaard, S., Danielsen, J., Daunt, F., Dehnhard, N., Erikstad, K. E., Ezhov, A., Gavrilo, M., Hallgrimsson, G. T., Hansen, E. S., Harris, M., Helberg, M., Jónsson, J. E., Kolbeinsson, Y., Krasnov, Y., Langset, M., Lorentsen, S. -H., Lorentzen, E., Newell, M., Olsen, B., Reiertsen, T. K., Systad, G. H., Thompson, P., Thórarinsson, T. L., Wanless, S., Wojczulanis-Jakubas, K., Strøm, H. 2021. Year-round distribution of Northeast Atlantic seabird populations: Applications for population management and marine spatial planning. Marine Ecology Progress Series 676: 255–276.

Fossheim M, Primicerio R, Johannesen E, Ingvaldsen RB, Aschan M and Dolgov AV. 2015. Recent warming leads to a rapid borealization of fish communities in the Arctic. Nature Climate Change 5, 673–677.

Strøm, H., Gavrilo, M.V., Krasnov, J.V. and Systad, G.H. 2009. Seabirds. In Joint Norwegian-Russian Environmental Status 2008 Report on the Barents Sea Ecosystem. Part II – Complete report, pp. 67-73. Ed. by J.E. Stiansen, O. Korneev, O. Titov, P. Arneberg, A. Filin, J.R. Hansen, Å. Høines and S. Marasaev. IMR/PINRO Joint Report Series, 3/2009.

Anthropogenic impact

Fishing activity

By Bjarte Bogstad (IMR) and Alexey Russkikh (PINRO)

Distribution of fishery

Fishing activity in the Barents Sea is tracked by the Vessel Monitoring System (VMS) which offer valuable information about temporal and spatial changes in fishing activity (Figure A5.114). The most widespread gear used in the Barents Sea is bottom trawl; but longlines, gillnets, Danish seines, and handlines are also used in demersal fisheries. Pelagic fisheries use purse-seines and pelagic trawls. The shrimp fishery used special bottom trawls.

From 2011 onwards, minimum mesh size for bottom-trawl fisheries for cod and haddock is 130 mm for the entire Barents Sea; previously the minimum mesh size was 135 mm in the Norwegian EEZ and 125 mm in the Russian EEZ. It is still mandatory to use sorting grids. Minimum legal catch size was harmonized at the same time: for cod from 47 cm (Norway) and 42 cm (Russia) to 44 cm for all, and for haddock from 44 cm (Norway) and 39 cm (Russia) to 40 cm for all.

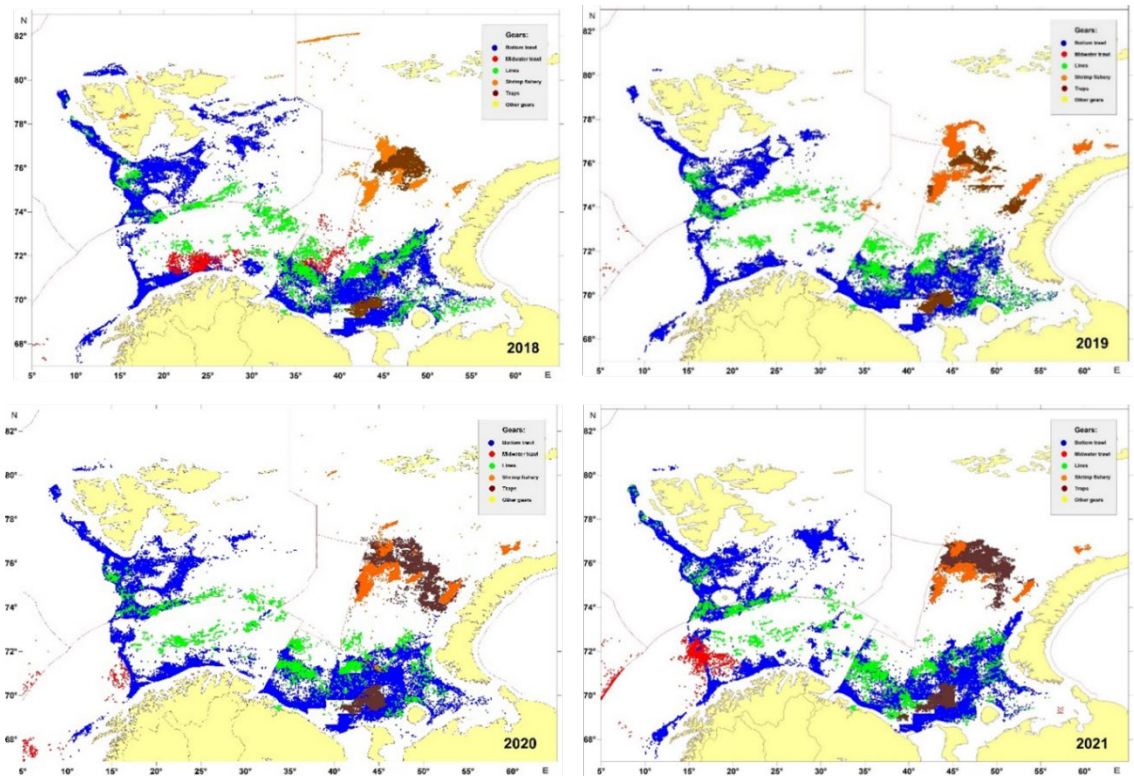

Figure A5.114: Location of Russian and foreign fishing activity from commercial fleets and fishing vessels used for research purposes in 2017–2021 as reported (VMS) to Russian authorities. These are VMS data linked with logbook data (source: PINRO Fishery statistics database).

Catch dynamic

The commercial fisheries in the Barents Sea Ecoregion target few stocks. The largest demersal fisheries target gadoid species: cod, haddock and saithe predominantly using trawls, gillnets, longlines, and handlines. Pelagic fishery using midwater trawl and purse seine target for capelin. The largest catches were observed in the 1960–80s and reached a total of 3-4 million tonnes, mainly due to the catch of capelin. In recent years, large catches of capelin have been sporadic, Gadoids catches varying around 1 million tonnes and the total catch has not exceeded 1.5 million tonnes (Figure A5.115).

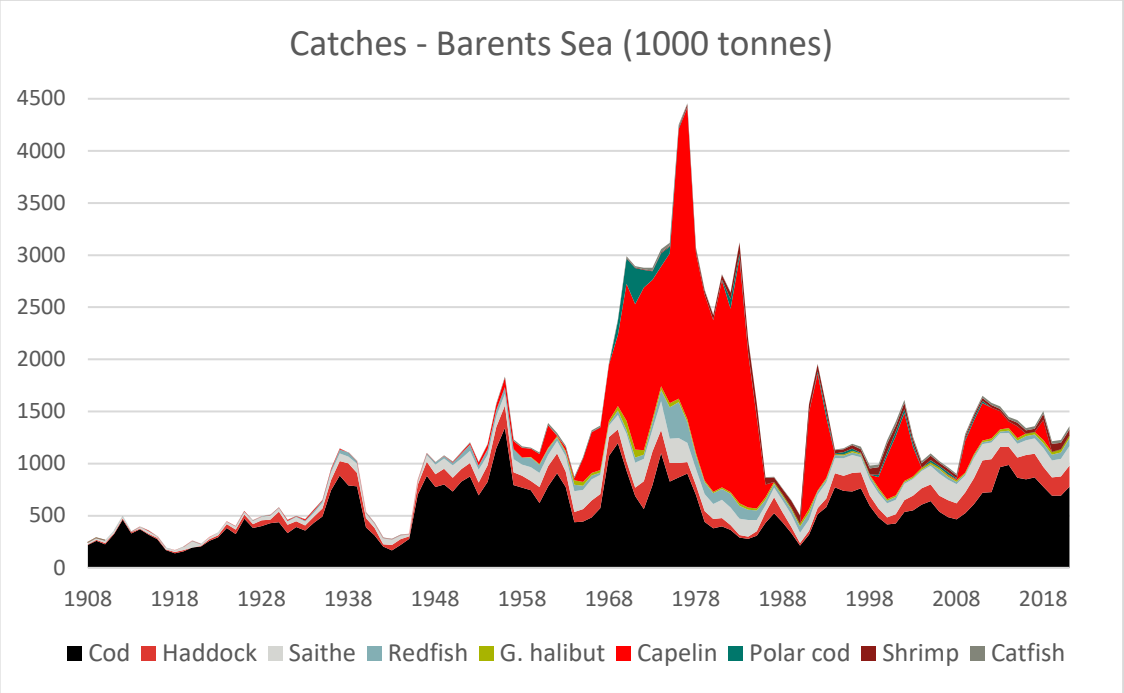

Figure A5.115: Catches of all species in the Barents Sea in 1908–2021 (Historical nominal catches 1950–2010, official nominal catches 2006–2019, preliminary catches 2020–2021, ICES, Copenhagen)

The catches of other species are much less. They are caught both as directed fisheries and as bycatch. Historically, very large catches of polar cod have been observed, but recently this species has not been harvested, and redfish and shrimp dominate in catches. The total catch of these species has been growing in recent years and is more than 150 thousand tonnes (Figure A5.116).

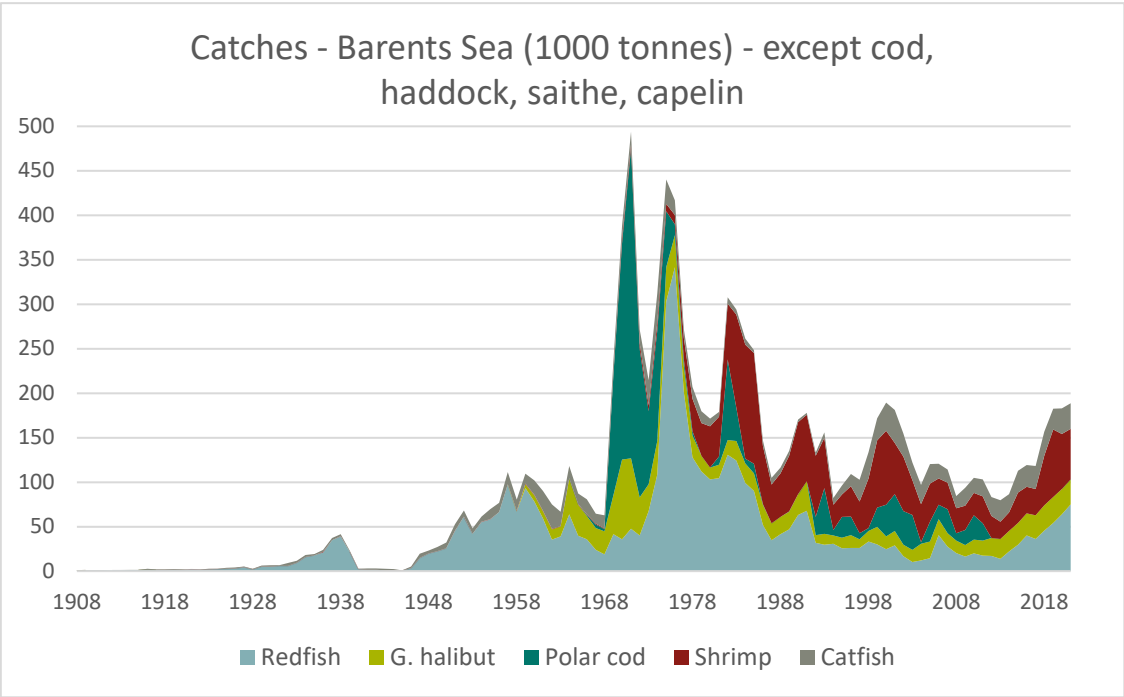

Figure A5.116: Catches of 'minor' species for fisheries in the Barents Sea in 1908–2021 (Historical nominal catches 1950–2010, official nominal catches 2006–2019, preliminary catches 2020–2021, ICES, Copenhagen).

The crustacean fisheries target also red king crab, and snow crab and using traps. Most catches of crabs are from coastal areas.

More information about the fisheries is available in the ICES Fisheries overview for the Barents Sea.

Catches of shellfish

By Aleksei V. Stesko (PINRO), Ann Merete Hjelset (IMR)

Northern shrimp (*Pandalus borealis*)

Norwegian and Russian vessels harvest northern shrimp over the stock's entire area of distribution in the Barents Sea. Vessels from other nations are restricted to trawl shrimp only in the Svalbard Fisheries Protection Zone and the Loophole. No overall TAC has been set for northern shrimp, and the fishery is regulated through effort control, licensing, and a partial TAC in the Russian zone. The regulated minimum mesh size is 35 mm.

The stock assessment indicates that the stock has been fished sustainably and has remained well above precautionary reference limits throughout the history of the fishery (NAFO/ICES 2021). Accordingly, ICES used the MSY-approach to advice a TAC of 150 000 and 140 000 metric tonnes in 2020 and 2021–2022 respectively (ICES 2021).

Geographical distribution of the fishery in 2009–2019 was more easterly directed compared to previous decades. As results, catch levels from some of the more traditional western fishing grounds have declined. Recent reports indicate lower catch rates than would be expected given the overall good stock condition. This may be related to operation costs for a relatively small fleet to move away from more traditional fishing grounds, and to find new grounds with commercially viable shrimp concentrations. There are currently no indications of a significant shift in the stock distribution itself.

Fisheries for northern shrimp in the Barents Sea and waters adjacent to Spitsbergen Archipelago have been carried out since the 1950s. The largest catches were recorded in the mid-1980s (more than 120 000 tonnes) and during 1990–1991, 2000 (approximately 80 000 tonnes). Since 2005, total annual catch of northern shrimp in this area have remained at the 20 000–40 000 thousand tonnes level (Figure A5.117) after 2018 total catch has rapidly grown mainly by Russian fishery, but in 2020 it decreased due to features of shrimp spatial distribution. In 2021 fishery effort was a bit higher than 2020, however of the TAC in the Russian EEZ only 71% was caught.

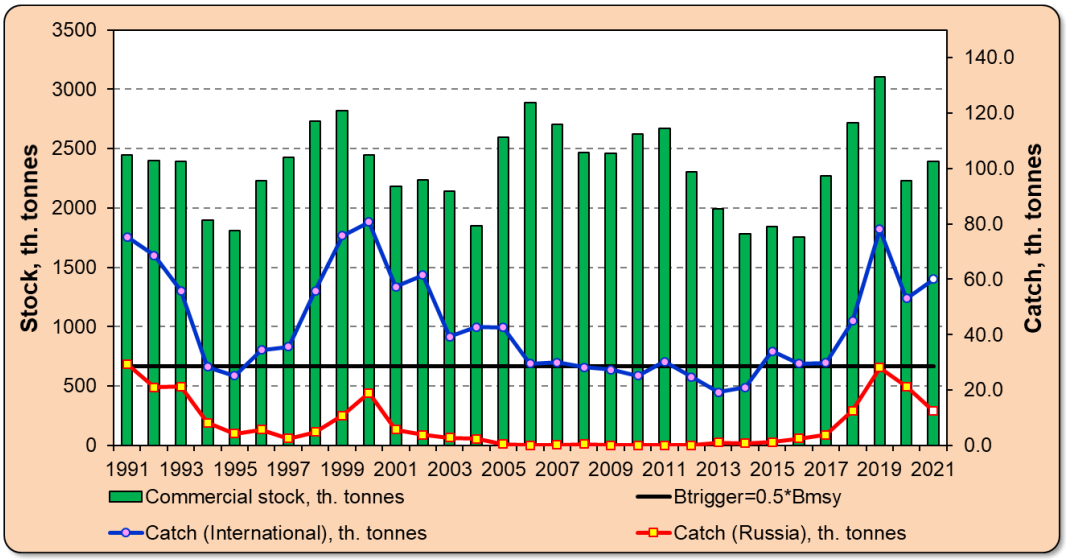

Figure A5.117: Catch and recommended TAC of the northern shrimp in the Barents Sea and waters around Spitsbergen archipelago in 1991–2021, 2022 is forecast (Bakanev, 2021; Bakanev, 2022 (in print)).

Trawl surveys of northern shrimp stocks have been carried out in the Barents Sea since 1982. During the 2005–2021 period, the stock has remained stable, showing fluctuations but without a clear trend.

Red king crab (Paralithodes camtschaticus)

Red king crab fishery has been managed separately in the Norwegian Economic Zone (NEZ) and Russian Economic Zone (REZ) from 2007 onwards.

The commercial fishery for red king crab in the Russian Economic Zone of the Barents Sea has been carried out since 2004. Russian Fisheries Regulations stipulate that males with carapace width greater than or equal to 150 mm can only be caught using traps. Trawl bycatch of crabs must be returned to sea alive.

Total catch also increased in subsequent years; in 2021, total catch of red king crabs in Russian Economic Zone was 12.9 thousand tonnes (Figure A5.118, the commercial stock index for red king crab was 200 thousand tonnes) bycatches. In 2021 also the fishing grounds in Eastern coast region was exploited, after having been closed for fishery due to high bycatch numbers of females and illegal males for several years.

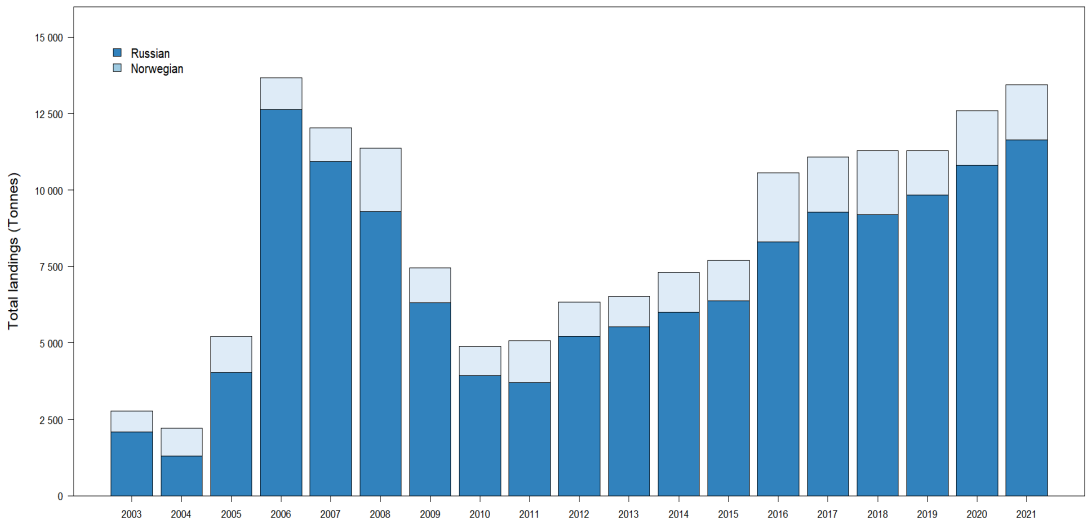

Figure A5.118: Total catch of the red king crab in the Russian Economic Zone and Norwegian coastal waters of the Barents Sea in 2003–2021.

Distribution of red king crab is assessed by trap and trawl surveys. In the coastal part of the Barents Sea Russian vessels have been using traps for investigations since 2008. The most density of egged female clusters was detected in Kanin peninsula region, in shallow waters 20–30 m depths. Modern stock assessment of red king crab in the Russian EEZ based on special trawl surveys 2017 to 2021. It increased until 2018–2019 but has particularly decreased since 2020. The main clusters of crab commercial stock shifted to north-eastward. The most eastern boundary of red king crab distribution was recorded in 2015 and 2017. Two adult individuals (male and female with eggclutch) in eastern Pechora Sea near Vaygach Island, and the southwestern coast of Novaya Zemlya Archipelago. Some crabs were caught in the "Gorlo" of the White Sea. Science observer worked in snow crab fishery reported about findings of king crabs near 75 N 48 E of the Barents Sea, but he didn't record it by photo or video (Stesko and Bakanev, 2022, in print). In 2021 PINRO's fishery observer had seen one specimen of crab near the Spitsbergen (Svalbard) area in approximate coordinates 77 10 N 29 30 E at a depth of 180 m.

The Norwegian fishery for the red king crab (RKC) is subjected to two different management regimes; a vessel quota fishery in the quota regulated area (QRA) and a free fishery with a discard ban in the free fishing area (FFA) west of 26°E (North Cape) (See Sundet and Hoel 2016, for detailed information).

In 2008 there was a change in the management of this fishery with the introduction of an annual vessel quota in tonnes, minimum legal-size restrictions fishery for both male and female crabs on 130 mm carapace length and trap limits of 30 traps among other things. For Norwegian landings of red king crab, see Figure A5.118.

Snow crab (Chionoecetes opilio)

The snow crab fishery carried out by Norwegian, Spanish, and Russian vessels began in international waters of the Barents Sea (Loophole) in 2013. During 2015–2016, average daily catch declined by 10–20% compared with the 2014 estimate (Bakanev and Pavlov, 2021).

Russian vessels fished crabs in this area until 2016. In 2016, Russian vessels started fishing snow crabs in Russian waters. In 2017–2021, the Russian fishery for snow crabs was conducted only within the Russian EEZ (Figure A5.119).

Total catches increased until 2015, then decreased until 2017 before increasing again to a record high value in 2021 (Figure A5.120).

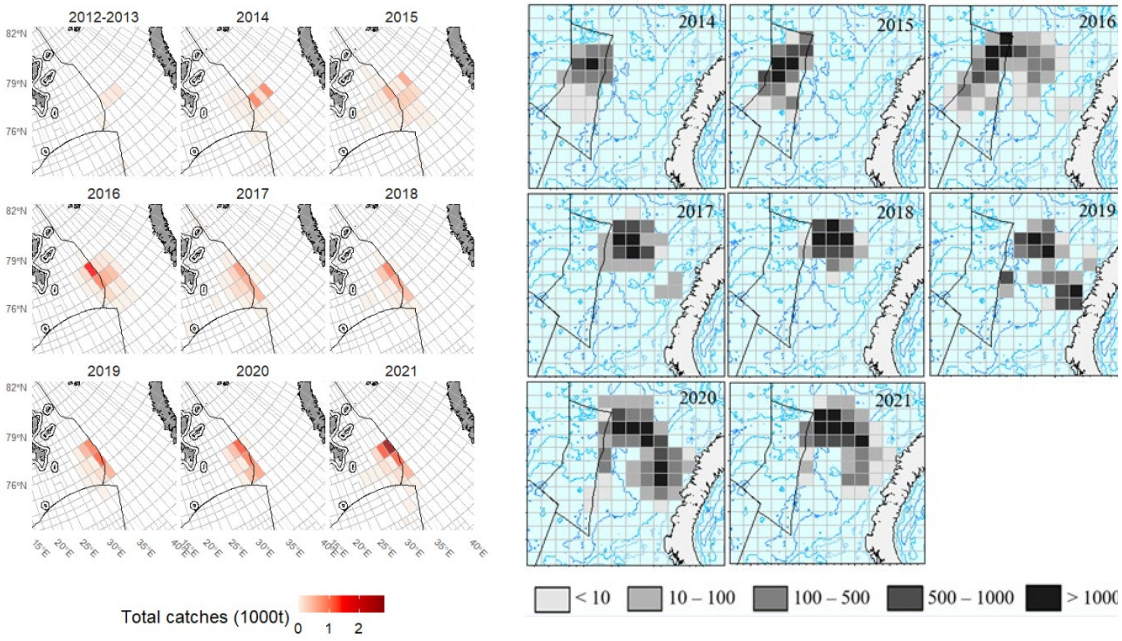

Figure A5.119: Spatial distribution of snow crab fishery from Norwegian (left panel) and Russian (right panel) vessels in the period 2013–2021.

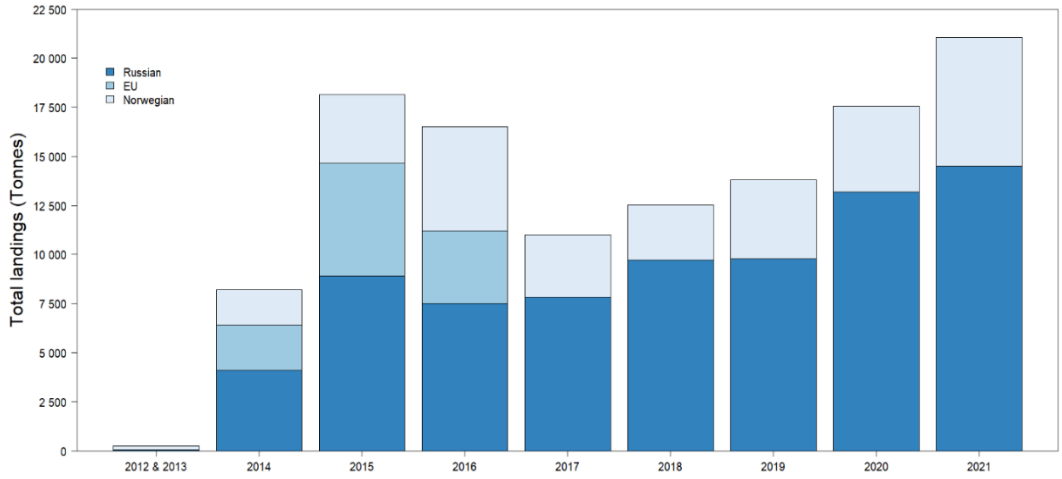

Figure A5.120: Total landings (in tonnes) of snow crab from the Barents Sea in the period 2012 to 2021.

Russian vessels used conical and trapezoidal traps for the snow crab fishery until 2018, but now they use mainly conical traps.

In July 2015, Norway and Russia agreed that the snow crab is a sedentary species. This decision changed the status from a water column species to a resource of continental shelf (Joint Norwegian-Russian Fisheries Commission, 2015).

The Norwegian fishery for snow crab commenced in 2012 with only 2.5 tones landed. The main fishing area for the Norwegian fishery is in the central part of the Barents Sea (see Figure A5.119). Snow crab in the Barents Sea fishery is exclusively harvested using conical pots deployed in strings connected to longline. The minimum legal size for male snow crab in the Norwegian fishery is now 95 mm carapace width (CW).

The further spread of the snow crab population to the west and northwest at the Norwegian continental shelf, will probably depend on temperature and food resources available for the

snow crab. The highest densities are still in central parts of the Barents Sea, with some scarce observations on the west coast of Spitsbergen Island.

References

Bakanev S.V. Shrimp State of biological resources of the Barents and the White seas and the North Atlantic in 2020, 40-41, 2021

Bakanev S.V. Shrimp State of biological resources of the Barents and the White seas and the North Atlantic in 2021, 40-41, 2022 (in print)

Bakanev S.V., Stesko A.V. Red king crab State of biological resources of the Barents and the White seas and the North Atlantic in 2021, 43-44, 2022 (in print)

Sundet, J.H.and Hoel. A.H. 2016. The Norwegian management of an introduced species: the Arctic red king crab fishery. Marine Policy, 72; 278-284. DOI: 10.1016/j.mar.pol.2016.04.041

Pavlov V.A., Bakanev S.V., Snow crab State of biological resources of the Barents and the White seas and the North Atlantic in 2020, 44-45, 2021

NAFO. 2020. Report of the Joint NAFO/ICES Pandalus Assessment Working Group (NIPAG), 27 October–2 November 2020, online meeting. NAFO SCS Doc. 20/21, Serial No. N7143.

ICES Advice on fishing opportunities, catch, and effort Arctic Ocean, Barents Sea, Faroes, Greenland Sea, Iceland Sea, and Norwegian Sea ecoregions Northern shrimp (*Pandalus borealis*) in subareas 1 and 2 (Northeast Arctic) pra.27.1-2. https://doi.org/10.17895/ices.advice.7833

Marine litter

T. Prokhorova (PINRO), B.E. Grøsvik (IMR) and R. Klepikovsky (PINRO)

Plastic dominated among anthropogenic pollutants on the water surface in 2021 as in 2020 (72.4% and 68.9% of observations, respectively) (Figure A5.121. The maximum surface observation of plastic litter was 5 m^3, with the average of 0.01 m^3 (except the single maximum catch of 5 m^3), and this is the same value, as in 2020. Due to currents, recorded debris could be dumped directly in some areas and transported from other areas. Wood was recorded in less observations in 2021 (13.2%) than in 2020 (22.1%). The maximum surface observation of wood in 2021 was lower, than in 2020 (1.13 m^3 in 2021 and 1.96 m^3 in 2020), but the average observation was higher (0.23 m^3 in 2021 and 0.12 m^3 in 2020). Metal, paper and rubber was observed singularly (3.9-5.3% of the observations).

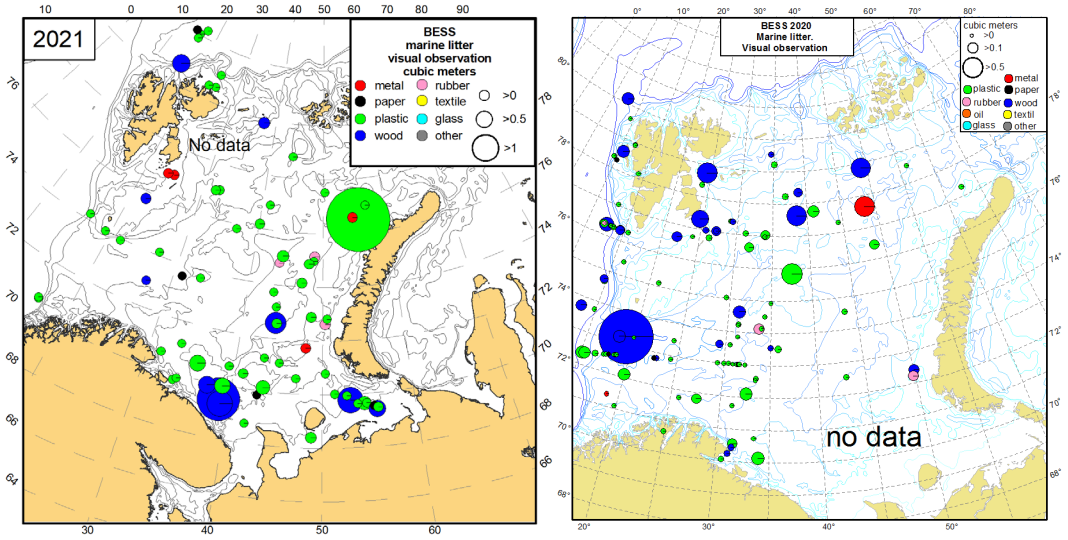

Figure A5.121: Type of observed anthropogenic litter (m^3) at the surface in the BESS 2021 and 2020. Taken from the 2021 and 2020 BESS survey report (Prokhorova *et al.*, 2022; Prokhorova *et al.*, 2021).

Anthropogenic litter was observed in 11.5% of pelagic trawl stations and 28.1% of bottom trawl stations in 2021 (in 24.6% of pelagic trawl stations and 27.4% of bottom trawl stations in 2020) (Figure A5.122 and A5.123). Plastic dominated from all anthropogenic matter in the both the pelagic and the bottom trawl stations in 2021 (10% of pelagic stations and 89.6% of bottom trawl stations with observed litter). This predominance of plastic among the anthropogenic litter is observed annually (Figure A5.124). Thus, plastic was recorded in 88.5% of pelagic stations with observed litter in 2020, in 96.5% in 2019, in 95.6% in the period of 2014–2018 and in 94.7% in the period of 2010–2013 (ICES, 2019). The same in the bottom trawls – 92.6% of bottom stations with observed litter in 2020, 82.3% in 2019, 81% of stations in the period of 2010–2013 and 88.7% in the period of 2014–2018 (ICES, 2019).

Weight of plastic litter from pelagic trawls in 2021 was from 0.5 g to 11 kg with average of 0.012 kg (except the single maximum catch of 11 kg). Weight of plastic litter in bottom trawls in 2021 was from 0.1 g to 6 kg with average of 0.04 g (except the single maximum catch of 6 kg). The average weight of plastic both in the pelagic and bottom stations was lower, than in 2020.

Processed wood was registered in 10.4% of the bottom trawl stations with observed litter in 2021 (compared with 5.8% in 2020, 24.8% in 2019, 11.3% in the period of 2010–2013 and 19% in the period of 2014–2018) (Figure A5.124) (ICES, 2019).

Other types of litter (textile, metal and rubber) was observed in trawls singularly.

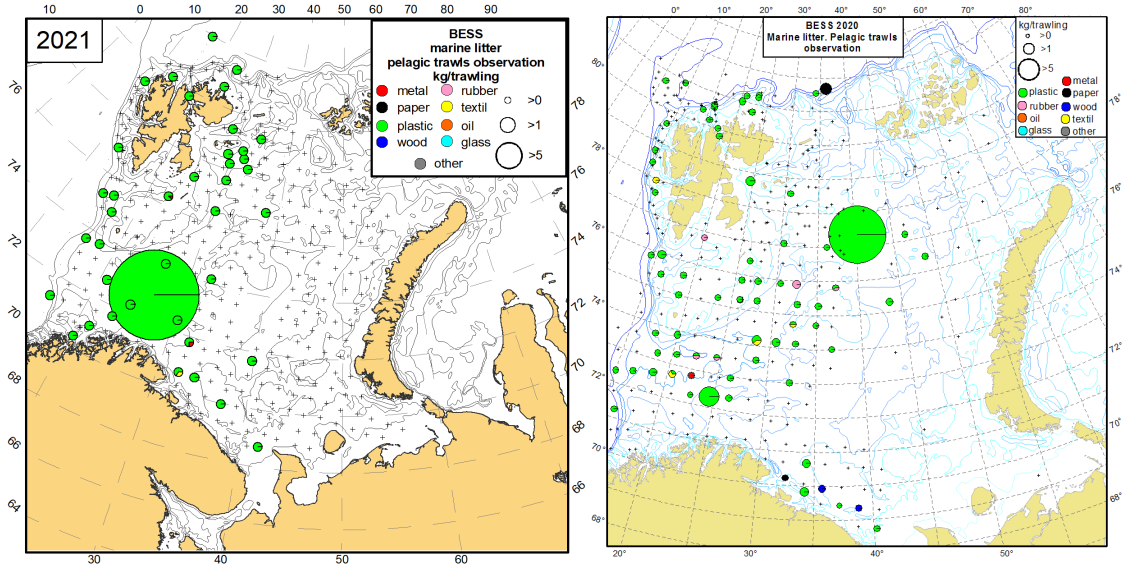

Figure A5.122: Type of anthropogenic litter collected in the pelagic trawls in 2021 and 2020. Crosses indicate trawl stations. Taken from the 2020 and 2019 BESS survey report (Prokhorova *et al.*, 2022; Prokhorova *et al.*, 2021).

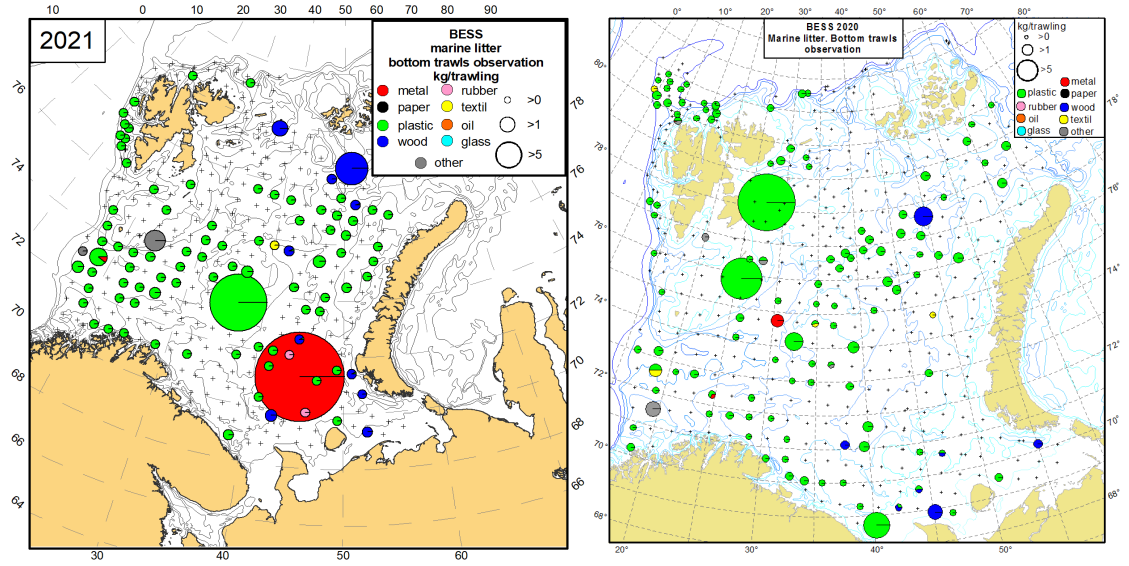

Figure A5.123: Type of anthropogenic litter collected in the bottom trawls in 2021 and 2020. Crosses indicate trawl stations. Taken from the 2020 and 2019 BESS survey report (Prokhorova *et al.* 2022; Prokhorova *et al.* 2021).

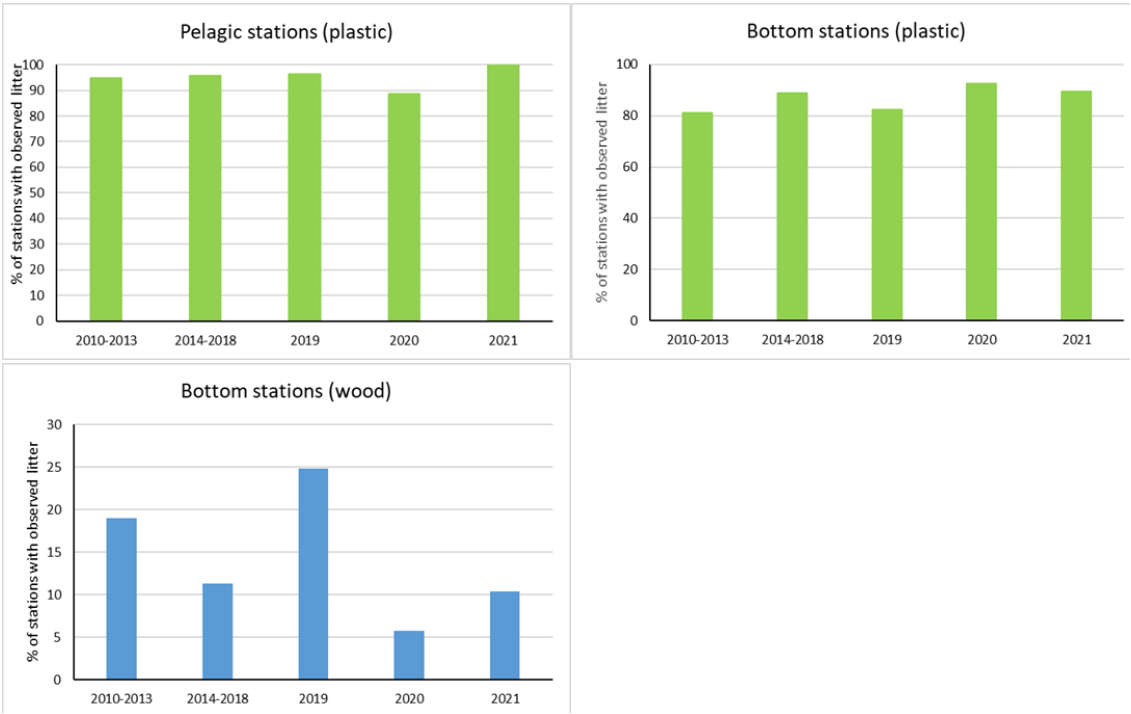

Figure A5.124: Frequency of occurrence of plastic in pelagic and bottom trawls that contained litter and of processed wood in bottom trawls in the period of 2010–2013, 2014–2018, 2019, 2020 and 2021 during the BESS survey.

Litter from fishery was a significant part of plastic litter both in the pelagic and bottom trawls in 2021 (36.6% and 66.1%, respectively), as in 2020 (50.7% and 67%, respectively) (Figure A5.125). Fishery related litter was recorded in 25.5% of plastic litter observations at the surface in 2021 and in 22.6% in 2020 (Figure A5.125). Fishery related litter was represented by ropes, rest of nets, floats/buoys etc.

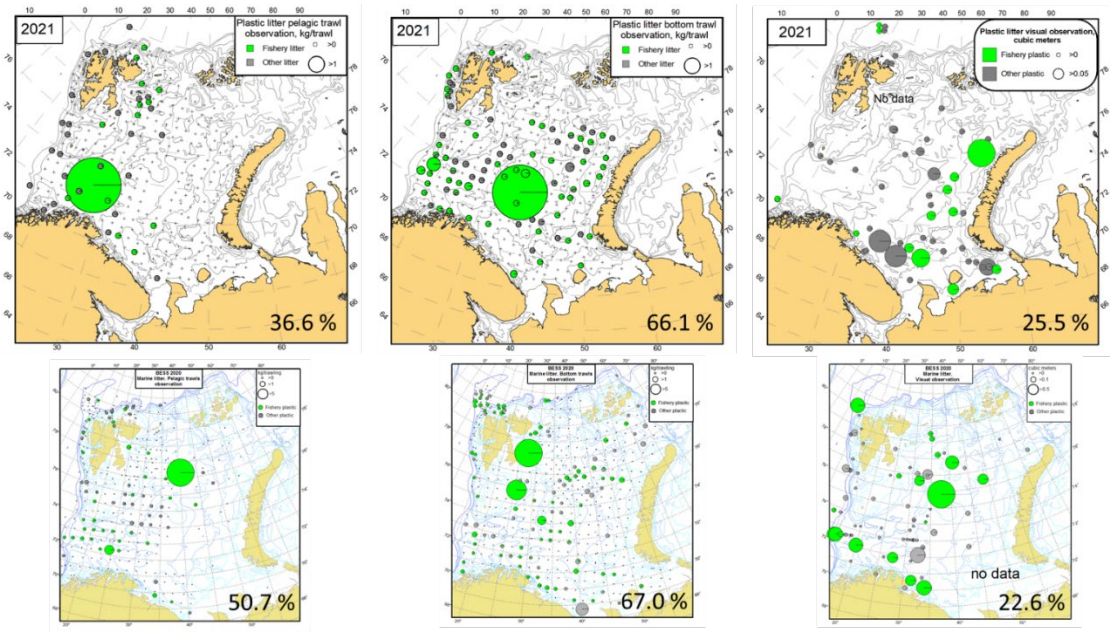

Figure A5.125: Proportion of fishery plastic of the plastic litter collected in the pelagic trawls (to the left), bottom trawls (in the middle) and at the surface (to the right) in the BESS 2021 and 2020 (crosses – trawl stations).

References

Prokhorova T, Grøsvik BE and Klepikovskiy R. 2022 in G.I. van der Meeren, D. Protozorkevich (eds). Survey report from the joint Norwegian/ Russian ecosystem survey in the Barents Sea and adjacent waters August-October 2021. IMR/PINRO Joint Report Series, *In prep.*

Prokhorova T, Grøsvik BE and Klepikovskiy R. 2021 in G.I. van der Meeren, D. Protozorkevich (eds). Survey report from the joint Norwegian/ Russian ecosystem survey in the Barents Sea and adjacent waters August-October 2020. IMR/PINRO Joint Report Series, 1-2021, 90 pp.

ICES. 2019. The Working Group on the Integrated Assessments of the Barents Sea (WGIBAR). ICES Scientific Reports. 1:42. 157 pp. http://doi.org/10.17895/ices.pub.5536.

ICES. 2020. The Working Group on the Integrated Assessments of the Barents Sea (WGIBAR). ICES Scientific Reports. 204 pp.

Contaminants in marine organisms

Metals and persistent organic pollutants (POPs)

By Sylvia Frantzen (IMR), Stepan Boitsov (IMR), Mikhail A. Novikov (VNIRO)

Levels of heavy metals and organic contaminants in fish and crustaceans from the Barents Sea are in general relatively low and below maximum levels set for food safety. One exception is arsenic, which is found in relatively high concentrations. For most substances, concentrations are stable or slightly decreasing.

IMR conducts regular monitoring of chemical contaminants in biota through two different programmes. 1) A three-year monitoring programme designed to monitor the level of pollution in the Barents Sea, last updated with sampling in 2018. 2) An annual monitoring programme with focus on seafood safety and pollution levels in indicator species, updated with new data from 2020.

In programme 1, levels of certain organic contaminants (PCB, chlorinated pesticides and PBDEs) are analysed mainly in liver of fish (Boitsov *et al*., 2016; 2019). The exact species sampled varies from year to year, but some species have been sampled repeatedly in three year cycles and temporal data exist for Greenland halibut (*Rheinhardtius hippoglossoides*), long rough dab (*Hippoglossoides platessoides*), haddock (*Melanogrammus aeglefinus*), capelin (*Mallotus villosus*), polar cod (*Boreogadus saida*), saithe (*Pollachius virens*), herring (*Clupea harengus*), cod (*Gadus morhua*), golden redfish (*Sebastes norvegicus*) and peeled shrimp (*Pandalus borealis*). The sampling programme is designed to monitor pollution levels over time. Samples are mainly taken on the ecosystem cruise in summer/early autumn.

In programme 2, levels of metals including As, Cd, Hg and Pb are analysed in fillet and liver of Atlantic cod, whole capelin and polar cod as well as whole and peeled boiled shrimp. Levels of persistent organic pollutants (POPs) are analysed in liver of cod, whole capelin and polar cod and whole boiled shrimp, and a few samples of cod fillet have also been analysed. The POPs include dioxins and dioxin-like PCBs, non-dioxinlike PCBs (PCB6, PCB7), organochlorine pesticides, brominated flame retardants (PBDEs, HBCD and TBBP-A), per- and polyfluoralkyl substances (PFAS) and PAHs. The monitoring programme is designed to document levels of contaminants with regards to food safety, while also gaining information on pollution levels by analysing indicator organisms representing varying trophic levels and niches. Samples are mainly taken on the winter cruise in January to March.

In addition to these regular monitoring programmes, some species have been sampled and analysed as a part of special surveys (Nilsen *et al.* 2020; Frantzen and Maage 2016; Julshamn *et al.* 2015). In 2021, a comprehensive baseline study of contaminants in haddock (*Melanogrammus aeglefinus*) was finalized and reported, where 545 fish from the Barents Sea sampled during 2005–2018 were analysed (Kögel *et al.* 2021). Saithe (*Pollachius virens*) and Greenland halibut are monitored for contaminants annually. Since the previous report, HI has analysed new samples of cod, saithe, Greenland halibut and haddock from the Barents Sea.

In both programme 1 and 2, where temporal data exist, samples are not taken at fixed positions or at fixed fish size, so temporal trends must be interpreted with caution.

Analyses are performed with accredited analytical methods according to ISO 17025.

Since 1986, scientists of the Polar Branch of VNIRO have been sampling fish annually for analysis of contaminants. Samples of some species were collected over a long period of time, whereas sampling of other species was carried out occasionally. In 2021, a comprehensive study of total arsenic content in cod, haddock, long rough dab (*Hippoglossoides platessoides*), Greenland halibut and European plaice (*Pleuronectes platessa*) was finalized and published, where hundreds of fish specimens from the Barents Sea sampled during 2009–2020 were analysed (Novikov *et al.* 2021). Muscle and liver of different fish species are analysed for metals including Hg, As, Cd, Pb, Cr, Ni, Co, polyaromatic hydrocarbons (PAH), alkanes and chlorinated pesticides including DDT, HCB, HCH and chlordane. Results for Hg and As until 2020 are presented here.

For fish species that are regularly monitored, there are available time-series that describe variations in the content of pollutants over time. Among species monitored regularly are Atlantic cod, Greenland halibut, plaice, haddock, and long rough dab.

Levels and temporal trends of contaminants in muscle of fish and crustaceans

In general, levels of contaminants in fillet of fish and muscle of crustaceans from the Barents Sea are very low and below EU and Norway's maximum levels for food safety for substances where such regulatory limits exist (Hg, Cd, Pb, sum dioxins and dioxin-like PCBs and sum PCB6) (Figure A5.126–A5.133; EU, 2021).

Arsenic levels in some of the fish species and all crustaceans were relatively high (Figure A5.126-A5.129). In Norway and EU, there is no maximum level for arsenic, whereas Russia has a maximum level of 5 mg/kg wet weight. For cod, haddock, Greenland halibut, Atlantic and spotted wolffish, plaice as well as shrimp, red king crab and snow crab, mean arsenic concentrations were above this limit. The levels of arsenic in the snow crab and shrimp were particularly high (Figure A5.128 and A5.129). The concentrations of arsenic were much higher in fish analysed in Norwegian monitoring than in fish analysed in Russian monitoring. In Russian monitoring, only plaice and spotted wolffish had mean concentrations of arsenic above 5 mg/kg. Sediments in the Norwegian part of the Barents Sea, monitored through the MAREANO programme (www.mareano.no/en) have higher levels of arsenic than sediments in the Norwegian Sea, and it is believed that this is caused by high natural background levels. The sediment monitoring also showed that arsenic concentrations in surface sediments were lower near the coast of Northern Norway than further north in the Barents Sea, showing that there are spatial differences in arsenic levels within the sea area.

With respect to food safety, arsenic present in fish and crustacean muscle is usually arsenobetain, which has very low toxicity (EFSA 2009). The most toxic species of arsenic is inorganic arsenic. A large number of fish samples from Norwegian sea areas, including cod and Greenland halibut,

were previously analysed for total and inorganic arsenic (Julshamn *et al.* 2012). Even samples with very high total arsenic concentrations had very low levels of inorganic arsenic (<0.003–0.006 mg/kg ww). More recently, fillet samples of 161 haddock from the Barents Sea were analysed for inorganic arsenic, and the concentrations varied from <0,002 to 0,0085 mg/kg wet weight in samples where total arsenic content varied between 1.1 and 41 mg/kg (Kögel *et al.* 2021). Also analyses of inorganic arsenic in red king crab have shown that inorganic arsenic makes only a very small portion (<0.4%) of the total arsenic concentrations (Julshamn *et al.* 2015). Differences between species in arsenic level may at least in part be related to their diet, where a more benthic diet seems to lead to higher arsenic levels than a predominantly pelagic diet (Neff 1997).

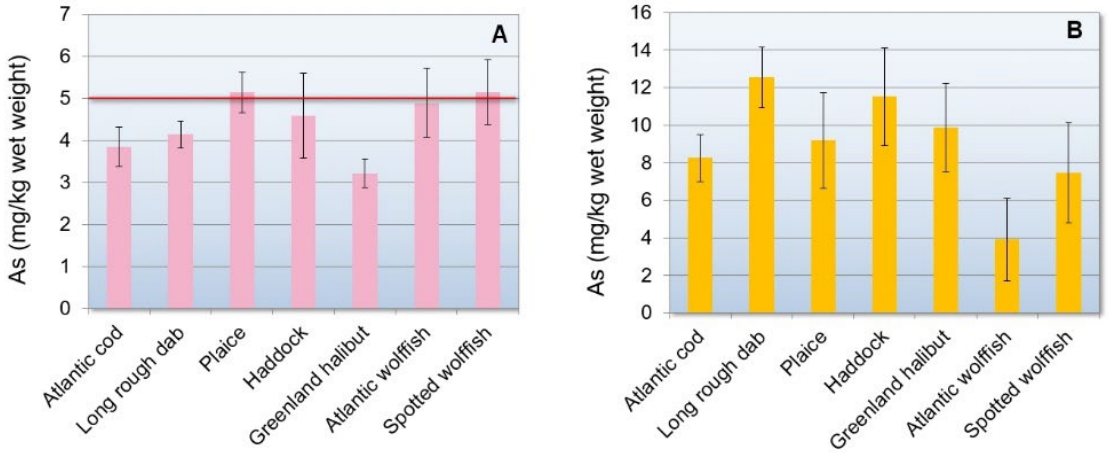

Figure A5.126: The total arsenic content (A) in muscle and (B) liver of bottom fish species from the Russian part of the Barents Sea in 2019–2020, in mg/kg wet weight. Species included (fillet/liver): Atlantic cod (n=54), long rough dab (n=44), plaice (n=23/22), Greenland halibut (n=55/21), haddock (n=22/20), spotted (n=15) and Atlantic (n=14) wolffish. The average in muscles is ± 2 m, the average in liver is ± 2 m (95% confidence interval). The red line shows the maximum permissible regulatory level of content in fish products (for Russia).

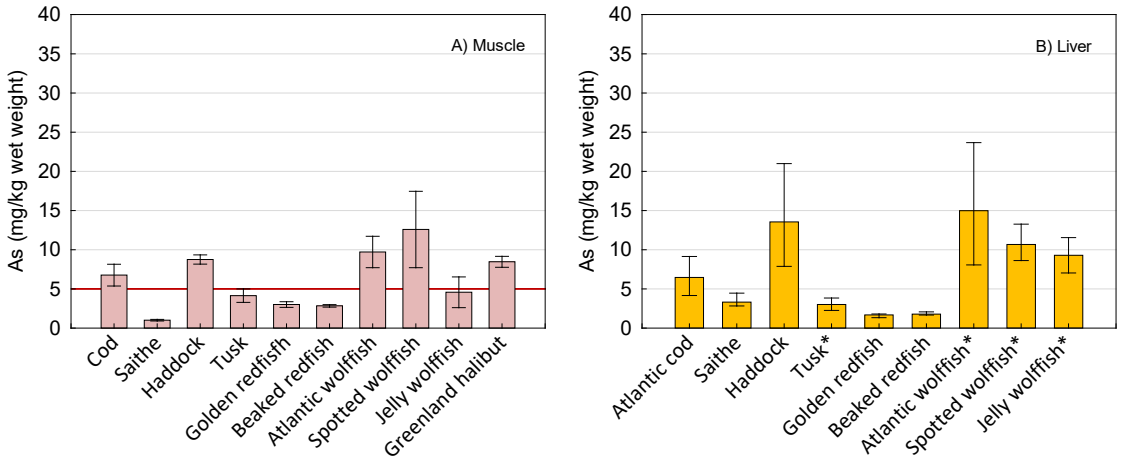

Figure A5.127: Concentrations of arsenic (As, mg/kg wet weight) in a) muscle and b) liver of fish species from the Norwegian part of the Barents Sea: Species included cod (2020–2021, n = 125), saithe (2020–2021, n = 98/50), haddock (2015–2018, n=557/539), tusk (2014, n=160/9*), golden redfish (2018, n = 50/4*), beaked redfish (2018, n = 249/19*), Atlantic wolffish (2014, n = 29/13*), spotted wolffish (2014, n = 27/13*), jelly wolffish (2014, n = 12/2*) and Greenland halibut (2020–2021, n= 249). Mean ± 95% confidence intervals are given. Red line indicates the maximum allowable level set for food safety in Russia. *Pooled samples of liver were analysed.

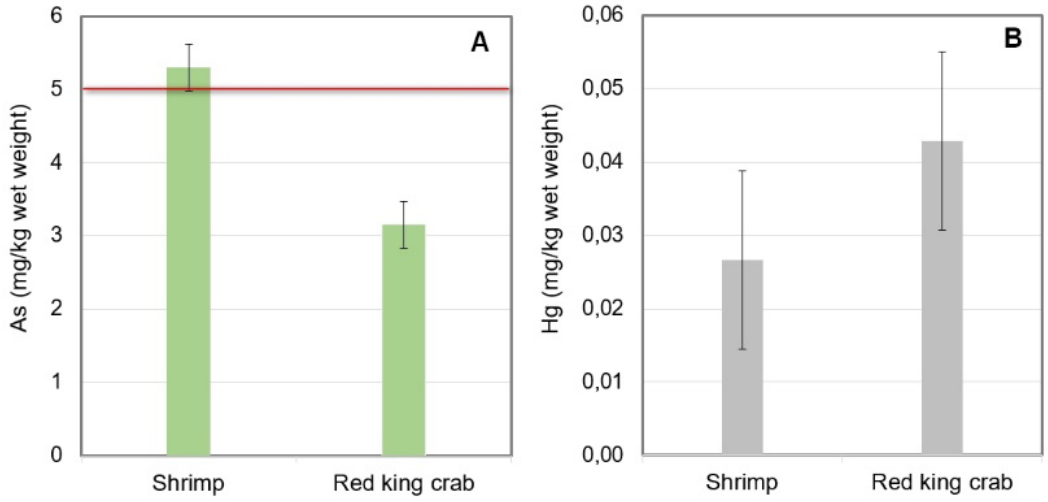

Figure A5.128: The content of (A) arsenic and (B) mercury in muscles of marine invertebrates of the Russian part of the Barents Sea in 2020–2021, in mg/kg wet weight. The average of ± 2 m (95% confidence interval) is shown. The red line shows the maximum permissible regulatory level of As content in marine invertebrates (for Russia).

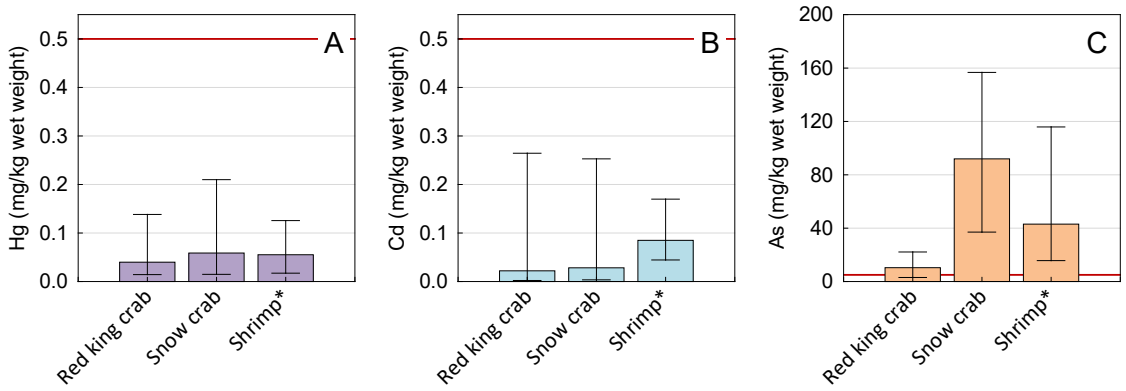

Figure A5.129: Concentrations in the Norwegian part of the Barents Sea of A) mercury (Hg, mg/kg wet weight), B) cadmium (Cd, mg/kg wet weight) and C) arsenic (As, mg/kg wet weight) in muscle of red king crab (*Paralithodes camtchaticus*, 2012, n=155), snow crab (*Chionoecetes opilio*, 2014 + 2016, n=64) and shrimp (*Pandalus borealis*, boiled, 2017–2021, n=15). Mean, minimum and maximum values are shown. Red lines indicate maximum allowable levels set for food safety. *Composite samples.

The levels of mercury in muscle of fish from the Norwegian part of the Barents Sea (Figure A5.130) are generally lower than in the same species sampled in the Norwegian Sea and the North Sea (Azad *et al.* 2019; miljostatus.no; Frantzen *et al.* 2022). Data from VNIRO also show low concentrations of mercury in muscle of Barents Sea fish, well below maximum levels set for food safety (Figure A5.131). However, the mercury concentrations in muscle and liver of cod and haddock from the Russian part of the Barents Sea were considerably higher than in the same species from the Norwegian part of Barents Sea. On the other hand, Atlantic and spotted wolffish from Norwegian monitoring had much higher mercury concentrations than the same species analysed in Russian monitoring. Only Greenland halibut muscle had relatively similar concentrations. The reason for these differences are not currently known. Some of the differences may be due to methodological differences such as size range of fish analysed or differences in the analytical methods. The fish from both areas were however sampled in the open Barents Sea, and muscle and liver samples of individual fish were analysed. A proper comparison of results should also include the fish physical parameters such as size/age and condition. Besides, a comparative laboratory study where both labs analyse the same samples would be useful in order to investigate whether the analytical methods provide the same results. It is, however, also possible that there are differences in mercury levels within different regions of the Barents Sea. This could

be due to factors such as different input of mercury from rivers or melting sea ice, or transport of mercury with currents from west towards the east. A relatively recent study showed that riverine input may have a greater influence on mercury flux to the Arctic than previously believed (Sonke *et al.* 2018).

Mercury in muscle of crustaceans from the Barents Sea analysed in Norwegian and Russian monitoring were low and well below maximum levels for food safety (Figure A5.128 and A5.129). The level of cadmium (Norwegian data) was considerably higher in shrimp than in both crab species (Figure A5.129). Cadmium levels in shrimp from the Barents Sea are higher than the levels in shrimp sampled in Norwegian sea areas further south (Frantzen *et al.* 2022). This corresponds well with findings from other studies of increasing cadmium levels in crustaceans from south to north (Wiech *et al.* 2020; Zauke *et al.* 1996, Zauke and Schmalenbach 2006). It likely has natural causes. However, a good explanation has so far not been found.

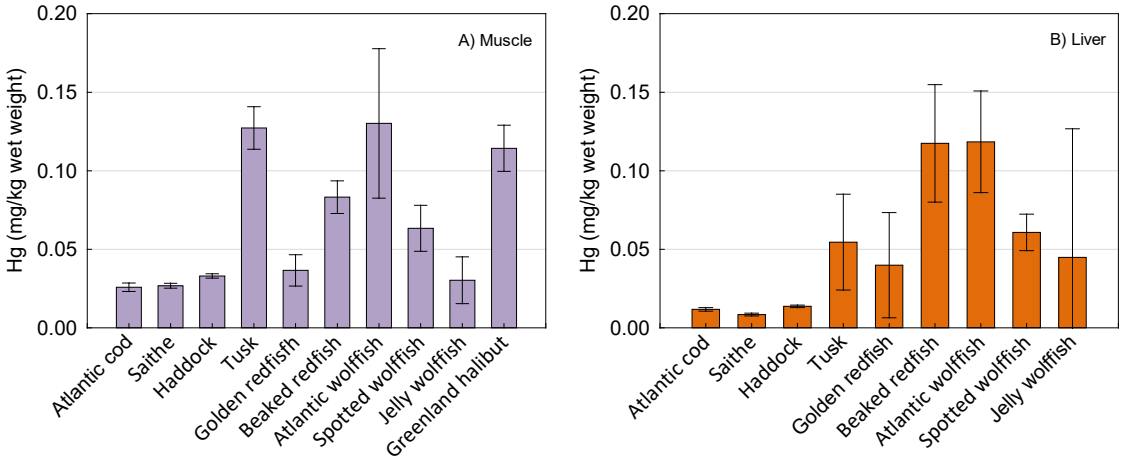

Figure A5.130: Concentrations of mercury (Hg, mg/kg wet weight) in a) muscle and b) liver of fish species from the Norwegian part of the Barents Sea: Species included (fillet/liver): cod (2020–2021, n = 125), saithe (2020–2021, n = 98/50), haddock (2015–2018, n=557/539), tusk (2014, n=160/9*), golden redfish (2018, n = 50/4*), beaked redfish (2018, n = 249/19*), Atlantic wolffish (2014, n = 29/13*), spotted wolffish (2014, n = 27/13*), jelly wolffish (2014, n = 12/2*) and Greenland halibut (2020–2021, n= 249). Mean ± 95% confidence intervals are given.
***Pooled samples of liver were analysed.**

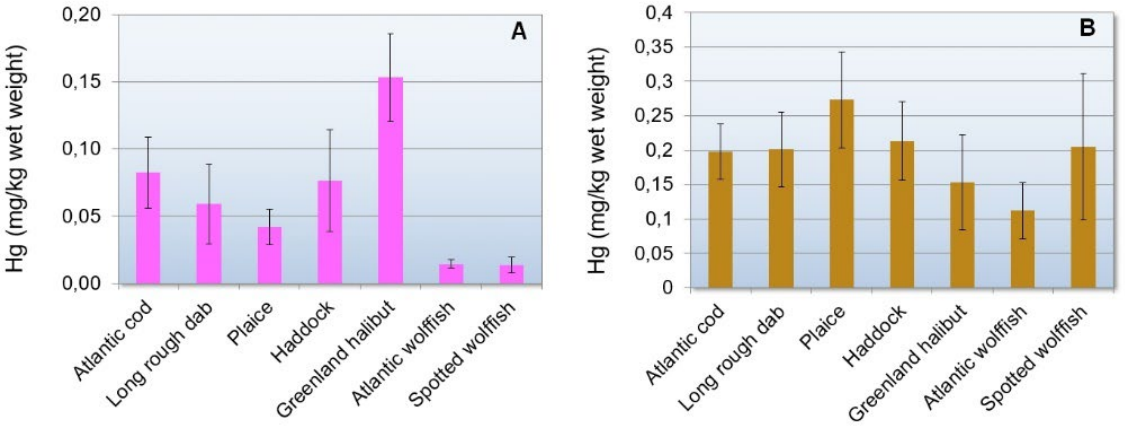

Figure A5.131: The total mercury content (A) in muscle and (B) liver of bottom fish species from the Russian part of the Barents Sea in 2019–2020, in mg/kg wet weight. Species included (fillet/liver): Atlantic cod (n=54), long rough dab (n=44), plaice (n=23/22), Greenland halibut (n=55/21), haddock (n=22/20), spotted (n=15) and Atlantic (n=14) wolffish. The average in muscles is ± 2 m, the average in liver is ± 2 m (95% confidence interval).

Concentrations of fat soluble organic contaminants, such as for instance dioxins and dioxin-like PCBs or non-dioxinlike PCBs (PCB6), are in general very low in muscle of fish and crustaceans

from the Barents Sea (Figure A5.132 and A5.133). The concentrations are higher in fish species that store a larger portion of their lipids in the fillet, such as Greenland halibut, than in lean fish species that mainly store lipids in the liver. The concentrations in boiled and peeled shrimp were on average similar as for cod muscle, and red king crab and snow crab had similar levels of these substances. For species such as shrimp, which are also analysed in other Norwegian sea areas, concentrations of dioxins and PCBs are lower in the Barents Sea than in shrimp from the North Sea and the Norwegian Sea.

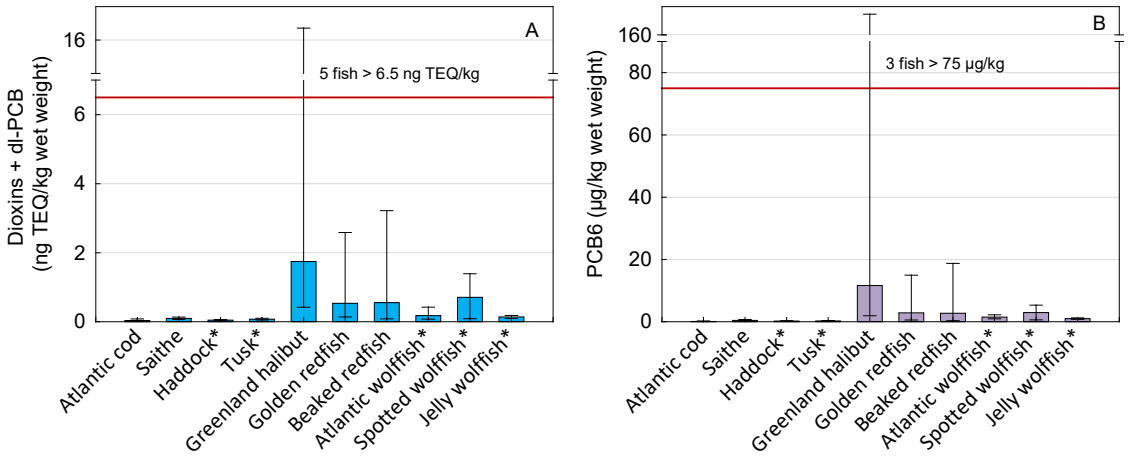

Figure A5.132: Concentrations of A) Sum of dioxins and dioxin-like (dl-) PCBs (ng TEQ/kg weight) and B) sum PCB6 (µg/kg wet weight) in muscle of cod (2020–2021, n = 30), saithe (2019–2020, n = 20), haddock (2014, n = 7*), tusk (2014+2016; n = 10*), Greenland halibut (2020, n = 149), golden redfish (2018, n = 49), beaked redfish (2018, n = 347), Atlantic wolffish (2014, n = 6*), spotted wolffish (2014, n = 4*) and jelly wolffish (2014, n = 2*). Mean, minimum and maximum values are shown. Red lines indicate maximum allowable levels set for food safety in EU and Norway. For non-dioxinlike PCBs, maximum level in EU and Norway applies to the sum PCB6.
***Composite samples analysed.**

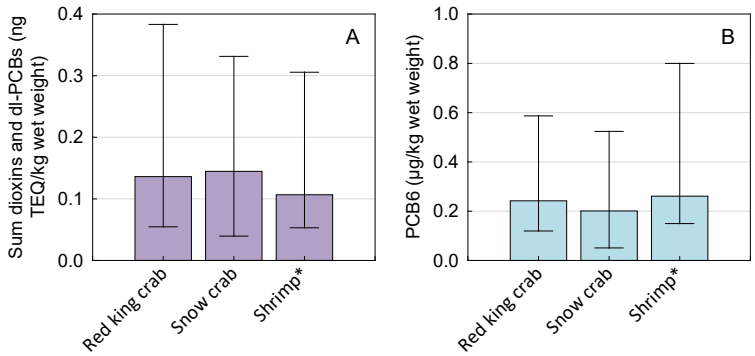

Figure A5.133: Concentrations of A) sum of dioxins and dioxin-like (dl-) PCBs (ng TEQ/kg weight) and B) sum PCB6 (µg/kg wet weight) in composite muscle samples of red king crab (2012, n = 29), snow crab (2014, n = 9*) and shrimp (2017–2021, n = 15* cooked and peeled). Mean, minimum and maximum values are shown.
***Composite samples analysed.**

Over the last decade, the levels of some pollutants in fish have decreased, while the levels of others remain relatively stable. Studies on the concentrations of metals in 2009–2020 by the Polar Branch of VNIRO indicated stable long-term decreasing trends in the contents of chromium and nickel in muscle of Greenland halibut cod, plaice and haddock (rf. last year's report). A decreasing trend, albeit less pronounced, also occurred for other examined metals such as cobalt, copper and lead

The decreasing levels of some metals in fish muscle may indicate a decrease in the overall pollution of the Barents Sea by some heavy metals in the last decade. This conclusion is in agreement with the data on the pollution of the Barents Sea waters in the same period (Novikov and

Draganov 2017, 2018). Additionally, the presented trend for cod may also be caused by shifts of its feeding areas northwards to the Arctic where the Barents Sea waters are cleaner than the Atlantic waters that are affected by the North Cape Current.

However, the results of Russian long-term studies (2012–2021) of arsenic and mercury contents in commercial bottom fish species Greenland halibut, cod, haddock and long rough dab of the Barents Sea, showed no temporal trend in the content of these elements in muscle or liver (Figure A5.134–A5.137). The values of the regression coefficients were low. Analysing these trends, we can note some isolation of the dynamics of the total arsenic content in Greenland halibut compared to other fish species. This is probably due to the biological features of this species in the Barents Sea. With respect to mercury content, there are practically no differences in trends between the studied fish species.

Also, in IMR's long-term monitoring of cod between 1994 and 2021, very stable mercury levels are observed (Figure A5.138). The mean concentration in 2021 was similar to 2020, and both years mean concentrations were slightly lower than most previous years.

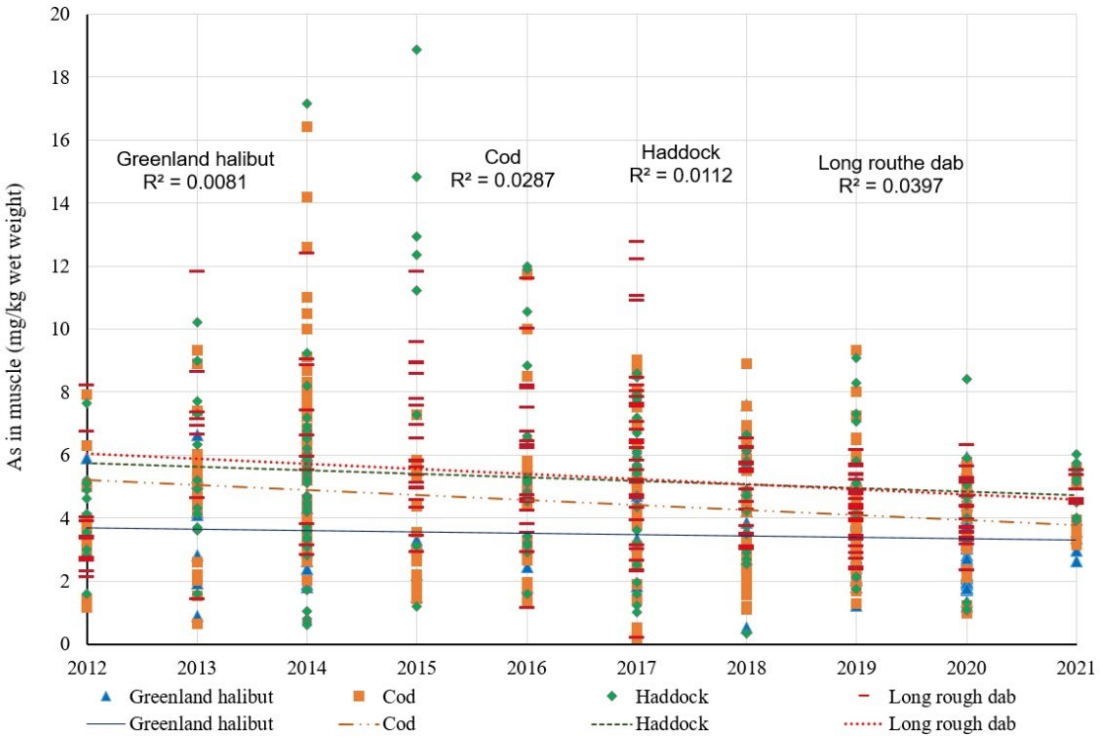

Figure A5.134: Trend (linear) of total arsenic content in muscle of bottom fish species of the Barents Sea 2012–2021.

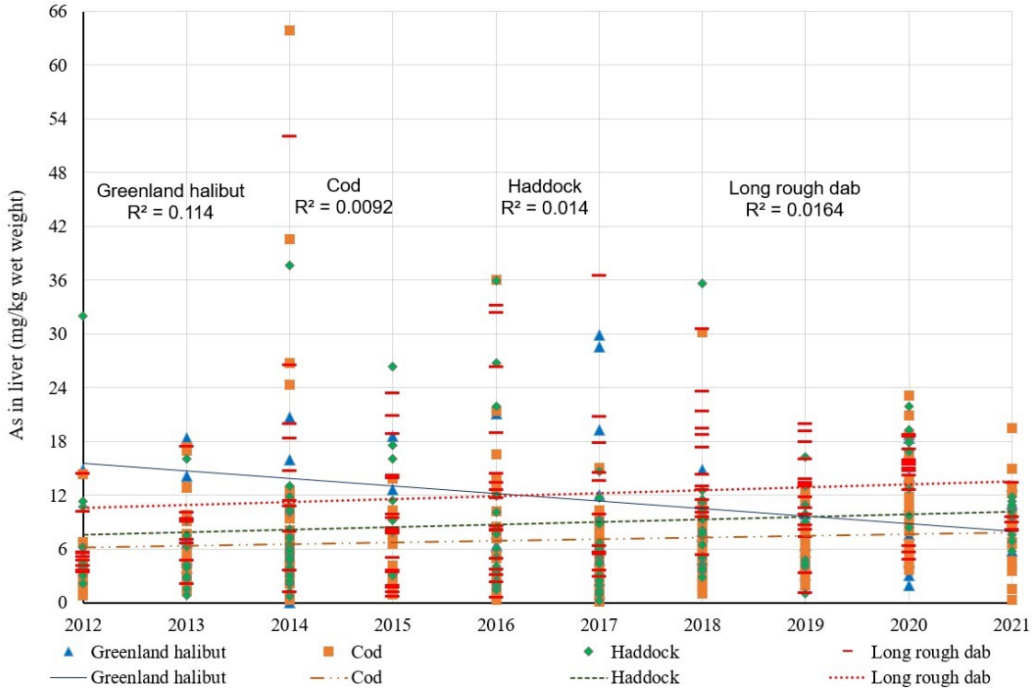

Figure A5.135: Trend (linear) of the total arsenic content in liver of bottom fish species of the Barents Sea.

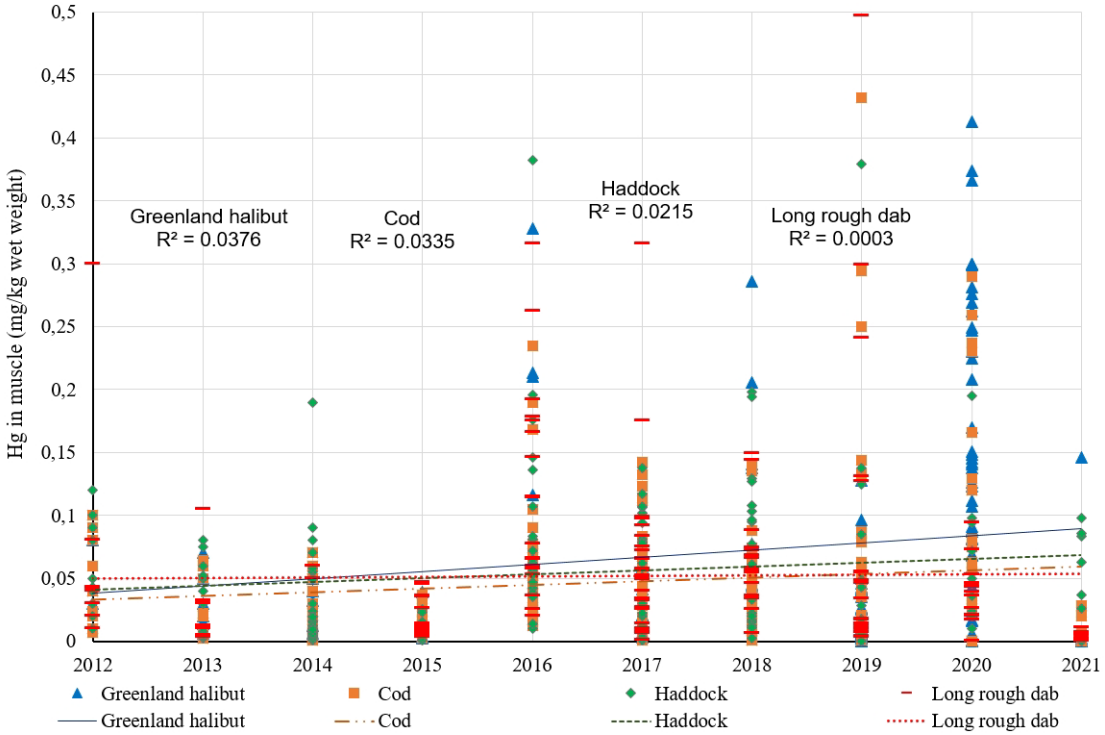

Figure A5.136: Trend (linear) of mercury content in muscle of bottom fish species of the Barents Sea.

Figure A5.137: Trend (linear) of mercury content in liver of bottom fish species of the Barents Sea.

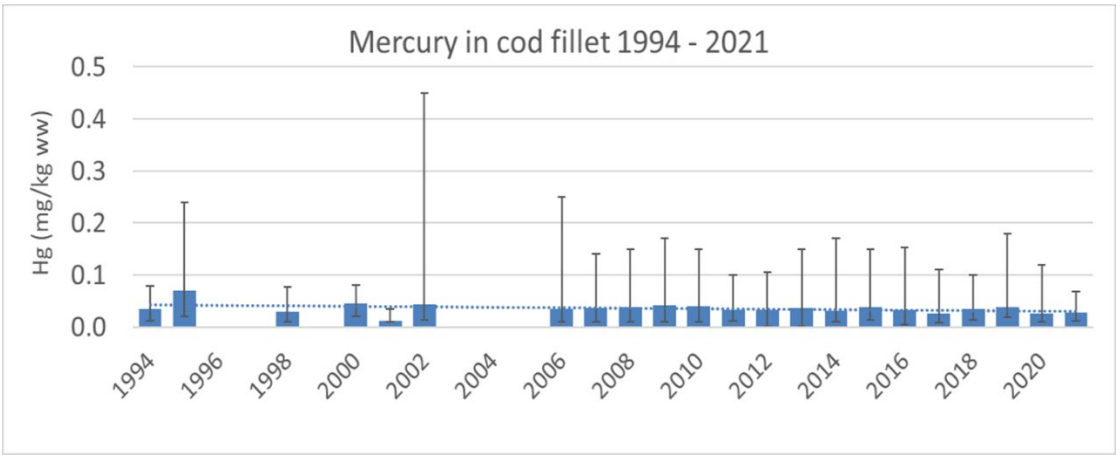

Figure A5.138: Annual concentrations of mercury in fillet of cod sampled in Norwegian monitoring from 1994 to 2021. For each year, mean, minimum and maximum values are shown.

Concentrations of mercury in polar cod and capelin were lower than in higher trophic level fish and were in general well below 0.01 mg/kg wet weight (Figure A5.139). Polar cod most years had a slightly lower mean Hg level than capelin. There have been weak, but significantly decreasing trends for the levels of mercury in both species since 2006/2007 (Figure A5.139). The trends were not related to sampling latitude, as there was significant decrease also when separating between fish sampled in different latitudes (Figure A5.139, bottom). For capelin the decrease seems to have tapered off after 2015.

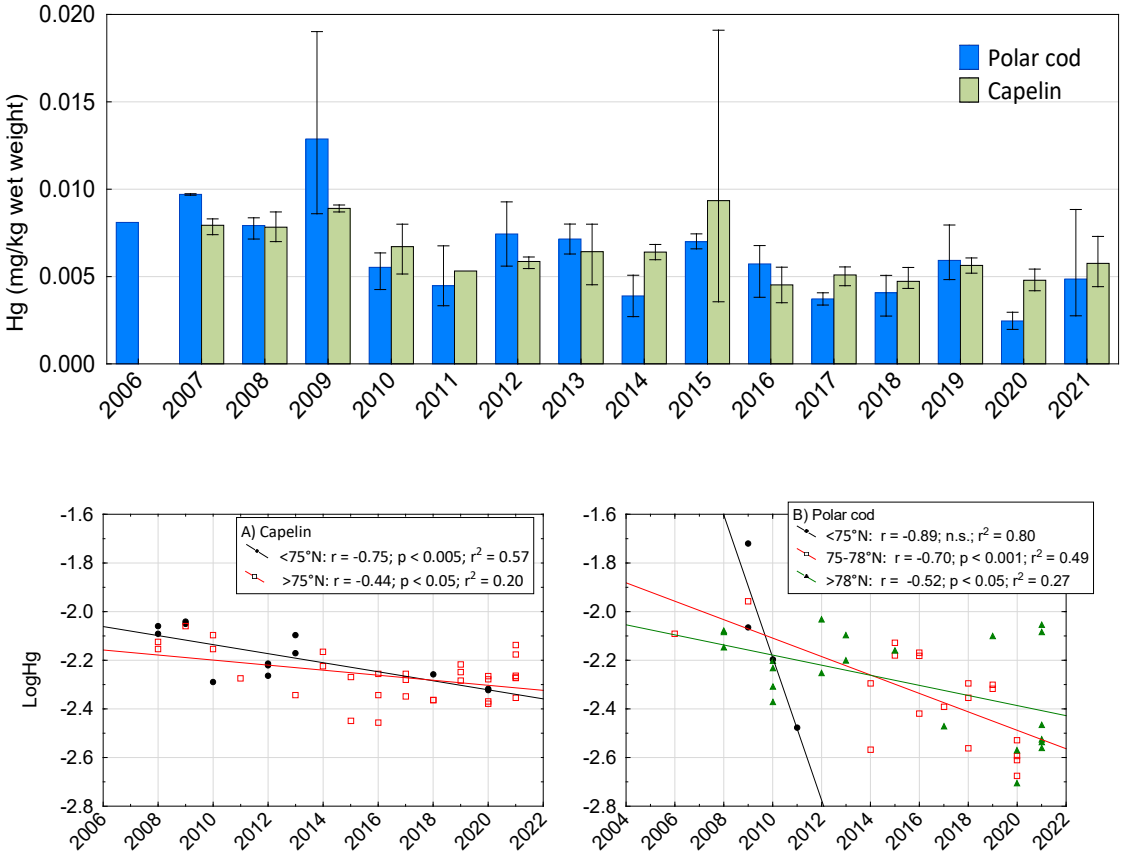

Figure A5.139: Temporal variation in mercury concentration (Hg, mg/kg wet weight) in composite samples of whole capelin and polar cod. Top: For each year (2006–2021) and species, mean, minimum and maximum values are given. Bottom: Temporal trend from of log-transformed mercury concentrations from 2006/2007 to 2021 for A) capelin south and north of 75°N and B) polar cod south of 75°N, 75-78°N and north of 78°N. Results of Pearson's one-way correlation between log_{10}-transformed mercury concentration (LogHg) and year are shown.

Levels and temporal trends of organic contaminants in fish liver or whole fish

Concentrations of organic contaminants are found in fish and crustaceans in the Barents Sea at measurable and significant levels, and the concentrations are higher in liver than in fillet of most fish species. The levels of the analysed substances are, however, relatively low in the Barents Sea compared to areas further south, except for the level of HCB, which is at the same level or higher in the Barents Sea than in the Norwegian Sea and the North Sea (Frantzen *et al.* 2022). The persistent organic pollutants PCBs and PBDEs are generally above environmental quality standard (EQS) values, which may indicate potentially harmful effects for animals at high trophic level such as for instance polar bears. There is evidence that the health of polar bears and seabirds may be negatively affected by contaminants (see references in Frantzen *et al.* 2022).

In order to evaluate time-trends for levels of persistent organic pollutants in the Barents Sea biota, data from analyses of liver of cod and whole capelin and polar cod have been assessed (Figure A5.140–A5.146).

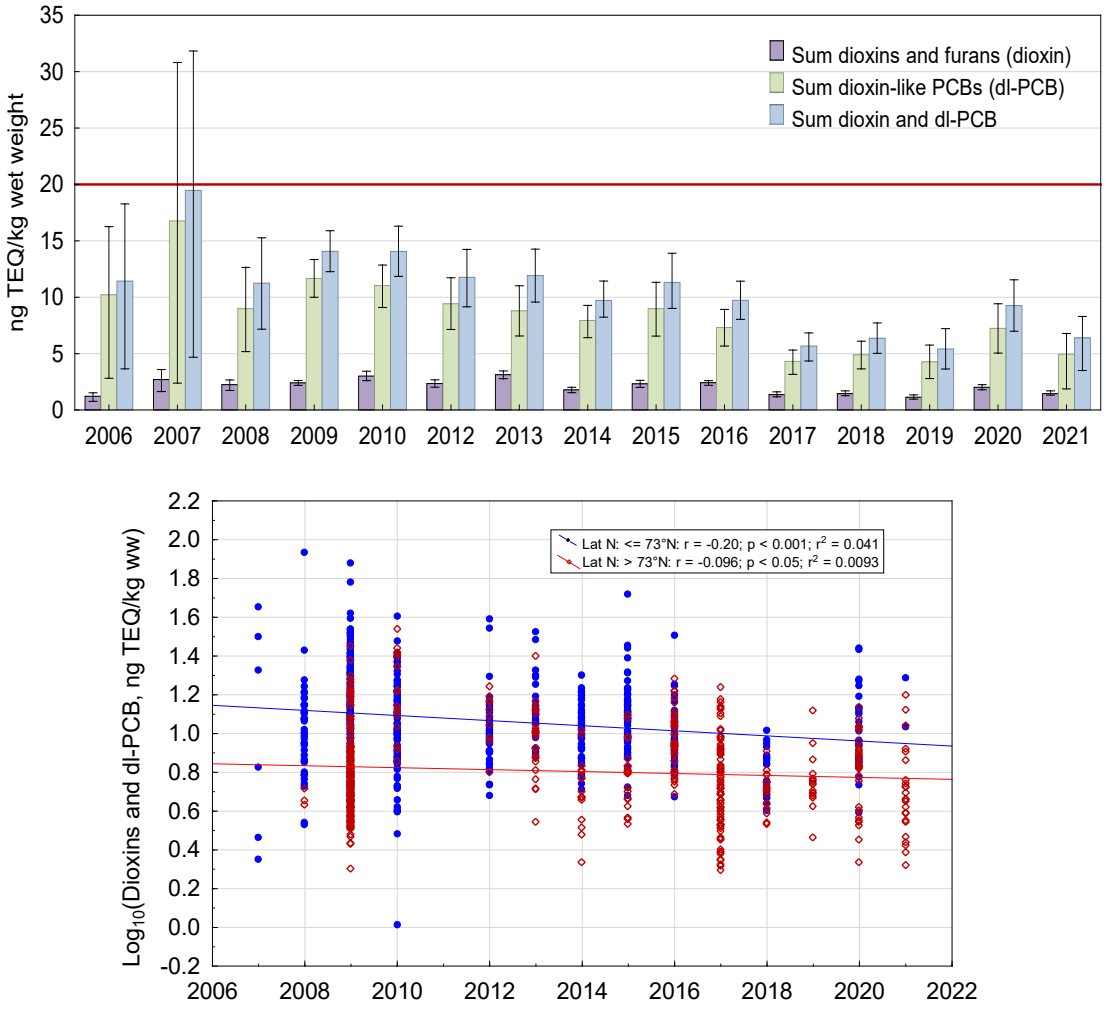

Figure A5.140: Temporal trend for dioxins and dioxin-like PCBs (ng TEQ/kg wet weight) in cod liver, including fish with lengths between 50 and 70 cm. Top: Concentrations per year of Sum dioxins and furans (dioxin), sum dioxin-like PCBs (dl-PCB) and sum dioxins and dl-PCB, given as mean values and non-outlier range. Red line represents EU's and Norway's maximum level for the sum of dioxins and dioxinlike PCBs applying to fish liver. Bottom: Correlation between log10-transformed concentration of the sum dioxins and dl-PCB and year, categorized by latitude south and north of 73°N. Results of Pearson's correlation with log10 transformed concentrations are shown for each category.

The level of dioxins and dioxin-like PCBs and non-dioxinlike PCBs in liver of cod appears to have decreased since 2007 (Figure A5.141 top, Figure A5.142 top). In 2007, the mean concentration of the sum of dioxin and dioxinlike PCBs was slightly above the special maximum level of 20 ng TEQ/kg wet weight applying to fish liver in Norway and EU, while in the years 2017 to 2020 mean concentrations were mostly below 10 ng TEQ/kg. However, because geography and fish size may affect the results, an analysis of the trend has been done separately for samples taken south and north of 73°N and including only fish between 50 and 70 cm length. For the sum of dioxins and dioxin-like PCBs there then was a significant, but very weak, decline in the level of dioxins and dl-PCB south of 73°N and no decline north of 73°N (Figure A5.141 bottom). Dioxin-like PCBs dominate the sum of dioxins and dioxin-like PCBs and the dioxins and furans initially had very low concentrations and changed much less over the years than the dioxin-like PCBs (Figure A5.141 top).

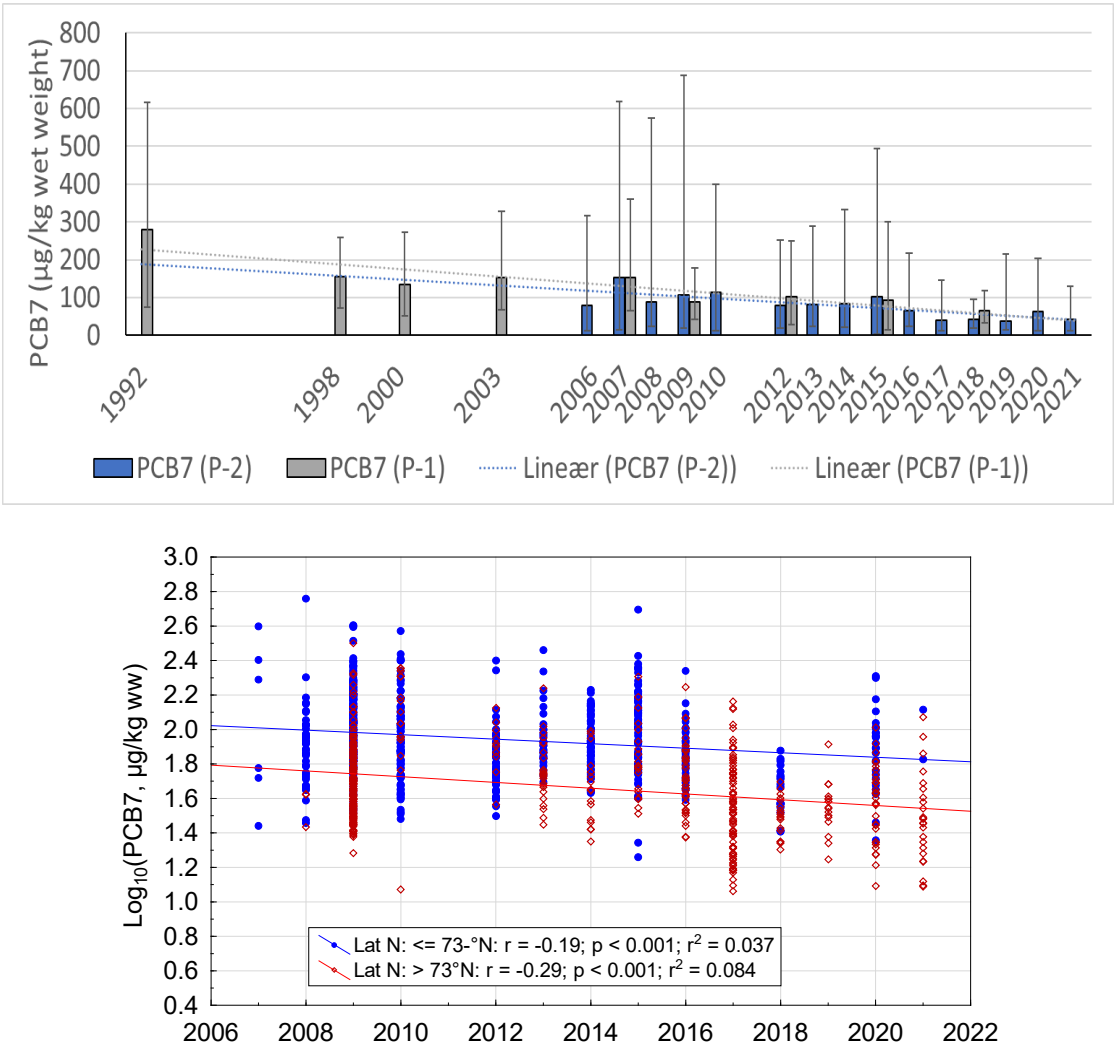

Figure A5.141: Temporal trend for non-dioxinlike PCBs, PCB7 (sum of PCB-28, 52, 101, 118, 138, 153, 180; µg/kg wet weight) in liver of cod. Top: Annual concentrations of sumPCB7, in Programme 1 (P-1) and Programme 2 (P-2) in liver of cod from 1992 to 2021. For each year, mean, minimum and maximum values are shown. Bottom: Correlation between concentrations of PCB7 in fish from P-2 between 50 and 70 cm, categorized by latitude south and north of 73°N. Results of Pearson's correlation are shown for each category.

The non-dioxinlike PCBs (given as PCB7 or PCB6) are often used as a proxy for total PCB contamination. The non-dioxinlike PCBs in cod liver have been analysed in programme 1 since 1992 and in programme 2 since 2006, during which time their levels seem to have decreased (Figure A5.142 top). Between 1992 and 2008, mean concentration more than halved from almost 300 to around 100 µg/kg, and in 2020 the mean concentration was only around 50 µg/kg. When including only cod between 50 and 70 cm from programme 2 (2007–2021) and categorizing between fish sampled south and north of 73°N, there was still significant, although weak, decrease in the PCB7 concentration for both geographical areas (Figure A5.142 bottom). It was clearly higher concentrations in liver of cod caught in the area south of 73°N than in those caught north of 73°N. Data from programme 1 has also shown a significant decrease with time since 1992 after correcting for fish size (weight basis) for cod from southern Barents Sea (Boitsov *et al.* 2019).

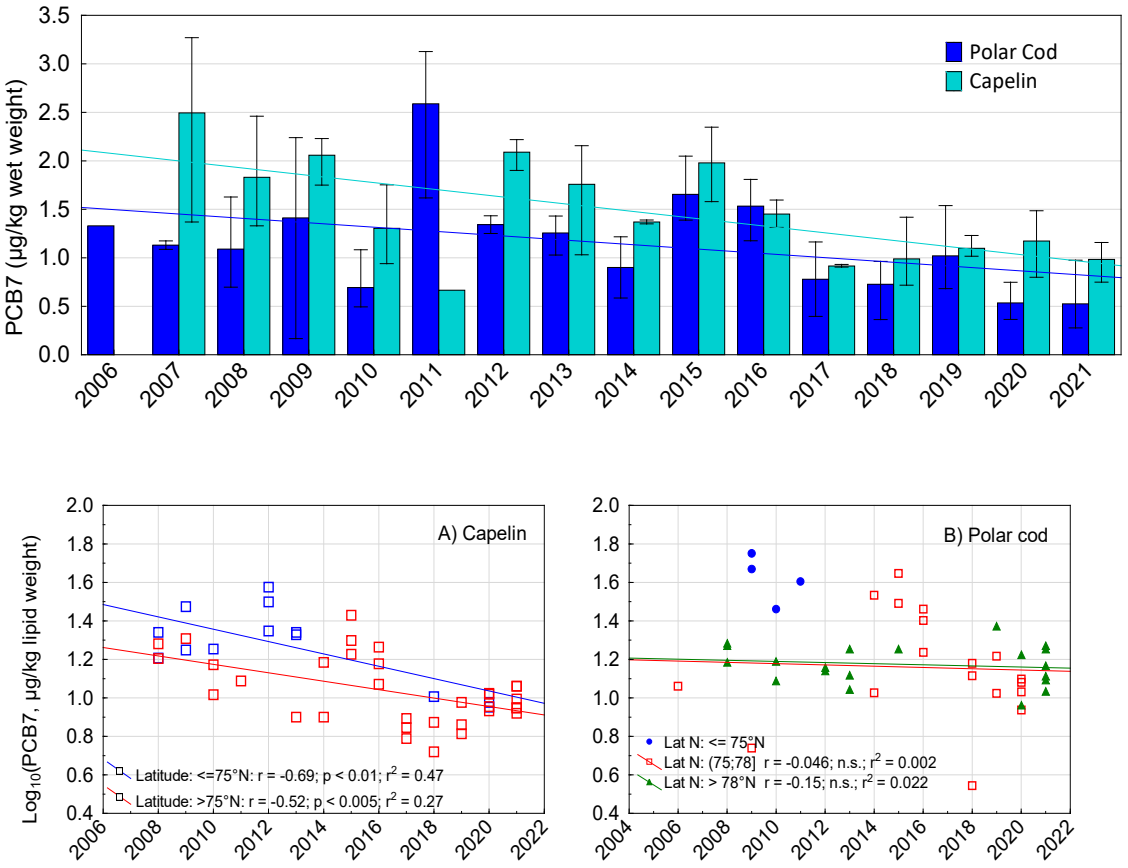

Figure A5.142: Temporal trends for concentrations of PCB7 (sum of PCB-28, 52, 101, 118, 138, 153, 180; µg/kg) in composite samples of whole capelin and polar cod in composite samples of whole capelin and polar cod from 2006 to 2021. Top: For each year from 2006 to 2020, mean, minimum and maximum values (µg/kg wet weight) are shown. Bottom: Correlation between lipid weight concentrations of PCB7 (µg/kg lipid weight) in A) Capelin, categorized by latitude south and north of 75°N, and B) polar cod, categorized by latitude south of 75°N (correlation not shown), between 75 and 78°N and north of 78°N. Results of Pearson's correlation are shown for each category.

The levels of PCB7 in capelin and polar cod also seem to have decreased somewhat since 2006, and perhaps more steeply in capelin than in polar cod (Figure A5.143 top). There was a significant decrease in concentrations with increasing latitude, and since the samples tended to be taken further north in later years, an effort has been made to separate the effects of latitude and year. Also, fat contents of the fish may affect the concentrations of PCBs, as they are fat soluble. However, lipid normalized concentrations of PCB7 (µg/kg lipid weight) in capelin showed significant decreasing trends both south and north of 75°N (Figure A5.143). Polar cod showed no temporal trend for lipid normalized PCB7 concentrations neither north of 78°N nor between 75 and 78°N (Figure A5.143). Samples of polar cod were only taken south of 75°N during 2009 to 2011.

Among chlorinated pesticides, there has been a clear decrease in concentrations of DDT in cod liver since 1992 (Figure A5.144). HCB levels in cod liver have remained very stable, although mean concentration of HCB in 2021 was the lowest since 2007. After correcting for fish size (weight), a significant decrease in the levels of both these contaminants was found in cod liver from the southern Barents Sea analysed in programme 1, although the decrease was very weak for HCB (Boitsov *et al.* 2019). For polar cod and capelin, the level of HCB seems to have been increasing up to 2019, and decreasing between 2019 and 2021 (Figure A5.145). The trends have not been analysed with regard to sampling latitude and fat content. HCB is one of a few contaminants which have been found in higher levels in biota and air of the Barents Sea region than in the North Sea and the Norwegian Sea (Frantzen *et al.* 2022).

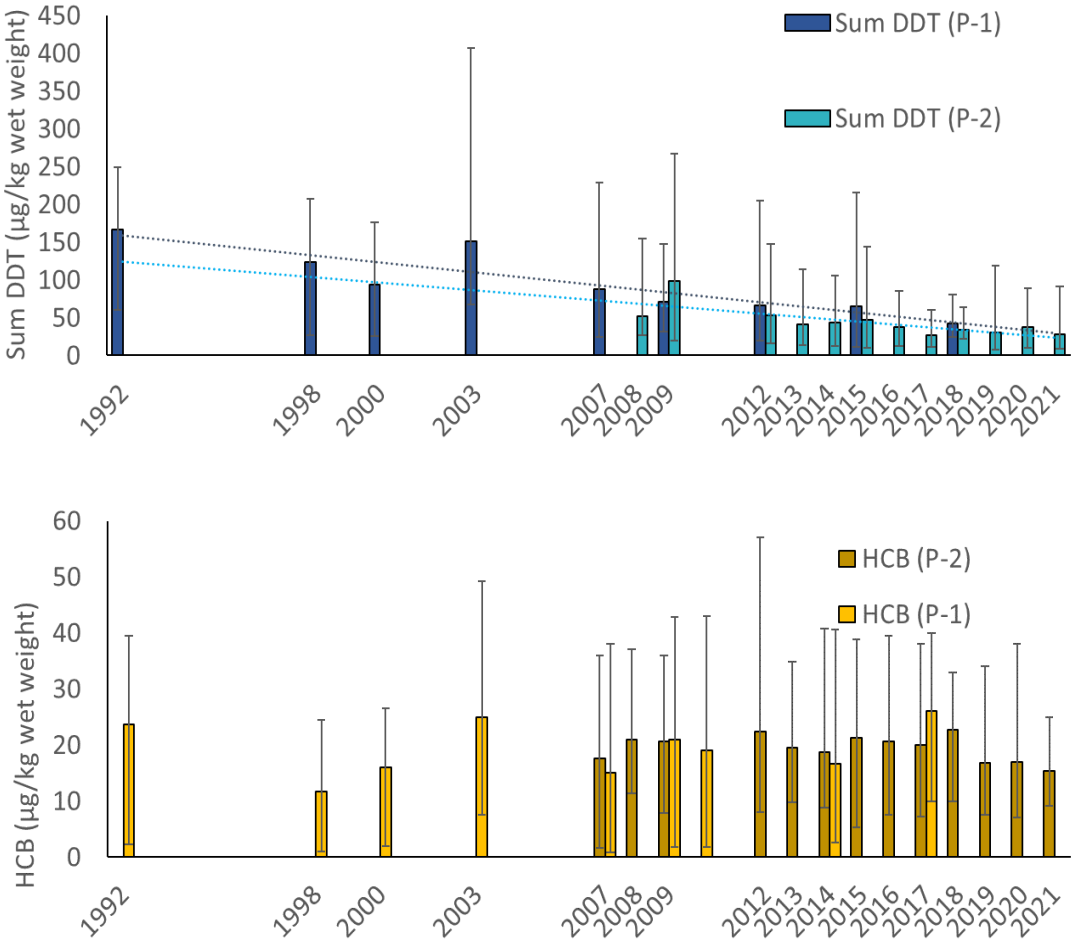

Figure A5.143: Annual concentrations of sum DDT (top) and hexachlorobenzene (HCB, bottom) in liver of cod from 1992 to 2021. Results from programme 1 (P-1) and programme 2 (P-2) are given separately. For each year, mean, minimum and maximum values are shown.

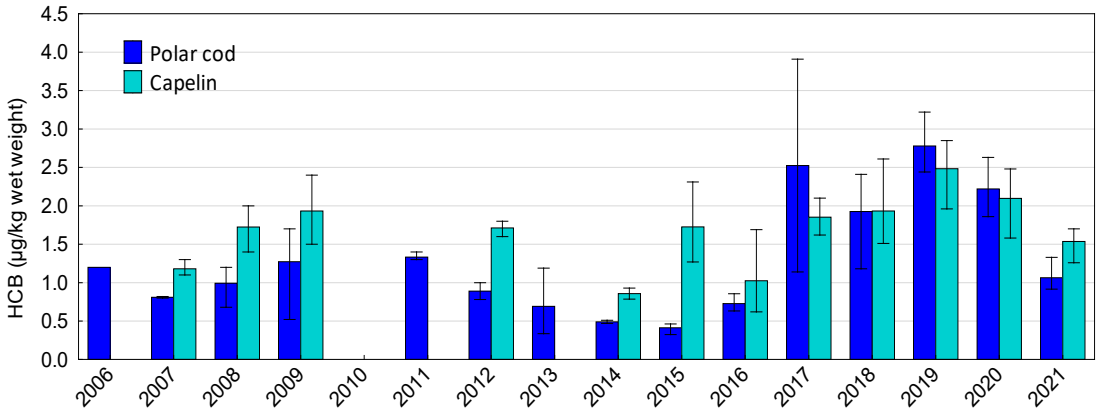

Figure A5.144: Annual concentrations of hexachlorobenzene (HCB) in composite samples of whole capelin and polar cod from 2006/2007 to 2021. For each year, mean, minimum and maximum values are shown.

The level of brominated flame retardants, PBDEs, appears to have decreased since 2006/2007, both in cod liver, capelin and polar cod (Figure A5.146). For cod liver, the decreasing trend was significant (here shown for the concentration of PBDE-47 the most dominating congener) in livers of cod sampled both south and north of 73°N (Figure A5.146 bottom). There was no change after 2015. For capelin, PBDE decreased significantly (PBDE7, µg/kg lipid weight) for samples

taken south of 75°N, but not for those taken further north (Figure A5.146A). For PBDE in polar cod, there was no significant trends when categorizing between samples taken at different latitudes (Figure A5.146B).

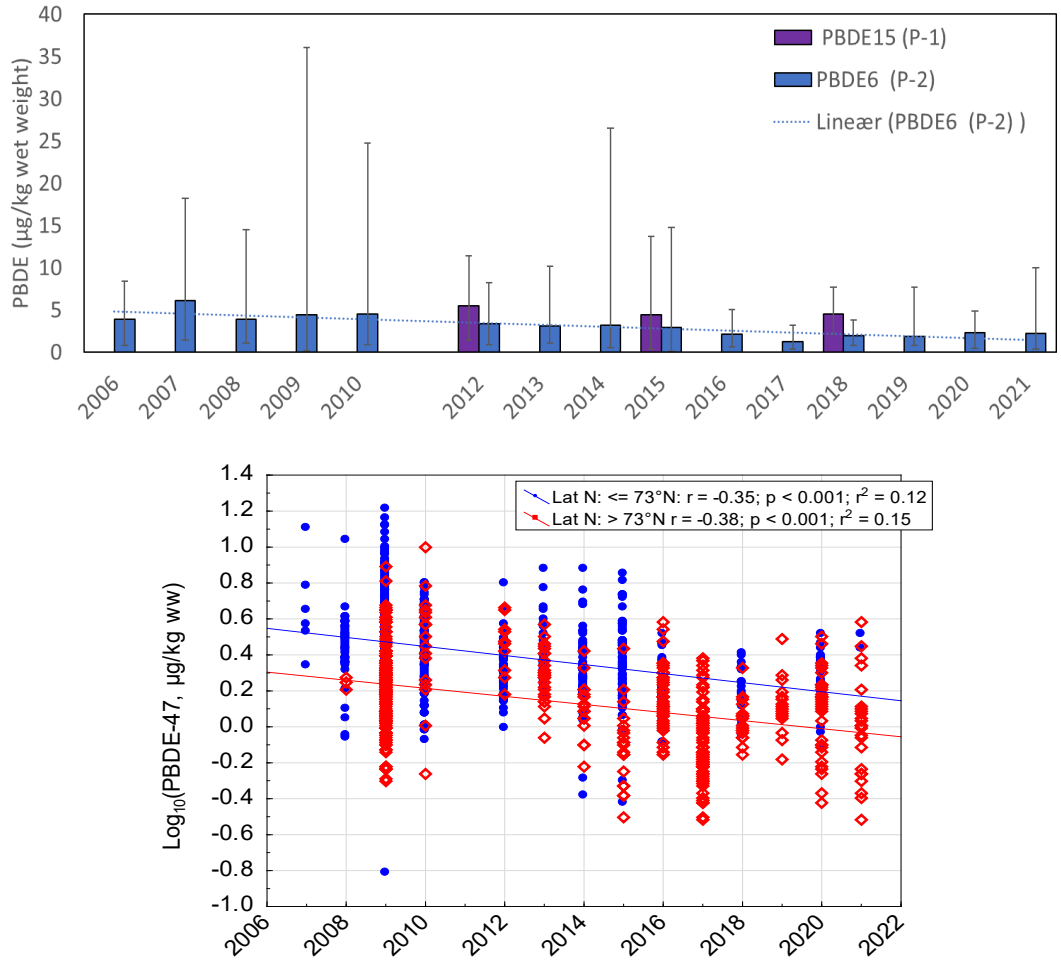

Figure A5.145: Temporal trend for polybrominated diphenyl ethers (PBDEs, µg/kg wet weight) in liver of cod from 2006 to 2021. Top: Results from programme 1 (P1) and programme 2 (P2) are given as mean, minimum and maximum values per year. In P1, PBDE15 is the sum of 15 PBDE congeners and for P2, PBDE6 is the sum of 6PBDE congeners (PBDE 28, 47, 99, 100, 153, 154). Bottom: Correlation between log10 transformed concentration of PBDE-47 and year, categorized by latitude south and north of 73°N. Only individuals between 50 and 70 cm sampled in programme 2 are included, and results of Pearson's correlation are shown for each category.

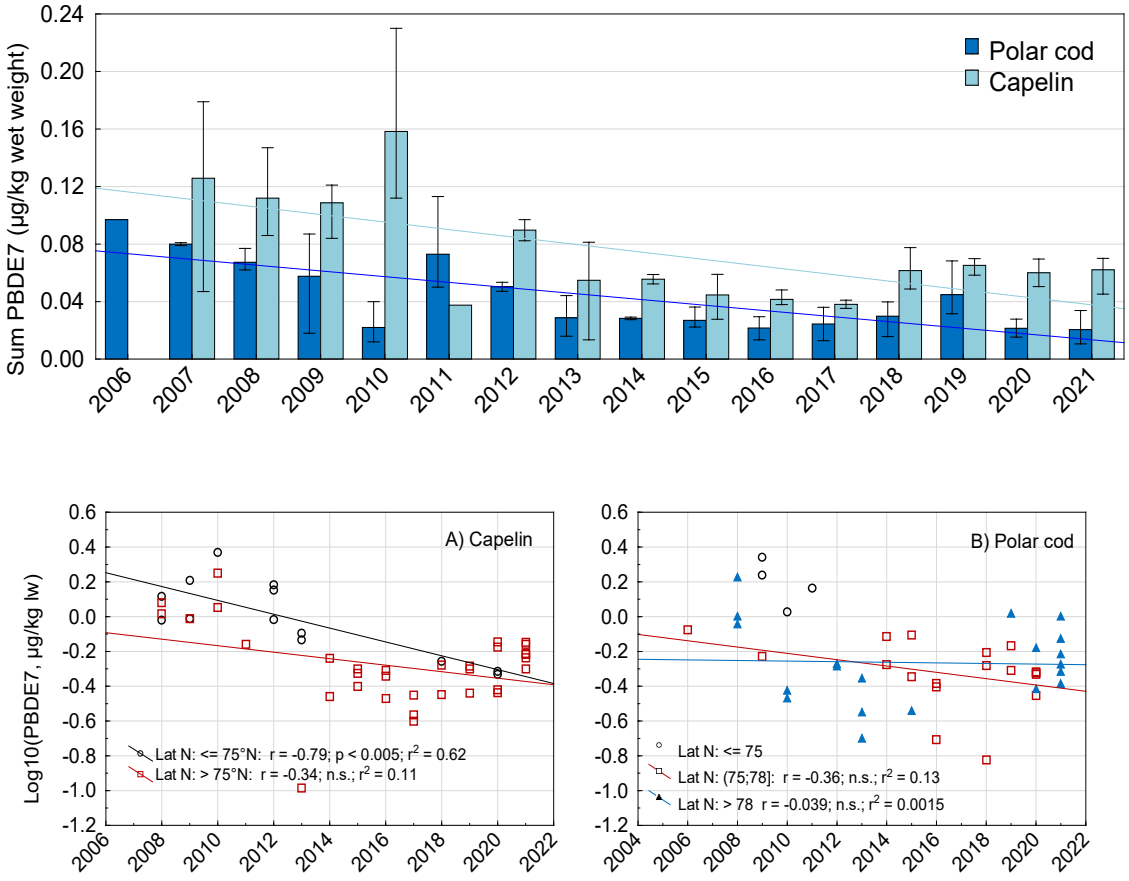

Figure A5.146: Temporal trend of concentrations of sum PBDE7 (sum of PBDE 28, 47, 99, 100, 153, 154, 180) in composite samples of whole capelin and polar cod from 2006 to 2021. Top: For each year, mean, minimum and maximum values of wet weight concentrations (µg/kg wet weight) are shown. Bottom: Correlation between lipid weight concentrations of PBDE7 (µg/kg lipid weight) and year in A) Capelin, categorized by latitude south and north of 75°N, and B) Polar cod, categorized by latitude south of 75°N (correlation not shown), between 75 and 78°N and north of 78°N. Result of Pearson's correlation is shown.

There are thus indications that the levels of persistent organic contaminants such as dioxins, PCBs and DDTs have been decreasing and are still slowly decreasing in the Barents Sea. This pattern seems to be the clearest for PBDEs, which were banned around 2005. HCB seems hardly to decrease at all. The latter may be because HCB can be breakdown product from other pesticides still in use, and also formed during incomplete combustion of industrial waste containing chlorinated organic materials. The mercury level in cod fillet has remained very stable since 1994, while concentrations may be decreasing in polar cod.

Radioactive pollution

By Hilde Elise Heldal (IMR)

Levels of radioactive pollution in the Barents Sea are low and generally decreasing. The levels in fish and seafood are far below the maximum permitted level for radioactive cesium in food set by the Norwegian authorities after the Chernobyl accident (600 Bq/kg). The Norwegian routine monitoring of the wreck of the Russian nuclear submarine "Komsomolets" has not revealed any elevated contamination levels in the area adjacent to the wreck. A dedicated expedition in 2019 with RV "G. O. Sars" and the advanced Remotely Operated Vehicle (ROV) Ægir 6000 did, however, confirm that releases of ^{137}Cs from the reactor are still occurring, 30 years after "Komsomolets" sank.

Background and sample collection

The most important sources for radioactive contamination in the Barents Sea are well known and include global fallout from atmospheric nuclear weapons testing during the 1950s and 1960s, river transport by the Ob and Yenisey rivers of radionuclides originating from Russian nuclear enterprises, discharges from European reprocessing plants for spent nuclear fuel (Sellafield and La Hague) and fallout from the Chernobyl accident in 1986. Additionally, liquid and solid radioactive wastes dumped in the Barents and Kara Seas and wrecks of sunken nuclear submarines represent potential sources.

Monitoring of radioactive contamination in Norwegian sea areas is performed within the national monitoring programme "Radioactivity in the Marine Environment" (RAME), which is coordinated by the Norwegian Radiation and Nuclear Safety Authority (DSA). We focus on the most abundant anthropogenic (man-made) gamma-emitting radionuclide cesium-137 (^{137}Cs), but the levels of other anthropogenic radionuclides like strontium-90 (^{90}Sr), plutonium-238 (^{238}Pu), plutonium-239,240 (^{239,240}Pu) and americium-241 (^{241}Am) are also determined in a selection of the samples. In recent years, there has been a growing focus on natural radionuclides like lead-210 (^{210}Pb), radium-226 (^{226}Ra) and radium-228 (^{228}Ra) in the marine environment. An additional anthropogenic source for these radionuclides to the marine environment is extraction of oil and gas. For example, produced water discharge natural radionuclides to the marine environment with activity concentrations about 1000 times higher than seawater concentrations (NRPA, 2004; Dowdall and Lepland, 2012).

The main sample collection for investigations of radioactive pollution in seawater, sediments and marine biota in the Barents Sea is carried out every third year. The last sampling campaign was in 2021, when samples were collected from R/V "Johan Hjort" and R/V "G. O. Sars" during the Barents Sea ecosystem survey in August/September.

In addition to the three-year sampling cycle, samples of cod (*Gadus morhua*) are caught along the coast of Finnmark and in the Bear Island area twice a year and analysed for ^{137}Cs. The results are part of a time-series from around 1990. Samples of surface sediments are also taken yearly at two locations in the Laksefjord in Finnmark. Further, levels of radioactive contamination are investigated once a year the near the wreck of the Russian nuclear submarine "Komsomolets", which sank in 1989 in the Norwegian Sea 180 to 190 km south-southwest of Bear Island. Samples of surface seawater (approximately 500 L) and bottom seawater (approximately 500 L) are collected with a CTD-rosette multi bottle sampler with large (10 L) water samplers. Sediment samples are collected with a sediment sampler of the type "Smøgen Boxcorer". The samples are analysed for a range of radionuclides (e.g. ^{238}Pu, ^{239,240}Pu, ^{137}Cs and ^{90}Sr) at IMR and DSA.

A joint Norwegian-Russian monitoring programme of radioactive contamination in the northern areas was established in 2006. The programme is a working group under the Joint Norwegian-Russian Expert Group on Investigation of Radioactive Contamination of the Northern Areas. The expert group is coordinated by Roshydromet on the Russian side and DSA on the Norwegian side. The monitoring programme is described and results are summarized in e.g. Jensen *et al.* 2017 and ICES 2020.

The results from the 2021 sampling campaign are not yet ready. Therefore, the present chapter summarizes results from the last Norwegian sampling campaign in the Barents Sea in 2018. Samples were prepared and analysed during 2019. Results from analyses of ^{137}Cs in sediments, seawater and marine organisms and ^{137}Cs, ^{40}K and ^{228}Ra in sediments are included. Analyses of ^{90}Sr, ^{238}Pu, ^{239,240}Pu and ^{241}Am in seawater have been performed by the DSA, but the results will not be presented here.

Sediments

Activity concentrations of ^{137}Cs in sediments collected in the Barents Sea in 2018 were below 10 Bq/kg dry weight (dw) (Figure A5.147, Table A5.7). These levels are low and comparable to previously reported values (e.g. Skjerdal *et al.* 2020; Gwynn *et al.* 2012). Elevated levels of ^{137}Cs are still found in sediments in fjords in mid-Norway, in areas which were heavily contaminated with fallout from the Chernobyl accident. These results are shown in Figure A5.147 for comparison.

Activity concentrations of the natural radionuclides ^{40}K and ^{228}Ra are given in Table A5.7. The levels of these radionuclides in marine sediments depend on e.g. the mineralogical composition and grain size distribution of the samples. The levels are comparable to those found in the Norwegian Trench (Dowdall and Lepland, 2012; Helvik, 2019) and in the Baltic Sea (Ilus *et al.* 2007). The ongoing project "NORM in Norwegian marine areas" aims at explaining observed geographical variations of natural radionuclides in sediments in Norwegian sea areas (DSA-info 2:2021; Heldal *et al.*, in press).

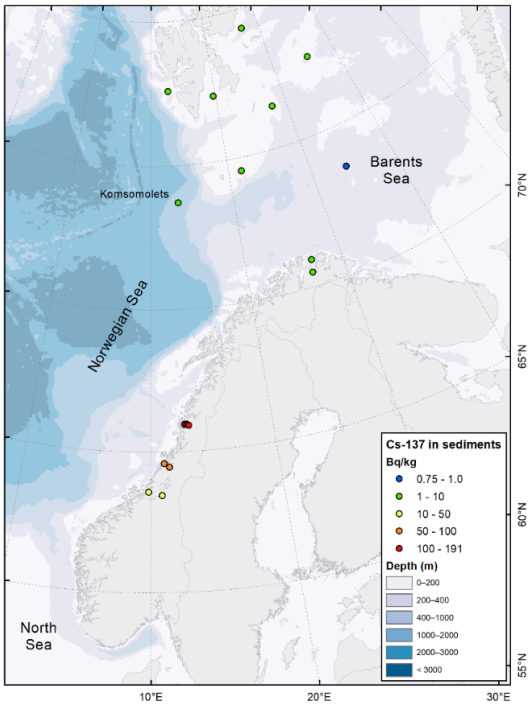

Figure A5.147: Activity concentrations of ^{137}Cs (Bq/kg dry weight) in sediments in the Barents Sea 2018. Results for samples collected in 2018 close to "Komsomolets" and in four Norwegian fjords are included for comparison (IMR/DSA/RAME).

Table A5.7: Activity concentrations of ^{137}Cs, ^{40}K, ^{228}Ra (Bq/kg dw) in sediments collected in 2018. n= number of samples.

	^{137}Cs (Bq kg^{-1} dw)		^{40}K (Bq kg^{-1} dw)		^{228}Ra (Bq kg^{-1} dw)		
	min	max	min	max	min	max	n
Barents Sea	0.8 ±0.1	4.8 ±0.6	552 ±52	1021 ±98	28 ±3	94 ±11	7
"Komsomolets"	4.3 ±0.5	6.3 ±0.6	510 ±48	555 ±53	22 ±3	26 ±3	4
Selected Norwegian fjords	5.4 ±0.6	191 ±17	525 ±50	820 ±78	24 ±3	50 ±6	8

Seawater

Levels of ^{137}Cs in seawater in the Barents Sea in 2018 are shown in Figure A5.148 and Table A5.8. The levels are low, and the results indicate that ^{137}Cs is relatively homogenously distributed throughout the Barents Sea except for a tendency to somewhat elevated levels in coastal waters along the coast of Troms and Finnmark. In general, levels of ^{137}Cs in seawater in the Barents Sea are slightly lower than levels in other Norwegian sea areas. The higher ^{137}Cs-levels in the Skagerrak are due to the closer proximity to important contamination sources, namely outflowing Baltic seawater, containing Chernobyl contamination, and the European reprocessing plants for spent nuclear fuel, Sellafield and La Hague. The ^{137}Cs-levels in seawater in fjords in mid-Norway are also somewhat elevated due to Chernobyl contamination (Figure A5.148).

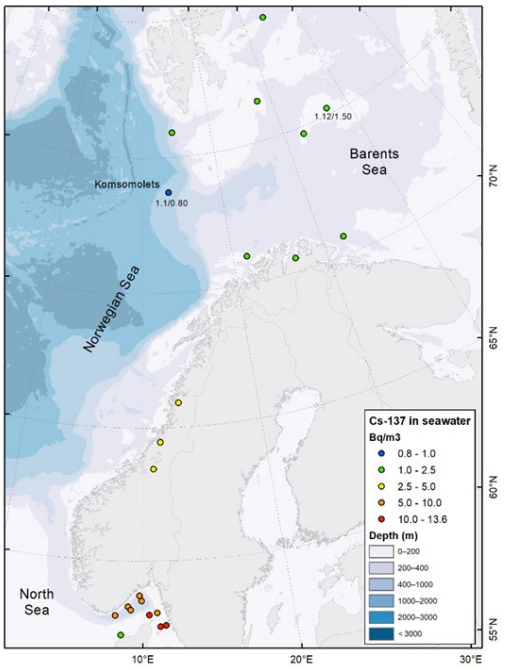

Figure A5.148: Levels of ^{137}Cs (Bq/m^3) in seawater collected in 2018 in the Barents Sea. Results for samples collected close to "Komsomolets", in four Norwegian fjords and in the Skagerrak are included for comparison (IMR/DSA/RAME). Where two numbers are given, the left hand refers to surface water and the right hand refers to bottom water.

Table A5.8: Activity concentrations of ^{137}Cs (Bq/m^3) in surface and bottom seawater in 2018. n= number of samples.

	^{137}Cs (Bq/m^3)		
	min	max	n
Barents Sea, surface	1.1 ±0.2	2.1 ±0.6	7
Barents Sea, bottom	1.5 ±0.4	-	1
"Komsomolets", surface	1.1 ±0.8	-	1
"Komsomolets", bottom	0.8 ±0.4	-	1
Selected Norwegian fjords, surface	1.8 ±0.5	3.0 ±0.5	4
Skagerrak, surface	2.5 ±0.6	13.6 ±0.8	10

Fish and marine organisms

Activity concentrations of ^{137}Cs in common species of fish collected in the Barents Sea in 2018 are below 0.2 Bq/kg fresh weigh (fw) (Figure A5.149). This is far below the maximum permitted level for radioactive cesium in food set by the Norwegian authorities after the Chernobyl accident (600 Bq/kg fw). To place the results into context, time-series of ^{137}Cs in cod along the coast of Troms and Finnmark, and in the Bear Island area from approximately 1990 until present are shown in Figures A5.150 and A5.151, respectively. It is evident that the levels have decreased during this period, and the levels in cod in the Barents Sea have been below 0.2 Bq/kg fw for the past ten years. The decrease is due to reduced discharges from Sellafield and La Hague and radioactive decay of pollution from nuclear testing during the 1950s and 1960s and the Chernobyl accident 1986. In addition, the pollution is diluted in seawater over time.

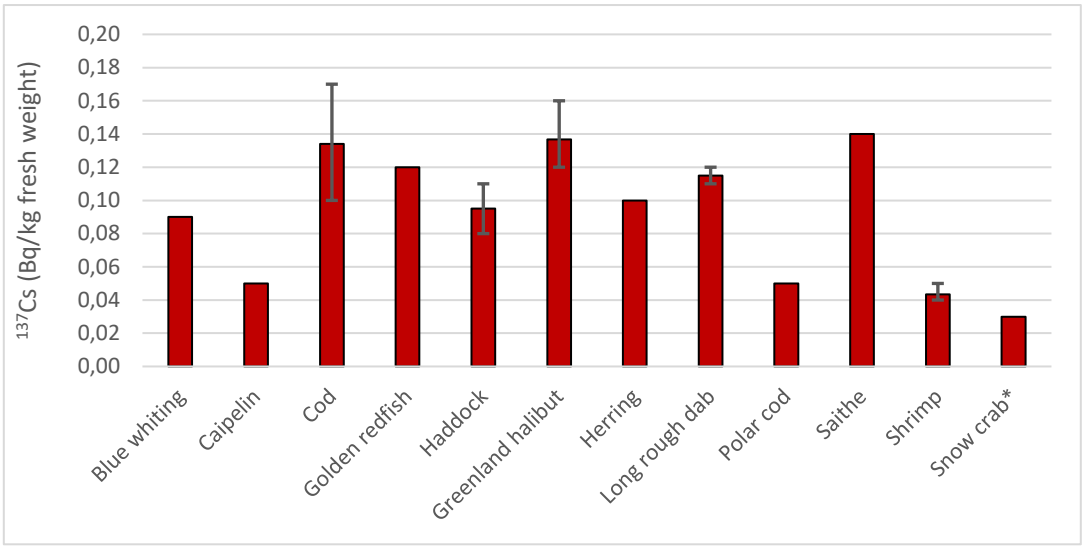

Figure A5.149: Activity concentrations (Bq/kg fw) of ^{137}Cs in common species of fish caught in the Barents Sea in 2018 (IMR/DSA/RAME). Between 1 and 5 samples of each species have been analysed. For species where more than one sample has been analysed, the average is shown, and the minimum and maximum activity concentrations are shown with bars. The activity concentration for snow crab was below the detection limit, and half the detection limit is plotted. The uncertainty in single measurements vary between 20 and 50%.

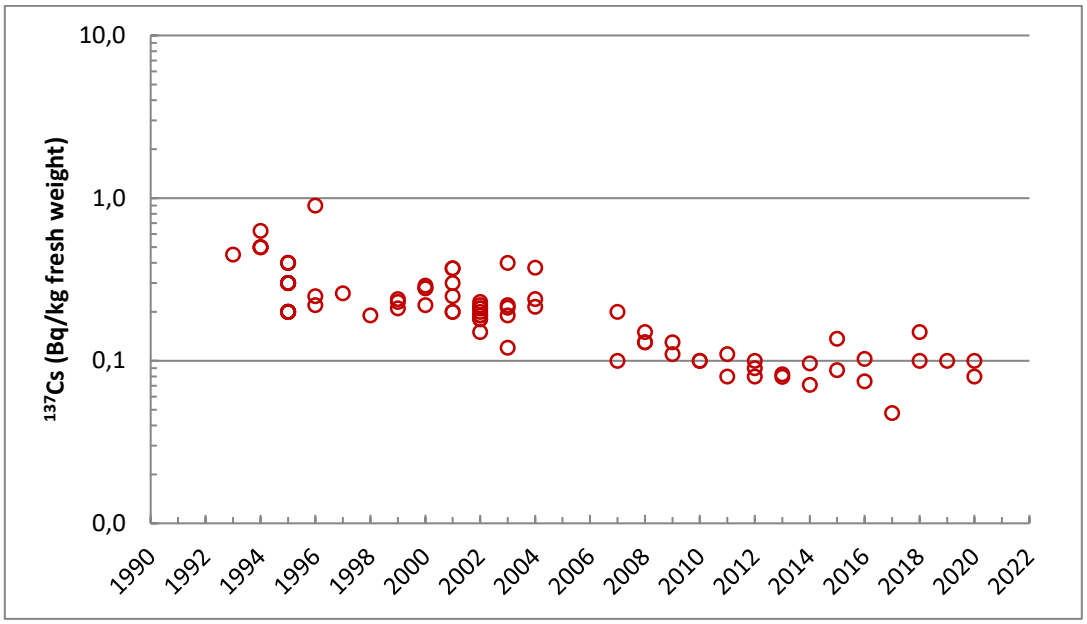

Figure A5.150: Activity concentrations of ^{137}Cs (Bq/kg fw) in cod caught in the Bear Island area in the period 1993 to 2020 (IMR/DSA/RAME). Uncertainties in single measurements are generally below 30%.

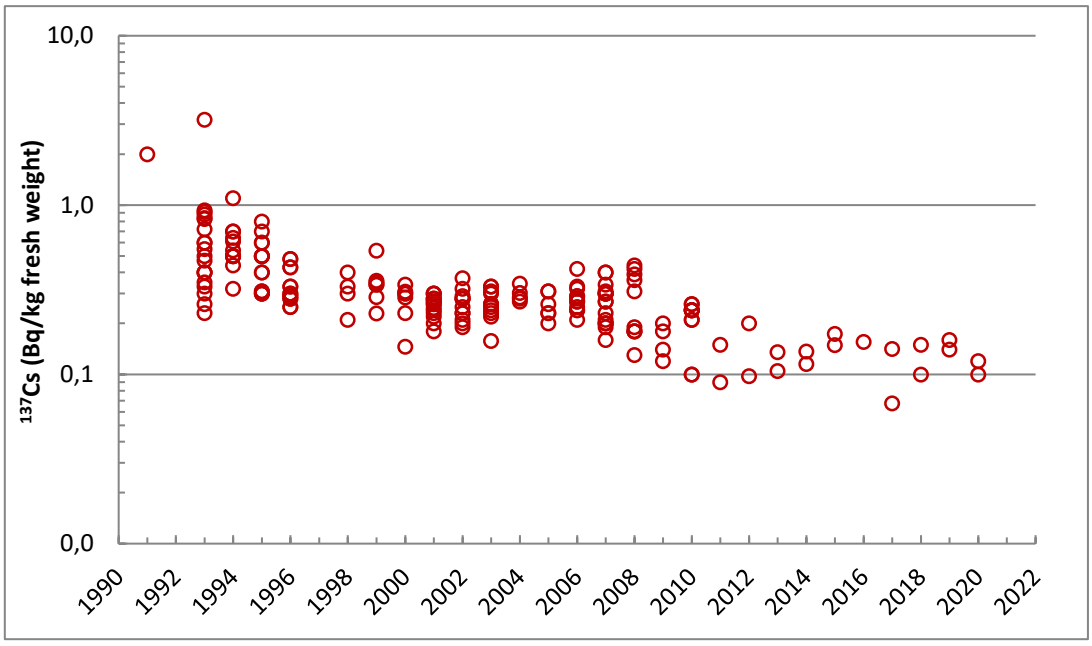

Figure A5.151: Activity concentrations of ^{137}Cs (Bq/kg fw) in cod caught along the coast of Troms and Finnmark in the period 1991 to 2020 (IMR/DSA/RAME). Uncertainties in single measurements are generally below 30%.

Komsomolets

Although "Komsomolets" rests in the Norwegian Sea, it is relevant to include here due to the proximity to the Barents Sea and the fact that it is known to leak radioactive contamination to the marine environment (Nejdanov, 1993; Gladkov *et al.*, 1994; Kazennov, 2010). Despite this fact, Norwegian routine monitoring has not revealed any elevated contamination levels in the area adjacent to the wreck (Gwynn *et al.*, 2018; Figure A5.152). Since 2013, sampling has been carried out using an acoustic transponder that allow samples to be collected at a distance of less than 20

m from the hull of the submarine. We have not found elevated levels of ^{137}Cs in these samples either.

In July 2019, a research cruise to "Komsomolets" was carried out with RV "G. O. Sars" and the advanced Remotely Operated Vehicle (ROV) Ægir 6000 (Heldal *et al*., 2019). The expedition was organized under the Joint Norwegian Russian Expert Group for investigation of radioactive contamination in Northern Areas. Using the ROV, the condition of "Komsomolets" was visually documented and samples of seawater, sediment and biota were taken at specific locations in the immediate vicinity of the submarine (Figure A5.153). Onboard analyses of seawater sampled directly from the ventilation pipe where releases have previously been documented, showed activity concentrations of ^{137}Cs between <8.0 and 857 Bq/L (Heldal *et al.*, 2019). This confirms that releases from the reactor are still occurring, 30 years after "Komsomolets" sank. The releases of ^{137}Cs from "Komsomolets" to the marine environment appeared to vary in amount and duration. Samples collected during the expedition will now be further analysed in the laboratory for ^{137}Cs, ^{90}Sr, plutonium-isotopes and other radionuclides as well as trace metals to further understand the nature of the releases from the reactor and to determine if any plutonium from the two nuclear warheads has been released into the marine environment. The analyses are delayed due to the COVID-19 pandemic, but we aim to compile and publish results from the investigation in a report under the Joint Norwegian Russian Expert Group for investigation of radioactive contamination in Northern Areas in 2022.

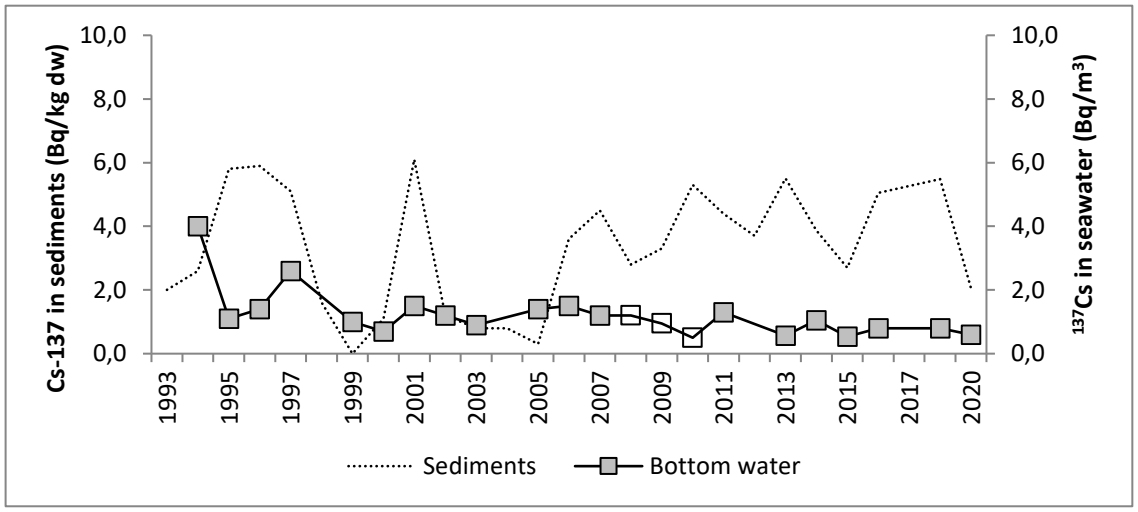

Figure A5.152. Activity concentrations of ^{137}Cs in sediments (Bq/kg dw) and bottom seawater (Bq/m^3) collected in the area adjacent to the sunken nuclear subarine «Komsomolets» in the period 1993 to 2020. Open symbols show activity concentrations below the detection limit. For these samples, half the detection limit is plotted.

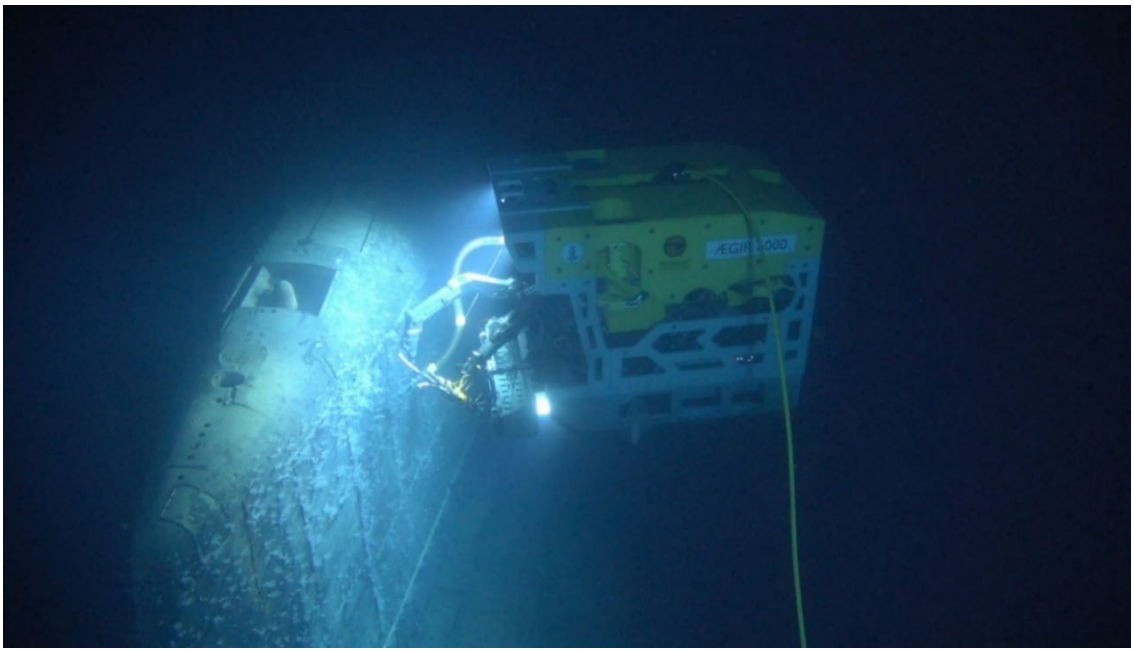

Figure A5.153: The Remotely Operated Vehicle (ROV) Ægir 6000 investigating "Komsomolets" in July 2019. Photo: IMR/Ægir 6000.

References

Azad, A.M., Frantzen, S., Bank, M.S., Nilsen, B.M., Duinker, A., Madsen, L. og Maage, A. (2019). Effects of geography and species variation on selenium and mercury molar ratios in Northeast Atlantic marine fish communities. Science of the Total Environment 652: 1482-1496.

Dowdall, M., Lepland, A., 2012. Elevated levels of radium-226 and radium-228 in marine sediments of the Norwegian Trench ("Norskerenna") and Skagerrak. Mar Pollut Bull 64, 2069-2076.

DSA-info 2:2021. Kan vi skille mellom forskjellige kilder til naturlig forekommende radioaktive stoffer i det marine miljø? Direktoratet for strålevern og atomsikkerhet. In Norwegian.

EFSA (2009). EFSA panel on contaminants in the food chain (CONTAM); Scientific opinion on arsenic in food. EFSA Journal 2009 7(10): 199 pp.

EU (2022). Commission regulation (EC) No. 1881/2006 of 19 December 2006 setting maximum levels for certain contaminants in foodstuffs (Text with EEA relevance). Official Journal of the European Union. Consolidated version 01.01.2022. http://data.europa.eu/eli/reg/2006/1881/2022-01-01

Frantzen, S. og Maage, A. (2016). Fremmedstoffer i villfisk med vekt på kystnære farvann. Brosme, lange og bifangstarter. Gjelder tall for prøver samlet inn i 2013-2015. [Contaminants in wild fish with focus on coastal waters. Tusk, ling and bycatch species. With data for samples collected during 2013-2015]. NIFES, Bergen. 116 pp. (In Norwegian).

Frantzen, S., Boitsov, S., Dehnhard, N., Duinker, A., Grøsvik, B.E., Heimstad, E., Hjermann, D., Jensen, H., Jensen, L.K., Leiknes, Ø., Nilsen, B.M., Routti, H., Schøyen, M. og Skjerdal, H.K. (2022). Forurensning i de norske havområdene - Barentshavet, Norskehavet og Nordsjøen - Rapport fra Overvåkingsgruppen 2021. Rapport fra havforskningen. 2022-3. 87 pp. (In Norwegian) https://www.hi.no/templates/reporteditor/report-pdf?id=54784&25976793

Gladkov, G.A., Khlopkin, N.S., Lystsov, V.N., Nejdanov, G.A., Pologikh, B.G., Sivintsev, Y.V., 1994. Assessment and Prognosis of the State of Nuclear Installation of Submarine Komsomolets. Working Group under leadership of Academician N. S. Khlopkin, RRC "Kurchatov Institute", Moscow, Russia.

Gwynn, J.P., Heldal, H.E., Flo, J.K., Sværen, I., Gäfvert, T., Haanes, H., Føyn, L., Rudjord, A.L., 2018. Norwegian monitoring (1990–2015) of the marine environment around the sunken nuclear submarine Komsomolets. J. Environ. Radioact. 182, 52–62.

Gwynn, J.P., Heldal, H.E., Gäfvert, T., Blinova, O., Eriksson, M., Sværen, I., Brungot, A.L., Strålberg, E., Møller, B., Rudjord, A.L., 2012. Radiological status of the marine environment in the Barents Sea. J. Environ. Radioact. 113, 155-62.

Heldal, H.E., Gwynn, J., Teien, H.-C., Volynkin, A., Jensen, L.K., Scheibener, S., Epifanov, A., 2019. Cruise report: Investigation of the marine environment around the nuclear submarine "Komsomolets" 6.-10. July 2019 (IMR cruise number 2019109). Toktrapport/Havforskningsinstituttet/ISSN 15036294/Nr. 9–2019.

Heldal, H.E., Volynkin, A., Haanes, H., Hevrøy, T., Skjerdal, H.K., Jensen, H., Lepland, A., 2022. Natural radionuclides in seafloor sediments of Norway's contintental shelf. Fram Forum 2022 (in press).

Helvik, L., 2019. A study in environmental chemistry: natural and anthropogenic radionuclides in sediment cores from the Norwegian Trench and the Vefsnfjord. Master of Science Thesis. Department of Chemistry, University of Bergen, Norway.

ICES, 2020. Working Group on the Integrated Assessments of the Barents Sea (WGIBAR). ICES Scientific Reports. 2:30. 206 pp. http://doi.org/10.17895/ices.pub.5998

Ilus, E., Mattila, J., Nielsen, S.P., Jakobson, E., Herrmann, J., Graveris, V., Vilimaite-Silobritiene, B., Suplinska, M., Stepanov, A., Lüning, M, 2007. Long-lived radionuclides in the seabed of the Baltic Sea, Report of the Sediment Baseline Study of HELCOM MORS-PRO in 2000-2005. Baltic Sea Enviroment Proceedings NO. 110, 44p.

Jensen, L.K., Shpinkov, V., Heldal, H.E., Gwynn, J.P., Møller, B. Bulgakov, V., Katkova, M., Artemyev, G., 2017. 10 years of joint monitoring of radioactive substances in the Barents Sea. Joint Norwegian-Russian expert Group for investigation of Radioactive Contamination in the Northern Areas (JNREG).

Julshamn, K., Nilsen, B.M., Frantzen, S., Valdersnes, S., Maage, A., Nedreaas, K. og Sloth, J.J. (2012). Total and inorganic arsenic in fish samples from Norwegian waters. Food Additives & Contaminants Part B-Surveillance 5(4): 229-235.

Julshamn, K., Valdersnes, S., Duinker, A., Nedreaas, K., Sundet, J.H. og Maage, A. (2015). Heavy metals and POPs in red king crab from the Barents Sea. Food Chemistry 167: 409-417.

Kazennov, A., 2010. Technologies of radiation monitoring of dumped objects. In: IAEACEG

Kögel, T., Frantzen, S., Bakkejord, J.A., Kjellevold, M., Maage, A. (2021). Basisundersøkelse av fremmedstoffer i hyse - Tungmetaller, sporelementer og organiske miljøgifter i hyse (Melanogrammus aeglefinus) fra Skagerrak, Nordsjøen, Norskehavet og Barentshavet. Rapport fra Havforskningen. 2021-35. 60 pp. (In Norwegian) https://www.hi.no/templates/reporteditor/report-pdf?id=48066&92043089

Neff, J.M. (1997). Ecotoxicology of arsenic in the marine environment. Environmental Toxicology and Chemistry 16(5): 917-927.

Nejdanov, G., 1993. Cs-137 Contamination of Seawater Around the "Komsomolets" Nuclear Submarine, in: Radioactivity and Environmental Security in the Oceans: New Research and Policy Priorities in the Arctic and North Atlantic, June 7-9, 1993. Woods Hole Oceanographic Institution, Massachusetts, USA, pp. 119-133.

Novikov, M.A. og Draganov, D. M. (2017). Kompleksnyj metodicheskij podhod k opredeleniyu fonovyh znachenij urovnej soderzhaniya mikroehlementov v vodnyh massah Barenceva morya na primere Cd, Co, Cu i Ni [Complex methodical approach to estimation of background levels of microelement content in water masses of the Barents Sea (Cd, Co, Cu and Ni)]. Vestnik KRAUNC. Nauki o Zemle 34 (2): 37-48 (In Russian).Novikov, M.A. og Draganov, D.M. (2018). Opredelenie fonovyh znachenij soderzhaniya Hg, Zn, Pb i Cr v vodnyh massah Barenceva morya [Estimation of background values of the Hg, Zn, Pb and Cr content in the water masses of the Barents Sea]. Vestnik KRAUNC. Nauki o Zemle 37 (1): 72-83 (In Russian).

Novikov, M.A., Gorbacheva, E.A. og Lapteva, A.M. (2021). Arsenic content in commercial fish of the Barents Sea (according to long-term data). Izv. TINRO 201 (3): 833–844 (In Russian).

NRPA, 2004. Natural Radioactivity in Produced Water from the Norwegian Oil and Gas Industry in 2003. StrålevernRapport 2005:2. Østerås: Norwegian Radiation Protection Authority.

Skjerdal, H.K., Heldal, H.E., Rand, A., Gwynn, J., Jensen, L.K., Volynkin, A., Haanes, H., Møller, B., Liebig, P.L., Gäfvert, T., 2020. Radioactivity in the Marine Environment 2015, 2016 and 2017. Results from the Norwegian National Monitoring Programme RAME. DSA Report 2020:04. Østerås: Norwegian Radiation and Nuclear Safety Authority.

Sonke, J.E., Teisserenc, R., Heimbürger-Boavida, L.-E., Petrova, M.V., Marusczak, N. et al. (2018) Eurasian river spring flood observations support net Arctic Ocean mercury export to the atmosphere and Atlantic Ocean. PNAS. 115 (50): E11586–E11594.

Wiech, M., Frantzen, S., Duinker, A., Rasinger, J.D. og Maage, A. (2020). Cadmium in brown crab Cancer pagurus. Effects of location, season, cooking and multiple physiological factors and consequences for food safety. Science of the Total Environment 703: 134922.

Zauke, G.P. og Schmalenbach, I. (2006). Heavy metals in zooplankton and decapod crustaceans from the Barents Sea. Science of the Total Environment 359(1-3): 283-294.

Zauke, G.P., Krause, M. og Weber, A. (1996). Trace metals in mesozooplankton of the North Sea: Concentrations in different taxa and preliminary results on bioaccumulation in copepod collectives (Calanus finmarchicus/C. helgolandicus). Internationale Revue Der Gesamten Hydrobiologie 81(1): 141-160.

Shipping activity

By Nina Mikkelsen and Gro I. van der Meeren (IMR)

Marine traffic is monitored by information obtained from the Automatic Identification System (AIS). All vessels >300 gross tonnage are required to transmit AIS after the International Maritime Organization (IMO) adopted this requirement in Regulation 19 of SOLAS chapter V in 2000. Since 2014, all fishing vessels >15 m operating in Norwegian waters are required to have AIS Class A transponders.

The marine traffic, excluding fishing vessels, cover less distance than in other ocean regions. Shipping activity measured by annual vessel density is highest in coastal areas and in areas with high fishing activity (Figure A5.154). In the Barents Sea Management Plan (BSMP) area covering the Norwegian sector of the Barents Sea, there was an annual increase in sailed distance (nm) in from 2015 to 2019, followed by a slight drop in 2020. The drop in marine traffic was largely generated by reduced activity by the vessels belonging to the vessel categories cruise ships, tankers, other activities and passenger ships (including domestic traffic by the coast such as ferries) (Table A5.9). When including fishing vessels, they account for approximately 40% of the annual sailed distance, followed by passenger ships and vessels classified to "Other activities" category by the Norwegian Coastal Administration (NCA).

Receding sea ice allows more frequent open passage for shipping in the Barents Sea and the Northeast passage between the Atlantic and Pacific Oceans. Shipping activity related to tourism, petroleum-related activities and marine cargo transport is expected to increase, while fisheries activities expand northwards (Fauchald *et al.*, 2021). Prognosis made by Norwegian Coastal Administration up to 2040 indicate that traffic in the Norwegian sector of the Barents Sea will increase with approximately 40% (DNV GL, 2018).

The shipping lanes between the Barents Sea and the North Atlantic are important for ship traffic and good surveillance reduce the risk for major pollutions due to accidents, as well as close monitoring of vessels carrying dangerous goods and petroleum products.

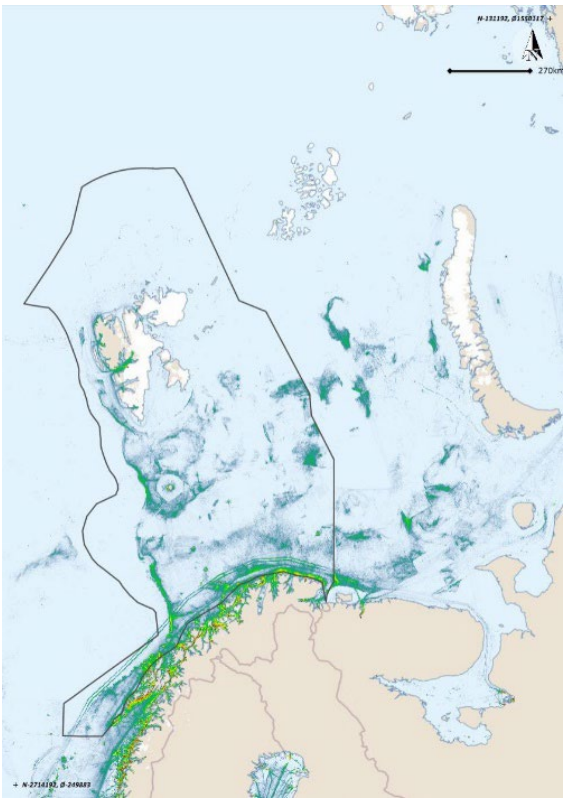

Figure A5.154: Shipping density, including fishing vessels, in the Barents Sea 2019. Black line illustrates the border of the Norwegian Barents Sea Management Plan area (Source EMODnet, BarentsWatch-Norwegian Coastal Administration).

Table A5.9: Sailed distance (nm) in the Norwegian sector of the Barents Sea by vessel categories (n=15) in the period 2015 to 2021 (Source Norwegian Coastal Administration).

Vessel category	2015	2016	2017	2018	2019	2020	2021
Bulk carriers	534 292	503 049	600 473	586 581	640 359	512 732	425 512
Chemical tankers	265 369	265 386	315 022	351 550	325 201	241 008	247 665
Container ships	7 989	2 213	7 520	22 712	24 772	23 279	13 577
Crude oil tankers	134 367	194 211	237 228	227 397	255 622	240 225	224 248
Cruise ships	227 953	264 298	294 569	344 900	383 789	61 391	35 735
Fishing vessels	4 277 153	4 470 835	4 465 287	4 393 803	4 095 986	4 396 588	4 368 417
Gas tankers	74 161	73 041	74 740	223 596	471 899	344 075	282 915
General cargo ships	1 239 784	1 386 177	1 372 945	1 335 260	1 310 613	1 325 157	1 379 263
Offshore supply ships	182 941	180 251	217 974	195 381	152 980	194 065	228 946
Oil product tankers	94 722	106 318	114 009	143 270	151 979	136 563	135 859
Other activities	1 079 946	1 039 217	1 214 171	1 048 646	1 257 220	1 064 146	1 938 278
Other service offshore vessels	71 874	41 401	63 394	43 340	58 685	58 368	48 348
Passenger ships	1 441 073	1 576 353	1 600 270	1 628 957	1 602 633	1 269 051	1 393 314
Refrigerated cargo ships	263 090	291 138	289 687	279 095	257 728	222 115	229 793
Ro-Ro cargo ships	44 983	29 471	38 248	38 791	39 241	28 229	33 959
Total	9 939 696	10 423 358	10 905 536	10 863 280	11 028 704	10 116 992	10 985 830

Table A5.10: Emission to air 2019 by vessel categories in the Norwegian sector of the Barents Sea (source Norwegian Coastal Administration)

Vessel category	CO_2	CO	NO_x	PM	SO_2
Bulk carriers	147 294	341	3 469	318	557
Chemical tankers	63 848	146	1 323	105	188
Container ships	2 547	6	39	1	3
Crude oil tankers	125 905	290	2 933	259	625
Cruise ships	130 054	284	2 569	205	491
Fishing vessels	409 564	956	5 725	155	233
Gas tankers	521 296	1 194	11 802	1 006	2 693
General cargo ships	118 305	275	1 886	51	161
Offshore supply ships	54 821	120	750	22	31
Oil product tankers	14 061	32	231	12	26
Other activities	132 629	301	1 869	51	92
Other service offshore vessels	18 851	39	279	11	26
Passenger ships	211 381	456	3 743	276	492
Refrigerated cargo ships	32 840	73	454	13	44
Ro-Ro cargo ships	5 736	12	83	3	8
Total sum	1 989 133	4 526	37 155	2 487	5 668

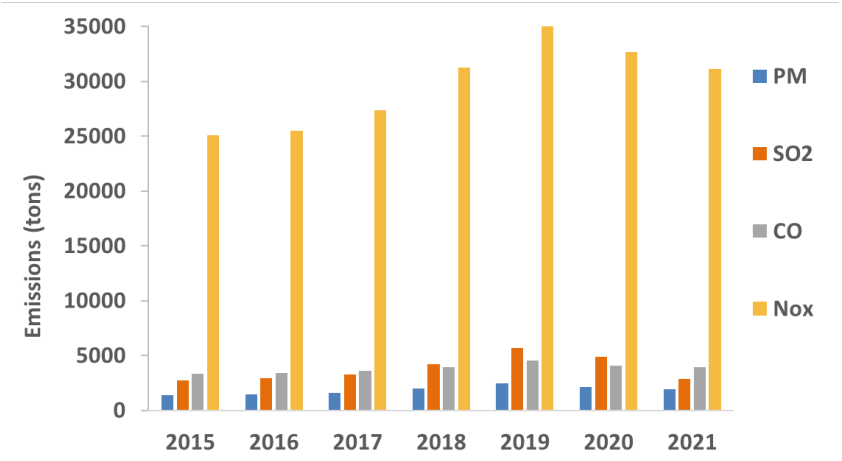

Figure A5.155: Emission (tons) to air of particles (PM), SO2, CO, NOx) by all vessels within the Norwegian Barents Sea Management Plan area 2015 to 2021 (source Norwegian Coastal Administration).

The impacts of shipping activity are generally linked to ordinary emission and pollutants due to normal cruising but does also include risk of introducing alien species through biofouling and ballast water, underwater noise and illegal release of pollutants. Underwater noise generated by vessels can travel hundreds of kilometers and is predominantly at low frequency (Popper and Hawkins, 2019). Vessel noise may cause disturbance in fish behavior, communication, detection of predator and prey and orientation and reproduction (Ivanova *et al.*, 2020; Popper and Hastings, 2009; Slabbekoorn *et al.*, 2010). There are also documented effects on marine mammals from vessel noise on behavioral and acoustic responses, auditory masking, stress and collisions (Erbe *et al.*, 2019; Hauser *et al.*, 2018; Schoeman *et al.*, 2020). Underwater noise from vessels may affect marine mammals when within 2 km for icebreaker vessels and as far as 52 km for tankers (Halliday *et al.*, 2017).

Release of pollutants from ordinary cruising may be countered by improved technology and fuel, reducing the environmental footprints even when the traffic increases. Several risk mitigating measures are already in place to reduce the environmental impacts caused by shipping activity and described in the International Convention for the Prevention of Pollution from Ships[1].

Pollution generated by estimated emissions to air by all vessel categories increased in the period from 2015 to 2021, followed by a slight decline in 2020 and 2021 (Figure A5.155). CO_2 is released in the highest quantity of all emissions by all vessels and usually most frequently by vessel categories with high values of sailed distance (Figure A5.156). The release of Nitrogen oxides (NOx) is the second most important, followed by Particular Matter (PM), Sulphur dioxide (SO_2) and Carbon monoxide (CO) is released in much lower quantities. In the period from 2016 to 2021, there has been an increase in CO_2 emissions by Gas tankers sailing in the Barents Sea, which also corresponds to the sharp increase in sailed distance by this vessel category from 2018 (Table A5.9). CO_2 emissions by Cruise ships had a sharp decline in 2020 and 2021 due to COVID-19 pandemic.

[1] https://www.imo.org/en/KnowledgeCentre/ConferencesMeetings/Pages/Marpol.aspx

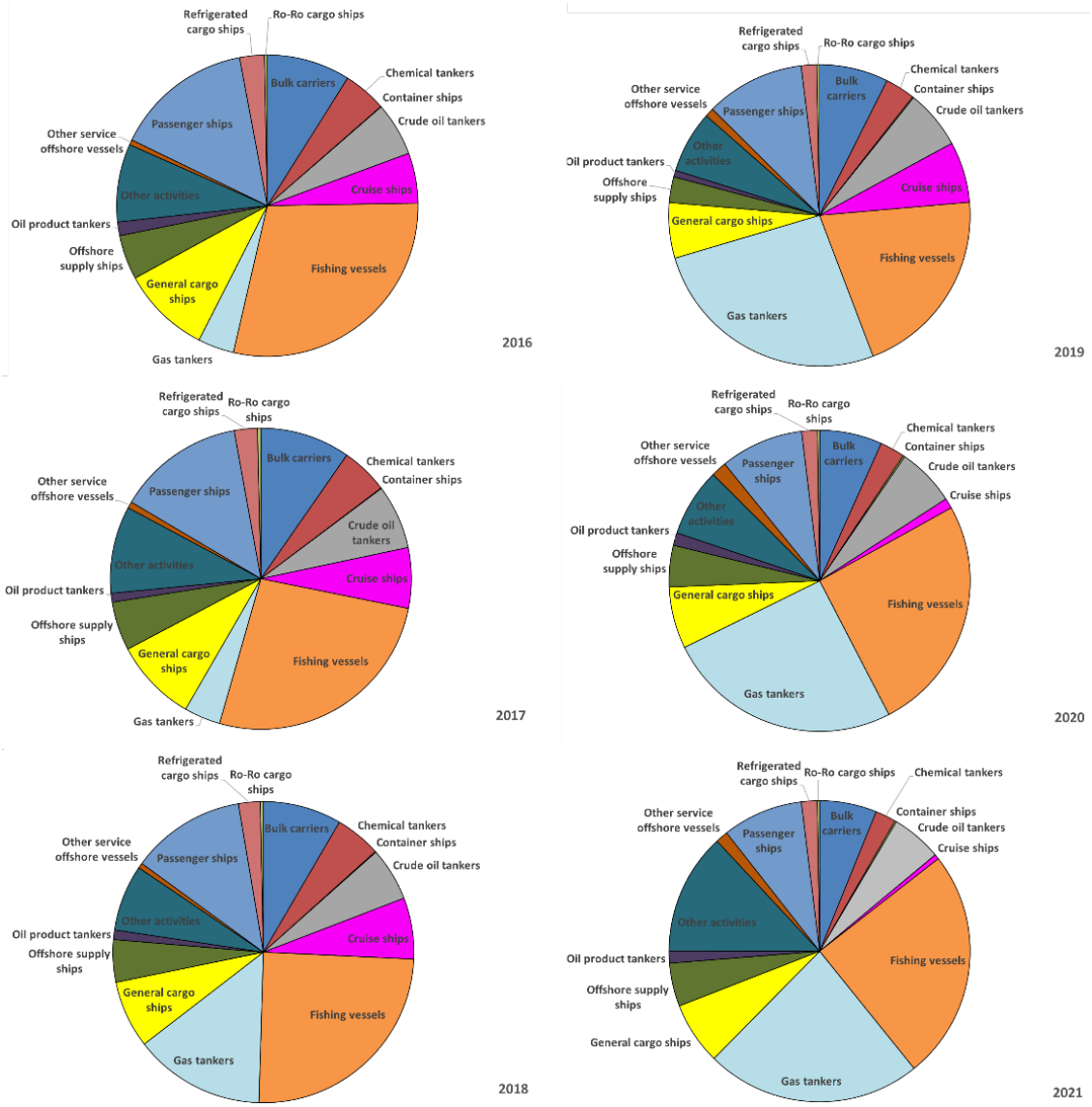

Figure A5.156: CO_2 emissions to air by vessel categories (n=15) in the Norwegian sector of the Barents Sea in the period 2016 to 2021 (Source Norwegian Coastal Administration).

The northern part of the Barents Sea is within the boundaries of the IMO's International Code for Ships Operating in Polar Waters (Polar Code)[2], which include mandatory measures covering both safety and prevention of pollution to protect the environment. The code entered into forces on 1 January 2017 and is mandatory under both the International Convention for the Safety of Life at Sea[3] and MARPOL.

[2] https://www.imo.org/en/MediaCentre/HotTopics/Pages/Polar-default.aspx

[3] https://www.imo.org/en/About/Conventions/Pages/International-Convention-for-the-Safety-of-Life-at-Sea-(SOLAS),-1974.aspx

References

DNV GL 2018. Prognoser for skipstrafikken mot 2040/ Forecasts for ship traffic towards 2040. Report No. 2014-1271, Rev. E. In Norwegian

Erbe, C., Marley, S.A., Schoeman, R.P., Smith, J.N., Trigg, L.E., Embling, C.B., 2019. The Effects of Ship Noise on Marine Mammals—A Review. Frontiers in Marine Science 6. https://doi.org/10.3389/fmars.2019.00606

Fauchald, P., Arneberg, P., Debernard, J.B., Lind, S., Olsen, E., Hausner, V.H., 2021. Poleward shifts in marine fisheries under Arctic warming. Environ Res Lett 16, 074057. https://doi.org/10.1088/1748-9326/ac1010

Halliday, W.D., Insley, S.J., Hilliard, R.C., De Jong, T., Pine, M.K., 2017. Potential impacts of shipping noise on marine mammals in the western Canadian Arctic. Marine Pollution Bulletin 123, 73-82. https://doi.org/10.1016/j.marpolbul.2017.09.027

Hauser, D.D.W., Laidre, K.L., Stern, H.L., 2018. Vulnerability of Arctic marine mammals to vessel traffic in the increasingly ice-free Northwest Passage and Northern Sea Route. Proceedings of the National Academy of Sciences 115, 7617. https://doi.org/10.1073/pnas.1803543115

Ivanova, S.V., Kessel, S.T., Espinoza, M., McLean, M.F., O'Neill, C., Landry, J., Hussey, N.E., Williams, R., Vagle, S., Fisk, A.T., 2020. Shipping alters the movement and behavior of Arctic cod (*Boreogadus saida*), a keystone fish in Arctic marine ecosystems. Ecological Applications 30. https://doi.org/10.1002/eap.2050

NCA (2022). BarentsWatch. Website maintained by the Norwegian Coastal Administration). Retrieved 26 February 2022. (https://www.barentswatch.no/en/)

Popper, A.N., Hastings, M.C., 2009. The effects of anthropogenic sources of sound on fishes. Journal of Fish Biology 75, 455-489. https://doi.org/10.1111/j.1095-8649.2009.02319.x

Popper, A.N., Hawkins, A.D., 2019. An overview of fish bioacoustics and the impacts of anthropogenic sounds on fishes. Journal of Fish Biology 94, 692-713.

Schoeman, R.P., Patterson-Abrolat, C., Plön, S., 2020. A Global Review of Vessel Collisions With Marine Animals. Frontiers in Marine Science 7. https://doi.org/10.3389/fmars.2020.00292

Slabbekoorn, H., N. Bouton, I. van Opzeeland, A. Coers, C. ten Cate, and A. N. Popper. 2010. A noisy spring: the impact of globally rising underwater sound levels on fish. Trends in Ecology & Evolution 25:419-427.https://doi.org/10.1016/j.tree.2010.04.005

Oil and gas

By Nina Mikkelsen and Gro I. van der Meeren (IMR)

Oil and gas exploration and exploitation in the Norwegian sector of the Barents Sea include seismic surveys, drilling of wellbores and production of oil and gas. Transport related to the activities is covered by separate vessel categories in the previous chapter.

The Norwegian authorities grants exclusive rights to conduct exploration drilling and production at the Norwegian continental shelf in two licensing rounds. The numbered licensing rounds include frontier parts of the shelf are normally held every other year while Awards in Predefined Areas (APA) are announced every year. APA comprise mature parts of the shelf with known geology and good infrastructure (NPD, 2022a). Few new numbered licenses in frontier areas has been granted since 2018, with only three licenses in 2021 (25th round), while the number of APA licenses increased sharply in 2019 (APA2018) and 2020 (APA2019) (Figure A5.157). In 2021, three APA licenses were offered in the Norwegian sector of the Barents Sea (APA2020). The offered APA in the period 2016 to 2020 were widely distributed (Figure A5.158).

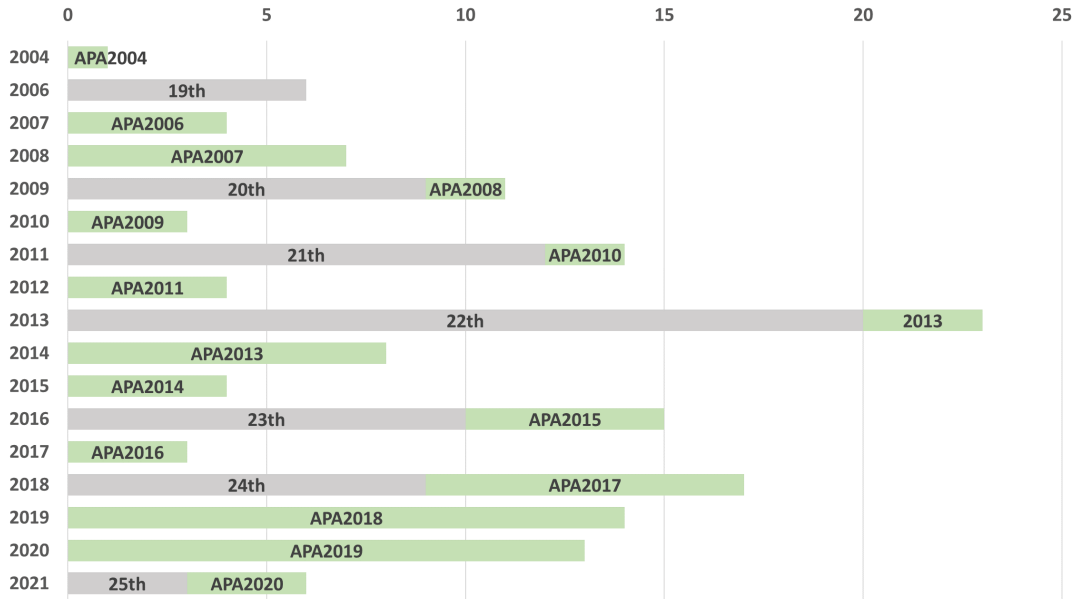

Figure A5.157: Number of licenses granting rights to conduct exploration drilling and production of oil and gas at the Norwegian continental shelf in the Barents Sea (2000–2021). Numbered licensing rounds (grey) in include frontier areas (19th to 25th licensing round) and Awards in Predefined Areas (APA2004-APA2020) (green) comprise the mature part of the shelf (Source the Norwegian Petroleum Directorate).

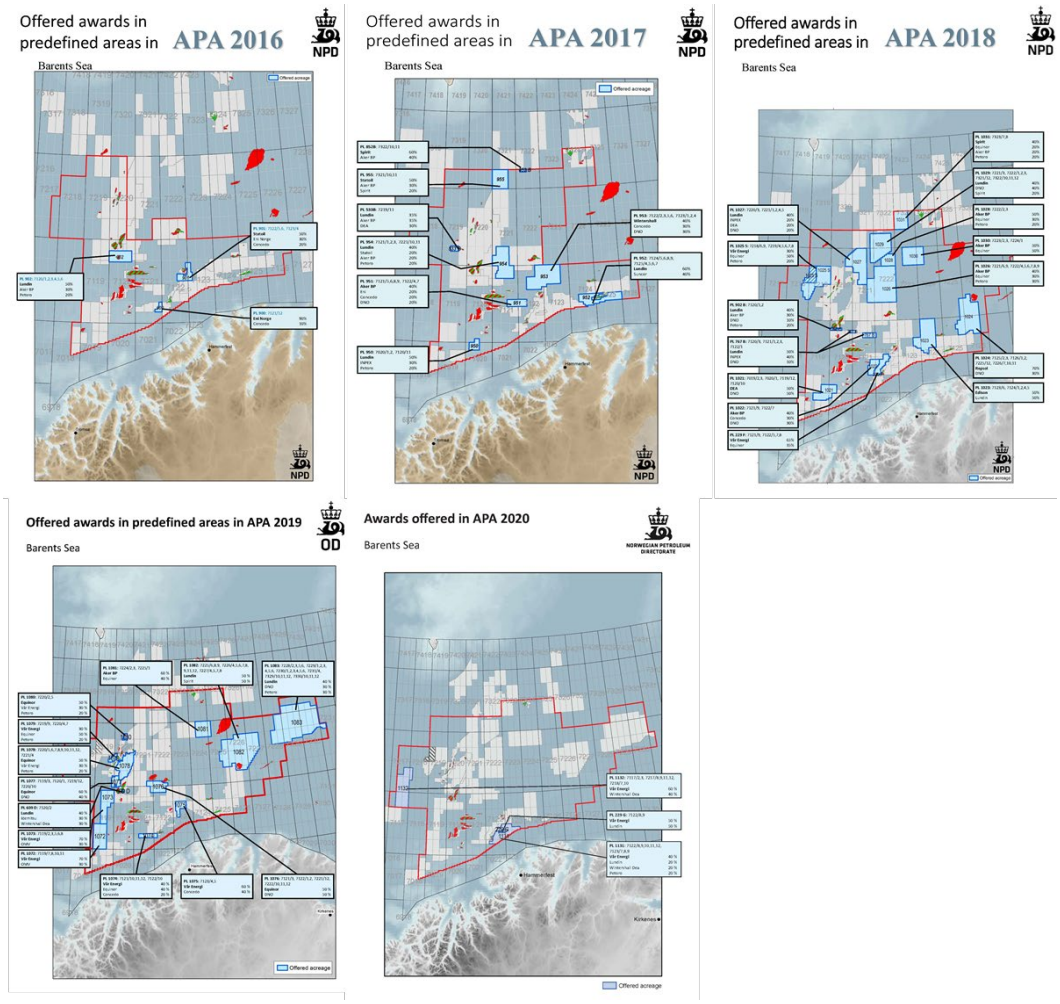

Figure A5.158: Offered Awards in Predefined Areas (APA) at the Norwegian Continental Self in the Barents Sea (source The Norwegian Petroleum Directorate).

There are currently two producing fields at the Norwegian continental shelf (NCS) in the Barents Sea. The fields, Snøhvit and Goliat, came on stream in 2007 and 2016, respectively. A third field, Johan Castberg is under development and expected to come on stream in 2024. Produced oil at Goliat field is exported in tankers, while gas from Snøhvit field is transported by pipeline to Melkøya onshore Liquified Natural Gas (LNG) facility at the coast of Northern Norway (Figure A5.159). After a record high production volume in 2018, the total production volume (million Sm^3 oil equivalents[4]) at the NCS in the Barents Sea has declined (Figure A5.160). LNG plant at Melkøya has been closed since Sept. 28, 2020 after a fire (OGJ 2020). The startup date for Hammerfest LNG had has been postponed due to consequences from Covid-19 pandemic and operational restrictions and the current plan is to start up in May 2022 (Equinor 2022). A large oil reservoir named Wisting (Figure A5.159) was proven in 2013, approximately 300 kilometers off the coast of Northern Norway. The discovery will most likely be developed as a stand-alone development and the plan for development and operation is expected to be submitted by the end of 2022 (NPD 2022b).

Drilling activity produce underwater noise and pollution, but the Norwegian authorities applies a zero environmental harmful discharge policy applies for the whole Norwegian continental

[4] standard cubic metres of oil equivalent (Sm3 o.e.)

shelf (Ministry of Petroleum and Energy, 2011). Visible drill cuttings can extend to less than 50 m after 3 or more years post-drilling (Cochrane *et al.*, 2019) and environmental impact has been confined to <30m from the wellhead (Dijkstra *et al.*, 2020). Bacterial community changes have been observed within 100 m from the drilling site and bacterial perturbations may last for more than eight years after drilling (Nguyen *et al.*, 2021).

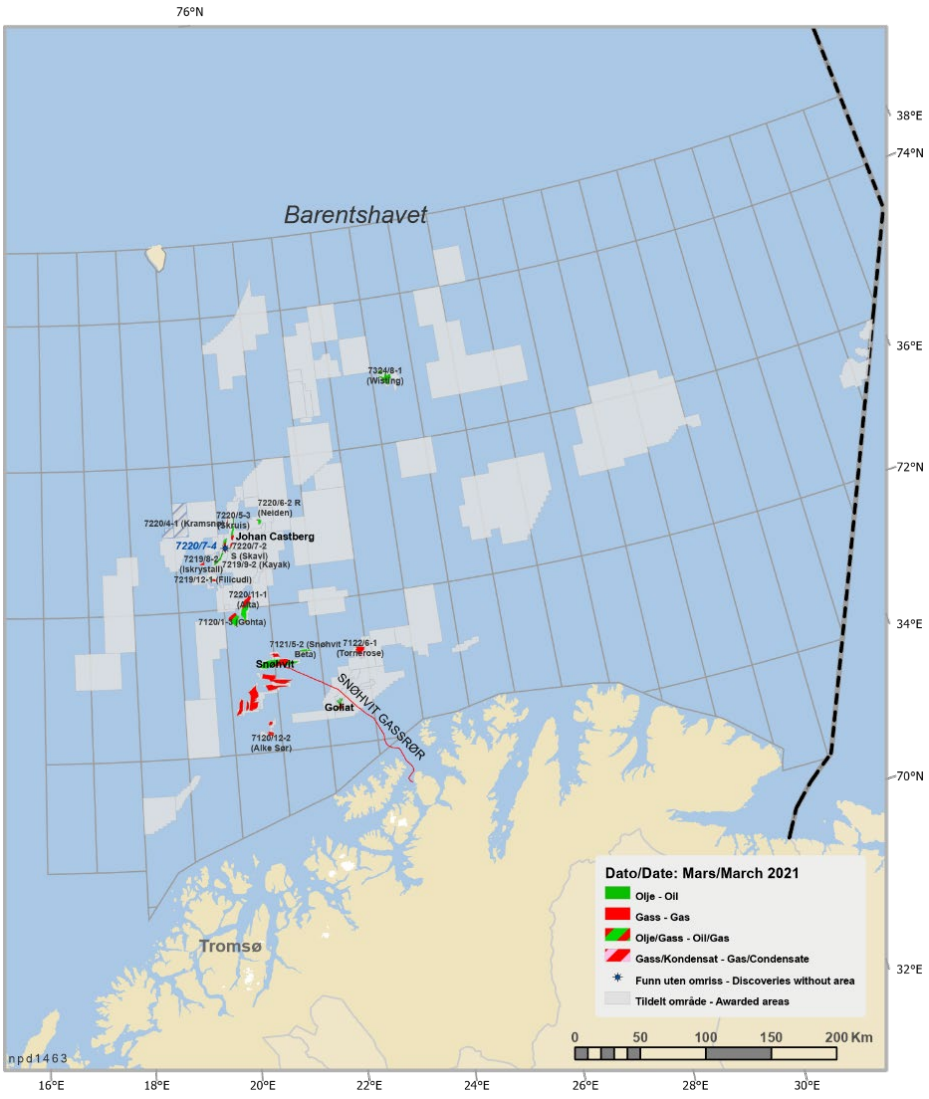

Figure A5.159: Active fields for oil- and gas exploitation in the Norwegian EEZ, by March 2021 (Source The Norwegian Petroleum Directorate).

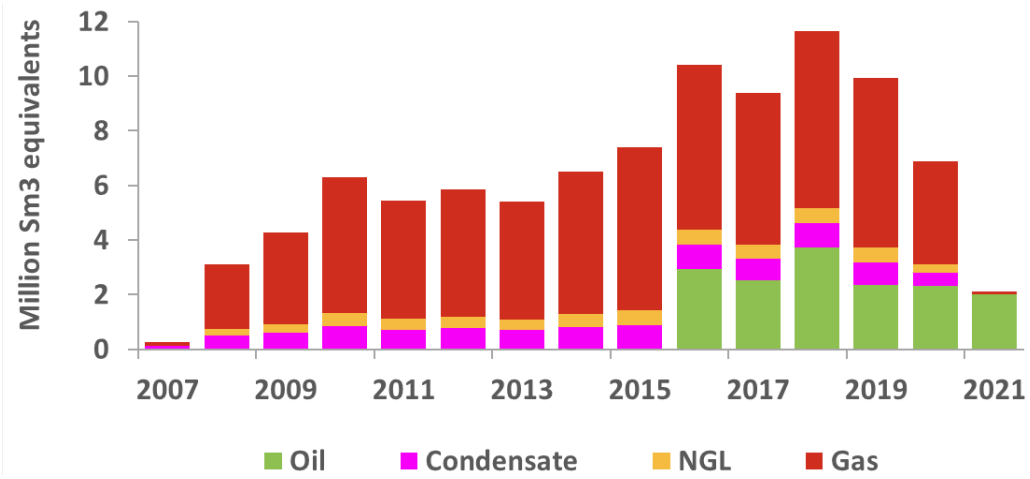

Figure A5.160: Annual production from the Barents Sea petroleum fields, from 2007 to 2021 (source The Norwegian Petroleum Directorate).

Seismic technology is used to analyse the ground below seabed to discover new oil and gas resources and to monitor production fields. The prevalence of geophysical surveys at the NCS in the Barents Sea vary greatly from year to year in terms of area covered, type of survey, shooting density and more (NPD 2022a). The ordinary seismic surveys are two-dimensional (2D), three-dimensional (3D) or four-dimensional (4D) (NPD 2020, Slabbekoorn *et al*., 2019). 2D surveys are often used in large regional aiming to discover oil and gas resources while 4D is largely used for reservoir monitoring (NPD 2019, Slabbekoorn *et al*., 2019). 3D surveys are increasingly used, as they provide more detailed information and an increasing average acreage per survey (NPD, 2020) (Figure A5.161).

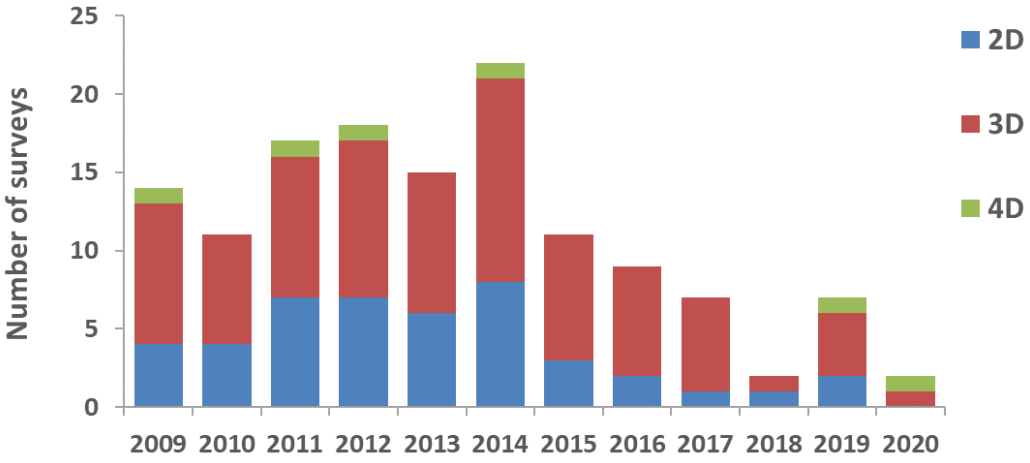

Figure A5.161: Number of seismic surveys in the Norwegian EEZ (Barents Sea) from 2009 to 2020 (source The Norwegian Petroleum Directorate).

Norway has managed seismic surveys based on potential impact of fish stocks since 1980s and since 2018, marine mammals are included in the advice (Sivle *et al*., 2021). An annual advice on seismic surveys is included in the annual advice on the impact of anthropogenic noise in Norwegian waters and includes temporal/spatial maps of areas where seismic and electromagnetic surveys are not recommended (Sivle *et al*., 2022). Spawning grounds for fish are closed for seismic surveys. Underwater noise created by seismic exploration of the seabed may have an impact on fish and marine mammals causing behavioural or physical change (Slabbekoorn *et al*., 2019). Although there is a lack of knowledge on population effects, effects from seismic shooting have been documented in several studies; reduced likelihood for social interaction in humpback

whales (Dunlop *et al.*, 2020), subtle changes to bowhead whale surfacing, respiration, and dive behaviour (Robertson *et al*., 2013), changed distribution, local abundance and catch-rates of fish (Engås *et al*., 1996; Løkkeborg *et al.*, 2012). Underwater noise from seismic survey may potentially mask communication up to 18 km from the source (Rogers *et al*. 2021)

References

Carroll, A. G., R. Przeslawski, A. Duncan, M. Gunning, and B. Bruce. 2017. A critical review of the potential impacts of marine seismic surveys on fish & invertebrates. Marine Pollution Bulletin 114:9-24. https://doi.org/10.1016/j.marpolbul.2016.11.038

Cochrane, S. K. J., S. Ekehaug, R. Pettersen, E. C. Refit, I. M. Hansen, and L. M. S. Aas. 2019. Detection of deposited drill cuttings on the sea floor - A comparison between underwater hyperspectral imagery and the human eye. Marine Pollution Bulletin 145:67

Dijkstra, N., Junttila, J., Aagaard-Sørensen, S., 2020. Impact of drill cutting releases on benthic foraminifera at three exploration wells drilled between 1992 and 2012 in the SW Barents Sea, Norway. Marine Pollution Bulletin 150, 110784. https://doi.org/10.1016/j.marpolbul.2019.110784

Dunlop, R. A., R. D. McCauley, and M. J. Noad. (2020). Ships and air guns reduce social interactions in humpback whales at greater ranges than other behavioral impacts. Marine Pollution Bulletin 154:111072. https://doi.org/10.1016/j.marpolbul.2020.111072

Engås, A., S. Løkkeborg, E. Ona, and A. V. Soldal. (1996). Effects of seismic shooting on local abundance and catch rates of cod (*Gadus morhua*) and haddock) (*Melanogrammus aeglefinus*). Canadian Journal of Fisheries and Aquatic Sciences 53:2238-2249. https://doi.org/10.1139/f96-177

Equinor (2022). Revised start-up date for Hammerfest LNG, Jan. 31,2022, Retrieved 20 March 2022 (https://www.equinor.com/)

Løkkeborg, S., E. Ona, A. Vold, and A. Salthaug. (2012). Sounds from seismic air guns: gear- and species-specific effects on catch rates and fish distribution. Canadian Journal of Fisheries and Aquatic Sciences 69:1278-1291. https://doi.org/10.1139/f2012-059

Ministry of Petroleum and Energy (2011). An industry for the future – Norway's petroleum activities. In: Meld. St. 28 (2010–2011) Report to the Storting, (White paper).

Nguyen, T.T., Paulsen, J.E., Landfald, B., (2021). Seafloor deposition of water-based drill cuttings generates distinctive and lengthy sediment bacterial community changes. Marine Pollution Bulletin 164, 111987. https://doi.org/10.1016/j.marpolbul.2021.111987

NPD (2019). Resource report Discoveries and Fields 2019. Norwegian Petroleum Directorate. ISBN-978-82-7257-294-4.

NPD (2020). Resource Report Exploration 2020. Norwegian Petroleum Directorate. ISBN-978-82-7257-330-9.

NPD (2022a). Norwegian Petroleum Directorate. Factpages. Retrieved 20 February 2022 (https://factpages.npd.no/en)

NPD (2022b). 'Norwegian Petroleum'. Facts and Figures about Norwegian Petroleum Production. Website maintained by the Norwegian Petroleum Directorate (NPD). Retrieved 20 February 2022. (https://www.norskpetroleum.no/en//)

Oil & Gas Journal (2020). Hammerfest LNG plant shut down upon report of fire, Sept. 28, 2020, Retrieved 20 March 2022 (https://ogj.com)

Sivle, L.D., Vereide, E.H., De Jong, K., Forland, T.N., Dalen, J., Wehde, H. (2021). Effects of Sound from Seismic Surveys on Fish Reproduction, the Management Case from Norway. Journal of Marine Science and Engineering 9, 436. https://doi.org/10.3390/jmse9040436

Sivle, L.D., Forland, T.N., de Jong, K., Pedersen, G., Kutti, T., McQueen, K., Zhang, G., Wehde, H., Grimsbø, E. (2022). Havforskningsinsituttets rådgivning for menneskeskapt støy i havet-Kunnskapsgrunnlag, vurderinger og råd for 2022/ Advice from the Institute of Marine Research on anthropogenic noise in the sea. Rapport fra havforskningen 2022-1.86 pp. Retrieved 5 March 2022 (https://www.hi.no/en/hi/nettrapporter).

Robertson, F., W. Koski, T. Thomas, W. Richardson, B. Würsig, and A. Trites. (2013). Seismic operations have variable effects on dive-cycle behavior of bowhead whales in the Beaufort Sea. Endangered Species Research 21:143-160. https://doi.org/10.3354/esr00515

Slabbekoorn, H., J. Dalen, D. Haan, H. V. Winter, C. Radford, M. A. Ainslie, K. D. Heaney, T. Kooten, L. Thomas, and J. Harwood. (2019). Population-level consequences of seismic surveys on fishes: An interdisciplinary challenge. Fish and Fisheries 20:653-685.10.1111/faf.12367

Interactions, drivers and pressures

By Bjarte Bogstad (IMR), Dmitri Prozorkevich (PINRO), Andrey Dolgov (PINRO), Georg Skaret (IMR), Irina Prokopchuk (PINRO), Padmini Dalpadado (IMR), Aleksandr Benzik (PINRO), Anna Gordeeva (PINRO), Johanna Fall (IMR)

Feeding data for capelin and polar cod could not be updated before this year's WGIBAR meeting, thus there are only minor updates of the diet information. For cod some updates including 2021 data were available, also estimates of historic consumption by cod are changed since last year due to updates in the cod assessment. Several papers on diet studies for these species will be presented at the 19th Norwegian-Russian symposium in Tromsø in June 2022.

Feeding and growth of capelin and polar cod

Capelin

Fourteen years (2006–2019) of capelin diet were examined from the Barents Sea where capelin is a key species both as a prey and predator. The PINRO/IMR mesozooplankton distribution usually shows low plankton biomass in the central Barents Sea, most likely due to predation pressure from capelin and other pelagic fish. This pattern was also observed during 2017 to 2020. In the Barents Sea, a pronounced shift in the diet from smaller (<14 cm) to larger capelin (≥14 cm) is observed. With increasing size, capelin shift their diet from predominantly copepods to euphausiids, (mostly *Thysanoessa inermis* - not shown), with euphausiids being the largest contributor to the diet weight in most years (Figure A5.162). However, in 2019 the portion of copepods slightly increased compared to 2018, while the portion of euphausiids somewhat decreased. Hyperiid amphipods contributed a small amount to the diet of capelin (4% on the average). The stomach fullness is the highest in the central and northern areas of the Barents Sea (Fig A5.163), where the capelin concentrations usually are the highest. The TFI values in 2019 were somewhat higher than in the two preceding years.

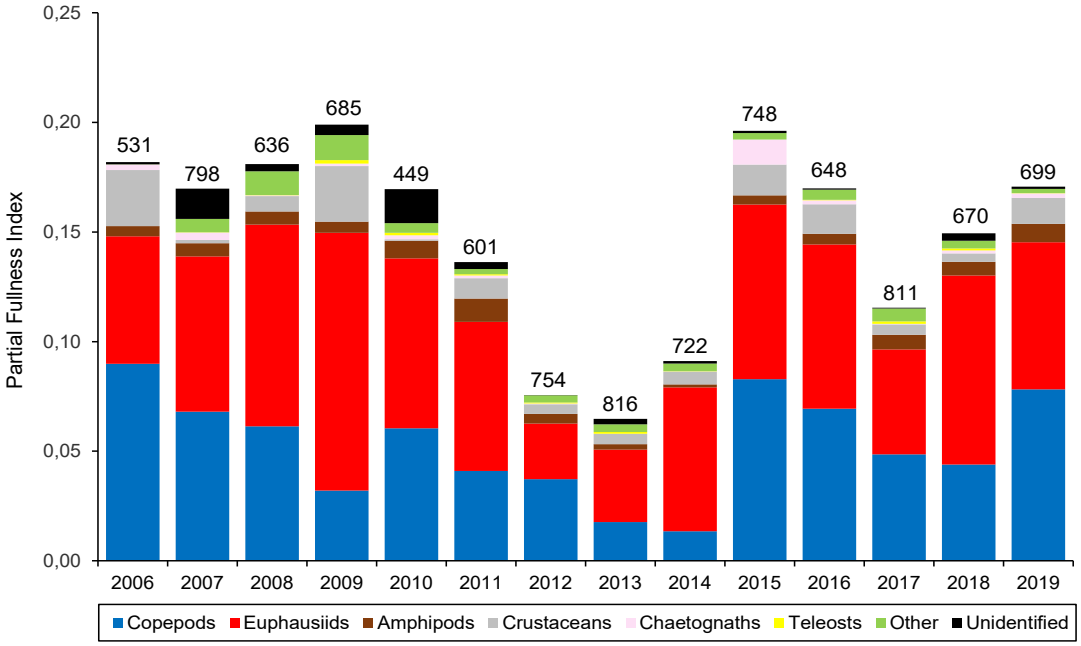

Figure A5.162: Stomach fullness (PFI, Lilly and Fleming 1981) of capelin during the BESS survey in August–September 2006–2019. Number of fish sampled in each year is indicated on top of the bars.

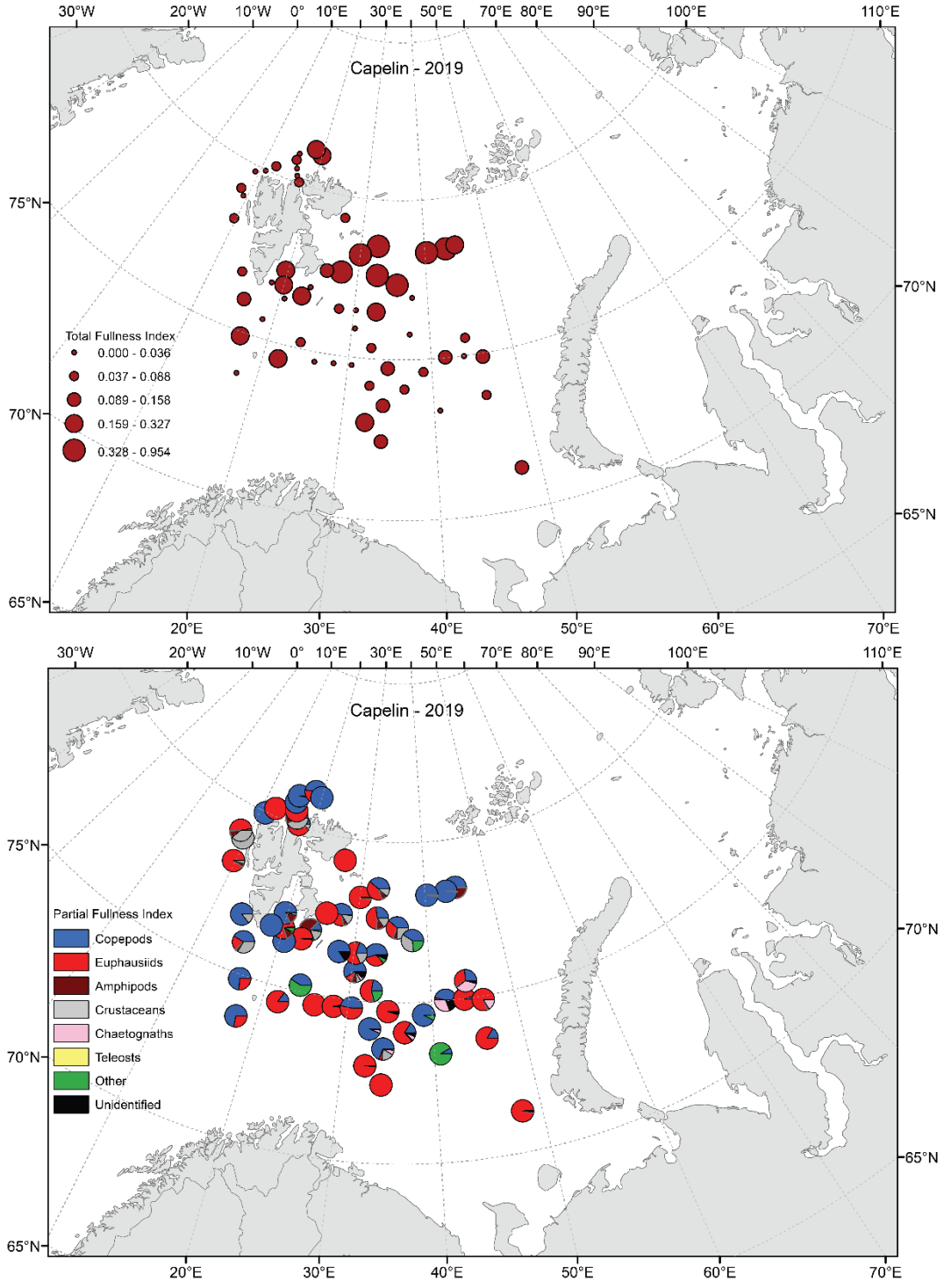

Figure A5.163: Geographic distribution of Total Fullness Index (TFI, Lilly and Fleming 1981) and PFI for capelin, in 2019.

Capelin growth decreased from 2009 onwards in a way similar to earlier periods of relatively high capelin abundance (1990–1992, 1998–2002) (Figure A5.164). There was a corresponding decrease in stomach fullness of capelin from 2009 onwards. These trends were reversed in 2014; both weight-at-age and stomach fullness were at high levels until 2019/2020 but capelin weight at age 2 decreased considerably in 2021 due to density-dependent growth (Figure A5.166).

The decrease in individual growth rate and condition of capelin observed before 2014 for the large capelin stock may have been caused by reduced food availability linked to strong grazing on the largest planktonic organisms; as suggested by reduction of the largest size fraction (>2

mm) in the Norwegian zone during the autumn survey (see section above about Zooplankton). Plankton species composition in the northeastern area has changed. Large calanoid copepods, *Calanus finmarchicus* and *C. glacialis* are important prey items for capelin. Abundance and biomass of boreal *C. finmarchicus* and arctic *C. glacialis* have increased since 2015 providing favourable conditions for capelin feeding. Small copepods *Pseudocalanus* spp. are one of the most numerous copepods species in the Barents Sea. However, this copepod is not consumed by capelin, likely due to its small size (approximately 2.5 times smaller than *C. finmarchicus*), though its abundance had been increased up to 2018 and stayed at high level in 2019.

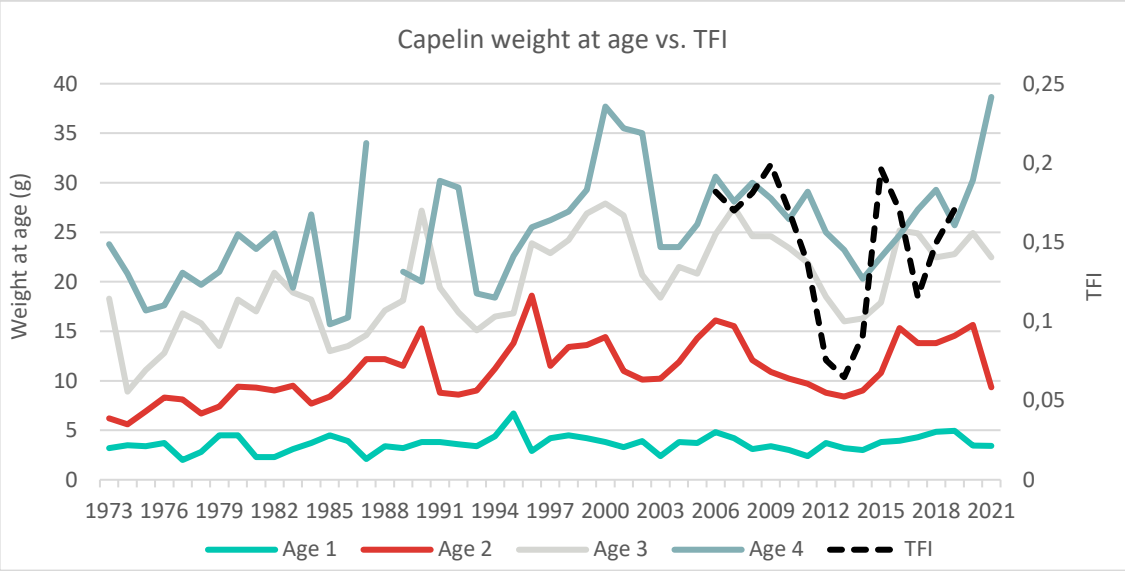

Figure A5.164: Growth (weight at age from ecosystem survey) and stomach fullness (TFI) of capelin in 1973–2021.

Capelin growth depends on the state of the plankton community (Skjoldal *et al.*, 1992; Dalpadado *et al.*, 2002; Orlova *et al.*, 2010). Capelin produces a strong feedback mechanism on zooplankton stock levels through predation (Figure A5.165, Dalpadado *et al.*, 2003; Stige *et al.*, 2014); it has been found to be particularly pronounced for krill in the central Barents Sea (Dalpadado and Skjoldal, 1996).

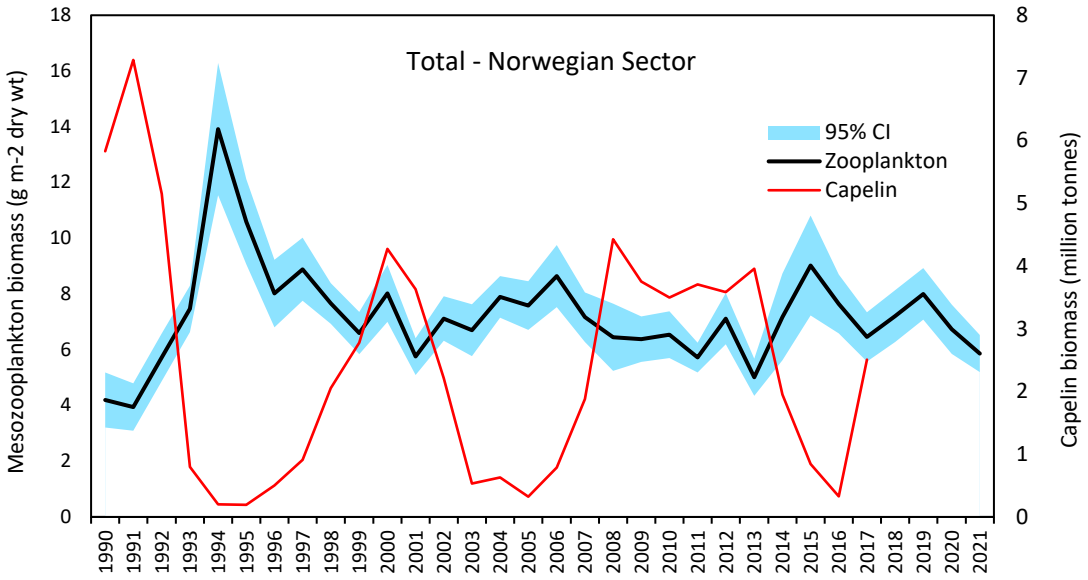

Figure A5.165. Fluctuation of capelin stock and zooplankton biomass in the Barents Sea in 1984–2021.

There is evidence of a density-dependent effect on capelin growth. This is reflected in decreasing length of individual capelin (2- and 3-year-olds) with increasing capelin abundance (Figure A5.166). The 2021 observation for age 2 (red dot) corresponds well with the general pattern of density-dependent growth for this age group.

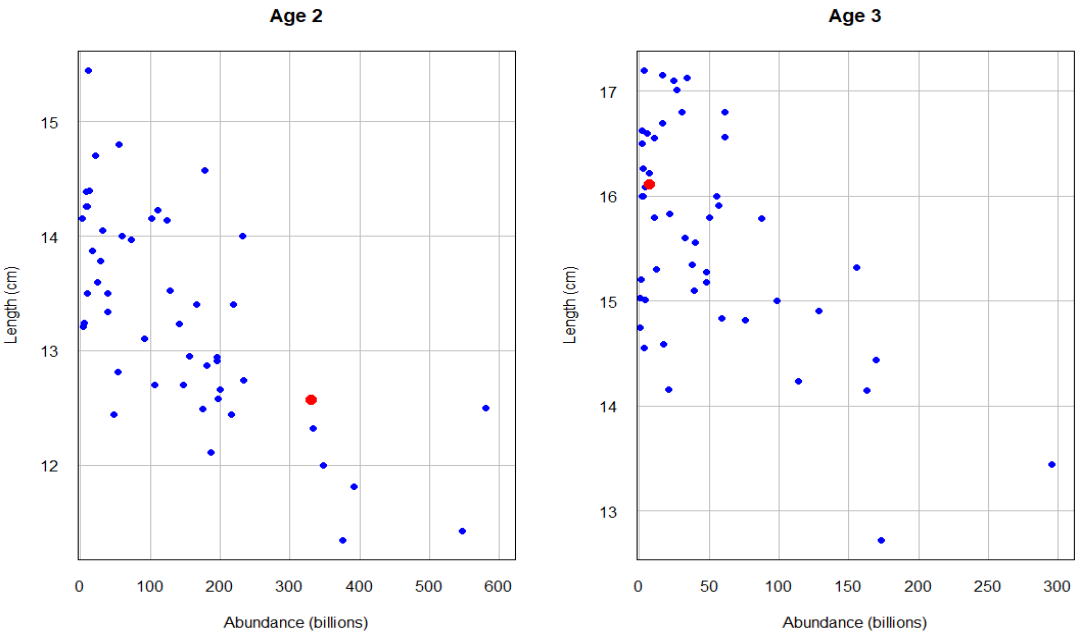

Figure A5.166: Average length as function of abundance for capelin at age 2 and 3. Red dots: 2021 observations.

Polar cod

Diet data from 2007 to 2019 indicate that polar cod mainly feed on copepods, amphipods (mainly hyperiids *Themisto libellula* and occasionally gammarids), euphausiids, and other invertebrates (to a lesser degree) (Figure A5.167). Large polar cod also prey on fish. The total stomach fullness

index decreased after 2011 and was at a fairly low level in 2012 to 2015; the index increased again in 2016 to the highest level measured in this 10-year time-series and remained relatively high in 2017 to 2019 (Figure A5.168). In 2019, the portion of copepods and euphausiids slightly increased, compared to 2018. Despite increased number of *Themisto libellula* in the Barents Sea in 2019, the portion of amphipods in polar cod diet slightly decreased compared to 2018.

The growth rate of polar cod was low for age 3 and intermediate for ages 1–2 in 2016 to 2018 (Figure A5.169) and, thus, does not reflect the increase in stomach fullness from the 2012–2015 to the 2016–2018 period. It should be noted that spatial coverage for polar cod is incomplete during most years of the BESS; thus, growth and stomach fullness data may not reflect the status of the entire population. The stomach fullness was the highest north of Spitsbergen and in the northern Barents Sea. The higher proportion stomach filling (high TFI) in the diet specially in 2018 but also in 2019, compared to 2017 may reflect the high abundances of *Themisto libellula* in the east Svalbard region.

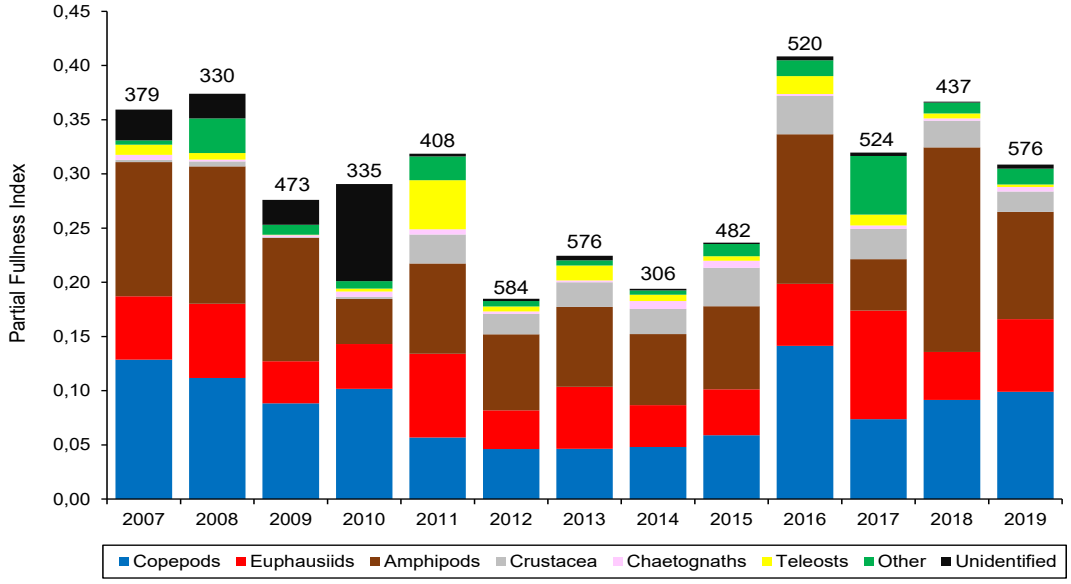

Figure A5.167: Stomach fullness (PFI) of polar cod during the BESS survey in August–September 2007–2019. Number of fish sampled in each year is indicated on top of the bars.

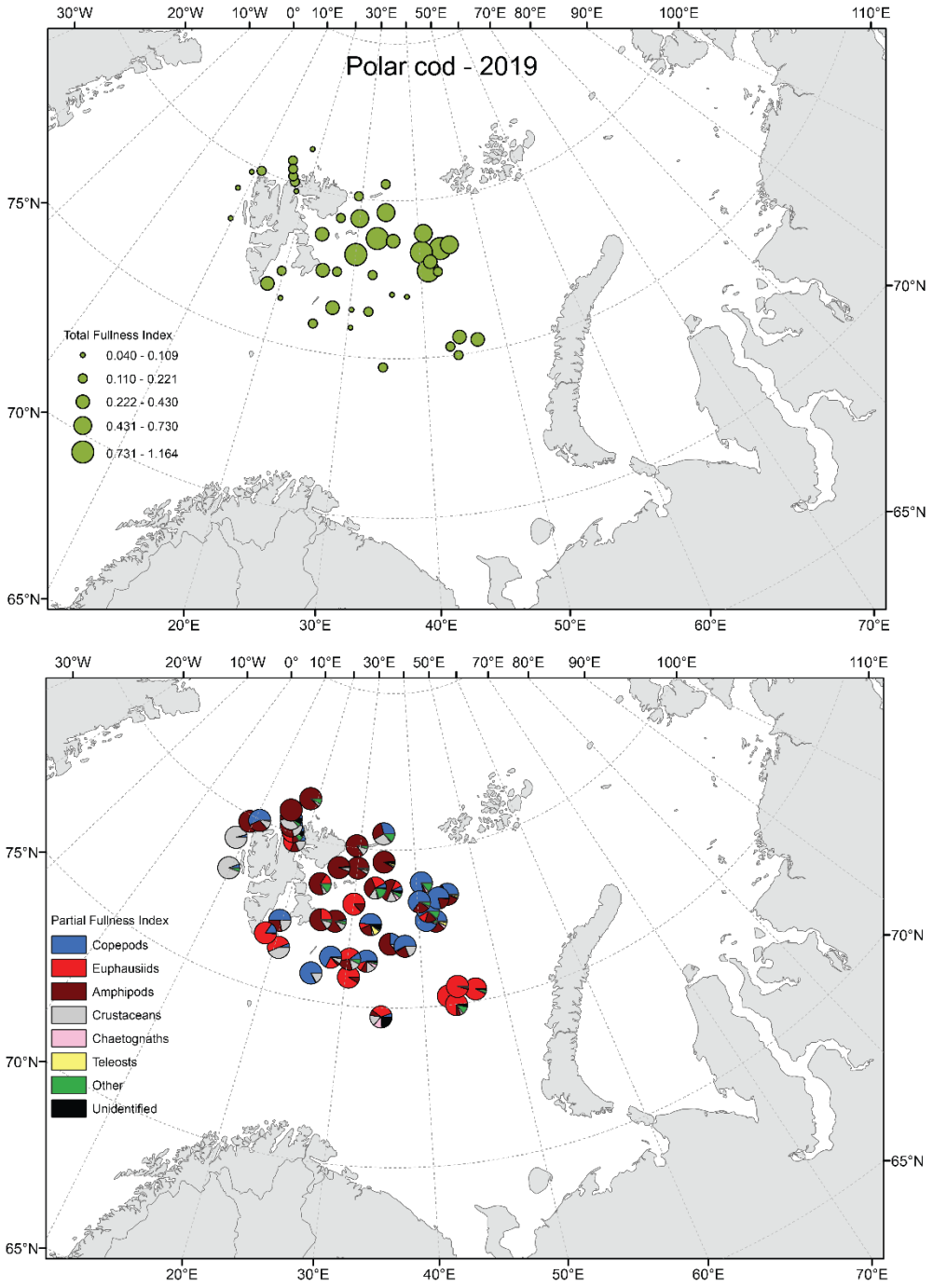

Figure A5.168: Geographic distribution of Total Fullness Index (TFI) and Partial Fullness Index (PFI) for polar cod in 2019.

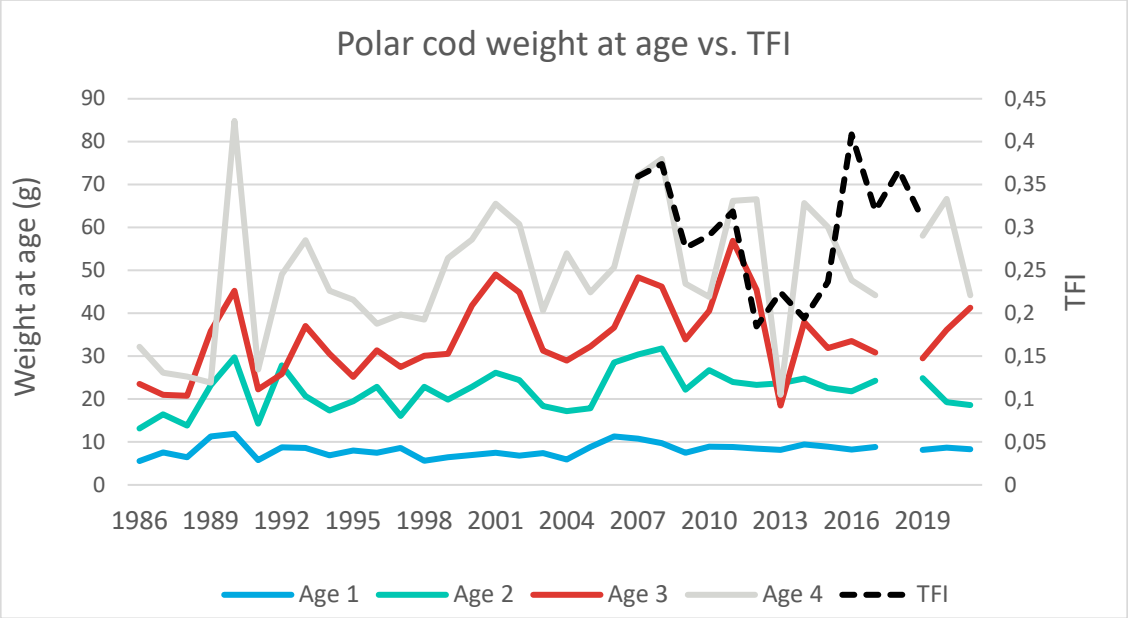

Figure A5.169: Growth (weight at age from ecosystem survey) and stomach fullness (TFI) of polar cod in 1986 to 2021.

Feeding, growth, and maturation of cod

Feeding

Figures A5.170 and A5.171 show the consumption and diet composition of cod.

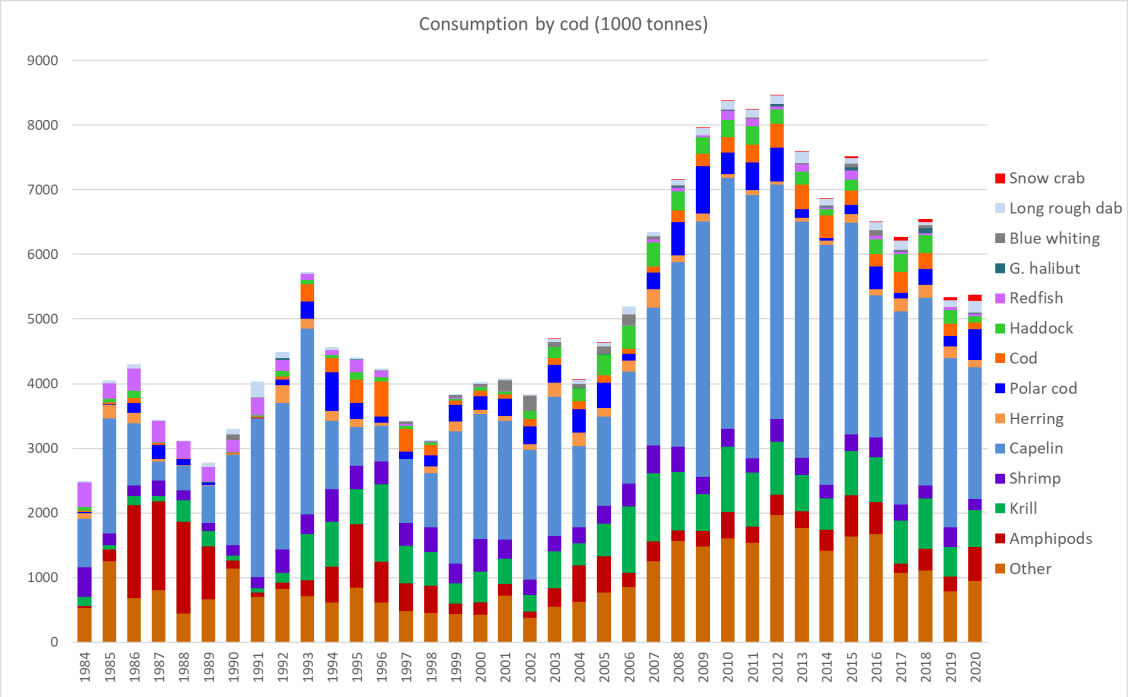

Figure A5.170: Cod consumption 1984 to 2020. Consumption by mature cod outside the Barents Sea (3 months during first half of year) not included. Norwegian calculations, from AFWG 2021.

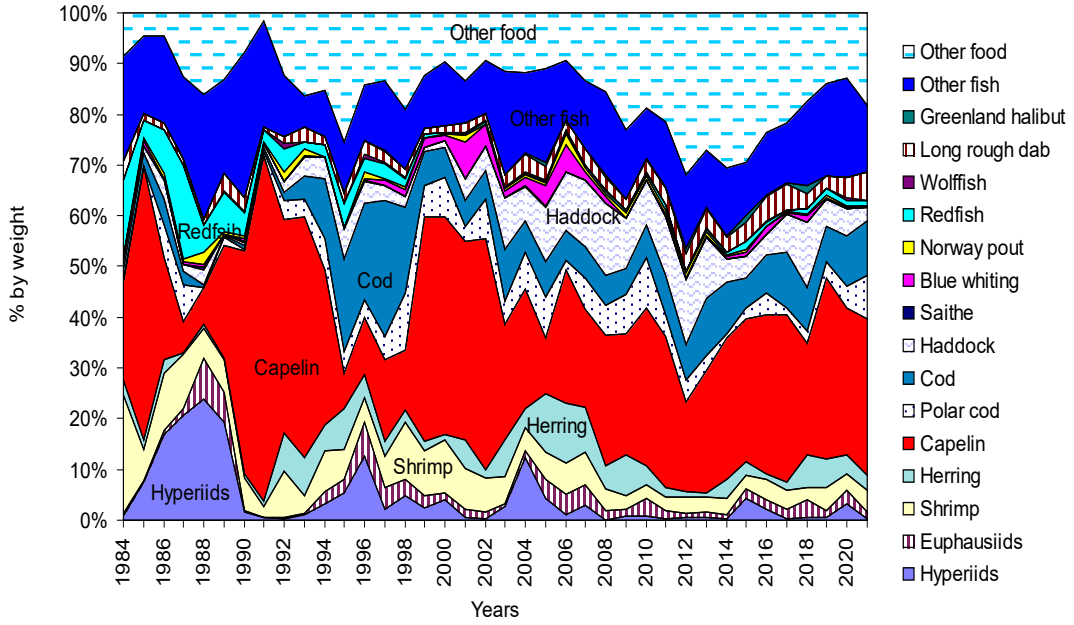

Figure A5.171: Cod stomach content composition in the Barents Sea in 1984 to 2021, by weight (aggregated over all size groups).

Cod is the major predator on capelin; although other fish species, seabirds and marine mammals are also important predators. The cod stock abundance in the Barents Sea peaked around 2013 and have declined since, although it is still above the long term average. The cod spawning stock and thus the abundance of old, large fish is still relatively high. Estimated biomass of capelin consumed by cod in recent years has been close and in some years above the biomass of the entire capelin stock (Figure A5.172). Abundance levels of predators other than cod are also high and, to our knowledge, stable.

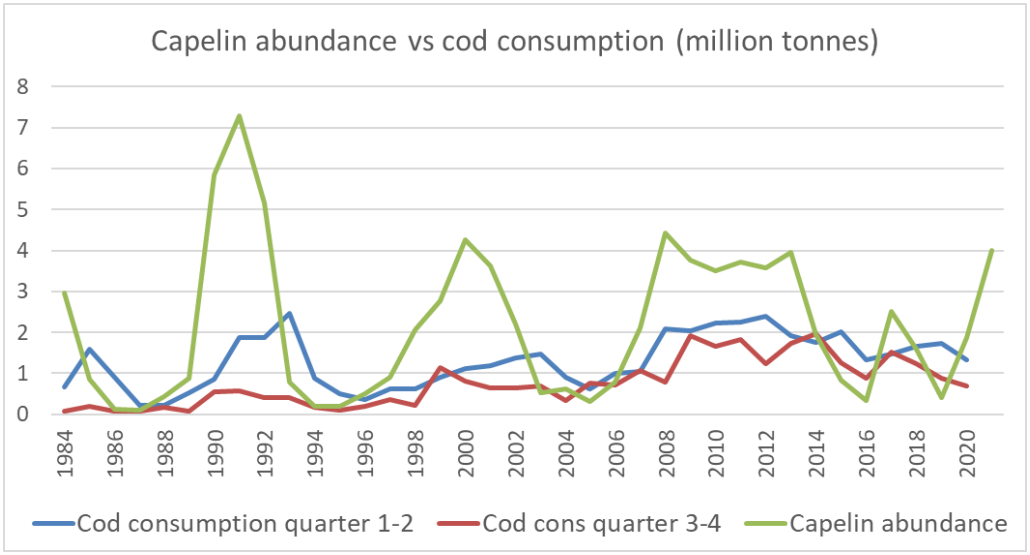

Figure A5.172: Size of the capelin stock and estimated consumption of capelin by cod. Note that the capelin biomass is estimated in September and may not be representative for the biomass available for cod during the year when year-to-year variability is high.

Estimated consumption of capelin by cod during first and second parts of the year has indicated different temporal patterns. Consumption during the 1st and 2nd quarters has been high during earlier periods and includes consumption during the spawning period, and during spring and early summer prior to seasonal capelin feeding migrations. From 2009 onwards, however, a

major difference has been the pronounced increase to a much higher level of consumption in the 3rd and 4th quarters (Figure A5.172). This reflects the northward movement of cod stock, and a larger spatial overlap between cod and capelin under the recent warm conditions. A declining trend is seen in the last years, which may be due to both a lower capelin stock and the northern limit of cod distribution moving southwards (see the section above about Zoogeographical groups of non-commercial species).

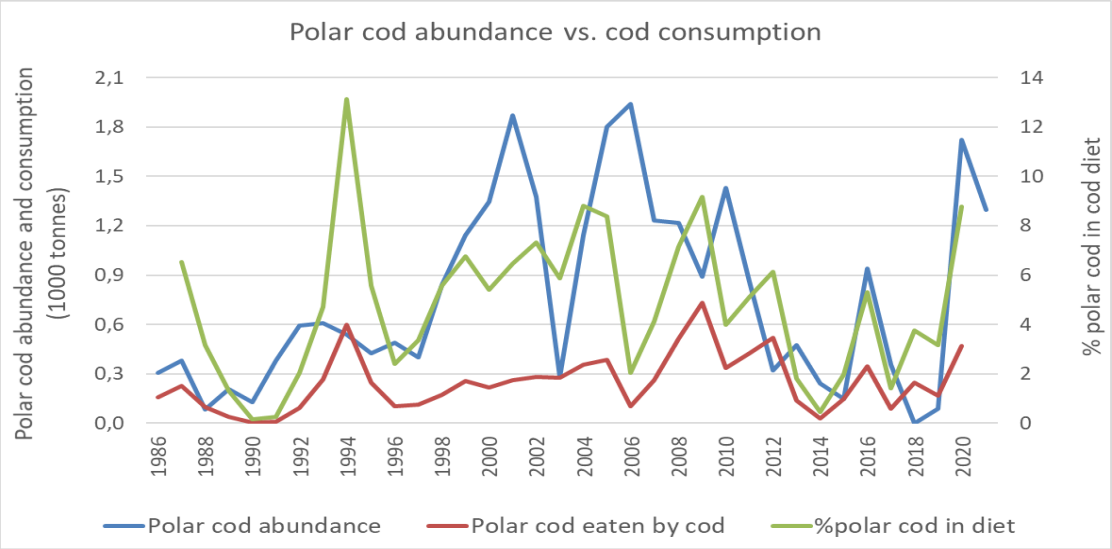

Figure A5.173: Acoustic estimates of polar cod compared to consumption of polar cod by cod and % of polar cod in cod diet, 1986–2020.

Figure A5.173 shows that there generally is a reasonable correspondence between the proportion of polar cod in the cod diet and acoustic estimates of polar cod.

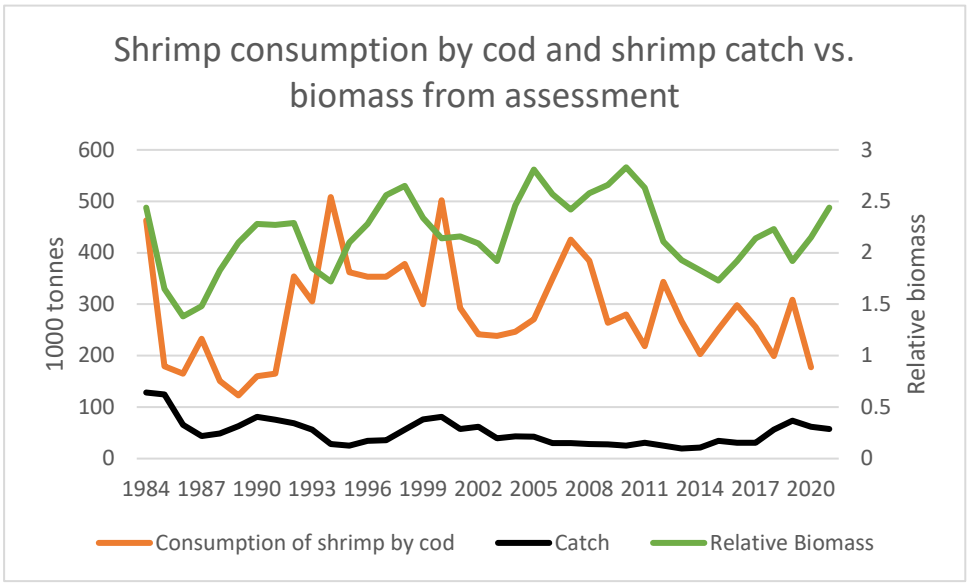

Figure A5.174: Shrimp consumption by cod and shrimp catch vs. biomass estimates of shrimp (ICES NIPAG 2021).

The estimated biomass of shrimp in the Barents Sea has increased in recent years. The trends in shrimp biomass are to some extent reflected in the cod diet (Figure A5.174). Note that the proportion of shrimp in the cod diet in 2019 was the highest since 2007.

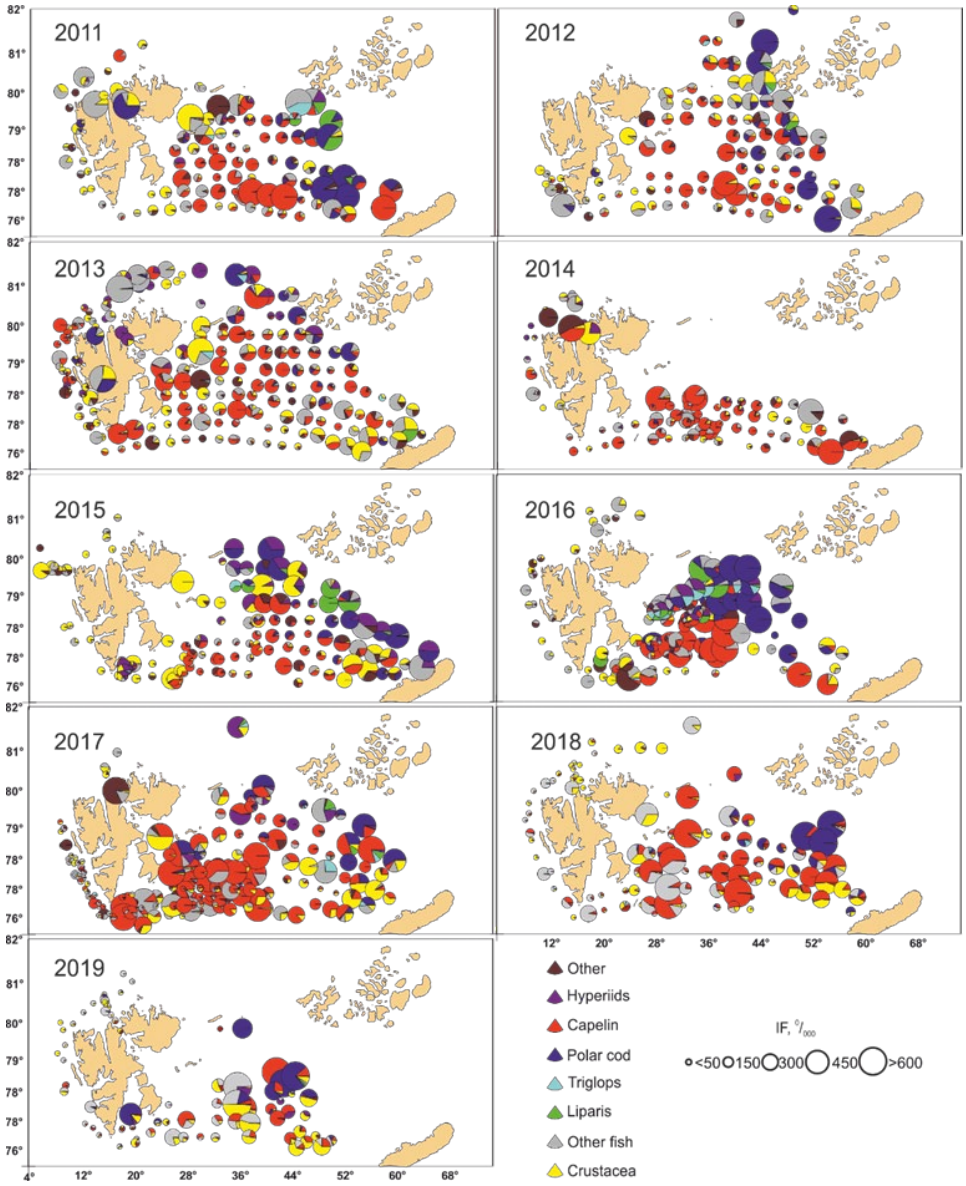

Figure A5.175. Cod diet composition in the northern part of the Barents Sea during the ecosystem survey in August–September 2011–2019. Red dots indicate capelin, and blue dots polar cod.

Capelin is the main prey item for cod. High or low stock biomass of capelin affect the biological state of cod.

During the first capelin collapse (1985–1989) the importance of capelin in cod diet decreased from 53% in 1985 to 20–22% (maximum) for the remainder of the collapse period. During that period, an increase of other prey was observed; in particular, hyperiids which constituted 7 to 23% of the capelin diet and redfish which constituted 3 to 18%.

During the second capelin collapse (1993–1997), the proportion (by weight) of capelin in the cod diet was high during the first 2 years (47% and 30%), followed by a decreased to 6 to 16%. During this period, cannibalism in cod increased sharply from 4–11% to 18–26% of the diet. In addition, more intensive consumption of hyperiids was observed (1–12%), but the proportion of hyperiids consumed was still much lower than during the first collapse.

During the third capelin collapse (2003–2006), consumption of capelin by cod was rather high (10–26%). Several alternative prey groups were present in the cod diet in similar quantities: juvenile haddock (6–11%) and cod (5–10%); herring (3–11%); blue whiting (1–5%); and hyperiids

(1–12%). Consumption of capelin by cod during the most recent years has remained somewhat stable (17–31%) but has been much lower than during earlier periods of high capelin abundance (average 36–51%). In recent years, a relatively diverse cod diet has been recorded: with stable high consumption of juvenile cod and haddock (6–11 and 5–11%, respectively); other fish species (11–15%); and other food types (21–33%) (mainly ctenophores and crabs).

Investigations of cod diet in the area north of 76°N showed different types of feeding intensity in three different local areas (Dolgov and Benzik, 2014). Cod feeding intensity was low (149–169 ‰) in areas near western and southern Spitsbergen — where cod feed on non-commercial fish. Other local areas were characterized by high feeding intensity (MFI 214-251-169 ‰) with capelin as dominant; non-target species (snailfish and sculpins), polar cod, and hyperiids were also consumed. These two are traditional areas of cod distribution during summer. The third area (Franz Josef Land, northern Novaya Zemlya, and adjacent areas) has become available habitat for cod only since 2008; in this area, cod (MFI 284-340 ‰) feed intensively on polar cod and capelin. Northward expansion of cod distribution, and their movement into northeastern Barents Sea results in better feeding conditions for cod under their high stock biomass and decreasing of main prey (capelin and polar cod). However, cod intensively fed on capelin and polar cod in 2015 to 2018 despite their low stocks (Figure A5.175). In 2019, consumption of these important prey was much lower and occurred in rather restricted areas in the northern Barents Sea compared to previous years.

In addition, some new prey items have recently appeared in the cod diet. The non-indigenous snow crab (*Chionoecetes opilio*) has become a rather important prey item for cod, especially in for large cod in the eastern Barents Sea alongside Novaya Zemlya (Dolgov and Benzik, 2016, Holt *et al.*, 2021). The percentage (by weight) of snow crab in the cod diet sharply increased from 2014 onwards (Figure A5.176). In contrast, two other non-indigenous crab species (red king crab and deep-water crab *Geryon trispinosus*) have not become more important in the cod diet. The difference is probably related to higher overlap between cod and snow crab, and more appropriate body shape and size of snow crab than the other crab species as prey for cod.

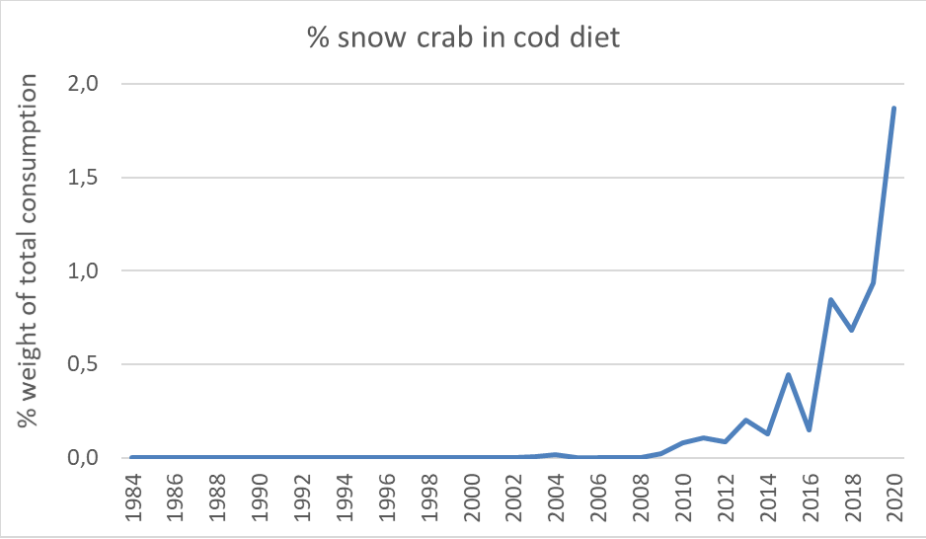

Figure A5.176. Importance of snow crab in cod diet (% weight of total consumption) in 1984 to 2020. Based on Norwegian consumption calculations.

Weight at age for young cod as measured from the winter survey has decreased in recent years (Figure A5.177) and was in 2021 the lowest observed or very close to that for age groups 3–7. The decreasing trend in growth seems to have been halted now, however. Concerning consumption, the biggest decrease in per capita consumption was observed for age 2 and this corresponds well

to the decrease in growth from age 2 to 3 as measured from the winter survey (Figure A5.178). Maturity-at-age for cod decreased considerably in 2015 to 2016 but then increased again. The 2021 values are however somewhat below the level observed in 2000 to 2010 (Figure A5.179).

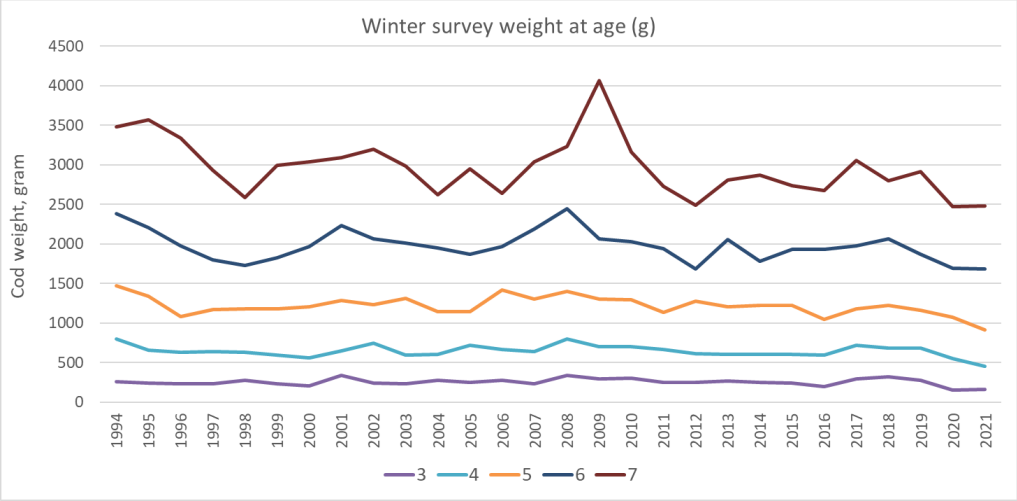

Figure A5.177: Cod weight at age 3-7 as calculated from the winter survey, for 1994 to 2021.

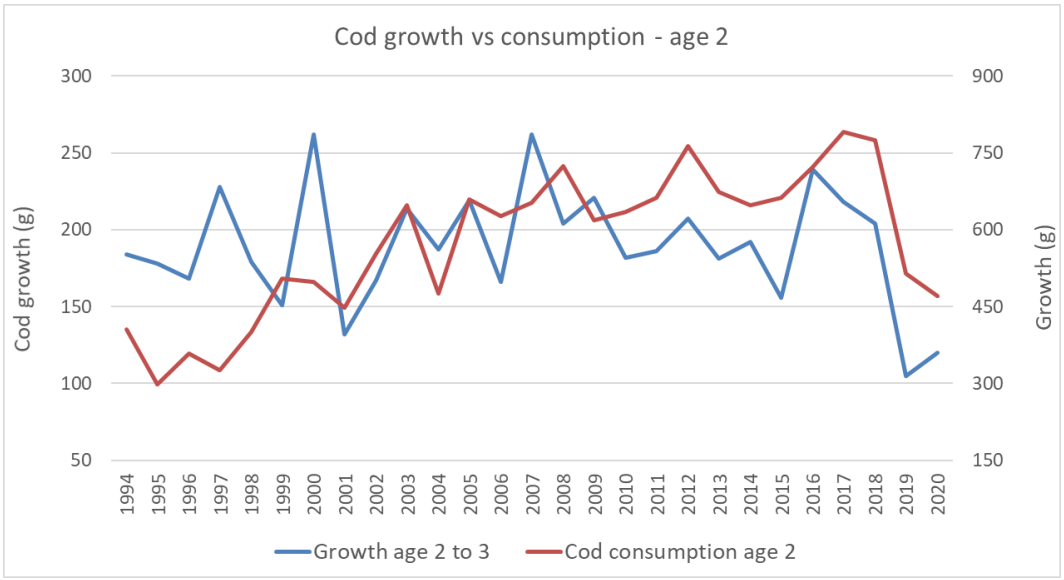

Figure A5.178: Cod consumption at age 2vs.growth from age 2 to 3.

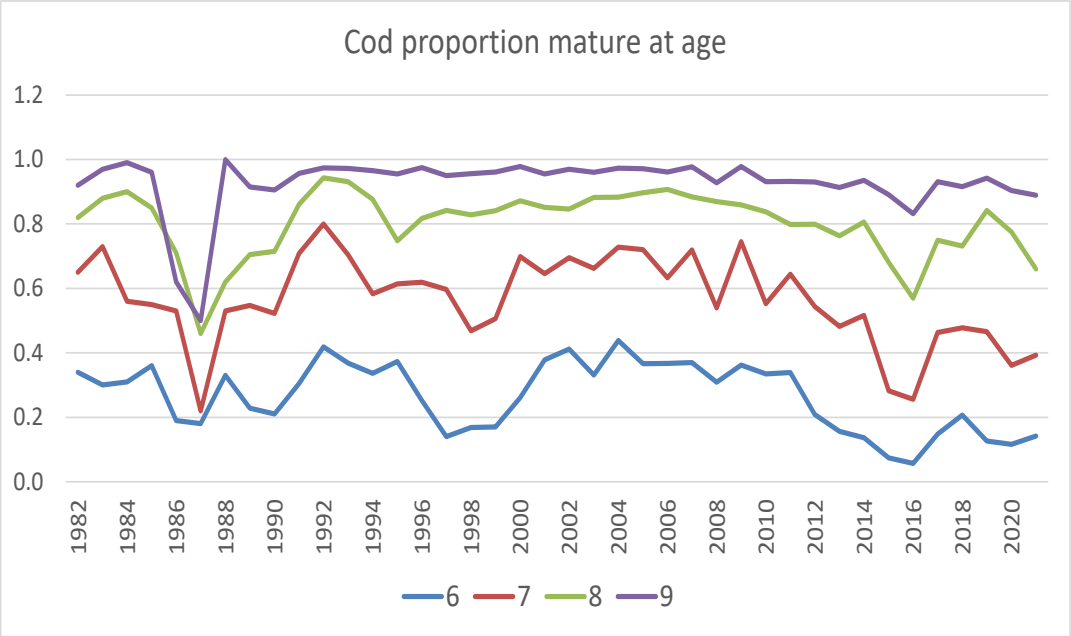

Figure A5.179: Maturity-at-age for cod ages 6-9 (ICES 2021).

Causes of capelin stock fluctuations

Stock size fluctuations

The Barents Sea capelin has undergone dramatic changes in stock size over the last four decades. Three major stock collapses (when abundance was low for several years and fishing moratoriums imposed) occurred during 1985–1989, 1993–1997, and 2003–2006. During the recent period 2014–2020 the stock size has fluctuated considerably. A rapid decline in stock size was recorded from 2014 and in 2015 to 2016 the total stock size was below 1 million tonnes. The capelin stock size estimate from 2016, however, must be considered an underestimate (Skaret *et al.*, 2019). Stock size again increased in 2017. The 0-group abundance in 2019 was record high, which was confirmed by high abundances of 1-year-olds in 2020 and 2-year-olds in 2021. The 2020 year class was also above average, so the abundance of capelin in autumn 2021 was the highest since 2008 and mostly consisting of 1 and 2-year-olds.

Previous capelin collapses have had serious effects cascading both upwards and downwards in the foodweb. Reduced predation pressure from capelin has led to increased amounts of zooplankton during periods of capelin collapse. When capelin biomass was drastically reduced, its predators were affected in various ways. Cannibalism became more prominent in the cod stock, cod growth was reduced, and maturation delayed. Seabirds experienced increased rates of mortality, and total recruitment failures; breeding colonies were abandoned for several years. Harp seals experienced food shortages, and recruitment failure, and increased mortality; partly because they invaded coastal areas and were caught in fishing gear. The effects were most serious during the 1985 to 1989 collapse, whereas the effects could hardly be traced during the third collapse. Gjøsæter *et al.* (2009) concluded that these differences in effect likely resulted from increased availability of alternative food sources during the second and third collapses (1990s and 2000s). It is too early to draw firm conclusions about cascading effects related to the "mini-collapses" observed recently, since it may take some years before lagged effects are observable.

The capelin stock collapses were caused by poor recruitment, most likely in combination with low growth and increased predation pressure. It is likely that high levels of fishing pressure during 1985 to 1986 amplified and prolonged the first collapse. After each collapse, the fishery has been closed and the stock has recovered within a few years due to good recruitment. Several authors have suggested that predation by young herring on capelin larvae has had a strong negative influence on capelin recruitment and, thus, has been a significant factor contributing to these capelin collapses (Gjøsæter *et al.*, 2016), while others (Dolgov *et al.*, 2019) claim that other reasons for the periodic recruitment failures could be more important.

Recruitment of capelin

Capelin is a short-lived species and thus the stock size variation is strongly influenced by the annual recruitment variability (Figure A5.180). There was a better correspondence between the abundance of 0-group and one-year-olds in the first half of the time period where both estimates are available. It should be noted that estimates of the abundance of the 0-group are carried out by the swept method and have a large uncertainty for small year classes. In recent years, very high but fluctuating estimates of 0-group were obtained and the mortality from age 0 to age 1 has seemingly increased (Figure A5.181). Especially the year classes 1985, 2008, 2015–2016 and 2018 were heavily reduced in size from the 0-group to the 1-group stage. While the three first capelin stock collapses were initiated by increased mortality at the early larval stage, between the larval survey in May-June and the 0-group survey in August, the increased mortality on young capelin in recent years is seemingly occurring later; between the 0-group survey and the acoustic measurement of the 1-year-olds. The reasons for this seemingly increased natural mortality at this stage is unknown but could likely be caused by other factors than those in effect during the collapses in the 1980s, the 1990s, and the 2000s. In 2019, a record strong year class occurred, and the 2020 year class was also strong, so there have now been two years in a row with recruitment above the long term mean.

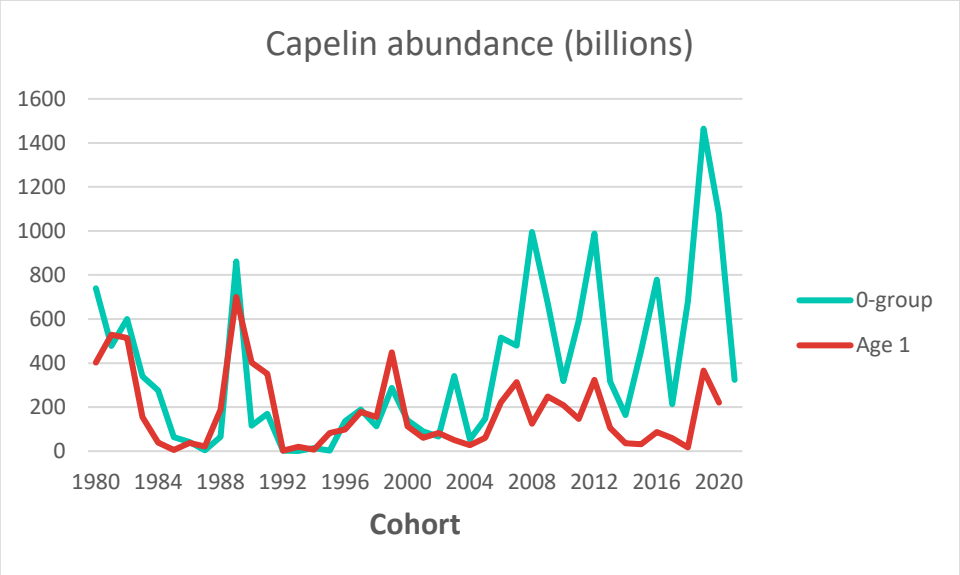

Figure A5.180: Capelin at age 0 and 1 for the year classes 1980 to 2021.

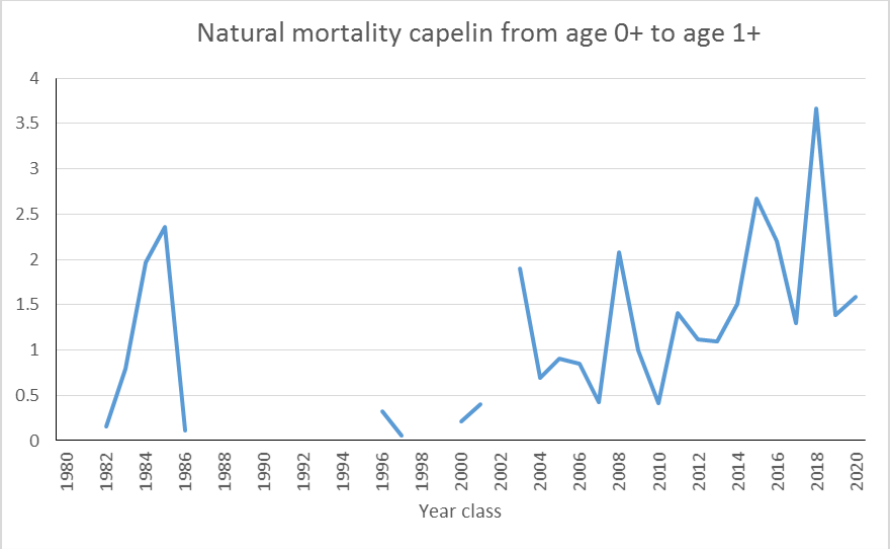

Figure A5.181: Fluctuation of capelin natural mortality from age 0 to age 1 for the year classes 1980 to 2020. The years with "negative" mortality was removed.

There is a strong positive correlation between first year growth of capelin and recruitment (Berg *et al.* 2021) (Figure A5.182). This indicates that good growth conditions in early life stages enhance survival, while the effect of density-dependent growth increases later in life.

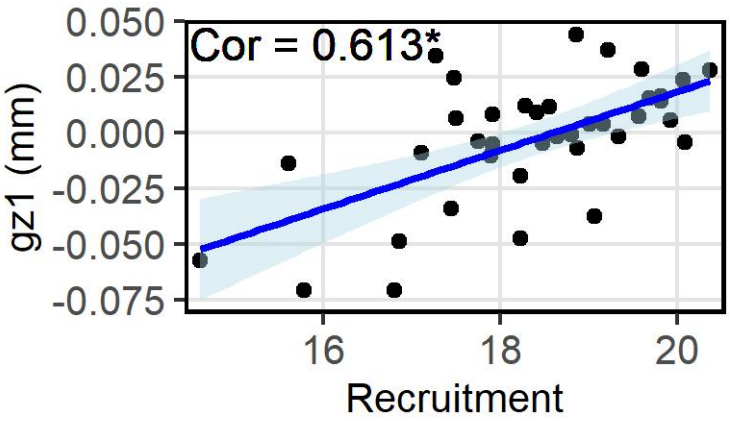

Figure A5.182: Model estimated deviation from the overall temporal trend of size of first otolith growth zone (gz1) as a function of log-transformed number of recruits (From Berg *et al.* 2021). The model used was a Bayesian hierarchical spatio-temporal model.

Figure A5.183 shows a stock–recruitment plot (updated from Gjøsæter *et al.* (2016)) for the year classes 1973 to 2020. The SSBs are those estimated by the assessment model for capelin (ICES 2021a).

The points are coloured according to the amount of young herring estimated to be in the Barents Sea in the spawning year. The amount of herring is the abundance of age 1 and age 2 herring from the assessment model times the mean weight of these age groups (ICES 2021b). The 1989-year class is the strongest year class at age 1 (700 billion). The average recruitment in the period is about 180 billion. It is seen that the recruitment in "red years" are below average recruitment in 13 out of 15 years, while in "green years" the recruitment is below average in 11 out of 18 years. In years with low numbers of young herring in the Barents Sea the recruitment is below average in 5 out of 11 years, and only when the SSB is below 100 kt. This supports the hypothesis that capelin recruitment is negatively affected in years with substantial amounts of young herring in the Barents Sea (Gjøsæter *et al.* 2016). On the other hand, the general shape of the stock–

recruitment relationship, where the highest recruitment is obtained for small to medium SSBs, points to the possibility of cannibalism or other density-dependent mortality mechanisms (Dolgov *et al.*, 2019). In any case, the large variability in recruitment clearly indicates an interplay of many factors affecting the recruitment of capelin.

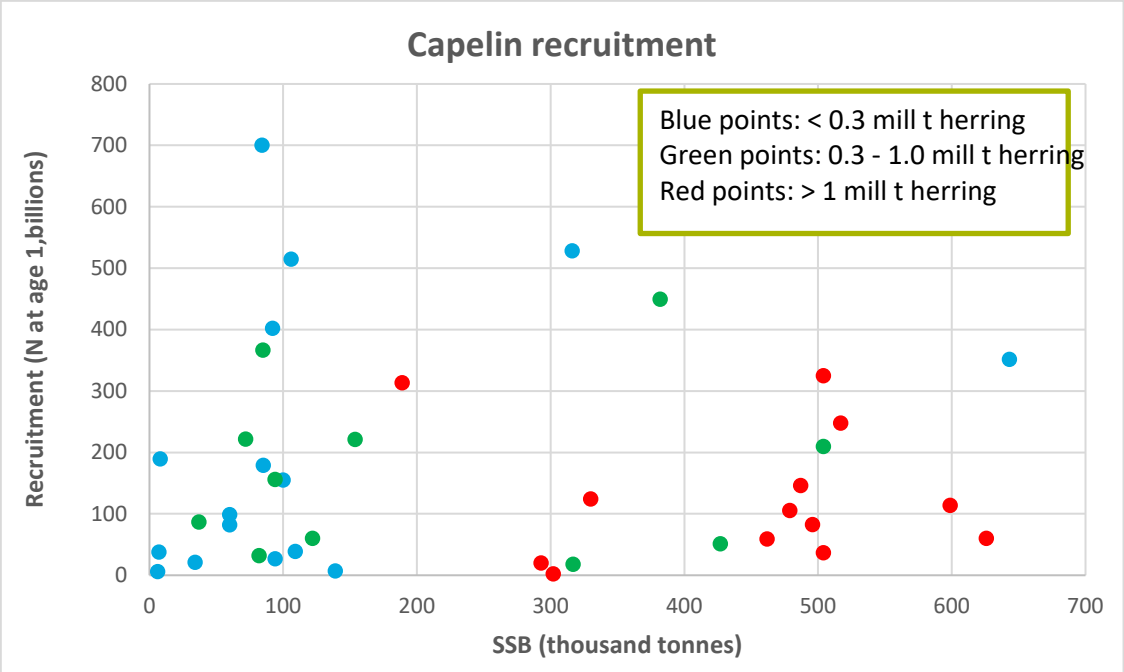

Figure A5.183: SSB/R plot for capelin. Cohorts 1981 to 2020. Points coded according to herring biomass as explained in the text. (Updated from Figure 7 in Gjøsæter *et al.* 2016).

Figure A5.184 depicts a stock-recruitment plot based on maturing stock size during autumn ½ year before spawning instead of estimated spawning stock size, and estimated number of 0-group capelin as an indicator of recruitment instead of one-year-olds.

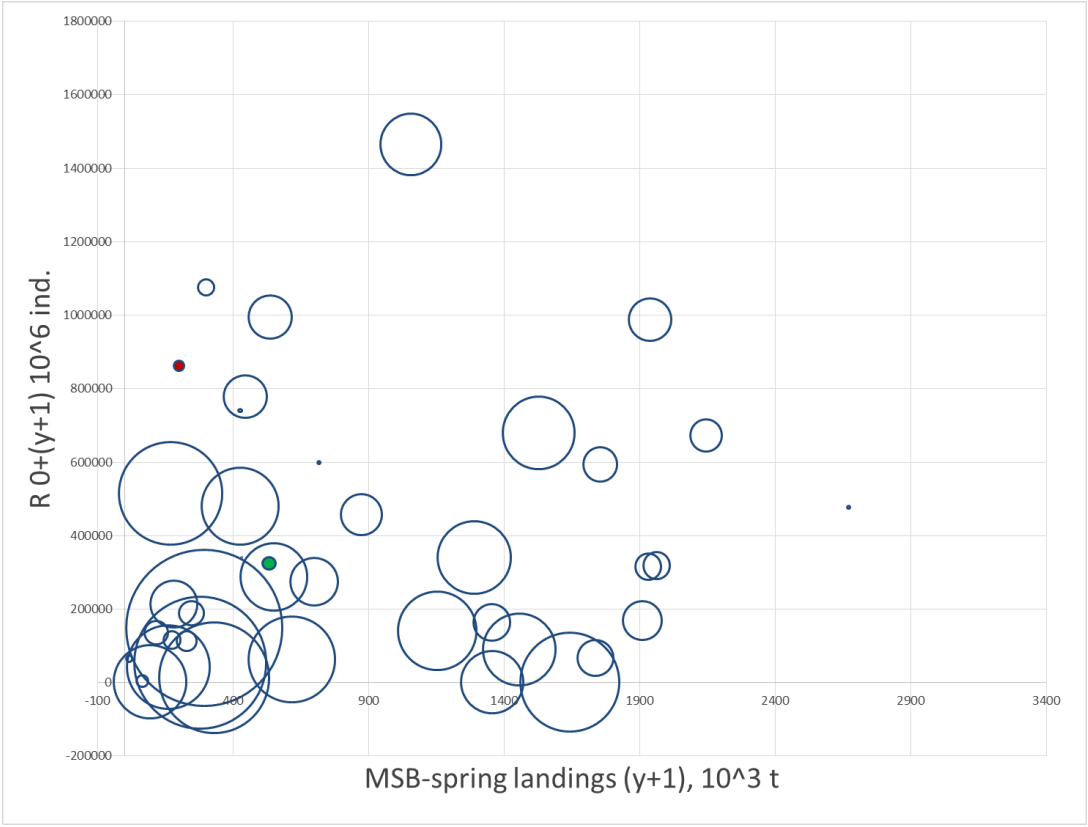

Figure A5.184: Relationship between mature stock biomass (>14 cm) with spring fishery subtracted (biomass at 1 Oct. Y, total landings from 1 January to 1 April. Y+1 are subtracted, 1000 tonnes) and 0-group index in millions (Y+1), covering the cohorts 1980 to 2021. The size of bubbles indicates the biomass of herring at age 1-3 (ICES WGIBAR data). Minimum diameter of bubble corresponds to 0.02 million tonnes of herring (1983), the maximum - 4.802 million tonnes. (2005). The red point is the 1989 cohort which is the basis for the current reference point (Blim). The green point is the 2021-year class.

Causes of polar cod stock fluctuations

The acoustic estimates of the Barents Sea polar cod stock (Figure A5.185) have been highly variable, and this is likely due to both natural variations in stock size and variable survey coverage. Consequently, the fluctuations in stock size are probably less than what is derived from the estimates of stock size.

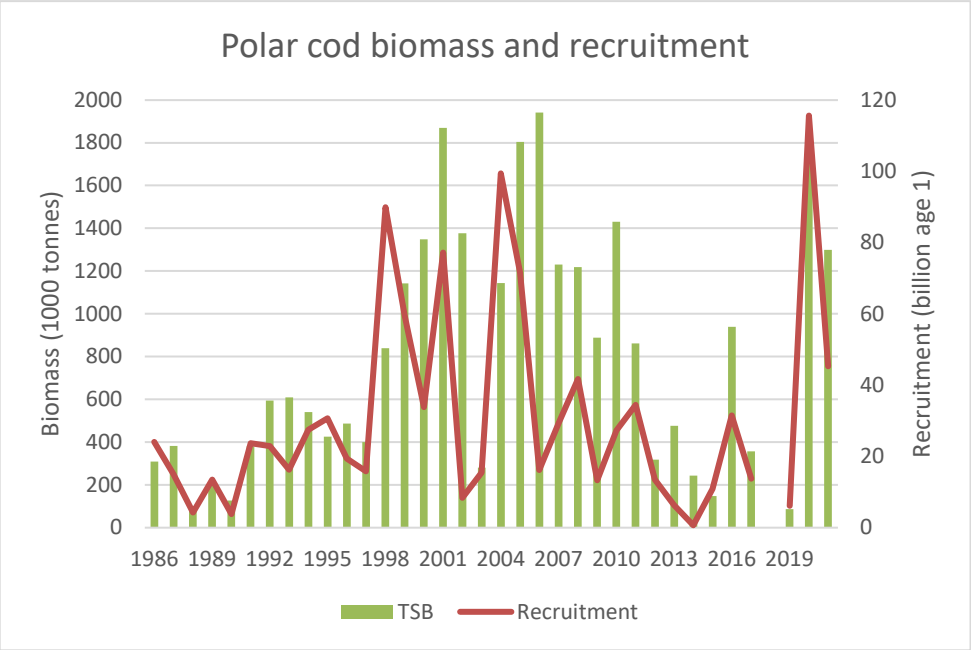

Figure A5.185: Total stock biomass and recruitment (acoustic estimate of 1-year-olds) of polar cod in the Barents Sea.

The reasons for this are unclear. Norway conducted commercial fisheries on polar cod during the 1970s; Russia has fished this stock on more-or-less a regular basis since 1970. However, the fishery has for many years been so small that it is believed to have very little impact on stock dynamics. Reasons for the stock fluctuations must therefore be sought in variable natural mortality and variable recruitment, or a variable part of the total stock may be found outside the Barents Sea.

The rate of natural mortality for this stock appears to be quite high; even in absence of fishing the total reduction in numbers from one age group to the next judged from the acoustic surveys are substantial in some years. It appears that polar cod mortality has increased in recent years, although "negative mortalities" in some years make it difficult to draw firm conclusions, as stated above. Presumably most of the natural mortality is caused by various predators. Although it is generally assumed that polar cod is a key forage species in the Arctic, and that large predatory fishes (like cod), seals, and seabirds are important consumers, not much is known about the details, like for instance who are the dominant predators on each of the polar cod age groups. Since polar cod are normally found at deeper waters as they grow older and larger, seabirds probably play a minor role in consuming larger polar cod. On the other hand, predatory demersal fish like cod, Greenland halibut, long rough dab and others probably mostly consume larger polar cod. Seals are able to feed over most depths in the Barents Sea, and polar cod is known to be a dominant prey for harp seals (Haug *et al.* 2021 and references therein). Only for cod do we have a year by year consumption estimate of polar cod, and the consumption estimates varies from less than 100 kt (in the 1980s and in 2014 and 2017) to more than 700 kt (in 2009). Preliminary analysis of cod consumption in the arctic Barents Sea in late summer shows a strong increase in cod's consumption of polar cod from the period 2004–2007 to 2008–2013, coinciding with a reduction in polar cod biomass. In the later period, the cod stock increased and expanded its distribution to the north and northeast, overlapping more with the polar cod habitat. After this period, consumption of polar cod has been reduced to similar, or slightly higher, levels as before the expansion. The consumption after 2013 has seemingly decreased somewhat in pace with the decrease in cod stock size, and the more southern distribution of cod during the feeding season. However, consumption increased in 2020 following the recruitment of the strong 2019-year class.

Since the mid-1990s, there has been a general trend of increase in both air and water temperature in the Barents Sea (see the section above about Meteorological and oceanographic conditions); record high temperatures have been recorded during the 2000s. The areal extent of sea ice coverage has never been lower than in 2016. In the Barents Sea, the area of Arctic water decreased, while a larger portion has been dominated by warmer Atlantic water. These climatic changes have likely affected the distribution and abundance of Arctic species like polar cod. It should be noted that, since 2016, the temperatures have decreased somewhat, and the ice coverage has shown an increasing trend. Nevertheless, the ice coverage in November 2020 was the smallest since 1951, that could affect spawning condition for polar cod in winter 2020/2021. At the same time, there is a lack of knowledge of the spawning area of polar cod. Previously, spawning was in the southeastern part of the Barents Sea, but in the last warm years it shifted to the southwestern part of the Kara Sea. Some spawning places have in 2013 been found in a shallow water area at 77°00′-77°30′ N 75°-80° E (Prokhorova *et al.*, 2013). How spawning places can affect polar cod recruitment and therefore stock size fluctuation is unknown.

0-group polar cod prey on small plankton organisms such as copepods and euphausiids, while adults feed mainly on large Arctic plankton organisms such as *Calanus hyperboreus* and *C. glacialis* and hyperiids. The biomass of Arctic forms of zooplankton decreased in recent years and most likely influenced negatively the feeding conditions for 0-group polar cod. However, no significant changes in the condition of adults were observed in recent years. This indicates a high degree of adaptability of this species to changes in the environment and enough available food resources.

The recruitment (Figure A5.185) has been spasmodic in recent years; mostly modest but with very strong year classes in 2014 and 2019. Less is known about recruitment mechanisms of polar cod than of capelin, but some recent studies of recruitment of polar cod (Eriksen *et al.*, 2019, Huserbråten *et al*., 2019, and Gjøsæter *et al.*, 2020) may shed some additional light on this topic.

Based on a particle tracking model, Eriksen *et al.* (2019) studied simulated drift patterns of polar cod eggs in the Svalbard area. It has been inferred from 0-group distributions that some spawning must have been taking place near Svalbard, but the location of this spawning is unknown. By releasing "eggs" several places around the Svalbard peninsula, from inner fjords to the outer coast, and letting these "eggs" drift with the currents until late summer and then compare their distribution with observed distributions of 0-group, the authors were able to backtrack the most probable spawning locations. Because there is a clockwise gyre flowing around Svalbard, they concluded that outer coastal areas both at the western, northern and eastern coasts of Svalbard would be possible spawning areas, but that spawning locations under the ice east of Svalbard was the most probable spawning area for the western component of polar cod. This finding was confirmed by similar studies carried out by Huserbråten *et al.* (2019), who expanded the particle drift experiment to many more years and included the whole Barents Sea. The data-driven biophysical model of polar cod early life stages used in the latter study predicted a strong mechanistic link between survival and variation in ice cover and temperature; ice cover was positively related to survival of polar cod eggs and larvae, while temperature was negatively related to survival. The backtracking model also suggested a northward retreat of the spawning assemblages in the eastern Barents Sea, possibly in response to warming.

Gjøsæter *et al.* (2020) used the same biophysical model to characterize the environmental and developmental properties of the early life history of individuals that reached the 0-group stage at the time and place of observations, and examined if and how ice cover, ice breakup time, maximum temperature, and spawning-stock biomass relate to modelled larval survival. Results indicate that high ice coverage has a significant positive effect and high temperature a significant negative effect on survival of eggs and larvae from an eastern spawning component. No

significant effects were found for the western spawning component, possibly because the variations in ice cover have been less noticeable there.

These recent studies support earlier findings that successful polar cod recruitment is associated with an ice cover until the eggs hatch. After hatching, however, larval survival depends on available food, which will only be available after ice break-up and onset of primary and secondary production. One may hypothesize, that ice break-up synchronizes these events, since the melting of ice and the associated stabilizing of the water column, warming of the surface layer, and deepening of the photic zone may initiate both hatching of eggs and onset of algal production.

References

Eriksen, E., M. Huserbråten, H. Gjøsæter, F. Vikebø and J. Albretsen (2019). "Polar cod eggs and larval drift pattern in the Svalbard archipelago." Polar Biology. https://doi.org/10.1007/s00300-019-02549-6

Gjøsæter, H., Huserbråten, M.B.O., Vikebø, F. and Eriksen, E.2020. Key processes regulating the early life history of Barents Sea polar cod. Polar Biology. https://doi.org/10.1007/s00300-020-02656-9

Huserbråten, M. B. O., E. Eriksen, H. Gjøsæter and F. Vikebø (2019). "Polar cod in jeopardy under the retreating Arctic sea ice." Communications Biology 2 407. https://doi.org/10.1038/s42003-019-0649-2

Cod-capelin-polar cod interaction

The interaction among cod, capelin, and polar cod is one of the key factors regulating the state of these stocks. However, this interplay is far from fully understood. Cod prey on capelin and polar cod and can strongly influence the numbers of these species, while the availability of these prey for cod varies. In addition, 0-group cod may also feed on 0-group capelin.

A prerequisite for feeding interactions is geographical overlap. The summer overlap between cod and capelin increased from 2008 to 2016, mainly due to an increasing cod stock and increased size of suitable habitat for cod. Similarly, the overlap with polar cod increased in this period. However, the northern limit of the summer cod distribution has moved southwards in recent years as the cod stock has declined, which may have been beneficial for the polar cod. The effect on cod's overlap with capelin is less clear. Figure A5.186 shows the overlap between cod and capelin from three recent BESS years with high capelin abundance and declining cod abundance: 2013, 2017 and 2021. Although cod overlaps with capelin in the north in all these years, the abundance of cod in the main capelin distribution area decreased from 2013 to 2017 and from 2017 to 2021. In general, there is low correspondence between changes in cod-capelin horizontal overlap and changes in capelin consumption in summer. The cod-capelin feeding interaction mainly takes place on the banks of the northern Barents Sea, where cod's consumption of capelin is more strongly related to vertical overlap with capelin than horizontal overlap.

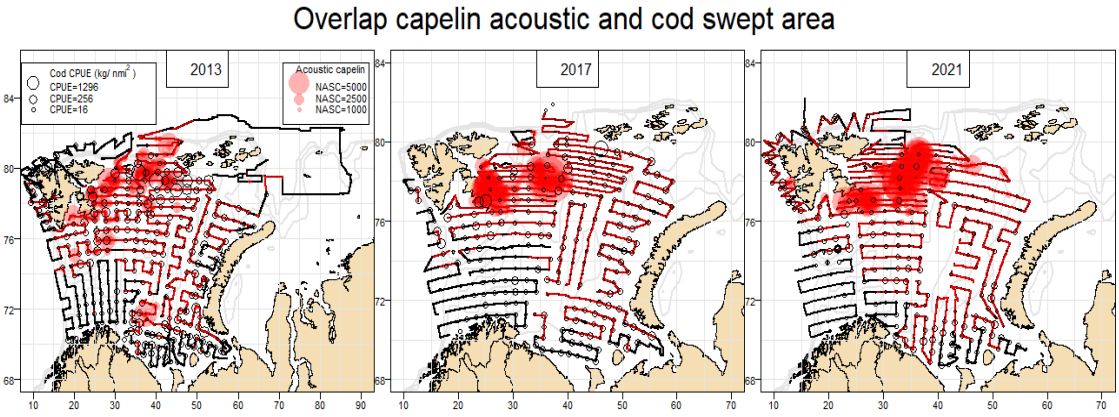

Figure A5.186: Capelin acoustic recordings overlaid with cod CPUE from BESS for three years of high capelin abundance, 2013, 2017 and 2021. The circle sizes for cod corresponds to the fourth root of CPUE (kg/nmi²) per demersal trawl station, while capelin circle sizes for capelin correspond to NASC per nautical mile. Different red colours indicate overlapping circles.

The cod-capelin overlap was relatively low in the period 2004 to 2015, suggesting a weak aggregative response of cod to capelin (Fall *et al.* 2018). However, increasing cod population size and water temperatures in this period influenced a northward shift of the late summer overlap area (Fall *et al.* 2018). The overlap between immature cod and capelin showed a rising trend, while the mature cod-capelin overlap had a less clear trend over time (Figure A5.187A). The overlap area also increased in size, particularly for immature cod, which reflects the northeastwards expansion of the cod stock. The observed increased overlap over time could be interpreted as facilitating increased consumption of capelin per unit of cod stock in recent years. However, when comparing the amount of capelin consumed by cod in the summer-autumn period with the overlap, there is no obvious relationship (Figure A5.187A and B). Consumption by immatures peaked during a period of average overlap, and for mature cod, the overlap trend is a near inverse of the trend in consumption. Generally, correlations between spatial overlap and consumption have been weak in summer, at several spatial scales (Fall, 2019).

Since cod is mainly distributed near the seabed and capelin in the free water masses, cod may overlap with capelin in the horizontal dimension but still be segregated by depth, always or during parts of the day. A recent study on drivers of variation in cod's consumption of capelin considered both capelin density (horizontal overlap) and capelin depth distribution (vertical overlap), finding that horizontal overlap had small effects on consumption, while vertical overlap was important (Fall *et al.* 2021). Even when accounting for variation in capelin depth distribution, changes in capelin density did not have a strong effect on cod consumption (Fall *et al.* 2021). A potential explanation for this is that once capelin is present, it is present in densities that allow cod to reach satiation (Fall and Fiksen 2019). Cod fed more intensively on capelin when capelin came close to the seabed, especially at banks and bank edges of the Barents Sea (Fall *et al.* 2021). Aarflot *et al.* (2018, 2020) showed that capelin also feed more effectively over the banks where plankton are trapped in shallow and light conditions during the day, pointing to a trade-off between foraging and predation risk for capelin. How these findings reflect the feeding dynamics in other seasons should be further explored.

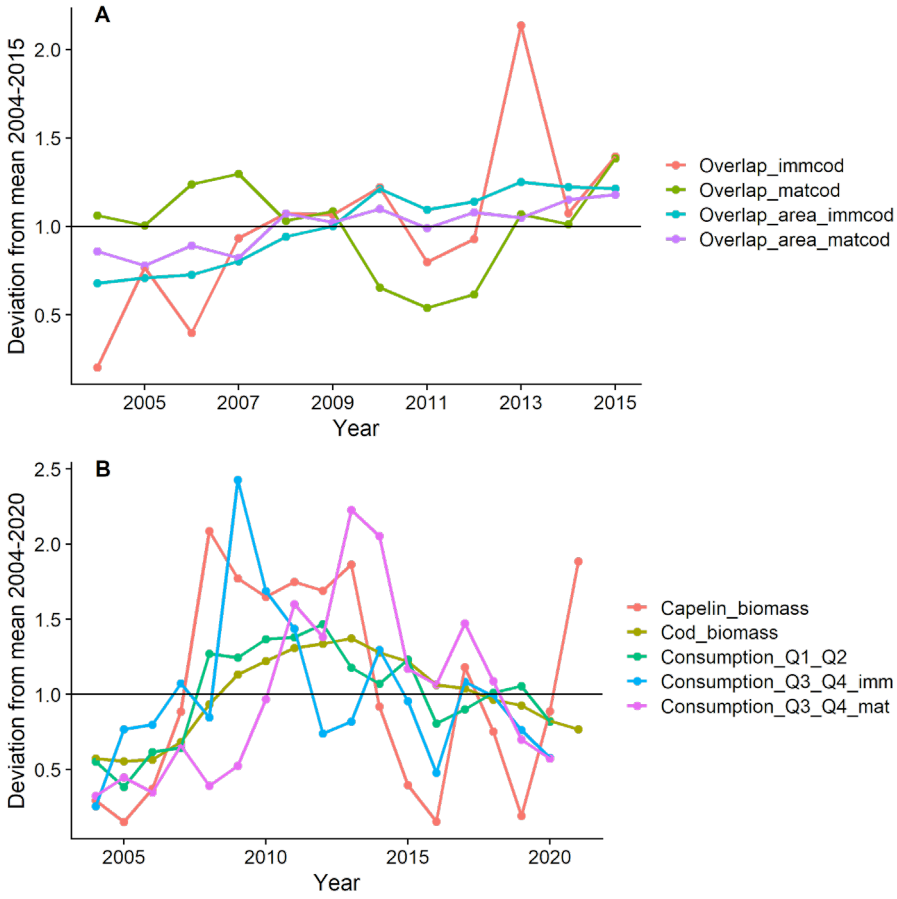

Figure A5.187: Deviations from A) mean overlap and size of the overlap area 2004–2015, and B) mean capelin biomass, cod biomass, and estimated capelin consumption by cod 2004–2020. Panel A shows mean overlap and size of the overlap area (overlap extent) from Fall *et al.* (2018) using predictions from the area north of 74 N. Panel B shows the same data as Figure A5.172 but split on cod maturity stage (age 3–6 were considered immature) with the addition of cod stock biomass. Quarterly consumption estimates for 2021 were not available for the working group.

Cod can prey intensively on polar cod. When polar cod and capelin occur in mixed concentrations, which they often do in northern and eastern areas, polar cod may be easier to catch due to lower swimming speeds (confirmed by trawl catch analyses) and distributions closer to the bottom. However, capelin is a fatter and energetically more valuable prey item. A potential example of this trade-off was seen in cod feeding on mixed aggregations of polar cod and capelin on the Great Bank, where the proportion of polar cod in cod stomachs was higher in the smallest cod (Skaret *et al.* 2020). According to the estimated consumption of various prey species by cod (Figure A5.170 abd A5.171) the consumption of polar cod is much lower than the consumption of capelin. Overlap between cod and polar cod varied between areas and seasons. In northern and eastern areas cod overlap with polar cod prespawners during late autumn–early winter and with younger polar cod during summer–autumn, and as seen during the cod expansion phase when overlap with polar cod increased in the northernmost Barents Sea. The polar cod biomass in the Barents Sea is currently (2021) much lower than the capelin biomass, and this situation is likely to persist for a couple of years.

Interspecific interactions in this trophic system are very complex and require more detailed study.

References

Aarflot, J., Aksnes, D., Opdal, A., Skjoldal, H.R., & Fiksen, Ø. 2018. Caught in broad daylight: Topographic constraints of zooplankton depth distributions. Limnology and Oceanography, 64(3), 849-859. doi:10.1002/lno.11079

Aarflot, J. M., et al. 2020. Foraging success in planktivorous fish increases with topographic blockage of prey distributions. - Marine Ecology Progress Series 644: 129-142.

Fall, J., Ciannelli, L., Skaret, G., & Johannesen, E. (2018). Seasonal dynamics of spatial distributions and overlap between Northeast Arctic cod (Gadus morhua) and capelin (Mallotus villosus) in the Barents Sea. PLoS One, 13(10), e0205921. doi:10.1371/journal.pone.0205921

Fall, J. (2019). Drivers of variation in the predator-prey interaction between cod and capelin in the Barents Sea. PhD thesis, University of Bergen.

Fall, J., & Fiksen, Ø. (2019). No room for dessert: A mechanistic model of prey selection in gut-limited predatory fish. Fish and Fisheries, 21(1), 63-79. doi:10.1111/faf.12415

Fall, J., et al. 2021. Predator–prey overlap in three dimensions: cod benefit from capelin coming near the seafloor. – Ecography. doi: 10.1111/ecog.05473

Skaret, G., et al. 2020. Diel vertical movements determine spatial interactions between cod, pelagic fish and krill on an Arctic shelf bank. - Marine Ecology Progress Series 638: 13-23.